frontiers | Research Topics

Oscillatory brain activity as a marker of brain function and dysfunction in aging and in neurodegenerative disorders

Edited by
Aneta Kielar, Priyanka Shah-Basak, Lars Meyer and Takako Fujioka

Published in
Frontiers in Aging Neuroscience

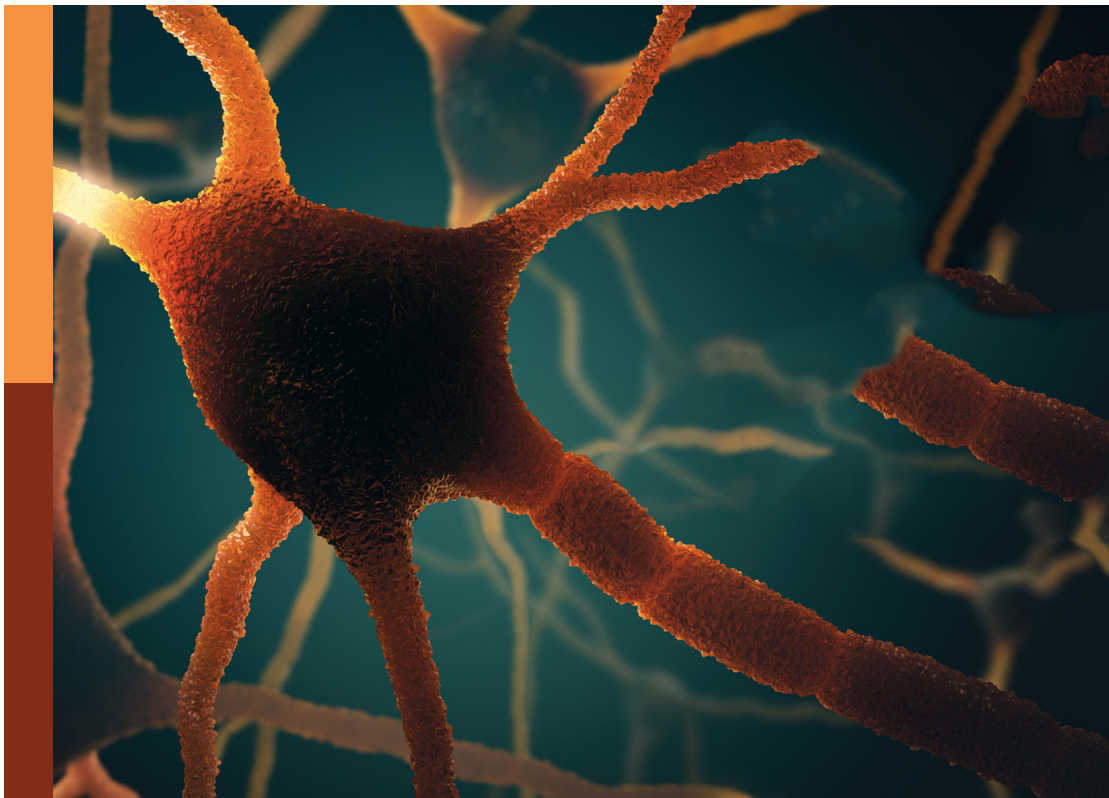

ISSN 1664-8714
ISBN 978-2-83251-790-1
DOI 10.3389/978-2-83251-790-1

About Frontiers

Frontiers is more than just an open access publisher of scholarly articles: it is a pioneering approach to the world of academia, radically improving the way scholarly research is managed. The grand vision of Frontiers is a world where all people have an equal opportunity to seek, share and generate knowledge. Frontiers provides immediate and permanent online open access to all its publications, but this alone is not enough to realize our grand goals.

Frontiers journal series

The Frontiers journal series is a multi-tier and interdisciplinary set of open-access, online journals, promising a paradigm shift from the current review, selection and dissemination processes in academic publishing. All Frontiers journals are driven by researchers for researchers; therefore, they constitute a service to the scholarly community. At the same time, the *Frontiers journal series* operates on a revolutionary invention, the tiered publishing system, initially addressing specific communities of scholars, and gradually climbing up to broader public understanding, thus serving the interests of the lay society, too.

Dedication to quality

Each Frontiers article is a landmark of the highest quality, thanks to genuinely collaborative interactions between authors and review editors, who include some of the world's best academicians. Research must be certified by peers before entering a stream of knowledge that may eventually reach the public - and shape society; therefore, Frontiers only applies the most rigorous and unbiased reviews. Frontiers revolutionizes research publishing by freely delivering the most outstanding research, evaluated with no bias from both the academic and social point of view. By applying the most advanced information technologies, Frontiers is catapulting scholarly publishing into a new generation.

What are Frontiers Research Topics?

Frontiers Research Topics are very popular trademarks of the *Frontiers journals series*: they are collections of at least ten articles, all centered on a particular subject. With their unique mix of varied contributions from Original Research to Review Articles, Frontiers Research Topics unify the most influential researchers, the latest key findings and historical advances in a hot research area.

Find out more on how to host your own Frontiers Research Topic or contribute to one as an author by contacting the Frontiers editorial office: frontiersin.org/about/contact

Oscillatory brain activity as a marker of brain function and dysfunction in aging and in neurodegenerative disorders

Topic editors

Aneta Kielar — University of Arizona, United States
Priyanka Shah-Basak — Medical College of Wisconsin, United States
Lars Meyer — Max Planck Society, Germany
Takako Fujioka — Stanford University, United States

Citation

Kielar, A., Shah-Basak, P., Meyer, L., Fujioka, T., eds. (2023). *Oscillatory brain activity as a marker of brain function and dysfunction in aging and in neurodegenerative disorders*. Lausanne: Frontiers Media SA. doi: 10.3389/978-2-83251-790-1

Table of contents

frontiers | Frontiers in Aging Neuroscience

TYPE Editorial
PUBLISHED 15 February 2023
DOI 10.3389/fnagi.2023.1153150

OPEN ACCESS

EDITED AND REVIEWED BY
Agustin Ibanez,
Latin American Brain Health Institute (BrainLat), Chile

*CORRESPONDENCE
Aneta Kielar
akielar@arizona.edu

SPECIALTY SECTION
This article was submitted to Alzheimer's Disease and Related Dementias, a section of the journal Frontiers in Aging Neuroscience

RECEIVED 29 January 2023
ACCEPTED 02 February 2023
PUBLISHED 15 February 2023

CITATION
Kielar A, Shah-Basak P, Meyer L and Fujioka T (2023) Editorial: Oscillatory brain activity as a marker of brain function and dysfunction in aging and in neurodegenerative disorders. *Front. Aging Neurosci.* 15:1153150. doi: 10.3389/fnagi.2023.1153150

Editorial: Oscillatory brain activity as a marker of brain function and dysfunction in aging and in neurodegenerative disorders

Aneta Kielar[1]*, Priyanka Shah-Basak[2], Lars Meyer[3,4] and Takako Fujioka[5]

[1]Speech Language and Hearing Sciences, University of Arizona, Tucson, AZ, United States, [2]Department of Neurology, Medical College of Wisconsin, Milwaukee, WI, United States, [3]Max Planck Institute for Human Cognitive and Brain Sciences, Leipzig, Germany, [4]Clinic for Phoniatrics and Pedaudiology, University Hospital Münster, Münster, Germany, [5]Department of Music, Stanford University, Stanford, CA, United States

KEYWORDS

neural oscillations, healthy aging, neurodegenerative disorders, biomarkers of neurodegeneration, oscillatory slowing

Editorial on the Research Topic
Oscillatory brain activity as a marker of brain function and dysfunction in aging and in neurodegenerative disorders

Neural oscillations support fundamental mechanisms of information processing in neural networks (Buzsáki, 2006; Singer, 2013, 2018). Properties such as phase and amplitude during task performance and at rest map onto cognitive processes and abilities. The articles in this issue discuss the scientific and clinical use of oscillations in neurological populations that exhibit altered cognition. The articles focus on understanding the oscillatory changes associated with healthy aging and progression of neurodegenerative disorders such as Alzheimer's Disease (AD), Mild Cognitive Impairment (MCI) and Parkinson's Disease (PD), and examine how oscillatory activity can inform development of interventions to slow down aging-related cognitive decline. Nine exciting contributions provide novel methods involving oscillatory signals as early indicators of healthy aging, biomarkers of neurodegeneration, and predictors of successful interventions.

Oscillatory changes associated with healthy aging

Griffa et al. investigated oscillatory connectivity, derived from resting-state MEG (rsMEG) signals in cognitively impaired and normal oldest-old adults (90+ years old) in terms of its relationships to their cognitive status. In the impaired oldest-old participants, increased theta but reduced beta power was found in frontoparietal regions and the default mode network, indicative of cortical slowing. Engagement during demanding cognitive tasks (indicator of cognitive reserve) was associated with stronger connectivity in the alpha and beta bands. Overall, the oscillatory changes in the oldest-old could not be readily distinguished from individuals younger than 85 years.

Fröhlich et al. examined differences in spectral power and oscillatory reactivity in 80+-year old adults across different cognitive status (cognitively unimpaired, possible MCI, non-amnesic MCI, amnesic MCI). No differences in power during eyes-closed condition

were found between healthy individuals and those with cognitive impairments. The authors noted that these findings might be related to anatomical changes associated with advanced aging such as cortical thinning which could lower baseline EEG amplitudes. Although this was not directly addressed in the study, the report highlights the importance of additional anatomical information in this population to reliably interpret scalp-level oscillations.

Changes in the EEG signal associated with neurodegeneration

Doan et al. examined the utility of resting-state and sensory and task-related EEG measures to predict dementia severity based on MMSE scores. After adjusting for demographic confounds, prefrontal EEG measures were found to be highly correlated with MMSE. Furthermore, relationships within EEG measures, including peak frequency, median frequency, alpha-to-theta ratio, alpha asymmetry, and theta-band power indicated increased risk of dementia. This preliminary evidence suggests a potential role of rsEEG as a screening tool. But larger-scale studies will need to substantiate these findings with cautious study designs, matching dementia and non-dementia groups on important demographic variables.

Smailovic et al. investigated the relative potential of rsEEG power, rsEEG connectivity and novel (neurogranin) and conventional CSF markers (amyloid and tau pathology) to differentiate subtypes of amnestic MCI. The strongest discriminator between single-domain and multi-domain MCI was a connectivity measure—global synchrony—in theta and delta bands. Connectivity in slow frequencies was related to early effects of AD-specific molecular pathology, further promising the utility of rsEEG measures as potential biomarkers of dementia.

Lopez et al. modeled connectivity hubs from resting-state alpha measurements in AD. Although both controls and individuals diagnosed with AD had significant parietal "degree" and "connector" hubs derived from alpha rhythms, outward directionality of parietal hubs was lower in AD.

Oscillatory power as a predictor of successful non-pharmacological and pharmacological interventions

Spironelli and Borella examined short- and long-term effects of working memory (WM) training among healthy older adults on behavioral and rsEEG-based oscillatory indices. Specific training, maintenance and transfer effects were reported in the WM treatment group compared to the active control group. For oscillatory responses, the treatment group showed increased oscillatory responses in bilateral anterior sites, which were correlated with better post-training performance.

Complementary to the assessment of resting-state power, Rodríguez-González et al. implemented a network-based approach that considered complex interactions among neurophysiological, cognitive (MMSE), and behavioral (Dementia Behavior Disturbance Scale) variables to assess treatment outcomes. Together the results indicate that changes in EEG parameters can serve as indicators of treatment-related changes in cognition and behavior.

Eyjolfsdottir et al. examined the effects of targeted encapsulated cell biodelivery of nerve growth factor (NGF-ECB) in the basal forebrain (a treatment approach for AD) on rsEEG parameters and cognition over a 12-month period. Increased theta power was associated with a decrease in CSF cholinergic marker (ChAT), whereas increased alpha power was related to increased ChAT and stabilization of MMSE scores.

Zhang et al. examined rsEEG oscillatory and non-oscillatory changes induced by dopaminergic medication in patients with PD. Beta-band phase synchronization was up-regulated by medication. Medication also increased the spectral slope of broadband non-oscillatory component, suggesting that spectral slope could serve as a marker of global efficiency.

In summary, cognitive impairment is found to be associated with increases in slow frequency and reduction in higher frequency cortical rhythms. Oscillatory reactivity is also modulated by behavioral and pharmacological interventions, and can serve as an indicator of treatment success alongside with other biomarkers. All studies here examined rsMEEG measures mainly including spectral power, ratio between bands, shifts in bands, and connectivity using phase- or amplitude-based metrics, suggesting possible mechanistic roles of oscillations.

Future directions

This Research Topic provides new methodologies and results with a potential to advance research and clinical practice for aging populations. Most reported results are preliminary, and signal a need for robust, well-designed, large-scale clinical trials with a focus on spectral oscillatory measures to replicate the said findings. Longitudinal studies are needed to validate reliability in predicting cognitive status. Specific to connectivity, approaches that overcome known challenges regarding volume conduction, linear mixing, and signal-to-noise ratio should be used (Palva and Palva, 2012). Consistent and reproducible findings related to connectivity are needed to better interpret normal and pathological oscillatory dynamics (Colclough et al., 2015; van Diessen et al., 2015).

Author contributions

AK: conceptualization, writing, review, and editing. PS-B and LM: writing, review, and editing. TF: review and editing. All authors contributed to the article and approved the submitted version.

Conflict of interest

The authors declare that the research was conducted in the absence of any commercial or financial relationships that could be construed as a potential conflict of interest.

Publisher's note

References

Buzsáki, G. (2006). *Rhythms of the Brain*. Oxford: Oxford University Press.

Colclough, G. L., Brookes, M. J., Smith, S. M., and Woolrich, M. W. (2015). A symmetric multivariate leakage correction for MEG connectomes. *Neuroimage* 117, 439–448. doi: 10.1016/j.neuroimage.2015.03.071

Palva, S., and Palva, J. M. (2012). Discovering oscillatory interaction networks with M/EEG: challenges and breakthroughs. *Trends Cogn. Sci.* 16, 219–230. doi: 10.1016/j.tics.2012.02.004

Singer, W. (2013). Cortical dynamics revisited. *Trends Cogn. Sci.* 17, 616–626. doi: 10.1016/j.tics.2013.09.006

Singer, W. (2018). Neuronal oscillations: unavoidable and useful? *Eur. J. Neurosci.* 48, 2389–2398. doi: 10.1111/ejn.13796

van Diessen, E., Numan, T., van Dellen, E., van der Kooi, A. W., Boersma, M., Hofman, D., et al. (2015). Opportunities and methodological challenges in EEG and MEG resting state functional brain network research. *Clin. Neurophysiol.* 126, 1468–1481. doi: 10.1016/j.clinph.2014.11.018

frontiers in Aging Neuroscience

ORIGINAL RESEARCH
published: 13 April 2021
doi: 10.3389/fnagi.2021.659817

Predicting Dementia With Prefrontal Electroencephalography and Event-Related Potential

Dieu Ni Thi Doan[1,2†], Boncho Ku[1†], Jungmi Choi[3], Miae Oh[4], Kahye Kim[1], Wonseok Cha[3] and Jaeuk U. Kim[1,2]*

[1]Korea Institute of Oriental Medicine, Daejeon, South Korea, [2]Korean Convergence Medicine, University of Science and Technology, Daejeon, South Korea, [3]Human Anti-Aging Standards Research Institute, Uiryeong-gun, South Korea, [4]Korea Institute for Health and Social Affairs, Sejong, South Korea

Objective: To examine whether prefrontal electroencephalography (EEG) can be used for screening dementia.

Methods: We estimated the global cognitive decline using the results of Mini-Mental Status Examination (MMSE), measurements of brain activity from resting-state EEG, responses elicited by auditory stimulation [sensory event-related potential (ERP)], and selective attention tasks (selective-attention ERP) from 122 elderly participants (dementia, 35; control, 87). We investigated that the association between MMSE and each EEG/ERP variable by using Pearson's correlation coefficient and performing univariate linear regression analysis. Kernel density estimation was used to examine the distribution of each EEG/ERP variable in the dementia and non-dementia groups. Both Univariate and multiple logistic regression analyses with the estimated odds ratios were conducted to assess the associations between the EEG/ERP variables and dementia prevalence. To develop the predictive models, five-fold cross-validation was applied to multiple classification algorithms.

Results: Most prefrontal EEG/ERP variables, previously known to be associated with cognitive decline, show correlations with the MMSE score (strongest correlation has $|r| = 0.68$). Although variables such as the frontal asymmetry of the resting-state EEG are not well correlated with the MMSE score, they indicate risk factors for dementia. The selective-attention ERP and resting-state EEG variables outperform the MMSE scores in dementia prediction (areas under the receiver operating characteristic curve of 0.891, 0.824, and 0.803, respectively). In addition, combining EEG/ERP variables and MMSE scores improves the model predictive performance, whereas adding demographic risk factors do not improve the prediction accuracy.

Conclusion: Prefrontal EEG markers outperform MMSE scores in predicting dementia, and additional prediction accuracy is expected when combining them with MMSE scores.

Significance: Prefrontal EEG is effective for screening dementia when used independently or in combination with MMSE.

Keywords: dementia, Alzheimer's disease, electroencephalography, electrophysiology, event-related potential, Mini-Mental Status Examination

OPEN ACCESS

Edited by:
Aneta Kielar,
University of Arizona, United States

Reviewed by:
Julie A. Onton,
University of California, San Diego, United States
Görsev Yener,
Dokuz Eylul University, Turkey
Regina Maria Baratho,
Pontifical Catholic University of São Paulo, Brazil

***Correspondence:**
Jaeuk U. Kim
jaeukkim@kiom.re.kr

†*These authors have contributed equally to this work*

Received: *28 January 2021*
Accepted: *19 March 2021*
Published: *13 April 2021*

Citation:
Doan DNT, Ku B, Choi J, Oh M, Kim K, Cha W and Kim JU (2021) Predicting Dementia With Prefrontal Electrencephalography and Event-Related Potential. Front. Aging Neurosci. 13:659817. doi: 10.3389/fnagi.2021.659817

INTRODUCTION

Dementia is a clinical syndrome that comprises a group of neurodegenerative disorders related to cognitive decline that influence memory, language presentation, social abilities, and executive functions, et cetera (McKhann et al., 2011; DSM-5). With the progression of cognitive decline, dementia patients gradually experience memory deficits, communication disorders, and difficulty performing activities of daily living and eventually become fully dependent on caregivers (Chertkow et al., 2013). Alzheimer's disease (AD) is the most common cause of dementia, representing 60%–70% of cases. Other common causes of dementia include cerebrovascular disease, Lewy Bodies disease, and frontotemporal dementia (World Health Organization, 2020).

Aging is the major risk factor for dementia, which has a prevalence of approximately 97% in population aged 65 years and above (Alzheimer's Association Report, 2020). The increasing world population and life expectancy have led to a rapid increase in the number of dementia patients, which is estimated to reach 82 million people worldwide by 2030 (World Health Organization, 2020). A substantial burden on social care and degradation of quality of life may follow. Furthermore, the deaths attributed to AD have positioned this condition as the fifth leading cause of death globally, causing 122,019 deaths in 2018 alone (Alzheimer's Association Report, 2020).

Although no known treatment is highly effective for any type of dementia, combined therapeutic tools which are available to mitigate the after effects of cognitive impairment, especially during the early stages of these diseases (Robinson et al., 2015; Tisher and Salardini, 2019). Moreover, the effectiveness of early therapeutic interventions can be increased to achieve disease modification when neuronal degeneration has not yet begun (Sperling et al., 2011; Tisher and Salardini, 2019). As the disease progresses, neurons accumulate abnormal proteins, such as beta-amyloid and tau proteins, and exhibit mitochondrial dysfunction and calcium homeostasis dysregulation (Niedowicz et al., 2011; Kocahan and Doan, 2017; Farooqui, 2019). In the later stages, the brain of the patient presents neuroinflammation and irreversible synaptic loss, leading to neuronal death and brain tissue damage (Niedowicz et al., 2011; Kocahan and Doan, 2017; Farooqui, 2019).

Early detection of neuronal damage in the brain that enables both timely therapeutic intervention to manage the symptoms and adequate preparation of patients and caregivers. Early prediction of dementia is possible when the underlying disease is defined with tangible biomarkers. Recently, the national institute on aging and the Alzheimer's association proposed an AD research framework using diagnostic biomarkers that are standardized in terms of beta-amyloid deposition, pathologic tau, and neurodegeneration, representing a shift from syndrome to biological constructions (Sperling et al., 2011; Jack et al., 2018). Beta-amyloid plaques and neurofibrillary tau tangles uniquely characterize AD among various neurodegenerative disorders that may progress to dementia (McKhann et al., 2011; Jack et al., 2018). Although these biomarker profiles are stated as core neuropathologic changes for defining AD and related terms in the research framework, they remain incomplete and inadequate for clinical practice (Jack et al., 2018). Furthermore, they are clinically accessible only at advanced hospitals and are frequently costly, invasive, and time consuming. Therefore, the development of cheap, fast, and easily accessible diagnostic and screening tools is needed (Humpel, 2011; Zvěřová, 2018).

At present, the most widely used tool for screening dementia is the Mini-Mental Status Examination (MMSE), which exhibits good internal consistency and concurrent validities (Boban et al., 2012; Baek et al., 2016). MMSE has been used as a clinical index to evaluate global cognitive performance with five domains: orientation, registration, attention and calculation, memory, and language (Folstein et al., 1975). Each MMSE domain functionally reflects neural activities by specific cognitive processing mechanisms. The noninvasive methods of EEG or ERPs can electrically record these neural activities. Several studies have validated the correlation between MMSE scores and EEG/ERPs variables. For instance, the study of Garn et al. (2014) explained 36%–51% of the variances associated with quantitative EEG markers by using MMSE scores and exhibited a strong correlation between MMSE scores and event-related potential (ERP) face-name encoding task. There was a significant negative correlation between MMSE scores with the temporal theta to alpha ratio, with $r = -0.69$ in AD group (Meghdadi et al., 2021). Significant correlations of MMSE with EEG beta activity were also observed (Lees et al., 2016) along with P300 latency (Tanaka et al., 1998; Lee et al., 2013). Notably, MMSE scores were effectively correlated with prefrontal EEG slowing biomarkers, as indicated from one of our previous publications (Choi et al., 2019).

Meta-analysis showed that using the MMSE alone yielded a pooled accuracy of 85%–87% for sensitivity and 82%–90% for specificity to screen dementia (cutoff value of 24–25); after adjusting for education level, the sensitivity and specificity were 97% and 70%, respectively (Creavin et al., 2014). In another review of the conversion from mild cognitive impairment (MCI) into AD dementia, the MMSE provided 27%–89% pooled sensitivity with 32%–90% specificity (Arevalo-Rodriguez et al., 2015). Although these meta-analyses have demonstrated a moderate to high accuracy of the MMSE for screening dementia, the cross-validation approach has frequently been neglected; this has led to questions regarding the overfitting of the selected models. In the medical sciences, a cross-validation approach is being increasingly adopted to obtain an unbiased prediction accuracy with high reliability (Wong and Yeh, 2020). Even though MMSE is the most prevalent screening tool for dementia, it suffers from some limitations such as barriers due to language or educational background, the learning effect, or low sensitivity in the early stage of cognitive decline (Scazufca et al., 2009; Duff et al., 2012; Carnero-Pardo, 2014; Gross et al., 2018).

Electroencephalography (EEG) may overcome or supplement the limitations of conventional screening tools such as the MMSE for the early detection of dementia, as it is non-invasive, relatively inexpensive, and portable, while allowing repeated measurements with none or minimal learning effects (Ben-David et al., 2011). Numerous studies have demonstrated that resting-state EEG biomarkers or event-related potential

(ERP) components obtained from EEG signals are reliable for distinguishing dementia from normal controls or other neurological disorders. For instance, by using quantitative EEG features with artificial neural networks, the classification of MCI from elderly normal individuals produced 95.87% sensitivity and 91.06% specificity (Rossini et al., 2008) and a classification model between AD and MCI achieved 94.10% accuracy (Buscema et al., 2007). Further, 92.2% accuracy was obtained for an Area Under the Receiver Operating Characteristic curve (AUROC) of 0.965 by using the cognitive data cluster of the Consortium to Establish a Registry for the Alzheimer's Disease (CERAD) neuropsychological battery, MMSE, and clinical dementia rating; however, in combination with a quantitative EEG analysis of the absolute band power at rest, 95.3% accuracy was achieved with an AUROC of 0.983 when distinguishing AD patients from non-AD persons (Fonseca et al., 2011). In addition, the N200 ERP component can identify memory changes better than MMSE (Papaliagkas et al., 2008).

With the recent advances in hardware and signal processing techniques, EEG systems with fewer channels have become emerging research topics as they can improve the simplicity and convenience of data acquisition and analysis in clinical environments. For instance, single-channel EEG signals have been tested for the detection of MCI, reaching 87.9% accuracy by using a support vector machine with leave-one-out cross-validation (Khatun et al., 2018). Similarly, single-channel EEG features, such as the power spectrum or amplitude, and ERP features (e.g., latency) have been used to distinguish early AD from normal controls, while reaching 81.90% accuracy (Cho et al., 2003). More recently, Choi et al. (2019) used the prefrontal EEG signals (channels Fp1 and Fp2 in the 10–20 system) and obtained a correlation of up to 0.757 in the regression model to predict the MMSE score for older individuals.

In this study, we intended to examine whether prefrontal EEG can be used for screening dementia. First, we examined the correlations between the MMSE score and selected EEG/ERP variables. Second, we compared the distributions of selected variables between the dementia and cognitively normal persons. Third, we estimated the associations of these variables with dementia using logistic regression. Finally, we developed prediction models for dementia by combining variables from resting-state EEG, sensory event-related potential (ERP), and selective-attention ERP results. We compared the model prediction accuracies with and without the MMSE score and demographic information, and we verified the applicability of the models by performing a double cross-validation test.

MATERIALS AND METHODS

Subjects

From September to October 2017, 155 elderly individuals from four health centers (two geriatric hospitals: sites 1 and 2; two public health centers: sites 3 and 4) were recruited for this study. The participants, aged 50 years or older, were located in Uiryeong County, Korea. This observational study was performed as part of the Brain Aging Map Project, a community welfare project conducted in Uiryeong County. Four clinical research nurses were trained to operate EEG systems and other devices and performed participation scheduling, data acquisition, and result consultations. County dwellers were recruited through phone calls, brochures, flyers, and poster advertisements.

The individuals participated voluntarily for approximately, 90 min to measure global cognitive decline [MMSE-DS, a Korean version of the MMSE (Tae et al., 2010)], geriatric depression [KGDS, a Korean version of the Geriatric Depression Scale (GDS; Kim et al., 2001; Bae and Cho, 2004)], and EEG/ERP examinations, among others. All the confirmed demented patients were clinically diagnosed in the current centers by their clinicians or by previous medical exams conducted from other hospitals. Medical records including the diagnostic details for dementia patients were not provided in this study. Despite this limitation, dementia patients were confirmed according to a standardized diagnostic guideline, according to "Clinical practice guideline for dementia by Clinical Research Center for Dementia of South Korea" (Bon et al., 2011). This so-called CREDOS CPG was established in 2011, and offers clinical standards for AD dementia and vascular dementia in South Korea; dementia is diagnosed by comprehensive assessment of dementia, which includes history-taking, neurological examinations, neuropsychological tests, physical evaluation, brain imaging, and laboratory tests. The Diagnostic and Statistical Manual of Mental Disorders IV (DSM-IV; American Psychiatric Association, 2013) was used for the dementia criteria (Bell, 1994), and the International Statistical Classification of Diseases and Related Health Problems 10th edition (ICD-10) was used to classify the disease stage (World Health Organization, 1992). All the normal individuals were recruited from public health centers with the assumption that they showed no evidence of dementia. The following individuals and subjects were excluded from the study: those who had a meal or performed intensive physical exercise within 1 h before beginning the experiments; those who had insufficient sleep (<4 h) during the previous night; those with physical abnormalities that impeded adequate EEG electrode placement; and those not apt for the study as assessed by the clinical research nurses.

Consent was obtained after providing complete descriptions about the purpose of the study to the participants or their caregivers. The study protocol was approved by the Institutional Review Board of the Korea Institute of Oriental Medicine (KIOM; approval number: I-1807/007-003). The study was performed in accordance with the Declaration of Helsinki. **Figure 1** shows the consolidated standards of reporting trials (CONSORT) diagram corresponding to this study.

The demographic data, including age, sex, education level, comorbidities, and current treatments, were obtained from the participants. Subsequently, they underwent the MMSE-DS, KGDS, and EEG/ERP experiments.

EEG/ERP Acquisition and Experiments

The brain activity was noninvasively recorded via EEG at two prefrontal monopolar scalp electrodes (channels Fp1 and Fp2)

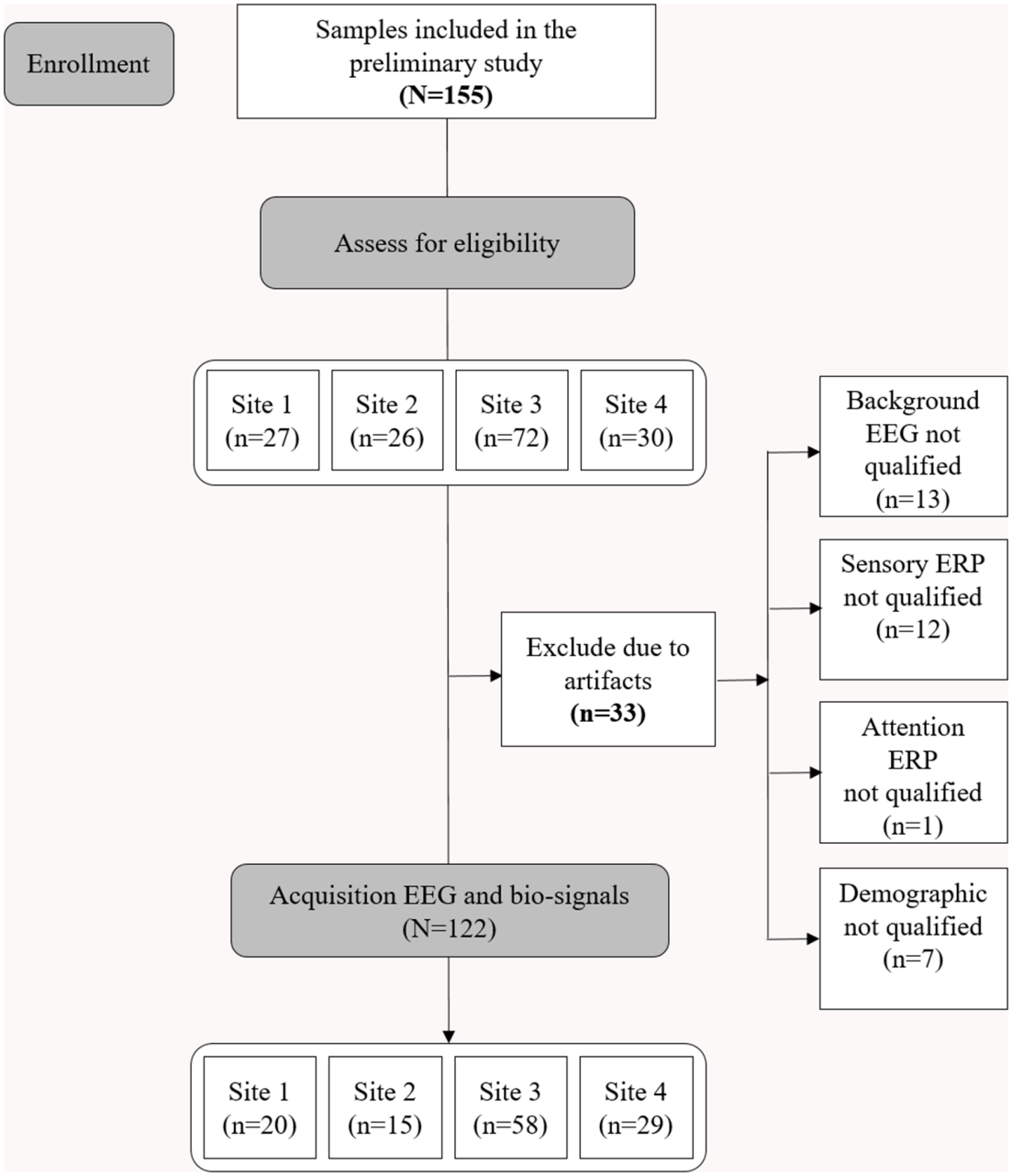

FIGURE 1 | Consolidated Standards of Reporting Trials (CONSORT) diagram illustrating enrollment and exclusion criteria for this study.

according to the International 10-20 system, with the right earlobe electrode serving as a reference. The EEG system used was the NeuroNicle FX2 (LAXTHA, Daejeon, South Korea) with band-pass filtering from 3–43 Hz and input voltages of ±393 μV (input noise below 0.6 μVrms). The signals passed through an infinite impulse response, including Butterworth highpass and lowpass filters with cutoff frequencies of 2.6 and 43 Hz, respectively. In addition, a bandstop filter was set between 55 and 65 Hz. All the EEG electrode contact impedances were maintained below 10 kΩ. The data were digitized in continuous recording mode at a 250 Hz sampling frequency and a 15-bit resolution (Choi et al., 2019). To eliminate muscle and eye movement artifacts and monitor sleepiness in the subjects, qualified operators inspected the individuals and EEG traces during the recordings. The operator guided the participants to remain comfortably seated with their eyes closed and alerted them whenever signs of behavioral or EEG drowsiness were detected. Thirty-three subjects were excluded from the study due to noise, artifacts, and incomplete demography information (**Figure 1**; Choi et al., 2019).

Electroencephalography (EEG) signals from the participants were acquired while they remained seated in an upright position under three sequential conditions: (1) spontaneous brain activity to establish background EEG signals in a resting state for 5 min (resting-state EEG); (2) sensory-evoked potentials (sensory ERP) for 8 min; and (3) a selective attention task to acquire the corresponding ERPs (selective-attention ERP) for 5 min. All participants were tested for auditory hearing ability before operating the experiments.

To elicit the sensory ERP, each participant was instructed to avoid motion while perceiving eight intonations from auditory stimuli at 125, 250, 500, 750, 1,500, 2,000, 3,000, and 4,000 Hz. The sequence of intonation was allocated by a pseudo-random function, in which the same intonation was not provided consecutively over the 480 stimuli presented. The pseudorandomized eight intonations function as non-repeated stimuli, which helps to avoid the sensory adaptation effect and therefore maintain the response sensitivity. Sensory adaptation leads to the attenuation of neuronal responsiveness over time after the sensory neurons are exposed to a repeated stimulation (Pérez-González and Malmierca, 2014). Another reason for selecting eight intonations, lies in the fact that hearing loss due to aging generally occurs in high frequency and low frequency regimes, which would be reflected in the frequency response pattern of sensory ERP (Ciorba et al., 2011; Rigters et al., 2016). Each participant received the auditory stimuli through earphones at a volume level of 70 dB. The duration of each stimulus was 50 ms, with rise and fall times being within 1 ms and the interval between consecutive stimuli being 1 s.

To elicit the selective-attention ERP, we adopted an active auditory oddball task presenting 64 rare random-sequenced target stimuli of 2,000 Hz (1/5 ratio) and 256 monotonic standard auditory stimuli of 750 Hz (4/5 ratio). The stimulus presentation was the same as that adopted to elicit the sensory ERP. The participants were asked to press a response key upon recognition of the target stimuli. The recordings were conducted while the participants kept their eyes closed in a soundless room with regular illumination.

Preprocessing and Variable Extraction

We tested data for contamination due to muscle and eye movement of the (Fp1, Fp2) prefrontal EEG signals as we did not reject any artifact in the signal processing. First, we checked that none of the EEG data were contaminated by large amounts of artifacts. Specifically, none of the participants contained more than 10% of epochs exceeding 200 μV in maximum amplitude; this value was a common exclusion threshold of each epoch due to serious artifacts (Noh et al., 2006). When applying a stricter voltage threshold of 100 μV, we still found no participants for whom 10% of the epochs exceeded this threshold. Therefore, none of the eye-closed resting-state EEG data were rejected due to artifacts in this study.

Frequency-domain (or spectral-domain) features are typically used in the quantitative analysis of EEG rhythms. To transform an EEG signal from the time domain into the frequency domain, a Fourier transform of the autocorrelation function was employed to provide the power spectral density. In the eye-closed resting EEG, intrinsic oscillation reflective of an idling cortical state becomes dominant, and the dominant peak frequency is usually located in the 4–13 Hz band. Previous reports have commonly revealed that the dominant oscillatory frequencies that appear in the alpha band during normal aging become lower in cognitively disordered patients (Jackson and Snyder, 2008; Jelic and Kowalski, 2009).

Some of the variables used in the resting-state EEG results are explained further. The resting-state EEG markers were derived from a frequency-domain analysis of EEG data measured over 5 min. Concretely, the median frequency measures the average frequency and the peak frequency measures the frequency at the maximum peak, in the dominant intrinsic oscillatory frequency band of 4–13 Hz of the EEG power spectrum. The alpha-to-theta ratio measures the power ratio of alpha rhythms (8–12.99 Hz) to theta rhythms (4–7.99 Hz). The EEG power spectrum was obtained by fast Fourier transform of the EEG signal using a rectangular window. The median frequency was calculated in two steps. Step 1: all spectral power values in the 4–13 Hz frequency domain were summed and divided by 2. Step 2: the frequency at which the cumulative power in the 4–13 Hz frequency domain first, exceeded the value calculated in step 1 was selected. The peak frequency was determined as the frequency at which the power of the EEG spectrum in the 4–13 Hz frequency domain was largest. The absolute power was calculated in the following four frequency regions: delta (0–3.99 Hz), theta (4–7.99 Hz), alpha (8–12.99 Hz), and beta (13–30 Hz). The power data were then logarithmically transformed to fulfill the normal distributional assumptions required for parametric statistical analysis (Choi et al., 2020). The alpha-to-theta ratio was obtained by dividing the alpha power by the theta power, and the frontal asymmetry was obtained by taking the difference between the right and left alpha powers and dividing by their sum.

The ERP markers were derived from event-related potentials extracted by the conventional ensemble averaging method in EEG with stimuli. Sensory ERP variables that are exogenous sensory components represent sensory processes that mainly depend on the stimuli physical parameters and also can be influenced by cognitive processes (Pratt, 2012). The selective attention ERP components measure higher processes of cognitive function, which are related to endogenous cognitive activity (Woodman, 2010). Five variables were considered from the sensory ERP results: The average voltage peak (amplitude), average response time, amplitude deviation, response time deviation, and center-to-edge amplitude difference. Four variables were extracted from the selective-attention ERP results: the number of correct responses, response time, weighted error percentile, and voltage peak difference between the response and background ERPs. Voltage peak is the maximum amplitude of the ERP signal. The response time is the time corresponding to the voltage amplitude peak and is calculated relative to the stimulus onset. All markers were averaged over the left and right signals. The extracted variables are summarized in **Table 1**.

TABLE 1 | EEG/ERP variables considered in this study.

Type	Variable	Notation	Unit	Definition/description	Alteration in dementia patients
Resting-state EEG	Median frequency	MEF	Hz	Frequency at which the cumulative power spectral density between 4 and 13 Hz is divided into two equal amounts (the 50% quantile). Median frequency is obtained by $\sum_{f=4}^{f=MEF} PSD[f] = \sum_{f=MEF}^{f=13} PSD[f] = \frac{1}{2}\sum_{f=4}^{f=13} PSD[f]$ PSD, power spectral density	Median frequency and peak frequency decrease in dementia patients (Garcés et al., 2013; Nina et al., 2014; Babiloni et al., 2018; Rossini et al., 2020)
	Peak frequency	–	Hz	Frequency at which peak power occurs in 4–13 Hz	
	Peak power	–	μV^2	Maximum PSD amplitude in 4–13 Hz	Shift to lower frequency in peak power in dementia patients (Raicher et al., 2008; Rodriguez et al., 2011)
	Alpha power	Alpha (avg.)	μV^2	Alpha band (8–12.99 Hz) power averaged over left and right hemispheres	General reduction in alpha band power is an EEG hallmark in AD (Li et al., 2020)
	Theta power	Theta (avg.)	μV^2	Theta band (4–7.99 Hz) power averaged over left and right hemispheres	Theta power significantly increases in patients with AD dementia. There are significant correlation between relative theta power and multiple neuropsychological measures and total tau proteins (Rodriguez et al., 2011; Vecchio et al., 2011; Musaeus et al., 2018)
	Beta power	Beta (avg.)	μV^2	Beta band (13–30 Hz) power averaged over left and right hemispheres	Decrement in relative and absolute beta band power was found in dementia patients (Coben et al., 1983; Holschneider and Leuchter, 1995; Christov and Dushanova, 2016)
	Alpha-to-theta ratio	Alpha/theta	–	Ratio of alpha to theta band power Alpha-to-theta ratio = alpha/theta	Lower alpha-to-theta ratio in early and moderate AD patients (Cibils, 2002; Schmidt et al., 2013; Choi et al., 2019)
	Frontal asymmetry	–	–	Asymmetry ratio of alpha band power between right and left hemispheres: $FA = (R - L)/(R + L)$, $R(L)$, absolute alpha band power from right (left) hemisphere	Alpha asymmetry is mainly reported in depression-related diseases as greater alpha power in the left frontal region in patients with major depression (Jesulola et al., 2017; Roh et al., 2020)
Sensory ERP	Voltage amplitude peak	Amplitude	μV	Voltage peak of ERP responses averaged over different frequencies	Sensory ERP components were found to be relatively low in sensitivity to detect changes in dementia (Hirata et al., 2000; Olichney et al., 2011)

(Continued)

TABLE 1 | Continued

Type	Variable	Notation	Unit	Definition/description	Alteration in dementia patients
	Response time	–	ms	Mean time delay between stimulus and response (i.e., voltage peak) averaged over different frequencies	Delayed response across different auditory and visual oddball tasks in dementia patients (Cecchi et al., 2015; Gu et al., 2018)
	Voltage amplitude deviation	Amplitude (deviation)	μV	Standard deviation between voltage peaks over different frequencies	–
	Response time deviation	Response time (deviation)	ms	Standard deviation between response times over different frequencies	–
	Center-to-edge amplitude difference	Amplitude (edge-center ratio)	–	Mean voltage peaks at 500, 750, 1,500, and 2,000 Hz minus mean voltage peaks at 125 and 4,000 Hz divided by their sum	–
Selective-attention ERP	Number of correct responses	# of correct	–	Number of correct responses for target stimulus (2,000 Hz tone) distinguished from background stimulus (750 Hz tone)	Reduced accuracy in ERP-related tasks in dementia patients (Mathalon et al., 2003; Cecchi et al., 2015; Gu et al., 2018)
	Response time	Resp. Time	s	Time between auditory stimulation and voltage peak of EEG voltage oscillations	Response time to evoked auditory stimuli increases in dementia patients (Yener and Başar, 2010; Gu et al., 2018)
	Weighted error percentile	wER	–	wER = (no. errors + 4 × (64 − no. correct recognitions)/(256 + 64 × 4) No. of target (background) stimuli = 64 (256)	–
	Amplitude difference between response and background ERP	Amp (resp) – Amp (bg)	μV	Difference in voltage peaks of EEG oscillations between target and background stimuli	Patients with AD dementia showed lower amplitude for ERP features (Vecchio and Määttä, 2011; Cecchi et al., 2015)

Eight variables from resting-state EEG, five from sensory ERP, and four from selective attention ERP. EEG, electroencephalography; ERP, event-related potential.

Statistical Analysis

The significant level for all statistical tests is set to $\alpha = 0.05$. The demographic and neuropsychological characteristics were summarized as the means and standard deviations (SDs) or medians and ranges (from minimum to maximum values) for continuous variables, and as the frequencies and proportions for categorical variables for the dementia and non-dementia groups. Either an independent two-sample *t*-test or a Mann-Whitney-Wilcoxon rank-sum test was performed after checking the normality of each group of data based on the Shapiro-Wilk test to assess the differences in the continuous variables across dementia and non-dementia individuals. The chi-squared (χ^2) test or the Fisher's exact test was used to check the independence of the categorical variables from the dementia status. The association between the MMSE score and each EEG/ERP variable was evaluated using the Pearson's correlation coefficient ($\hat{\rho}$) and slope of each EEG measurement ($\hat{\beta}$) obtained from univariate linear regression analysis.

The distribution of every EEG/ERP variable for the dementia and non-dementia individuals was obtained using kernel density estimation to visualize the natural differences in both groups for illustrative purposes. Univariate and multiple logistic regression analyses were conducted to estimate the unadjusted or adjusted odds ratios for dementia in each EEG/ERP variable to assess the associations between the EEG/ERP variables and dementia prevalence. In the multiple logistic regression analysis, sex, age, education level, and GDS score were used as covariates. The underlying diseases of the participants described in **Table 2** were not considered as covariates due to the small sample size. Furthermore, the MMSE score was included as an additional covariate in the regression model to identify the independent association of the EEG/ERP variables for dementia.

Dementia prediction models were developed based on all EEG/ERP and demographic variables (age, sex, and education level) that are directly associated with cognitive status. The MMSE score was also used as a single predictor to compare the performances of the models using EEG/ERP features or to investigate the improvement of the predictive models using EEG/ERP features in combination with the MMSE score. All continuous predictors were standardized to a mean of 0 and SD of 1 for data preprocessing. For the model comparisons, we generated 12 datasets based on combination of the variable groups: MMSE score, demographics, resting-state EEG, sensory ERP, and selective attention ERP. The

TABLE 2 | Demographic information and neuropsychological test results of dementia and non-dementia subjects.

	Total (n = 122)	No (n = 87)	Yes (n = 35)	Test Statistic
Age [years]				
Mean (SD)	71.0 (±11.9)	68.2 (±11.2)	78.1 (±10.7)	
Median [range]	73.9 [42.3–95.9]	68.7 [48.3–90.6]	78.6 [42.3–95.9]	W = 777.0, p = 0.0000
Sex				
Male	30 (25%)	22 (25%)	8 (23%)	
Female	92 (75%)	65 (75%)	27 (77%)	$\chi^2_{(df\ =\ 1)}$ = 0.0, p = 9.605E-1
Education level [year]				
Mean (SD)	6.0 (±5.0)	7.1 (±5.0)	3.4 (±3.9)	W = 2,148.5, p = 0.0003
Median [range]	6.0 [0.0–18.0]	6.0 [0.0–18.0]	0.0 [0.0–12.0]	
Systolic BP [mmHg]				
Mean (SD)	125.6 (±16.4)	125.1 (±15.5)	126.9 (±18.6)	$t_{120.0}$ = –0.6, p = 0.5716
Median [range]	123.5 [80.0–170.0]	123.0 [80.0–170.0]	130.0 [98.0–169.0]	
Diastolic BP [mmHg]				
Mean (SD)	73.5 (±11.7)	74.3 (±12.0)	71.4 (±10.8)	$t_{120.0}$ = 1.3, p = 0.2091
Median [range]	70.0 [41.0–100.0]	73.0 [41.0–100.0]	70.0 [45.0–95.0]	
MMSE score				
Mean (SD)	23.2 (±5.7)	25.3 (±4.6)	18.0 (±5.0)	W = 2630.0, p < 1E-6
Median [range]	25.0 [5.0–30.0]	27.0- [12.0–30.0]	18.0 [5.0–28.0]	
GDS score				
Mean (SD)	12.2 (±6.5)	10.7 (±6.0)	16.0 (±6.1)	W = 810.5, p = 0.0001
Median [range]	11.0 [1.0–28.0]	9.0 [1.0–24.0]	16.0 [2.0–28.0]	
Diabetes				
No	101 (83%)	73 (84%)	28 (80%)	$\chi^2_{(df\ =\ 1)}$ = 0.1, p = 0.8010
Yes	21 (17%)	14 (16%)	7 (20%)	
Hypertension				
No	60 (49%)	46 (53%)	14 (40%)	$\chi^2_{(df\ =\ 1)}$ = 1.2, p = 0.2774
Yes	62 (51%)	41 (47%)	21 (60%)	
Hyperlipidemia				
No	105 (86%)	73 (84%)	32 (91%)	FE-test, p = 0.3900
Yes	17 (14%)	14 (16%)	3 (9%)	
Thyroid disease				
No	115 (94%)	81 (93%)	34 (97%)	FE-test, p = 0.6718
Yes	7 (6%)	6 (7%)	1 (3%)	
Mental disorder				
No	93 (76%)	81 (93%)	12 (34%)	$\chi^2_{(df\ =\ 1)}$ = 44.5, p < 1E-6
Yes	29 (24%)	6 (7%)	23 (66%)	
Nervous system disease				
No	111 (91%)	79 (91%)	32 (91%)	FE-test, p = 1.0000
Yes	11 (9%)	8 (9%)	3 (9%)	
Circulatory disease				
No	118 (97%)	84 (97%)	34 (97%)	FE-test, p = 1.0000
Yes	4 (3%)	3 (3%)	1 (3%)	

The values represent the mean (±SD), median and range (minimum–maximum) for the continuous variables and N (%) for the categorical variables. The test statistics and p-values for the continuous variables were obtained from an independent two sample t-test (t value with degree of freedom, df) or a Mann-Whitney-Wilcoxon rank sum test (W) after checking the normality of each group of data based on the Shapiro-Wilk test. For the categorical variables, the p-values were derived from the chi-squared test statistics. FE-test: Fisher's exact test.

interaction terms between sex and other variables were included as predictors in each candidate model containing demographic features.

In total, 122 participants were randomly split, with 80% being in the training set (n = 98) and 20% in the test set (n = 24). The dementia cases in both the training and test sets were distributed proportionally to the total sample size. Before assigning data to the training and test sets, the total dataset was stratified by the dementia status. Consequently, 20% of the data were randomly selected according to each stratum, and then the selected data from both strata were merged into the test dataset. The rest 80% of the data of both strata were merged into the training set. We trained several learning algorithms using a five-fold cross-validation approach, for which the training dataset was again stratified according to the dementia status; subsequently, the randomly generated fold identifiers were given to each stratified group. The learning algorithms employed in this study included binary logistic regression with stepwise variable selection based on Akaike information criteria; penalized logistic regression including ridge, elastic net, and least absolute shrinkage selection operator (Friedman et al., 2020); random forest algorithm (Wright et al., 2020); and extreme gradient boosting (Chen et al., 2020). The model performance was evaluated using the AUROC and binomial deviance. The optimal model (with the highest AUROC and lowest binomial deviance) was selected within each combination of learning algorithms and 12 datasets, and its prediction power was evaluated with the test set. All statistical analyses and predictive model development were conducted using the statistical software R (version 4.0.2, released 2019-06-22; R Core Team, 2020).

RESULTS

"Subject Characteristics" section describes the basic characteristics of the participants with regard to their demographics, neuropsychological information, and comorbidities. "Correlation Between MMSE Score and EEG Measures" section demonstrates the correlation between the EEG/ERP variables and conventional MMSE scores for screening dementia using linear regression analysis. "Densities of EEG/ERP Variables Between Dementia and Non-dementia Subjects" section reports the distribution of each EEG/ERP variable by its density in the dementia and non-dementia groups. "Relation Between EEG/ERP Variables and Dementia" section clarifies the relations between the EEG/ERP variables and dementia, using the estimated odds ratios in the unadjusted and the two adjusted models based on logistic regression. Finally, "Prediction Models for Dementia" section provides an evaluation of the various dementia prediction models based on the EEG/ERP variables, MMSE scores, and demographic data.

Subject Characteristics

The overall demographic information, neuropsychological characteristics, and comorbidities of the 122 persons enrolled in this study are listed in **Table 2**. Among the participants, 87 were non-dementia individuals, and the remaining 35 were confirmed dementia patients. Further, 25% of the participants were male and the remaining 75% were female. The ages of the dementia and non-dementia groups were 78.1 ± 10.7 and 68.2 ± 11.2 years (mean $\pm$ standard deviation), respectively, and their education levels were 3.4 ± 3.9 and 7.1 ± 5.0 years ($p < 0.05$), respectively. The MMSE score was 18.0 ± 5.0 for the dementia patients and 25.3 ± 4.6 for the non-dementia individuals and ranged from 5.0–30.0 ($p < 0.05$). Thus, the dementia patients exhibited lower MMSE scores and education levels and higher mean ages than the non-dementia individuals (Pedraza et al., 2013; Qin et al., 2020). Moreover, the GDS score was higher in the dementia individuals (16.0 ± 6.1, mean $\pm$ standard deviation) than in the non-dementia subjects (10.8 ± 6.2). The physiological and psychological information, such as blood pressure, diabetes, hypertension, and mental disorders, showed no statistically significant differences.

Correlation Between MMSE Score and EEG Measures

We investigated the relations between the MMSE score and prospective EEG/ERP variables from the resting-state EEG, sensory ERP, and selective-attention ERP using linear regression models and the Pearson correlation coefficients, obtaining the results shown in **Figure 2**. Weak to moderate linear correlations are observed between the MMSE score and EEG/ERP variables.

Among the resting-state EEG variables, the median frequency, peak frequency, and alpha-to-theta ratio show positive moderate linear correlations with the MMSE score, with average Pearson correlation coefficient ($\hat{\rho}$) of 0.55–0.68 and average regression coefficients ($\hat{\beta}$) of 2.55–10.29. The theta power shows a negative linear correlation with the MMSE score, with $\hat{\rho} = -0.43$ and $\hat{\beta} = -4.34$. Individual variables from the sensory ERP show weak negative correlations with the MMSE scores, with $\hat{\rho}$ from -0.12 to -0.24. For the selective-attention ERP variables, the MMSE scores show moderate linear correlations with the most variables, including positive correlations with the number of correct responses and amplitude difference between responses, with $\hat{\rho} = 0.58$ and $\hat{\rho} = 0.27$, respectively, and negative correlations with the response time and weighted error percentile, with $\hat{\rho}$ ranging from -0.40 to -0.68.

Densities of EEG/ERP Variables Between Dementia and Non-dementia Subjects

We determined the distribution of each EEG/ERP variable based on its density in the dementia and non-dementia groups, obtaining the results shown in **Figure 3**. Overlapping distributions are observed for some variables obtained from the resting-state EEG and sensory ERP results. However, the variables exhibiting moderate correlations with the MMSE score (reported in "Correlation Between MMSE Score and EEG Measures" section) consistently show significant differences between the dementia and non-dementia groups. Specifically, the median frequency, peak frequency, alpha-to-theta ratio, and theta power from the resting-state EEG results; average response time from the sensory ERP results; and all selective-attention ERP variables exhibit significant differences between the dementia and non-dementia groups. Overall, the observed differences in the distributions of the EEG/ERP variables reflect the different cognitive statuses of the dementia and non-dementia groups.

Relation Between EEG/ERP Variables and Dementia

We obtained the forest plots shown in **Figure 4** for the estimated odds ratios and the 95% confidence intervals of the EEG/ERP variables for predicting dementia. Three logistic regression models were considered, namely, the unadjusted model (first model); the first model adjusted for sex, age, education level, and GDS score (second model); and the second model also adjusted for the MMSE score (third model).

In the first model, most variables from the resting-state EEG and selective-attention ERP reflect the risk of dementia, with odds ratios and 95% confidence intervals, significantly different from 1. Specifically, small peak frequency, median frequency, alpha-to-theta ratio, frontal asymmetry, and large theta band power in the resting-state EEG results indicate increased risk of dementia with mean odds ratios of 0.255, 0.285, 0.289, 0.546, and 1.699 (p-values from 1.09E-2 to 5.58E-7), respectively. Similarly, all variables from the selective-attention ERP contribute with mean odds ratios from 0.349–0.521 and from 2.130–2.364 (p-values from 1.96E-2 to 4.31E-5). In addition, the delayed average response time between the left and right hemispheres in sensory ERP also indicates increased risk of dementia with a mean odds ratio of 1.967 (p-value of 1.25E-3). The detailed odds ratios and p-values are presented in **Appendix Table A1**.

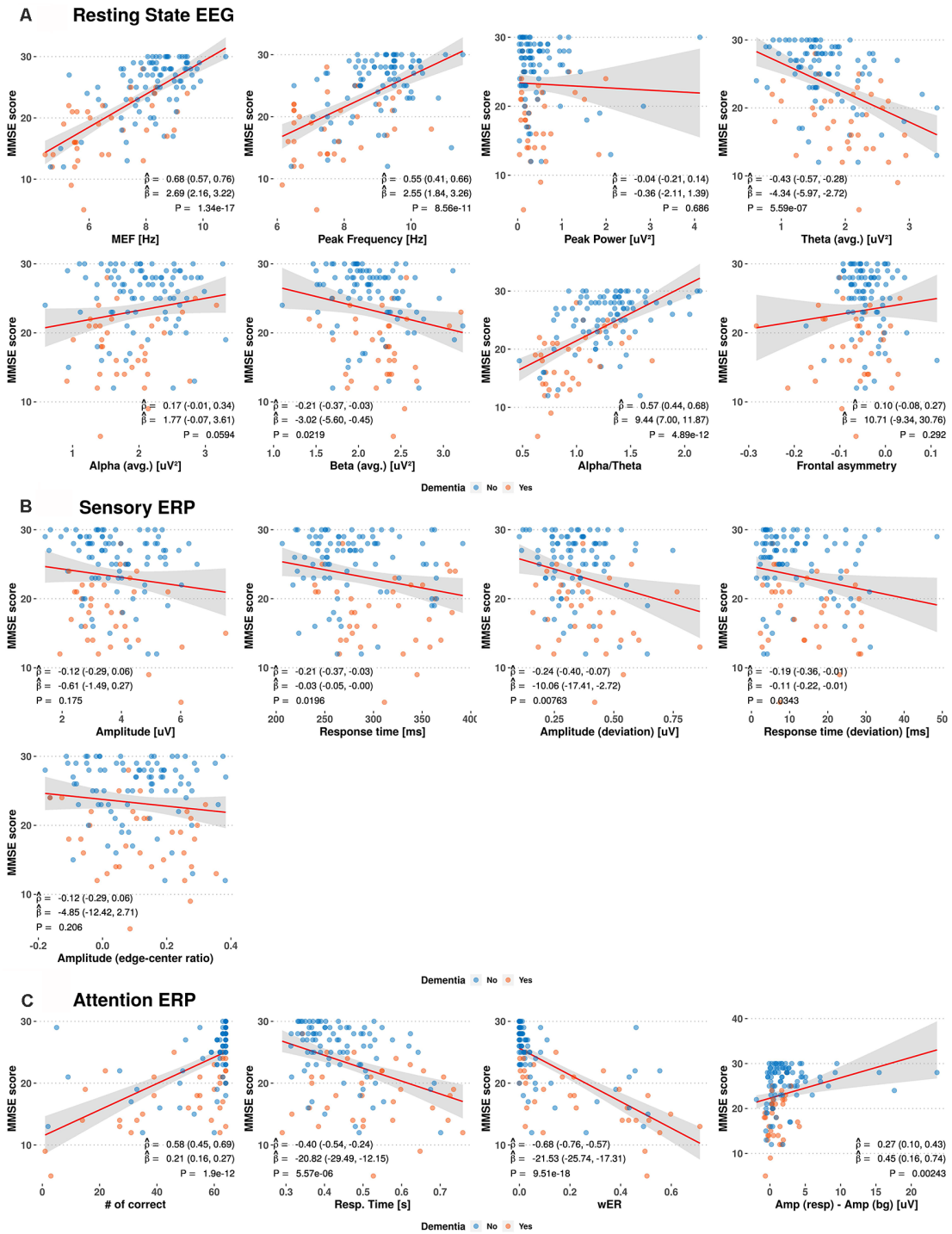

FIGURE 2 | Scatterplots between Mini-Mental Status Examination (MMSE) scores and electroencephalography (EEG)/event-related potential (ERP) variables. The red and blue circles indicate the dementia and non-dementia subjects, respectively. The red line and shaded area show the estimated regression curves and 95% confidence intervals derived from univariate regression analysis. The estimated Pearson correlation coefficient ($\hat{\rho}$), regression coefficient ($\hat{\beta}$), and p-value (P) for each EEG/ERP variable are shown with their 95% confidence intervals (MEF, median frequency; wER, weighted error percentile).

In the second model, only the median frequency, peak frequency, alpha-to-theta ratio, and frontal asymmetry in the resting-state EEG results and the average response time in the sensory ERP results are effective to identify dementia after adjustment, with odds ratios and 95% confidence intervals different from 1. Notably, the bounds of the 95% confidence

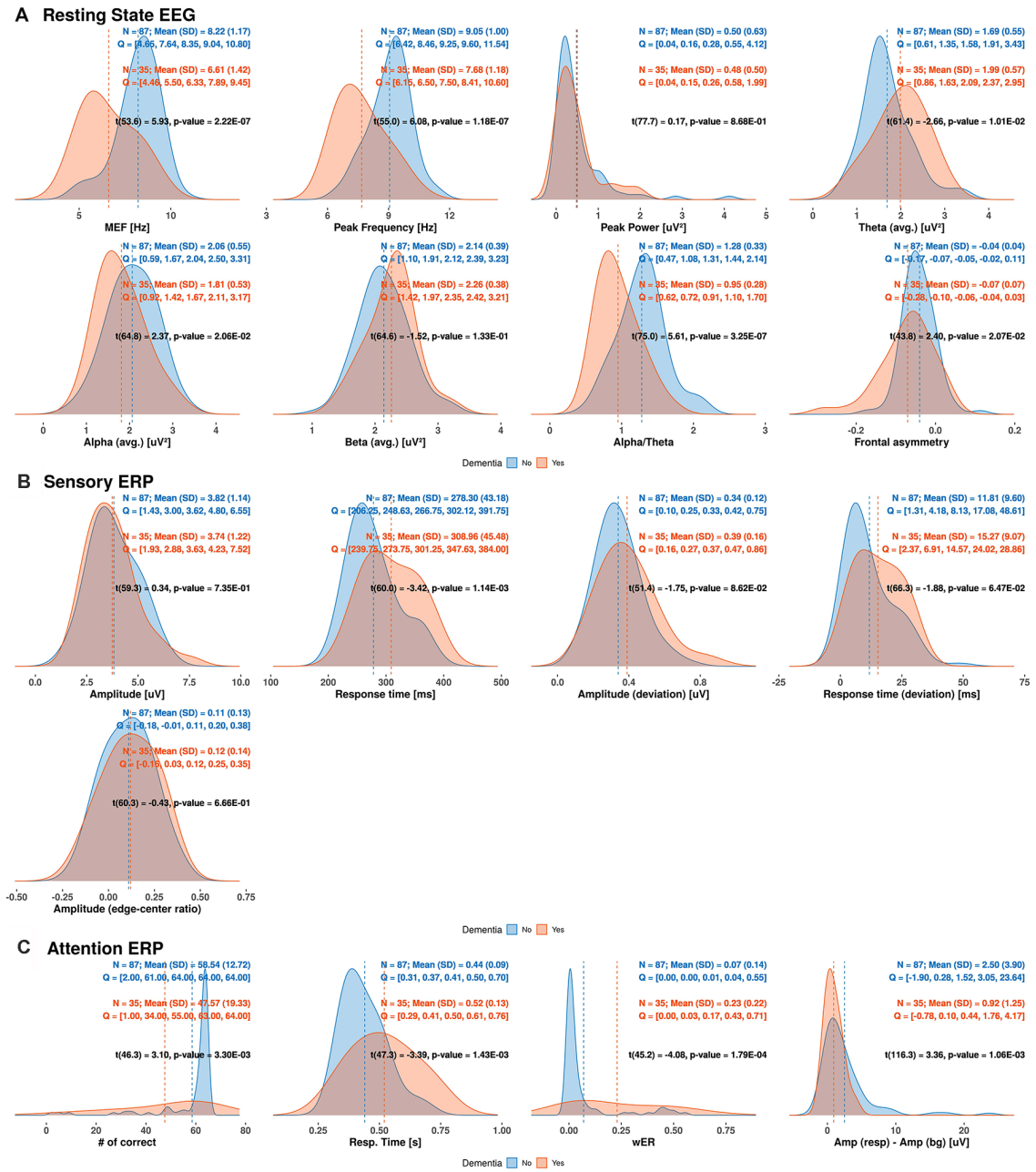

FIGURE 3 | Estimated densities of EEG/ERP variables in dementia and non-dementia subjects. Q indicates values divided into four quantiles (MEF, median frequency; wER, weighted error percentile; SD, standard deviation).

intervals of these variables in the second model are wider than those in the first model, but they still reflect the risk factors of dementia with $p < 0.05$. Hence, the median frequency, peak frequency, alpha-to-theta ratio, frontal asymmetry and average response time tend to be independent from the demographic risk factors and may represent risk factors of dementia.

In the third model, most variables correlated with the MMSE score no longer represent risk factors, and only a few variables, including the peak frequency and frontal asymmetry in the resting-state EEG results and average response time in the sensory ERP results enable identification of dementia. Interestingly, frontal asymmetry shows no correlation with the MMSE score, but it represents a considerable risk factor for dementia after adjustment for demographic covariates and the MMSE score.

Variables such as the median frequency, peak frequency, and alpha-to-theta ratio in the resting-state EEG results

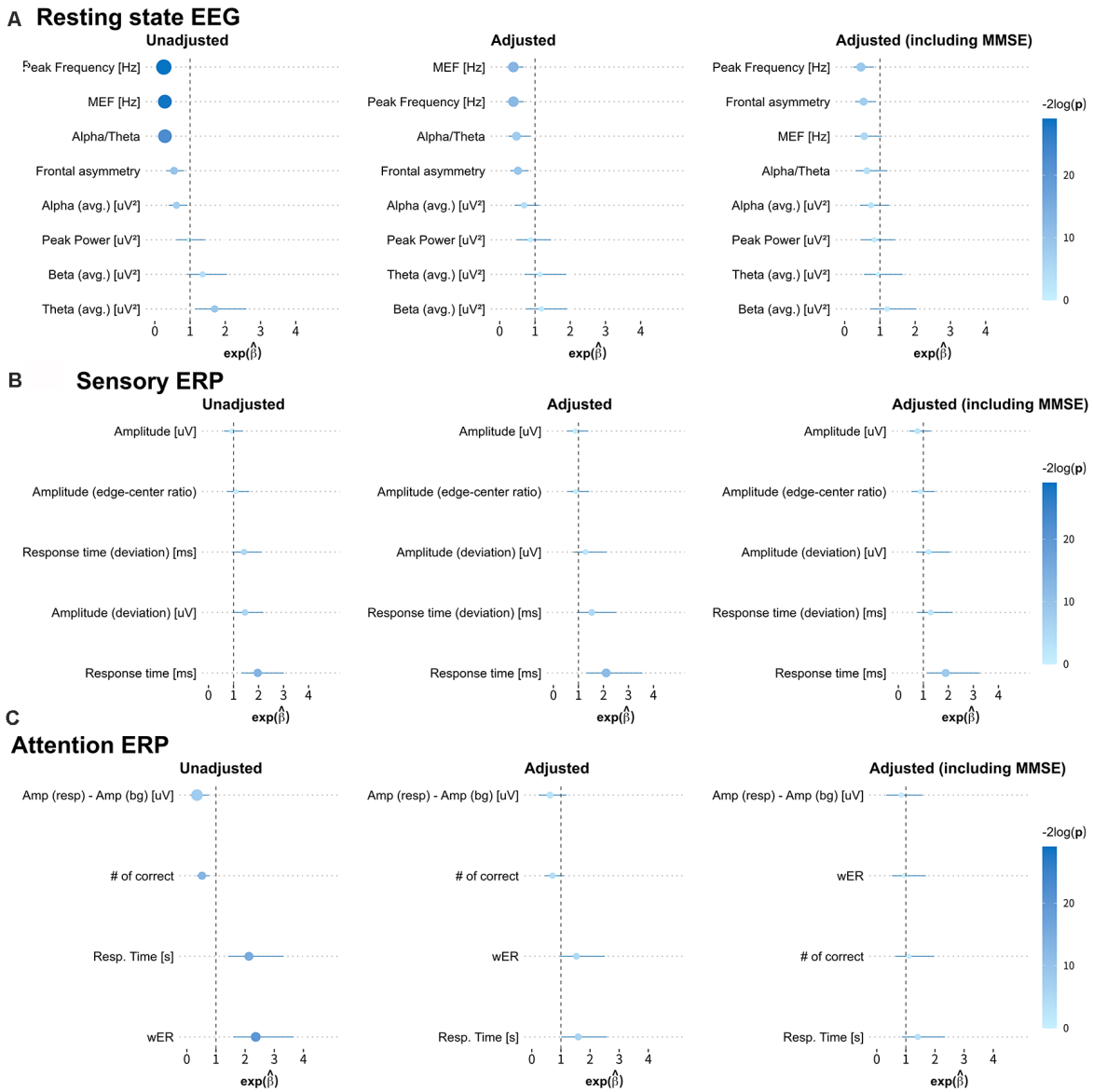

FIGURE 4 | Estimated odds ratios and 95% confidence intervals derived from three logistic regression models. The first, second, and third columns show the results from the unadjusted univariate logistic regression model; the model adjusted for sex, age, education level, and geriatric depression scale (GDS) score; and the model adjusted for all these covariates and the MMSE score, respectively. The size of each circle indicates the magnitude of the estimated odds ratio, and the line across the circle represents its 95% confidence interval. The color map represents the magnitude of the log-transformed *p*-values (−2log p) for the odds ratios (MEF, median frequency; wER, weighted error percentile). The quantitative results are summarized in **Appendix Table A1**.

present moderate to strong correlations with the MMSE score (reported in "Correlation Between MMSE Score and EEG Measures" section) and provide consistent odds ratio values for classifying dementia. On the other hand, the frontal asymmetry in the resting-state EEG results and the average response times from the left and right hemispheres in the sensory ERP results show no or weak correlations with the MMSE score. Nevertheless, they exhibit valid odd ratios for classifying dementia, suggesting that they could be candidate biomarkers for dementia screening independently from the MMSE score.

Prediction Models for Dementia

We categorized the prediction model results into five groups (**Table 3**). The first group contained univariate analysis of MMSE, multivariate analysis of individual sets of MMSE plus demographic information, resting-state EEG, sensory ERP, and selective-attention ERP. The logistic regression model using the ordinary least squares approach for parameter estimation predicted dementia using only the MMSE score, achieving a 0.803 AUROC and 23.845 deviance. Adding demographic information to the MMSE score did not improve the accuracy. In fact, the prediction model based on logistic regression plus

TABLE 3 | Evaluation results of prediction models according to type of data and classification model.

	Logistic regression (Ordinary least square)		Logistic regression + Elastic net		Random forest		Extreme gradient boosting	
	AUROC	**Deviance**	**AUROC**	**Deviance**	**AUROC**	**Deviance**	**AUROC**	**Deviance**
MMSE	**0.803**	**23.845**	-	-	-	-	-	-
DM + MMSE	0.664	31.380	0.803	25.234	0.748	26.200	0.752	26.995
RSEEG	**0.824**	**23.037**	0.824	22.183	0.773	23.843	0.807	23.929
sensERP	0.697	30.332	0.647	28.832	0.605	28.465	0.500	28.979
attERP	**0.891**	**20.363**	0.882	21.608	0.857	20.679	0.882	24.134
RSEEG + sensERP + attERP	0.739	42.722	0.849	21.146	0.832	22.569	0.849	21.193
DM + RSEEG + sensERP + attERP	0.571	73.514	0.832	21.439	0.832	21.954	0.832	21.295
MMSE + RSEEG	0.798	25.300	0.849	22.141	0.807	21.581	0.849	22.123
MMSE + sensERP	0.807	25.795	0.798	23.338	0.790	22.598	0.756	29.949
MMSE + attERP	0.803	23.845	0.849	23.064	0.798	24.330	0.739	26.390
MMSE + RSEEG + sensERP + attERP	0.782	40.182	0.866	20.855	0.866	20.875	0.866	20.986
DM + MMSE + RSEEG + sensERP + attERP	0.605	86.032	0.849	22.048	0.866	21.140	0.874	21.150
Significant-variables	0.874	20.628	**0.891**	**19.397**	0.798	22.908	0.874	20.461

The MMSE score, demographic information (i.e., sex, age, education level, interaction between sexes, and other variables), resting-state EEG (eight variables), sensory ERP (five variables), and selective-attention ERP (four variables) were the data sources. For the models with demographic variables, the terms corresponding to the interaction between sex and other variables were included in each model. DM, Demographic information; RSEEG, resting state EEG; sensERP, sensory ERP; attERP, selective-attention ERP. For models with demographic variables, the terms corresponding to the interaction between sex and other variables are included in each model."Significant-variables" models contain MEF, peak frequency, alpha/theta, frontal asymmetry from resting state EEG, response time from sensory ERP, and number of correct responses, response time and weighted error percentile from attention ERP. The bold fonts indicate outstanding prediction accuracies.

elastic net using the MMSE score and demographic information provided equal AUROCs of 0.803 with deviances of 25.234. In this first group, the predictor based on selective-attention ERP variables yielded the highest AUROC of 0.891 and lowest deviance of 20.363 using logistic regression. In addition, the resting-state EEG variables enabled higher accuracy than the MMSE score or the MMSE score combined with demographic information.

The second group combined resting-state EEG, sensory ERP, and selective-attention ERP before and after adding demographic information. Loosely speaking, these prediction models failed to improve accuracy compared with the models from the EEG/ERP variables in the first group.

The third group combined the MMSE score with different EEG/ERP variables. Combining the MMSE score with resting-state EEG or sensory ERP provided better prediction accuracy than using the EEG variables from the single groups or the MMSE score alone, reaching an AUROC of 0.849 and a deviance of 22.141 when using logistic regression and elastic net regularization. In comparison with selective-attention ERP alone, combining the MMSE score with selective-attention ERP or with all three EEG/ERP variables did not increase the prediction accuracy.

The fourth group combined demographic information with the MMSE score, resting-state EEG, sensory ERP, and selective-attention ERP. This group provided a lower AUROC with higher deviance than the third group, in which demographic information was neglected.

Finally, the fifth group ("significant-variables" model) contained eight most likely potential markers among all the variables, including MEF, peak frequency, alpha-theta, and frontal asymmetry from resting state EEG, response time from sensory ERP, and number of correct responses, response time, and weighted error percentile from selective-attention ERP. These variables were shown to have high correlations with MMSE score ("Correlation Between MMSE Score and EEG Measures" section), less overlapping in their distribution between dementia and non-dementia groups ("Densities of EEG/ERP Variables Between Dementia and Non-dementia Subjects" section), and indicated as risk factors of dementia after adjusting for covariates ("Relation Between EEG/ERP Variables and Dementia" section). This combination provided a similar AUC of 0.891 but lower deviance of 19.397 using logistic regression with elastic net in comparison with selective-attention ERP cluster (deviance 20.363) using logistic regression with ordinary least square. In this "significant-variables" model based on the elastic net, the accuracy went up to 92.7%.

The prediction model results show that the groups of resting-state EEG and selective-attention ERP variables predict dementia better than the MMSE score. In addition, the EEG/ERP variables combined with the MMSE score further improve dementia prediction, except for selective-attention ERP, whereas adding demographic information to either the EEG/ERP variables or MMSE score does not improve the prediction accuracy. The ineffectiveness of demographic information may be due to the diversity of the participants and the small sample size. The evaluation results of the prediction models are summarized in **Table 3**.

DISCUSSION

In this study, spontaneous resting state EEG, sensory ERP and selective-attention ERP were used as three methods to obtain the important brain oscillations (Başar et al., 2016). Both EEG and ERP variables have been investigated as potential biomarkers to detect MCI and its progression to AD dementia, as well as to directly detect AD dementia (Herrmann and Demiralp, 2005; Uhlhaas and Singer, 2006; Jackson and Snyder, 2008). In resting-state EEG, frequency components shift from high-frequency

bands (i.e., alpha and beta) to lower frequency bands (i.e., delta and theta), and the alterations develop gradually according to the disease severity (Jelles et al., 2008; Smailovic and Jelic, 2019). Similarly, the peak frequency, median frequency, and alpha-to-theta ratio in dementia patients drift towards lower frequencies compared with non-dementia individuals (Raicher et al., 2008; Dauwels et al., 2010; Schmidt et al., 2013). In ERP, amplitude reduction and increased latency have been reported (Başar et al., 2010), as well as reduced accuracy and increased response time in a target detection task (Cecchi et al., 2015) in dementia patients. Our findings are consistent with the results of these studies.

The MMSE has been used widely in clinical practice as an effective and sensitive test to detect and screen cognitive impairment and dementia (Benson et al., 2005; Arevalo-Rodriguez et al., 2015). The MMSE enables dementia detection with 92% accuracy, 78%–84% sensitivity, and 87%–91% specificity (cutoff value of 23/24) (Tsoi et al., 2015). However, the MMSE has bias according to the socio-educational backgrounds of participants, practice effect, and low sensitivity in the early stage of cognitive decline (Scazufca et al., 2009; Duff et al., 2012; Carnero-Pardo, 2014). These disadvantages can be overcome while enhancing the diagnostic accuracy by combining the MMSE score with EEG/ERP data.

Selective-attention ERP examines the cognitive performance using auditory oddball paradigm, which elicits P300 in response to the target intonations through the use of prompt button pushing. This motoric response can cause a distinct movement-related potential, which has been reported to interfere with the topography of P300 and alter its amplitude in comparison with the silent-count task (Salisbury et al., 2001; van Vliet et al., 2014; Kim et al., 2020). Despite these reported influences on P300 with button-pushing behavior, for old participants with as many as 64 deviant stimuli, the button-press was an optimal task touse the counts of correct and erroneous responses as the two salient variables in evaluating cognitive performance.

Selective-attention ERP variables include the number of correct responses, response time, weighted error percentile, and amplitude difference between deviant and background stimuli. Selective attention ERP has been shown to provide the highest AUROC values, while demonstrating the best dementia predictor among all the possible combinations of dementia risk factors. Selective-attention ERP or attention components of P300 have been studied as indicators for cognitive processing. Selective-attention ERP endogenous components reflect the ability of cognitively processing the stimulus based on the levels of attention and arousal (Polich and Kok, 1995). A prolonged P300 response time implies that more time is required to process information, which represents an index of abnormal cognition ability (Williams et al., 1991; van Deursen et al., 2009). P300 amplitude reduction in dementia patients shows that lower attentional resources were devoted to the task performance (van Deursen et al., 2009; Hedges et al., 2016). Furthermore, decreasing number of correct answers and increasing weighted error percentile in the dementia group as compared to those in the normal group indicate a reduction in attentional maintenance and action control ability during cognitive processing throughout the task (Vecchio and Määttä, 2011). All changes in selective-attention ERP variables indicate a decrease in intrinsic brain activation to the responses in demented patients. Selective-attention ERP provides a sensitive and reliable measure for the early detection of cognitive impairment related to AD (Cecchi et al., 2015; Gu et al., 2018). Our findings upheld the literature associated with using attention ERP for detecting dementia.

As indicated by the significant odds ratios before and after adjusting for sex, age, education level, and GDS score, the EEG/ERP variables show high correlations with the MMSE score and indicate dementia risk factors. Furthermore, variables with low correlations with the MMSE score (e.g., frontal asymmetry in resting-state EEG) may be suitable for classifying dementia independently from the MMSE score, as indicated by the significant odds ratios that are obtained after adjusting for the covariates plus the MMSE score. Frontal asymmetry has been used as an indicator of depression due to the hyperactivity of the right prefrontal lobe and the withdrawal behavior to aversive stimuli (Thibodeau et al., 2006; Jesulola et al., 2015). However, to the best of our knowledge, frontal asymmetry has not been reported as a candidate indicator of dementia. Thus, our findings establish a new direction for research on dementia by considering frontal alpha asymmetry.

Considering dementia and its relation to depression, half of the patients with late-onset depression may exhibit cognitive impairment, and the prevalence of depression in dementia patients is between 9% and 68% (Muliyala and Varghese, 2010). Asymmetry in frontal cortex activity reflected in EEG signals has been described as a potential discriminator for depression, such that frontal alpha asymmetry has been found to be significantly higher in depressed subjects than healthy controls (Gollan et al., 2014; Adolph and Margraf, 2017; Brzezicka et al., 2017); however, contradicting results have also been reported (van der Vinne et al., 2017; Kaiser et al., 2018). Our results may suggest that the frontal alpha asymmetry as one of the potential EEG variables for dementia detection.

We derived prediction models using different combinations of EEG/ERP variables, MMSE scores, and demographic data. Selective-attention ERP variables and resting-state EEG variables produced more accurate predictions than MMSE scores or MMSE scores combined with demographic information. Hence, these variables may be representative in the identification of cognitive changes due to dementia. In contrast, adding demographic information tended to decrease the accuracy compared to the cases in which demographic information was neglected. Hence, demographic information may undermine predictive modeling of dementia.

The variable selection in the prediction model based on the statistical test often leads to serious bias in maximizing the performance of the predictive model, as explained by Lo et al. (2015). To overcome this limitation, we adopted penalized regression approaches that performed the variable selection continuously. In our case, a model with the variables that showed highest statistical significances resulted in best accuracy among various prediction models (**Table 3**). In particular, the model

exhibiting the highest AUROC (0.891) and lowest deviance (19.397) employed the eight most significant-variables in the logistic regression approach with elastic net regularization, followed by the selective-attention ERP variables in a logistic regression model via the ordinary least squares method. It implies that a prediction model with only few EEG/ERP variables that showed high statistical significance can be used for effective screening of dementia, which would lead to the cost effective utility of "prefrontal EEG" in clinics.

Overall, the logistic regression model with elastic net regularization tended to perform better than the random forest or extreme gradient boosting approach in terms of AUROC and deviance from individual EEG/ERP variables with or without MMSE. Again, adding demographic information to this model reduced the predictive performance. The adverse effects of demographics may be due to the diversity of participants considered in this study regarding aspects such as age, sex, education level, GDS score, and the underlying disease causing dementia.

Some limitations of this study remain to be addressed. The dementia patients in this study were registered in the Korean National Health Insurance Service, and we were not able to obtain further medical records of the patients, such as imaging data, to identify the underlying causes and statuses of dementia. Therefore, hidden comorbidities inducing diversity of EEG/ERP features may have affected our results. In addition, our findings cannot be generalized due to the small sample size (122 participants) and discrepancies in age and education level among groups. Even though we attempted to remove confounding effects by adjusting for age, sex, education level and depression level, the prediction models could increase clinical usability if the data had no such discrepancies in other risk factors between dementia patients and normal controls. Finally, we could not examine the exposures or suspected risk factors over time. Thus, a prospective or case-control study with a larger and more representative sample is still required to clinically validate the diagnostic value of the EEG/ERP variables considered in our study.

CONCLUSION

Prefrontal EEG variables, which are related to EEG slowing, left–right asymmetry in the resting state, and sensory and selective-attention ERPs, have been correlated with the MMSE score. Logistic regression for dementia prediction shows that most of the selected variables remain significant after adjustment for GDS and demographic risk factors of dementia, such as age, education level, and sex. In contrast, when the model is adjusted for the MMSE score and demographic covariates, these prefrontal EEG variables become non-significant, except for the frontal asymmetry among the activity in the left and right hemispheres, peak frequency in resting-state EEG, and the response time in sensory ERP. The other variables have no or minimal correlations with the MMSE score after such adjustment. From multivariate regression models with five-fold cross-validation, we found that the prefrontal EEG variables outperform the MMSE score in dementia prediction. In particular, the prediction accuracy was the highest when using the eight variables that showed highest statistical significances among tested EEG/ERP variables. Adding demographic information fails to improve the prediction accuracy. Overall, the slowing and asymmetry of prefrontal EEG activity seem promising for dementia screening, and can be used in combination with the MMSE score or function as its alternative. In a future study, the clinical usability of few-channel EEG can be improved by recruiting more participants with balanced demographic risk factors among patient and control groups and by including preceding stages of dementia such as MCI; screening MCI patients effectively allows early medical intervention that can prevent or deter the progression to dementia.

DATA AVAILABILITY STATEMENT

The original contributions presented in the study are included in the article, further inquiries can be directed to the corresponding author.

ETHICS STATEMENT

The studies involving human participants were reviewed and approved by Declaration of Helsinki. The patients/participants provided their written informed consent to participate in this study.

AUTHOR CONTRIBUTIONS

DD led the manuscript preparation. BK analyzed the data and wrote the manuscript. JC extracted relevant EEG variables and controlled the EEG data quality. MO analyzed the data. WC designed and led the Brain Aging Map Project. KK worked to obtain the institutional review board approval. JK designed the study and wrote the manuscript. All authors commented on and approved the contents of the manuscript. All authors contributed to the article and approved the submitted version.

FUNDING

This study was conducted as a part of the Brain Aging Map Project and was supported by the Korea Institute of Oriental Medicine (KIOM; Grant no.: KSN2021130) funded by the Korean government. The Brain Aging Map Project was supported by the Human Anti-Aging Standards Research Institute, the Uiryeong Community Health Center, and the KIOM.

ACKNOWLEDGMENTS

We thank all the contributors to the Brain Aging Map Project, especially for acquiring the data used in this study. The contributors include Young Gooun You, Miok Jo, Minji Kwon, Youyoung Choi, Segyeong Jung, Soyoung Ryu, and Eunjeong Park.

REFERENCES

Adolph, D., and Margraf, J. (2017). The differential relationship between trait anxiety, depression and resting frontal α-asymmetry. *J. Neural Transm.* 124, 379–386. doi: 10.1007/s00702-016-1664-9

Alzheimer's Association Report. (2020). Alzheimer's disease facts and figures. *Alzheimers Dement.* 16, 391–460. doi: 10.1002/alz.12068

American Psychiatric Association. (2013). *Diagnostic and Statistical Manual of Mental Disorders.* 4th Edn. Arlington, VA: American Psychiatric Association.

Arevalo-Rodriguez, I., Smailagic, N., Roquéi Figuls, M., Ciapponi, A., Sanchez-Perez, E., Giannakou, A., et al. (2015). Mini-mental state examination (MMSE) for the detection of Alzheimer's disease and other dementias in people with mild cognitive impairment (MCI). *Cochrane Database Syst. Rev.* 2015:CD010783. doi: 10.1002/14651858.CD010783.pub2

Babiloni, C., Del Percio, C., Lizio, R., Noce, G., Lopez, S., Soricelli, A., et al. (2018). Abnormalities of resting state cortical EEG rhythms in subjects with mild cognitive impairment due to Alzheimer's and lewy body diseases. *J. Alzheimers Dis.* 62, 247–268. doi: 10.3233/JAD-170703

Bae, J. N., and Cho, M. J. (2004). Development of the korean version of the geriatric depression scale and its short form among elderly psychiatric patients. *J. Psychosom. Res.* 57, 297–305. doi: 10.1016/j.jpsychores.2004.01.004

Baek, M. J., Kim, K., Park, Y. H., and Kim, S. Y. (2016). The validity and reliability of the mini-mental state examination-2 for detecting mild cognitive impairment and Alzheimer's disease in a korean population. *PLoS One* 11:e0163792. doi: 10.1371/journal.pone.0163792

Başar, E., Gölbaşı, B. T., Tülay, E., Aydın, S., and Başar-Eroğlu, C. (2016). Best method for analysis of brain oscillations in healthy subjects and neuropsychiatric diseases. *Int. J. Psychophysiol.* 103, 22–42. doi: 10.1016/j.ijpsycho.2015.02.017

Başar, E., Güntekin, B., Tülay, E., and Yener, G. G. (2010). Evoked and event related coherence of Alzheimer patients manifest differentiation of sensory-cognitive networks. *Brain Res.* 1357, 79–90. doi: 10.1016/j.brainres.2010.08.054

Bell, C. C. (1994). DSM-IV: diagnostic and statistical manual of mental disorders. *JAMA* 272, 828–829. doi: 10.1001/jama.1994.03520100096046

Ben-David, B. M., Campeanu, S., Tremblay, K. L., and Alain, C. (2011). Auditory evoked potentials dissociate rapid perceptual learning from task repetition without learning. *Psychophysiology* 48, 797–807. doi: 10.1111/j.1469-8986.2010.01139.x

Benson, A. D., Slavin, M. J., Tran, T. T., Petrella, J. R., and Doraiswamy, P. M. (2005). Screening for early Alzheimer's disease: is there still a role for the mini-mental state examination? *Prim. Care Companion J. Clin. Psychiatry* 7, 62–67. doi: 10.4088/pcc.v07n0204

Boban, M., Malojčić, B., Mimica, N., Vuković, S., Zrilić, I., Hof, P. R., et al. (2012). The reliability and validity of the mini-mental state examination in the elderly croatian population. *Dement. Geriatr. Cogn. Disord.* 33, 385–392. doi: 10.1159/000339596

Bon, D. K., Kim, S. G., Lee, J. Y., Park, K. H., Shin, J. H., Kim, K. K., et al. (2011). Clinical practice guideline for dementia by clinical research center for dementia of south korea. *J. Korean Med. Assoc.* 54, 861–875. doi: 10.5124/jkma.2011.54.8.861

Brzezicka, A., Kamiński, J., Kamińska, O. K., Woyńczyk-Gmaj, D., and Sedek, G. (2017). Frontal EEG α band asymmetry as a predictor of reasoning deficiency in depressed people. *Cogn. Emot.* 31, 868–878. doi: 10.1080/02699931.2016.1170669

Buscema, M., Capriotti, M., Bergami, F., Babiloni, C., Rossini, P., and Grossi, E. (2007). The implicit function as squashing time model: a novel parallel nonlinear EEG analysis technique distinguishing mild cognitive impairment and Alzheimer's disease subjects with high degree of accuracy. *Comput. Intell. Neurosci.* 2007:35021. doi: 10.1155/2007/35021

Carnero-Pardo, C. (2014). Should the mini-mental state examination be retired? *Neurologia* 29, 473–481. doi: 10.1016/j.nrl.2013.07.003

Cecchi, M., Moore, D. K., Sadowsky, C. H., Solomon, P. R., Doraiswamy, P. M., Smith, C. D., et al. (2015). A clinical trial to validate event-related potential markers of Alzheimer's disease in outpatient settings. *Alzheimers Dement.* 1, 387–394. doi: 10.1016/j.dadm.2015.08.004

Chen, T., He, T., Benesty, M., Khotilovich, V., Tang, Y., Cho, H., et al. (2020). *Xgboost: Extreme Gradient Boosting.* Available online at: https://CRAN.R-project.org/package=xgboost.

Chertkow, H., Feldman, H. H., Jacova, C., and Massoud, F. (2013). Definitions of dementia and predementia states in Alzheimer's disease and vascular cognitive impairment: consensus from the canadian conference on diagnosis of dementia. *Alzheimers Res. Ther.* 5:S2. doi: 10.1186/alzrt198

Cho, S. Y., Kim, B. Y., Park, E. H., Kim, J. W., Whang, W. W., Han, S. K., et al. (2003). "Automatic recognition of Alzheimer's disease with single channel EEG recording," in *Proceedings of the 25th Annual International Conference of the IEEE Engineering in Medicine and Biology* (Cancun, Mexico: IEEE), 2655–2658.

Choi, J., Ku, B., You, Y. G., Jo, M., Kwon, M., Choi, Y., et al. (2019). Resting-state prefrontal EEG biomarkers in correlation with MMSE scores in elderly individuals. *Sci. Rep.* 9:10468. doi: 10.1038/s41598-019-46789-2

Choi, J., Lim, E., Park, M. G., and Cha, W. (2020). Assessing the retest reliability of prefrontal EEG markers of brain rhythm slowing in the eyes-closed resting state. *Clin. EEG Neurosci.* 51, 348–356. doi: 10.1177/1550059420914832

Christov, M., and Dushanova, J. (2016). Functional correlates of the aging brain: β frequency band responses to age-related cortical changes. *Int. J. Neurorehabil.* 76, 98–109. doi: 10.21307/ane-2017-009

Cibils, D. (2002). "Chapter 43 Dementia and qEEG (Alzheimer's disease)," in *Supplements to Clinical Neurophysiology*, Vol. 54 (Elsevier Science B.V.), 289–294.

Ciorba, A., Benatti, A., Bianchini, C., Aimoni, C., Volpato, S., Bovo, R., et al. (2011). High frequency hearing loss in the elderly: effect of age and noise exposure in an Italian group. *J. Laryngol. Otol.* 125, 776–780. doi: 10.1017/S0022215111001101

Coben, L. A., Danziger, W. L., and Berg, L. (1983). Frequency analysis of the resting awake EEG in mild senile dementia of Alzheimer type. *Electroencephalogr. Clin. Neurophysiol.* 55, 372–380. doi: 10.1016/0013-4694(83)90124-4

Creavin, S. T., Noel-Storr, A. H., Smailagic, N., Giannakou, A., Ewins, E., Wisniewski, S., et al. (2014). Mini-mental state examination (MMSE) for the detection of Alzheimer's dementia and other dementias in asymptomatic and previously clinically unevaluated people aged over 65 years in community and primary care populations. *Cochrane Database Syst. Rev.* 2014:CD011145. doi: 10.1002/14651858.CD011145.pub2

Dauwels, J., Vialatte, F., and Cichocki, A. (2010). Diagnosis of Alzheimer's disease from EEG signals: where are we standing? *Curr. Alzheimer Res.* 999, 1–19. doi: 10.2174/156720504558652050

Duff, K., Chelune, G., and Dennett, K. (2012). Within-session practice effects in patients referred for suspected dementia. *Dement. Geriatr. Cogn. Disord.* 33, 245–249. doi: 10.1159/000339268

Farooqui, A. A. (2019). "Neurochemical aspects of dementia," in *Molecular Mechanisms of Dementia* (Elsevier), 1–38. doi: 10.1016/b978-0-12-816347-4.00001-5

Folstein, M. F., Folstein, S. E., and McHugh, P. R. (1975). "Mini-mental state". A practical method for grading the cognitive state of patients for the clinician. *J. Psychiatr. Res.* 12, 189–198. doi: 10.1016/0022-3956(75)90026-6

Fonseca, L. C., Tedrus, G. M. A. S., Fondello, M. A., Reis, I. N., and Fontoura, D. S. (2011). EEG theta and α reactivity on opening the eyes in the diagnosis of Alzheimer's disease. *Clin. EEG Neurosci.* 42, 185–189. doi: 10.1177/155005941104200308

Friedman, J., Hastie, T., Tibshirani, R., Narasimhan, B., Tay, K., and Simon, N. (2020). *Glmnet: Lasso and Elastic-Net Regularized Generalized Linear Models.* Available online at: https://CRAN.R-project.org/package=glmnet.

Garcés, P., Vicente, R., Wibral, M., Pineda-Pardo, J. á., López, M. E., Aurtenetxe, S., et al. (2013). Brain-wide slowing of spontaneous α rhythms in mild cognitive impairment. *Front. Aging Neurosci.* 5:100. doi: 10.3389/fnagi.2013.00100

Garn, H., Waser, M., Deistler, M., Schmidt, R., Dal-Bianco, P., Ransmayr, G., et al. (2014). Quantitative EEG in Alzheimer's disease: cognitive state, resting state and association with disease severity. *Int. J. Psychophysiol.* 93, 390–397. doi: 10.1016/j.ijpsycho.2014.06.003

Gollan, J. K., Hoxha, D., Chihade, D., Pflieger, M. E., Rosebrock, L., and Cacioppo, J. (2014). Frontal α EEG asymmetry before and after behavioral activation treatment for depression. *Biol. Psychol.* 99, 198–208. doi: 10.1016/j.biopsycho.2014.03.003

Gross, A. L., Chu, N., Anderson, L., Glymour, M. M., and Jones, R. N. (2018). Do people with Alzheimer's disease improve with repeated testing? Unpacking the role of content and context in retest effects. *Age Ageing* 47, 866–871. doi: 10.1093/ageing/afy136

Gu, L., Chen, J., Gao, L., Shu, H., Wang, Z., Liu, D., et al. (2018). Cognitive reserve modulates attention processes in healthy elderly and amnestic mild cognitive impairment: an event-related potential study. *Clin. Neurophysiol.* 129, 198–207. doi: 10.1016/j.clinph.2017.10.030

Hedges, D., Janis, R., Mickelson, S., Keith, C., Bennett, D., and Brown, B. L. (2016). P300 amplitude in Alzheimer's disease: a meta-analysis and meta-regression. *Clin. EEG Neurosci.* 47, 48–55. doi: 10.1177/1550059414550567

Herrmann, C. S., and Demiralp, T. (2005). Human EEG γ oscillations in neuropsychiatric disorders. *Clin. Neurophysiol.* 116, 2719–2733. doi: 10.1016/j.clinph.2005.07.007

Hirata, K., Hozumi, A., Tanaka, H., Kubo, J., Zeng, X. H., Yamazaki, K., et al. (2000). Abnormal information processing in dementia of Alzheimer type. A study using the event-related potential's field. *Eur. Arch. Psychiatry Clin. Neurosci.* 250, 152–155. doi: 10.1007/s004060070033

Holschneider, D. P., and Leuchter, A. F. (1995). β activity in aging and dementia. *Brain Topogr.* 8, 169–180. doi: 10.1007/BF01199780

Humpel, C. (2011). Identifying and validating biomarkers for Alzheimer's disease. *Trends Biotechnol.* 29, 26–32. doi: 10.1016/j.tibtech.2010.09.007

Jack, C. R. Jr., Bennett, D. A., Blennow, K., Carrillo, M. C., Dunn, B., Budd Haeberlein, S., et al. (2018). NIA-AA research framework: toward a biological definition of Alzheimer's disease. *Alzheimers Dement.* 14, 535–562. doi: 10.1016/j.jalz.2018.02.018

Jackson, C. E., and Snyder, P. J. (2008). Electroencephalography and event-related potentials as biomarkers of mild cognitive impairment and mild Alzheimer's disease. *Alzheimers Dement.* 4, S137–S143. doi: 10.1016/j.jalz.2007.10.008

Jelic, V., and Kowalski, J. (2009). Evidence-based evaluation of diagnostic accuracy of resting EEG in dementia and mild cognitive impairment. *Clin. EEG Neurosci.* 40, 129–142. doi: 10.1177/155005940904000211

Jelles, B., Scheltens, W. M., van der Flier, E. J., Jonkman, F. H., Lopes da Silva, F. H., and Stam, C. J. (2008). Global dynamical analysis of the EEG in Alzheimer's disease: frequency-specific changes of functional interactions. *Clin. Neurophysiol.* 119, 837–841. doi: 10.1016/j.clinph.2007.12.002

Jesulola, E., Sharpley, C. F., and Agnew, L. L. (2017). The effects of gender and depression severity on the association between α asymmetry and depression across four brain regions. *Behav. Brain Res.* 321, 232–239. doi: 10.1016/j.bbr.2016.12.035

Jesulola, E., Sharpley, C. F., Bitsika, V., Agnew, L. L., and Wilson, P. (2015). Frontal α asymmetry as a pathway to behavioral withdrawal in depression: research findings and issues. *Behav. Brain Res.* 292, 56–67. doi: 10.1016/j.bbr.2015.05.058

Kaiser, A. K., Doppelmayr, M., and Iglseder, B. (2018). α-asymmetrie im elektroenzephalogramm bei geriatrischer depression: valide oder verschwunden? *Z. Gerontol. Geriatr.* 51, 200–205. doi: 10.1007/s00391-016-1108-z

Khatun, S., Morshed, B. I., and Bidelman, G. M. (2018). "Single channel EEG based score generation to monitor the severity and progression of mild cognitive impairment," in *IEEE International Conference on Electro Information Technology* (Rochester, MI: IEEE), 882–886.

Kim, J., Lee, K., and Lee, E. (2020). N100, N200, and P300 auditory event-related potentials depending on handedness and response tasks such as button pressing and mental counting. *Audiol. Speech Res.* 16, 314–320. doi: 10.21848/asr.200059

Kim, J. M., Prince, M. J., Seon Shin, I. L., and Yoon, J. S. (2001). Validity of korean form of geriatric depression scale (KGDS) among cognitively impaired koren elderly and development of a 15-item short version (KGDS-15). *Int. J. Methods Psychiatr. Res.* 10, 204–210. doi: 10.1002/mpr.117

Kocahan, S., and Doan, Z. (2017). Mechanisms of Alzheimer's disease pathogenesis and prevention: the brain, neural pathology, N-methyl-D-aspartate receptors, tau protein and other risk factors. *Clin. Psychopharmacol. Neurosci.* 15, 1–8. doi: 10.9758/cpn.2017.15.1.1

Lee, M.-S., Lee, S.-H., Moon, E.-O., Moon, Y.-J., Kim, S., Kim, S.-H., et al. (2013). Neuropsychological correlates of the P300 in patients with Alzheimer's disease. *Prog. Neuropsychopharmacol. Biol. Psychiatry* 40, 62–69. doi: 10.1016/j.pnpbp.2012.08.009

Lees, T., Khushaba, R., and Lal, S. (2016). Electroencephalogram associations to cognitive performance in clinically active nurses. *Physiol. Meas.* 37, 968–980. doi: 10.1088/0967-3334/37/7/968

Li, X. Y., Yang, X. L., and Sun, Z. K. (2020). α rhythm slowing in a modified thalamocortico-thalamic model related with Alzheimer's disease. *PLoS One* 15:e0229950. doi: 10.1371/journal.pone.0229950

Lo, A., Chernoff, H., Zheng, T., and Lo, S. H. (2015). Why significant variables aren't automatically good predictors. *Proc. Natl. Acad. Sci. U S A* 112, 13892–13897. doi: 10.1073/pnas.1518285112

Mathalon, D. H., Bennett, A., Askari, N., Max Gray, E., Rosenbloom, M. J., and Ford, J. M. (2003). Response-monitoring dysfunction in aging and Alzheimer's disease: an event-related potential study. *Neurobiol. Aging* 24, 675–685. doi: 10.1016/s0197-4580(02)00154-9

McKhann, G. M., Knopman, D. S., Chertkow, H., Hyman, B. T., Jack, C. R., Kawas, C. H., et al. (2011). The diagnosis of dementia due to Alzheimer's disease: recommendations from the national institute on aging-Alzheimer's association workgroups on diagnostic guidelines for Alzheimer's disease. *Alzheimers Dement.* 7, 263–269. doi: 10.1016/j.jalz.2011.03.005

Meghdadi, A. H., Karić, M. S., McConnell, M., Rupp, G., Richard, C., Hamilton, J., et al. (2021). Resting state EEG biomarkers of cognitive decline associated with Alzheimer's disease and mild cognitive impairment. *PLoS One* 16:e0244180. doi: 10.1371/journal.pone.0244180

Muliyala, K. P., and Varghese, M. (2010). The complex relationship between depression and dementia. *Ann. Indian Acad. Neurol.* 13, S69–S73. doi: 10.4103/0972-2327.74248

Musaeus, C. S., Engedal, K., Høgh, P., Jelic, V., Mørup, M., Naik, M., et al. (2018). EEG theta power is an early marker of cognitive decline in dementia due to Alzheimer's disease. *J. Alzheimers Dis.* 64, 1359–1371. doi: 10.3233/JAD-180300

Niedowicz, D. M., Nelson, P. T., and Murphy, M. P. (2011). Alzheimers disease: pathological mechanisms and recent insights. *Curr. Neuropharmacol.* 9, 674–684. doi: 10.2174/157015911798376181

Nina, B., Florian, H., Habib, B., Ehrensperger Michael, M., Ute, G., Martin, H., et al. (2014). Slowing of EEG background activity in Parkinson's and Alzheimer's disease with early cognitive dysfunction. *Front. Aging Neurosci.* 6:314. doi: 10.3389/fnagi.2014.00314

Noh, G.-J., Kim, K.-M., Jeong, Y.-B., Jeong, S.-W., Yoon, H.-S., Jeong, S.-M., et al. (2006). Electroencephalographic approximate entropy changes in healthy volunteers during remifentanil infusion. *Anesthesiology* 104, 921–932. doi: 10.1097/00000542-200605000-00006

Olichney, J. M., Yang, J.-C., Taylor, J., and Kutas, M. (2011). Cognitive event-related potentials: biomarkers of synaptic dysfunction across the stages of Alzheimer's disease. *J. Alzheimers Dis.* 26, 215–228. doi: 10.3233/JAD-2011-0047

Papaliagkas, V., Kimiskidis, V., Tsolaki, M., and Anogianakis, G. (2008). Usefulness of event-related potentials in the assessment of mild cognitive impairment. *BMC Neurosci.* 9:107. doi: 10.1186/1471-2202-9-107

Pedraza, O., Clark, J. H., O'Bryant, S. E., Smith, G. E., Ivnik, R. J., Graff-Radford, N. R., et al. (2013). Diagnostic validity of age and education corrections for the mini-mental state examination in older african americans. *J. Am. Geriatr. Soc.* 60, 328–331. doi: 10.1111/j.1532-5415.2011.03766.x

Pérez-González, D., and Malmierca, M. S. (2014). Adaptation in the auditory system: an overview. *Front. Integr. Neurosci.* 8:19. doi: 10.3389/fnint.2014.00019

Polich, J., and Kok, A. (1995). Cognitive and biological determinants of P300: an integrative review. *Biol. Psychol.* 41, 103–146. doi: 10.1016/0301-0511(95)05130-9

Pratt, H. (2012). "Sensory ERP components," in *The Oxford Handbook of Event-related Potential Components*, eds E. S. Kappenman and S. J. Luck (New York, NY: Oxford University Press), 1–3.

Qin, H.-Y., Zhao, X.-D., Zhu, B.-G., and Hu, C.-P. (2020). Demographic factors and cognitive function assessments associated with mild cognitive impairment progression for the elderly. *Biomed Res. Int.* 2020:3054373. doi: 10.1155/2020/3054373

R Core Team. (2020). *R: A Language and Environment for Statistical Computing*. Vienna, Austria: R Foundation for Statistical Computing. Available online at: https://www.R-project.org/.

Raicher, I., Yasumasa Takahashi, D., Medeiros Kanda, P. A., Nitrini, R., and Anghinah, R. (2008). QEEG spectral peak in Alzheimer's disease: a possible tool for treatment follow-up. *Dement. Neuropsychol.* 2, 9–12. doi: 10.1590/S1980-57642009DN20100003

Rigters, S. C., Metselaar, M., Wieringa, M. H., Baatenburg de Jong, R. J., Hofman, A., and Goedegebure, A. (2016). Contributing determinants to hearing loss in elderly men and women: results from the population-based rotterdam study. *Audiol. Neurootol.* 21, 10–15. doi: 10.1159/000448348

Robinson, L., Tang, E., and Taylor, J. P. (2015). Dementia: timely diagnosis and early intervention. *BMJ* 350:h3029. doi: 10.1136/bmj.h3029

Rodriguez, G., Arnaldi, D., and Picco, A. (2011). Brain functional network in Alzheimer's disease: diagnostic markers for diagnosis and monitoring. *Int. J. Alzheimers Dis.* 2011:481903. doi: 10.4061/2011/481903

Roh, S.-C., Kim, J. S., Kim, S., Kim, Y., and Lee, S. H. (2020). Frontal α asymmetry moderated by suicidal ideation in patients with major depressive disorder: a comparison with healthy individuals. *Clin. Psychopharmacol. Neurosci.* 18, 58–66. doi: 10.9758/cpn.2020.18.1.58

Rossini, P. M., Buscema, M., Capriotti, M., Grossi, E., Rodriguez, G., Del Percio, C., et al. (2008). Is it possible to automatically distinguish resting EEG data of normal elderly vs. mild cognitive impairment subjects with high degree of accuracy? *Clin. Neurophysiol.* 119, 1534–1545. doi: 10.1016/j.clinph.2008.03.026

Rossini, P. M., Di Iorio, R., Vecchio, F., Anfossi, M., Babiloni, C., Bozzali, M., et al. (2020). Early diagnosis of Alzheimer's disease: the role of biomarkers including advanced EEG signal analysis. report from the IFCN-sponsored panel of experts. *Clin. Neurophysiol.* 131, 1287–1310. doi: 10.1016/j.clinph.2020.03.003

Salisbury, D. F., Rutherford, B., Shenton, M. E., and McCarley, R.-W. (2001). Button-pressing affects P300 amplitude and scalp topography. *Clin. Neurophysiol.* 112, 1676–1684. doi: 10.1016/s1388-2457(01)00607-1

Scazufca, M., Almeida, O. P., Vallada, H. P., Tasse, W. A., and Menezes, P. R. (2009). Limitations of the mini-mental state examination for screening dementia in a community with low socioeconomic status: results from the sao paulo ageingand health study. *Eur. Arch. Psychiatry Clin. Neurosci.* 259, 8–15. doi: 10.1007/s00406-008-0827-6

Schmidt, M. T., Kanda, P. A. M., Basile, L. F. H., da Silva Lopes, H. F., Baratho, R., Demario, J. L. C., et al. (2013). Index of α/theta ratio of the electroencephalogram: a new marker for Alzheimer's disease. *Front. Aging Neurosci.* 5:60. doi: 10.3389/fnagi.2013.00060

Smailovic, U., and Jelic, V. (2019). Neurophysiological markers of Alzheimer's disease: quantitative EEG approach. *Neurol. Ther.* 8, 37–55. doi: 10.1007/s40120-019-00169-0

Sperling, R. A., Aisen, P. S., Beckett, L. A., Bennet, D. A., Craft, S., Fagan, A. M., et al. (2011). Toward defining the preclinical stages of Alzheimer's disease: recommendations from the national institute on aging. *Alzheimers Dement.* 7, 280–292. doi: 10.1016/j.jalz.2011.03.003

Tae, H. K., Jin, H. J., Joon, H. P., Jeong, L. K., Seung, H. R., Seok, W. M., et al. (2010). Korean version of mini mental status examination for dementia screening and its short form. *Psychiatry Investig.* 7, 102–108. doi: 10.4306/pi.2010.7.2.102

Tanaka, F., Kachi, T., Yamada, T., and Sobue, G. (1998). Auditory and visual event-related potentials and flash visual evoked potentials in Alzheimer's disease: correlations with Mini-Mental State Examination and Raven's Coloured Progressive Matrices. *J. Neurol. Sci.* 156, 83–88. doi: 10.1016/s0022-510x(98)00004-5

Thibodeau, R., Jorgensen, R. S., and Kim, S. (2006). Depression, anxiety, and resting frontal EEG asymmetry: a meta-analytic review. *J. Abnorm. Psychol.* 115, 715–729. doi: 10.1037/0021-843X.115.4.715

Tisher, A., and Salardini, A. (2019). A comprehensive update on treatment of dementia. *Semin. Neurol.* 39, 167–178. doi: 10.1055/s-0039-1683408

Tsoi, K. K. F., Chan, J. Y. C., Hirai, H. W., Wong, S. Y. S., and Kwok, T. C. Y. (2015). Cognitive tests to detect dementia a systematic review and meta-analysis. *JAMA Intern. Med.* 175, 1450–1458. doi: 10.1001/jamainternmed.2015.2152

Uhlhaas, P. J., and Singer, W. (2006). Neural synchrony in brain disorders: relevance for cognitive dysfunctions and pathophysiology. *Neuron* 52, 155–168. doi: 10.1016/j.neuron.2006.09.020

van der Vinne, N., Vollebregt, M. A., van Putten, M. J. A. M., and Arns, M. (2017). Frontal α asymmetry as a diagnostic marker in depression: fact or fiction? A meta-analysis. *Neuroimage Clin.* 16, 79–87. doi: 10.1016/j.nicl.2017.07.006

van Deursen, J. A., Vuurman, E. F., Smits, L. L., Verhey, F. R., and Riedel, W. J. (2009). Response speed, contingent negative variation and P300 in Alzheimer's disease and MCI. *Brain Cogn.* 69, 592–599. doi: 10.1016/j.bandc.2008.12.007

van Vliet, M., Manyakov, N. V., Storms, G., Fias, W., Wiersema, J. R., and Van Hulle, M. M. (2014). Response-related potentials during semantic priming: the effect of a speeded button response task on ERPs. *PLoS One* 9:e87650. doi: 10.1371/journal.pone.0087650

Vecchio, F., and Määttä, S. (2011). The use of auditory event-related potentials in Alzheimer's disease diagnosis. *Int. J. Alzheimers Dis.* 2011:653173. doi: 10.4061/2011/653173

Vecchio, F., Lizio, R., Frisoni, G. B., Ferri, R., Rodriguez, G., and Babiloni, C. (2011). Electroencephalographic rhythms in Alzheimer's disease. *Int. J. Alzheimers Dis.* 2011:927573. doi: 10.4061/2011/927573

Williams, P. A., Jones, G. H., Briscoe, M., Thomas, R., and Cronin, P. (1991). P300 and reaction-time measures in senile dementia of the Alzheimer type. *Br. J. Psychiatry* 159, 410–414. doi: 10.1192/bjp.159.3.410

Wong, T. T., and Yeh, P. Y. (2020). Reliable accuracy estimates from K-fold cross validation. *IEEE Trans. Knowl. Data Eng.* 32, 1586–1594. doi: 10.1109/tkde.2019.2912815

Woodman, G. F. (2010). A brief introduction to the use of event-related potentials in studies of perception and attention. *Atten. Percept. Psychophys.* 72, 2031–2046. doi: 10.3758/APP.72.8.2031

World Health Organization. (1992). *International Statistical Classification of Diseases and Related Health. Problems*. 10th Edn. World Health Organization.

World Health Organization. (2020). *Dementia*. World Health Organization. Available online at: https://www.who.int/news-room/fact-sheets/detail/dementia.

Wright, M. N., Wager, S., and Probst, P. (2020). *Ranger: A Fast Implementation of Random Forests*. Available online at: https://CRAN.R-project.org/package=ranger.

Yener, G. G., and Başar, E. (2010). Sensory evoked and event related oscillations in Alzheimer's disease: a short review. *Cogn. Neurodyn.* 4, 263–274. doi: 10.1007/s11571-010-9138-5

Zvěřová, M. (2018). Alzheimer's disease and blood-based biomarkers—potential contexts of use. *Neuropsychiatr. Dis. Treat.* 14, 1877–1882. doi: 10.1016/j.clnu.2021.02.024

Conflict of Interest: The authors declare that the research was conducted in the absence of any commercial or financial relationships that could be construed as a potential conflict of interest.

APPENDIX

TABLE A1 | Estimated odds ratios and 95% confidence intervals derived from three logistic regression models.

		Unadjusted		Adjusted		Adjusted (including MMSE)	
		OR (95% CI)	**Wald Z (p-value)**	**OR (95% CI)**	**Wald Z (p-value)**	**OR (95% CI)**	**Wald Z (p-value)**
Resting state EEG							
	Alpha (avg.) [μV^2]	0.615 (0.40, 0.93)	−2.26 (2.39E−02)	0.693 (0.42, 1.12)	−1.47 (1.41E−01)	0.747 (0.43, 1.26)	−1.08 (2.80E−01)
	Alpha/Theta	0.289 (0.16, 0.49)	−4.39 (1.14E−05)	0.474 (0.24, 0.87)	−2.33 (1.99E−02)	0.630 (0.32, 1.21)	−1.36 (1.75E−01)
	Beta (avg.) [μV^2]	1.355 (0.91, 2.05)	1.49 (1.37E−01)	1.186 (0.74, 1.92)	0.71 (4.76E−01)	1.204 (0.72, 2.04)	0.71 (4.78E−01)
	Frontal asymmetry	0.546 (0.34, 0.83)	−2.68 (7.47E−03)	0.516 (0.30, 0.82)	−2.58 (9.75E−03)	0.535 (0.30, 0.87)	−2.29 (2.21E−02)
	Peak frequency [Hz]	0.255 (0.14, 0.42)	−5.01 (5.58E−07)	0.387 (0.20, 0.69)	−3.07 (2.11E−03)	0.460 (0.24, 0.83)	−2.50 (1.26E−02)
	MEF [Hz]	0.285 (0.17, 0.45)	−4.97 (6.64E−07)	0.387 (0.21, 0.68)	−3.19 (1.40E−03)	0.555 (0.28, 1.06)	−1.76 (7.79E−02)
	Peak power [μV^2]	0.969 (0.61, 1.42)	−0.15 (8.79E−01)	0.868 (0.48, 1.45)	−0.51 (6.13E−01)	0.842 (0.46, 1.43)	−0.60 (5.52E−01)
	Theta (avg.) [μV^2]	1.699 (1.14, 2.60)	2.54 (1.09E−02)	1.143 (0.70, 1.89)	0.53 (5.94E−01)	0.952 (0.55, 1.65)	−0.18 (8.60E−01)
Sensory ERP							
	Amplitude (deviation) [μV]	1.459 (0.99, 2.19)	1.88 (5.95E−02)	1.282 (0.80, 2.12)	1.01 (3.13E−01)	1.213 (0.71, 2.07)	0.72 (4.72E−01)
	Amplitude (edge−center ratio)	1.094 (0.74, 1.63)	0.45 (6.56E−01)	0.903 (0.57, 1.43)	−0.44 (6.61E−01)	0.884 (0.53, 1.47)	−0.48 (6.33E−01)
	Amplitude [μV]	0.931 (0.62, 1.38)	−0.35 (7.24E−01)	0.875 (0.54, 1.40)	−0.56 (5.78E−01)	0.768 (0.44, 1.30)	−0.97 (3.32E−01)
	Response time (deviation) [ms]	1.424 (0.97, 2.11)	1.79 (7.32E−02)	1.538 (0.95, 2.51)	1.75 (7.96E−02)	1.292 (0.76, 2.17)	0.96 (3.35E−01)
	Response time [ms]	1.967 (1.32, 3.01)	3.23 (1.25E−03)	2.109 (1.31, 3.56)	2.96 (3.09E−03)	1.892 (1.15, 3.26)	2.42 (1.55E−02)
Attention ERP							
	# of correct	0.521 (0.34, 0.77)	−3.18 (1.46E−03)	0.711 (0.45, 1.10)	−1.54 (1.24E−01)	1.106 (0.65, 1.97)	0.36 (7.19E−01)
	Amp (resp) − Amp (bg) [μV]	0.349 (0.13, 0.75)	−2.33 (1.96E−02)	0.626 (0.23, 1.20)	−1.13 (2.59E−01)	0.844 (0.32, 1.57)	−0.43 (6.70E−01)
	Resp. Time [s]	2.130 (1.42, 3.32)	3.53 (4.21E−04)	1.593 (1.01, 2.59)	1.96 (5.04E−02)	1.408 (0.86, 2.34)	1.36 (1.74E−01)
	wER	2.364 (1.59, 3.66)	4.09 (4.31E−05)	1.533 (0.95, 2.51)	1.75 (8.02E−02)	0.950 (0.52, 1.69)	−0.17 (8.61E−01)

*The table shows the exact values for **Figure 4**. Due to the small sample size in this study, the covariates related to the disease status (e.g., hypertension, diabetes, and so on) were not included in the multiple logistic regression model. OR (95% CI), Odds ratios with 95% confident interval; Wald Z (p-value), P-value obtains from Wald test.*

frontiers in Aging Neuroscience

ORIGINAL RESEARCH
published: 29 July 2021
doi: 10.3389/fnagi.2021.696174

Exploring the Interactions Between Neurophysiology and Cognitive and Behavioral Changes Induced by a Non-pharmacological Treatment: A Network Approach

Víctor Rodríguez-González[1], Carlos Gómez[1,2], Hideyuki Hoshi[3], Yoshihito Shigihara[3], Roberto Hornero[1,2,4] and Jesús Poza[1,2,4]*

[1]Biomedical Engineering Group, Universidad de Valladolid, Valladolid, Spain, [2]Centro de Investigación Biomédica en Red en Bioingeniería, Biomateriales y Nanomedicina (CIBER-BBN), Madrid, Spain, [3]Precision Medicine Centre, Hokuto Hospital, Obihiro, Japan, [4]IMUVA, Instituto de Investigación en Matemáticas, Universidad de Valladolid, Valladolid, Spain

OPEN ACCESS

Edited by:
Priyanka Shah-Basak, Medical College of Wisconsin, United States

Reviewed by:
Laura Lorenzo-López, University of A Coruña, Spain
Dianne Patterson, University of Arizona, United States

***Correspondence:**
Víctor Rodríguez-González
victor.rodriguez@gib.tel.uva.es

Received: *16 April 2021*
Accepted: *13 July 2021*
Published: *29 July 2021*

Citation:
Rodríguez-González V, Gómez C, Hoshi H, Shigihara Y, Hornero R and Poza J (2021) Exploring the Interactions Between Neurophysiology and Cognitive and Behavioral Changes Induced by a Non-pharmacological Treatment: A Network Approach. Front. Aging Neurosci. 13:696174. doi: 10.3389/fnagi.2021.696174

Dementia due to Alzheimer's disease (AD) is a neurological syndrome which has an increasing impact on society, provoking behavioral, cognitive, and functional impairments. AD lacks an effective pharmacological intervention; thereby, non-pharmacological treatments (NPTs) play an important role, as they have been proven to ameliorate AD symptoms. Nevertheless, results associated with NPTs are patient-dependent, and new tools are needed to predict their outcome and to improve their effectiveness. In the present study, 19 patients with AD underwent an NPT for 83.1 ± 38.9 days (mean ± standard deviation). The NPT was a personalized intervention with physical, cognitive, and memory stimulation. The magnetoencephalographic activity was recorded at the beginning and at the end of the NPT to evaluate the neurophysiological state of each patient. Additionally, the cognitive (assessed by means of the Mini-Mental State Examination, MMSE) and behavioral (assessed in terms of the Dementia Behavior Disturbance Scale, DBD-13) status were collected before and after the NPT. We analyzed the interactions between cognitive, behavioral, and neurophysiological data by generating diverse association networks, able to intuitively characterize the relationships between variables of a different nature. Our results suggest that the NPT remarkably changed the structure of the association network, reinforcing the interactions between the DBD-13 and the neurophysiological parameters. We also found that the changes in cognition and behavior are related to the changes in spectral-based neurophysiological parameters. Furthermore, our results support the idea that MEG-derived parameters can predict NPT outcome; specifically, a lesser degree of AD neurophysiological alterations (i.e., neural oscillatory slowing, decreased variety of spectral components, and increased neural signal regularity) predicts a better

NPT prognosis. This study provides deeper insights into the relationships between neurophysiology and both, cognitive and behavioral status, proving the potential of network-based methodology as a tool to further understand the complex interactions elicited by NPTs.

Keywords: non-pharmacological treatment (NPT), Mini-Mental State Examination (MMSE), Dementia Behavior Disturbance Scale (DBD-13), magnetoencephalography (MEG), networks, predict

INTRODUCTION

Dementia is a neurological syndrome that induces cognitive, behavioral, and functional alterations (Cummings, 2003). It is estimated that, in 2019, about 50 million people suffered from dementia worldwide, and this number is expected to increase to 132 million in 2050 (Alzheimer's Disease International, 2019). Furthermore, its global economic impact is currently estimated at $1 trillion, and it is expected to be doubled by 2030 (Alzheimer's Disease International, 2019). Alzheimer's disease (AD) is the most common cause of dementia, with an exponentially growing incidence, especially in developed countries, due to the increase in life expectancy (Alzheimer's Association, 2019). These figures show that AD is becoming a problem of utmost importance, highlighting the need to develop new treatments to help ameliorate the increasing impact of AD.

Some pharmacological treatments for AD have been developed over the past few years (Alzheimer's Disease International, 2019). Nonetheless, their effectiveness to mitigate dementia symptoms is very limited and patient-dependent and, in addition, they are often expensive (Qaseem et al., 2008; Alzheimer's Association, 2019; Alzheimer's Disease International, 2019). On the other hand, non-pharmacological treatments (NPTs) are showing promising results when dealing with AD-related cognitive alterations (Zucchella et al., 2018; Alzheimer's Association, 2019). NPTs include a wide variety of strategies, ranging from physical training to cognitive stimulation, through psychological therapy (Dyer et al., 2018). As pharmacological therapies, they are not able to repair or stop the neuronal death caused by AD, but they are beneficial to patients with the disease (Dyer et al., 2018; Alzheimer's Association, 2019). NPTs have been proven to effectively treat behavioral and psychological dementia symptoms, as well as to improve cognitive function and scores in depression tests (Oliveira et al., 2015; Dyer et al., 2018; Alzheimer's Association, 2019). Therefore, NPTs are recommended as first-line managers to cope with behavioral and psychological symptoms of dementia, as they do not have adverse effects (Dyer et al., 2018). Nonetheless, their effectiveness has been shown to be patient-dependent (Kurz et al., 2011; Maki et al., 2018; Alzheimer's Association, 2019). Many factors could influence the outcome of NPTs, such as previous cognitive level, symptom severity, or anti-psychotic use, but their impact is still unclear (Hsu et al., 2017). Therefore, being able to *a-priori* predict NPT outcome is a problem of paramount importance, since it would lead to personalized treatments and, consequently, to increased treatment efficiency.

Neuroimaging techniques could be useful in this regard. They record neuronal activity on different levels, providing a quantitative framework to assess NPT influence on higher cognitive functions. Resting-state electroencephalography (EEG) and magnetoencephalography (MEG) have already been proven to be sensitive to changes induced by NPTs in brain activity (Amjad et al., 2019; Shigihara et al., 2020a,b), as well as to be potential predictors of NPT outcome (Amjad et al., 2019; Shigihara et al., 2020a,b). Both EEG and MEG are noninvasive neurophysiological techniques, though only MEG provides simultaneously high spatial and temporal resolution, as well as low distortion of scalp recordings due to the resistive properties of brain structures (Babiloni et al., 2009). MEG records brain activity in the range of milliseconds, which is of paramount importance to understand the function of a dynamic system like the brain (Babiloni et al., 2009). MEG recordings, and specifically resting-state signals, are often analyzed in patients with AD because they are able to detect the subtle changes that the disease provokes in neural activity (Engels et al., 2017; Mandal et al., 2018). Likewise, as previously mentioned, past studies found individual correlations between MEG-based parameters in specific brain regions and both, cognitive and behavioral variations due to NPTs (Amjad et al., 2019; Shigihara et al., 2020a,b). These results support the potential of MEG to quantify the effects of these therapeutic interventions. In the current research, we propose to further explore the complex interactions between the diverse variables under study by means of a network-related framework, which enables us to glimpse the footprint of the therapy in neural signals in a comprehensive and intuitive way. This approach is based on the generation of the so-called "association networks" that simplify the interpretation of the complex interactions between variables of diverse nature (Borsboom and Cramer, 2013; Fornito et al., 2016; Borsboom, 2017). Association networks are increasingly used as a tool for conceptualizing the interactions between symptoms in mental disorders, given their ability to capture all the intriguing complexity of these pathologies (Borsboom and Cramer, 2013; Borsboom, 2017). To the best of our knowledge, this is the first time that a network framework has been applied to assess the complex associations due to an NPT between neurophysiology, cognition, and behavior in AD. This framework provides a powerful tool to analyze the impact of NPT on neurophysiological signals and its potential predictors in a simple and integrated way.

In this work, we hypothesize that NPT elicits several changes in different cognitive and behavioral dimensions, which in turn modify functional brain activity. The relationships between brain function and higher-order capacities are governed by a complex pattern of interactions between neurophysiological, cognitive, and behavioral variables. Consequently, new methodological

approaches are needed to identify the changes in oscillatory brain activity that could be used to quantitatively assess NPT outcomes and, eventually, to design personalized therapeutic interventions. To address these issues, 19 patients with AD went through an NPT. Resting-state MEG activity, cognitive state, and behavioral status were evaluated at the beginning and end of the NPT. Different spectral and non-linear parameters of the MEG recordings were calculated to evaluate their interactions with the NPT outcome, which was measured by means of cognitive and behavioral tests. Specifically, we will address the following research questions: (i) are the association networks able to reflect the influence of the NPT on the relationships between neurophysiological and cognitive/behavioral variables?; (ii) what are the particular changes in the structure of the association networks due to the NPT?; and (iii) can the neurophysiological parameters predict the cognitive and behavioral changes associated with the NPT?

MATERIALS AND METHODS

Participants

Nineteen patients with dementia from the geriatric health services facility "Kakehashi" (Obihiro, Japan) were recruited for this study. It is an official facility authorized by the Ministry of Health, Labor, and Welfare in Japan, recognized as a transient facility between hospitals and patients' homes. The main role of this facility is to improve the physical and cognitive conditions of aged individuals to enable them to return to their homes. All the participants were diagnosed with AD, and two of them were also diagnosed with other pathologies: one with Parkinson's disease, and the other one with vascular dementia. The diagnoses were carried out by clinicians before admission in the "Kakehashi" facility, and according to the National Institute on Aging-Alzheimer's Association criteria (McKhann et al., 2011). If possible, patients' medication remained unchanged during the NPT period.

Patients underwent the NPT for 83.1 ± 38.9 days (mean ± standard deviation, see **Figure 1** for a graphical description of the NPT period), being treated every day by the NPT professionals. NPT is composed of five types of activities commonly used in geriatric health services facilities in Japan:

1. **Physical training**. It is aerobic exercise and resistance training, which are effective to improve cognitive function in aged individuals (Nagamatsu et al., 2012; Amjad et al., 2019).
2. **Therapeutic role-playing**. This therapeutic intervention is called "Otona-no-gakko" ("School for adults") and it is used to both re-introduce patients to active life and enhance their daily motivation (Cotelli et al., 2012).
3. **Nursing care**. Nursing care provides proper eating, drinking, and a sanitary environment, which are essential to keep brain activity healthy. Furthermore, it has been previously suggested that diet has some relevant impact on AD (Rege et al., 2016; McGrattan et al., 2019).
4. **Horticultural therapy**. This therapy is based on gardening and planting activities to improve physical and cognitive conditions (Lu et al., 2020). Patients were familiar with these activities since our facility is located in an agricultural area.
5. **Self-cognitive training**. Self-cognitive training includes activities such as coloring books or crossword puzzles (Anderson and Grossberg, 2014).

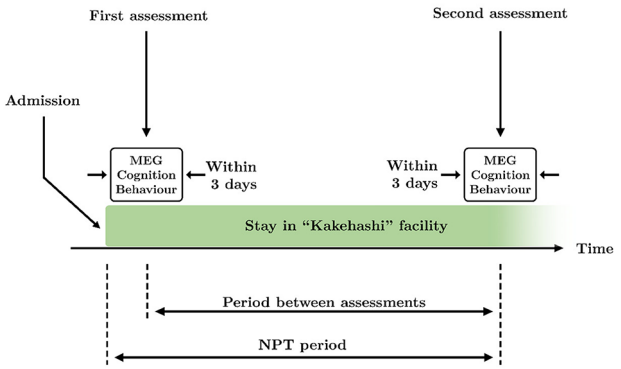

FIGURE 1 | Schematic overview of the time course of the study. Two assessments took place during the study: at the beginning and the end of the therapy. Each assessment consisted of MEG recording and application of Mini-Mental State Examination (MMSE) and Dementia Behavior Disturbance (DBD)-13 tests, that were performed within 3 days. The period between assessments is defined as the time between the first and the second assessments. The non-pharmacological treatment (NPT) period is defined as the time between the admission in the facility and the second assessment.

TABLE 1 | Sociodemographic and clinical information of the sample.

Sociodemographic data		
Number of subjects	19	
Age (years)	86.00 ± 3.86	
Gender (M:F)	7:12	
NPT Period (days)	83.05 ± 38.88	
	Pre	**Post**
MMSE	14.11 ± 5.95	16.00 ± 7.32
DBD-13	10.89 ± 9.93	9.84 ± 10.55

Data are shown as mean ± standard deviation. M, male; F, female; MMSE, Mini-Mental State Examination; DBD-13, Dementia Behavior Disturbance scale.

Each NPT session was designed each day by the experts to adapt it to the clinical features and mood of each patient (Maki et al., 2018), with a duration ranging from 20 to 40 min, according to the Japanese regulations. See **Table 1** for a description of the sociodemographic and clinical information of the sample.

All participants and their families or caregivers gave their informed consent to participate in the present study. The investigation was carried out in accordance with the Code of Ethics of the World Medical Association (Declaration of Helsinki). The protocol was approved by the Ethics Committee of Hokuto Hospital.

Cognitive and Behavioral Assessment

Cognitive and behavioral performance was assessed twice for each patient, at the beginning and at the end of the NPT. Each assessment session consisted of two different tests conducted on the same day: an abbreviated version of the Dementia

Behavior Disturbance Scale (DBD-13; Machida, 2012), and the Japanese Mini-Mental State Examination (MMSE; Folstein et al., 1975; Sugishita et al., 2010). The DBD-13 scale is a 52-point test consisting of 13 items of the original DBD-28 scale (Baumgarten et al., 1990; Machida, 2012). It measures the behavioral disturbance induced by dementia, assigning higher values to more behavior problems. The MMSE is a test with a maximum score of 30, which measures cognitive impairment by assessing different cognitive domains (Folstein et al., 1975; Sugishita et al., 2010). Lower values correspond to more impaired cognition.

MEG Recordings

All MEG recordings were acquired at the Hokuto Hospital (Obihiro, Japan). As for the cognitive and behavioral assessments, brain signals were recorded twice: at the beginning and end of the treatment. MEG recordings, cognitive state, and behavioral status were evaluated within 3 days in order to: (i) accurately match each MEG recording with a cognitive and behavioral assessment; and (ii) make the intervals between MEG recordings and both cognitive and behavioral assessments as similar as possible. Thereby, 76.1 ± 36.0 days (mean ± standard deviation) passed between the initial and final assessments. See **Figure 1** for a graphical description of the period between assessments.

For each subject, 5 min of resting-state brain activity was recorded using a 160-channel axial gradiometers MEG system (MEG Vision PQ1160C, Yokogawa Electric), with a sampling rate of 1,000 Hz and a low-pass filter at 200 Hz. Head position was registered with three fiducial markers placed on the patient's head during the MEG scan: 5 mm above the nasion, and 10 mm in front of the tragus on each side of the head. Patients were asked to stay calm and awake with eyes closed, in a supine position during the recording. For security reasons, as well as to prevent somnolence, MEG recordings were monitored in real time.

MEG Analysis

Signals were preprocessed before the application of the source inversion algorithm. Next, different spectral and non-linear local activation parameters were calculated from the signals at the source level. Finally, these parameters were used to construct the networks based on the Spearman correlations between them. The next subsections describe the steps followed in the MEG analysis in detail.

Preprocessing of MEG Signals

To limit the presence of noise in the MEG recordings, signals were preprocessed using a 4-step pipeline (Rodríguez-González et al., 2020): (i) artifact removal using the SOUND algorithm (Mutanen et al., 2018; Rodríguez-González et al., 2019); (ii) finite impulse response (FIR) filtering: 1–70 Hz band-pass to limit noise bandwidth, and 49–51 Hz band-stop to remove line noise; (iii) artifact removal using independent component analysis; and (iv) visual selection of 5-s artifact-free epochs.

Source Inversion

Source-level signals were obtained using the Brainstorm toolbox, which is documented and freely available for download online under the GNU general public license[1] (Tadel et al., 2011). A forward model with 15,000 sources was created by means of boundary element model using the ICBM152 head template (Montreal Neurological Institute) and OpenMEEG software (Fonov et al., 2009; Gramfort et al., 2010; Douw et al., 2018). The head model was segmented into three tissues: brain, skull, and scalp, with conductivities of 1, 0.0125, and 1 Siemens per meter, respectively (Mahjoory et al., 2017). Sources were restricted to the cortex, and their direction was set normal to it (Mahjoory et al., 2017; Lai et al., 2018; Rodríguez-González et al., 2020). No noise recordings were available, so an identity matrix was used as noise covariance (Lai et al., 2018; Rodríguez-González et al., 2020). The 15,000 source-level time courses were projected into the 68 regions of interest (ROIs) provided by the Desikan-Killiany atlas, in order to have a manageable number of ROIs to work with Desikan et al. (2006), Lai et al. (2018), and Rodríguez-González et al. (2020). This source projection was done by averaging the reconstructed activation time courses of all the voxels in each ROI after flipping the sources of opposite direction (Lai et al., 2018; Rodríguez-González et al., 2020).

As, we were working with resting-state signals, no *a-priori* assumptions about sources could be made. Thus, we used the weighted minimum-norm estimation (wMNE) algorithm, which restricts the solutions by minimizing the energy (L_2 norm) weighting deep sources to facilitate their identification (Lin et al., 2004). This method has been proven to be useful to reconstruct the underlying sources of resting-state MEG datasets (Lin et al., 2004).

Feature Extraction

Diverse signal processing methods have been widely used to describe the properties of brain activity. These methods characterize the electromagnetic fields generated by the synchronized neuronal pools responsible for the observed brain activity. In this study, we have used several local activation parameters, which measure the activation of single functional units (i.e., synchronized neuronal pools; Stam and van Straaten, 2012) They can be grouped in two main categories: (i) spectral parameters, which evaluate the time-frequency content of the recorded signal; and (ii) non-linear parameters, which measure relevant non-linear properties of the signal, such as variability, irregularity, or complexity. In this study, we have calculated a wide variety of parameters in both categories to fully characterize the properties of the resting-state MEG activity using its source reconstructed time courses on the 68 estimated ROIs.

Spectral Parameters

They are useful to characterize the spectral content of the signal. They were derived from the normalized power spectral density (PSDn), which was calculated using the Blackman-Tuckey method (Blackman and Tukey, 1958; Ruiz-Gómez et al., 2018; Rodríguez-González et al., 2020). The parameters computed in this category are listed below:

- **Relative power (RP)**. It summarizes the neural activation in a certain frequency range, relative to the full spectral content of

[1] http://neuroimage.usc.edu/brainstorm

the signal. RP was calculated in the well-known conventional frequency bands: delta (δ, 1–4 Hz), theta (θ, 4–8 Hz), alpha (α, 8–13 Hz), beta 1 (β_1, 13–19 Hz), beta 2 (β_2, 19–30 Hz), and gamma (γ, 30–70 Hz).

- **Median frequency (MF)**. MF is the frequency that divides the PSDn into two halves of equal power. It is commonly used to measure the global signal slowing provoked by AD disruptions (Poza et al., 2007; Dauwels et al., 2011).
- **Individual alpha frequency (IAF)**. It measures the frequency where the alpha peak can be found. It is calculated as the frequency that divides the extended alpha band (4–15 Hz) into two halves of equal power (Klimesch, 1999; Poza et al., 2007). Alpha peak is related to higher cognitive functions, so this parameter is widely used to assess cognitive disfunction (Klimesch, 1999; Poza et al., 2007).
- **Spectral entropy (SE)**. This parameter measures the flatness or uniformity of the PSDn using Shannon entropy. It has been proven that patients with AD show a less distributed spectral content of the PSDn than controls, which suggests less variety of neural oscillatory components (Poza et al., 2008b; Gómez and Hornero, 2010).
- **Spectral edge frequency (SEF)**. It is quantified as the upper limit of the PSDn. This parameter is calculated as the frequency that comprises 95% of the power of the PSDn, and is identified as the bandwidth of the signal (Poza et al., 2007). Due to the slowing and the reduction in the variety of neural oscillatory activity associated with AD, this parameter has been used to characterize brain signals in patients with dementia (Poza et al., 2007).

Non-linear Parameters

Non-linearity is a fundamental property of complex systems, such as the brain (Stam, 2005). Non-linear analyses of brain signals are then commonly used to describe the alterations produced by a neuropathology like AD. The non-linear parameters assessed in this study are:

- **Lempel-Ziv complexity (LZC)**. It is a coarse-grain complexity measure. LZC estimates the complexity by counting the number of subsequences that the binarized version of the analyzed signal contains (Lempel and Ziv, 1976). It assigns higher values to more complex time series (Fernández et al., 2010, 2011). A decrease in complexity has been associated with AD progression (Gómez et al., 2006; Fernández et al., 2010).
- **Sample entropy (SampEn)**. SampEn is an irregularity measure that assigns higher values to more irregular time sequences. It has two tuning parameters: the sequence length and the tolerance, which were respectively set to 1 and 0.25·std (std: standard deviation of the signal) based on previous studies (Gómez et al., 2009; Hornero et al., 2009; Rodríguez-González et al., 2020). A decrease in irregularity has been observed in the neural activity of patients with AD (Escudero et al., 2009; Gómez et al., 2009; Hornero et al., 2009).
- **Central tendency measure (CTM)**. This parameter is useful to quantify the variability of a signal. It is based on calculating the second-order differences diagram of the time series and then counting the points within a radius. In the present study, the radius has been set to 0.025, based on previous analyses (Ruiz-Gómez et al., 2018; Rodríguez-González et al., 2020). CTM assigns higher values to less variable signals. Previous studies have reported that AD is associated with lower CTM values (Ruiz-Gómez et al., 2018).

In addition to the spectral and non-linear parameters, a new measure is presented in the current study: the spatial Shannon entropy (SSE). Specifically, the SSE computes the entropy of the spatial distribution of values for a given local activation parameter. The spatial distribution of the considered parameter is estimated as the normalized histogram of its values considering the 68 ROIs. The calculation of the SSE of a local activation parameter enables us to quantify the changes induced by the NPT in the spatial patterns of brain oscillatory activity. A parameter with similar values across the brain (i.e., showing a delta-like distribution of values) would yield a low SSE value, whereas a high SSE value would be obtained by a parameter with a wide range of variation (i.e., displaying a uniform distribution). It is noteworthy that in the previous examples the parameters could have similar mean values, but their SSE values would be different. Hence, the SSE was computed for each spectral and non-linear parameter; the SSE of a given parameter will be referred to as S with the parameter name in brackets, e.g., the SSE of the IAF will be denoted as S(IAF).

Construction of Association Networks

In this study, we have generated different networks to account for the potential relationships between the neurophysiological, cognitive, and behavioral parameters. Thereby, the network nodes were individual variables (all the neurophysiological parameters, the score in the cognitive examination—i.e., MMSE–, and the score in the behavioral test—i.e., DBD-13), and the network edges (or weights) were the associations between them. These associations were estimated as the Spearman rank correlations between pairs of variables to detect both linear and non-linear monotonic interactions; age and gender were introduced in the correlation analysis as covariates to control for their effect. Non-significant correlations (i.e., network edges with p-values > 0.05) were removed from the network (Zhang, 2011; Barberán et al., 2012). For the sake of simplicity, negative correlations were converted to positive, as we were interested in the association, and not in the nature of that association. Afterward, networks were constructed using Gephi software[2]. The width of the edges was linked to the magnitude of the relationship, with a wider edge meaning stronger association. The Force Atlas 2 algorithm was employed to group nodes with higher correlations while taking nodes with lower correlations away (Jacomy et al., 2014). No regularization algorithm was applied, as we were interested in exploring all the associations, especially those of cognitive and behavioral parameters, even if they are weaker than others.

[2]https://gephi.org/

Four different associations networks were generated:

- **Pre-NPT network**. The nodes were the neurophysiological, cognitive, and behavioral parameters obtained before the application of the NPT.
- **Post-NPT network**. The nodes were the neurophysiological, cognitive, and behavioral parameters obtained after the application of the NPT.
- **Changes network**. The nodes were the variation of neurophysiological, cognitive, and behavioral parameters during the NPT, i.e., the difference between their values before and after the NPT.
- **Prediction network**. The nodes were the neurophysiological parameters before the application of the NPT, and the variation of the cognitive and behavioral parameters during the NPT.

Furthermore, networks stability was analyzed. To do that, the probability of obtaining similar results was assessed by using a bootstrapping methodology with 2,000 iterations to generate new random network instances (Efron, 1992; Epskamp et al., 2018). In each iteration, a new network is created by randomly selecting 19 subjects of the original dataset, being possible to select the same subject more than once (Efron, 1992). From the four bootstrapped instances (one for each network), the 95% confidence interval of the edges' weights was reported (Jimeno et al., 2020).

Another network was generated using the bootstrapped samples from Pre-NPT and Post-NPT networks: the **Variability network**. This network shows the differences in the association pattern between Pre-NPT and Post-NPT. Each network edge from the Variability network was computed as the test statistic obtained when comparing the bootstrapped samples from Pre-NPT and Post-NPT networks for that particular edge. Thus, the higher the edge weight in the Variability network, the higher the differences between Pre-NPT and Post-NPT networks. Although all the edge weights were statistically significant (p-values < 0.05, Wilcoxon signed rank test), only the 5% strongest connections (i.e., showing the biggest differences between Pre-NPT and Post-NPT networks) were displayed.

RESULTS

Changes in Cognition and Behavior Induced by the NPT

The average MMSE value before conducting the NPT was 14.11 ± 5.95 (mean ± SD), while the average for DBD-13 was 10.89 ± 9.93. Then, after applying the NPT, the average value for the MMSE was 16.00 ± 7.32, and the average for DBD-13 9.84 ± 10.55. The effectiveness of the NPT was assessed by comparing the MMSE and DBD-13 before and after conducting the NPT. Both, MMSE and DBD-13 show a statistically significant improvement after the NPT, with MMSE significantly increasing (p-value = 0.0323, one-tailed Wilcoxon signed rank test) and DBD-13 significantly decreasing (p-value = 0.007, one-tailed Wilcoxon signed rank test).

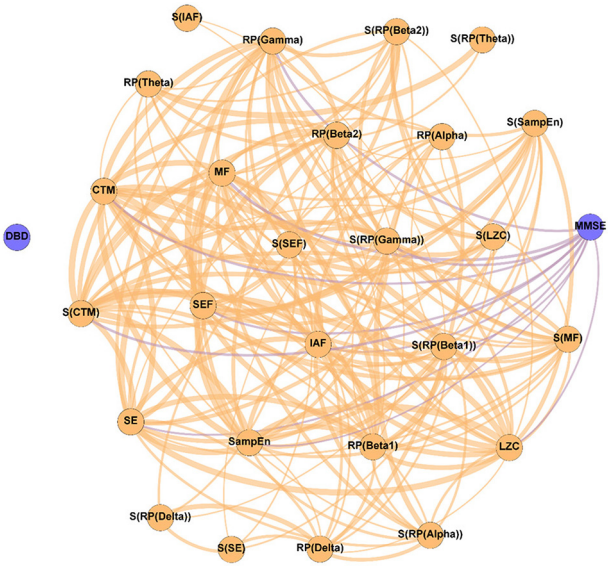

FIGURE 2 | Parameter network of the patients with Alzheimer's disease (AD) before the NPT (Pre-NPT network). Wider edges correspond with stronger associations. Nodes corresponding to cognitive and behavioral parameters are shown in blue, while nodes of neurophysiological parameters are shown in orange.

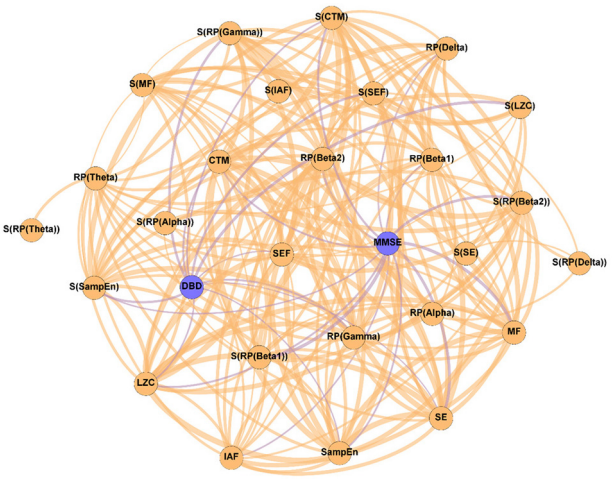

FIGURE 3 | Parameter network of the patients with AD after the NPT (Post-NPT network). Wider edges correspond with stronger associations. Nodes corresponding to cognitive and behavioral parameters are shown in blue, while nodes of neurophysiological parameters are shown in orange.

Changes in Network Structure Induced by the NPT

In order to evaluate the changes induced by the NPT in the patients' network structure, three different networks were evaluated: (i) Pre-NPT network (**Figure 2**); (ii) Post-NPT network (**Figure 3**); and (iii) Variability network (**Figure 4**). The figures depicting the stability of the networks shown in **Figures 2**, **3** can be found in the **Supplementary Figures 1, 2**.

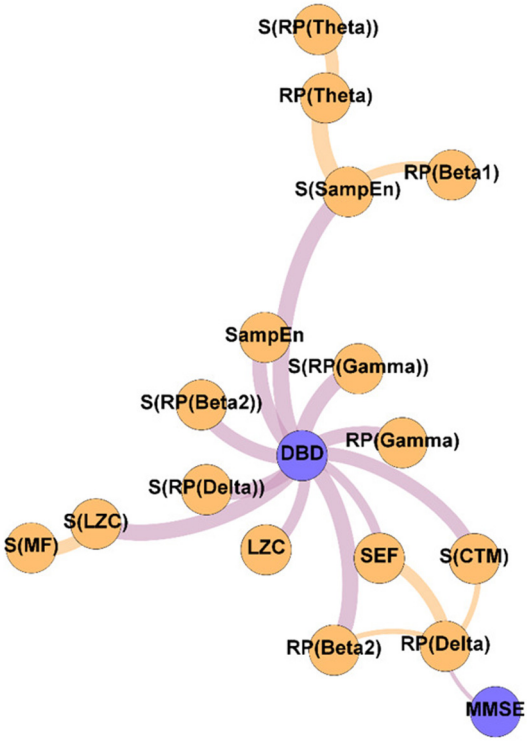

FIGURE 4 | Variability network, showing the 5% strongest connections corresponding to the network edges that obtained the most significant differences between Pre-NPT and Post-NPT networks. Wider edges correspond with stronger associations. Nodes corresponding to cognitive and behavioral parameters are shown in blue, while nodes of neurophysiological parameters are shown in orange.

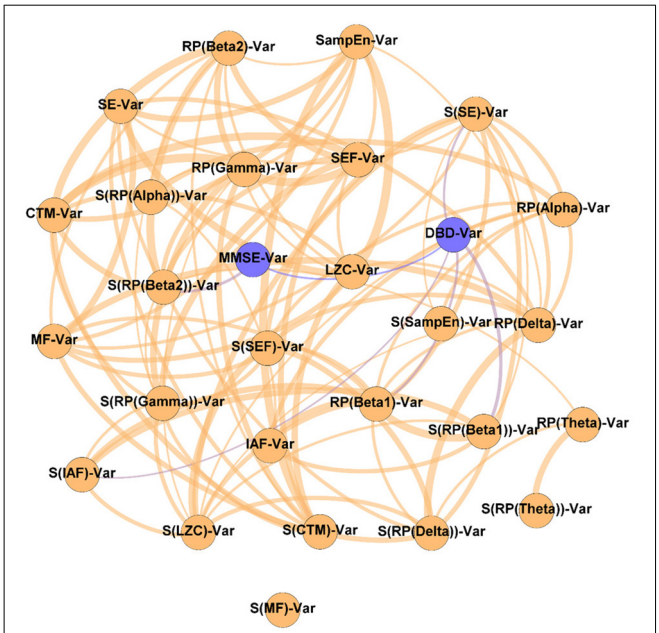

FIGURE 5 | Network of changes. As indicated by the "Var" suffix, this network displays the relationships between the variation of the parameters under study during the NPT (i.e., $Parameter_{Post} - Parameter_{Pre}$). Wider edges correspond with stronger associations. Nodes corresponding to cognitive and behavioral parameters are shown in blue, while nodes of neurophysiological parameters are shown in orange.

Figure 2 displays the relationships between the parameters under study without the influence of the NPT, as they were calculated with the samples obtained at the beginning of the therapeutic intervention. It can be observed that while DBD-13 is disconnected (i.e., it has no relationship with any other parameter), MMSE is related with another 11 parameters: RP(Gamma), MF, IAF, SE, SEF, LZC, SampEn, CTM, S(RP(Gamma)), S(RP(Beta 1)), and S(CTM). Interestingly, no associations were observed for any RP parameter apart from RP(Gamma).

On the other hand, **Figure 3** shows the association network, but including the influence of the NPT, as it has been calculated with the parameters obtained after conducting the NPT. The Post-NPT network has a higher number of connections on cognitive and behavioral parameters in comparison with the Pre-NPT network: MMSE now has 13 connections, while DBD-13 has 11. Of note, eight out of the 13 associations of MMSE were maintained from the Pre-NPT network (MF, IAF, SE, LZC, SampEn, CTM, S(RP(Beta 1)), and S(CTM)), while the other five were new associations (RP(Delta), RP(Beta 1), RP(Beta 2), S(RP(Beta 2)), and S(SampEn)). In contrast to the Pre-NPT network, three parameters based on RP are now associated with the MMSE, but RP(Gamma) is no longer significant. Furthermore, the significant relationships for DBD-13 that can be appreciated in the Post-NPT network are with: RP(Gamma), SE, SEF, LZC, SampEn, CTM, S(RP(Gamma)), S(SEF), S(LZC), S(SampEn), and S(CTM).

To get deeper insights on the changes induced by the NPT in the parameter network, the Variability network was constructed, depicting the 5% strongest differences between Pre-NPT and Post-NPT networks (**Figure 4**). As expected, the parameter whose relationships have changed most between both networks is DBD-13, with 11 connections, while MMSE only showed one connection. Interestingly, six out of those 11 connections (S(RP(Delta), S(RP(Beta 2)), S(RP(Gamma)), S(LZC), S(SampEn), and S(CTM)) are spatial entropies.

Relationship Between Neurophysiological and Cognitive and Behavioral Changes

The network of changes can be observed in **Figure 5**. This network describes the associations between the variation of the parameters under study (neurophysiological, cognitive, and behavioral) by computing: $Parameter_{Post} - Parameter_{Pre}$. A positive value indicates an increase in the parameter provoked by the NPT, while a negative value is associated with a decrease. The figure showing the stability of the network depicted in **Figure 5** can be found in the **Supplementary Figure 3**.

It could be observed that apart from the DBD-13 - MMSE relationship, DBD-13 displays four connections RP(Beta 1), S(IAF), S(SE), and S(RP(Beta 1)), while MMSE only one S(RP(Beta 2)). Interestingly, four out of five significant associations involve spatial entropies: S(RP(Beta

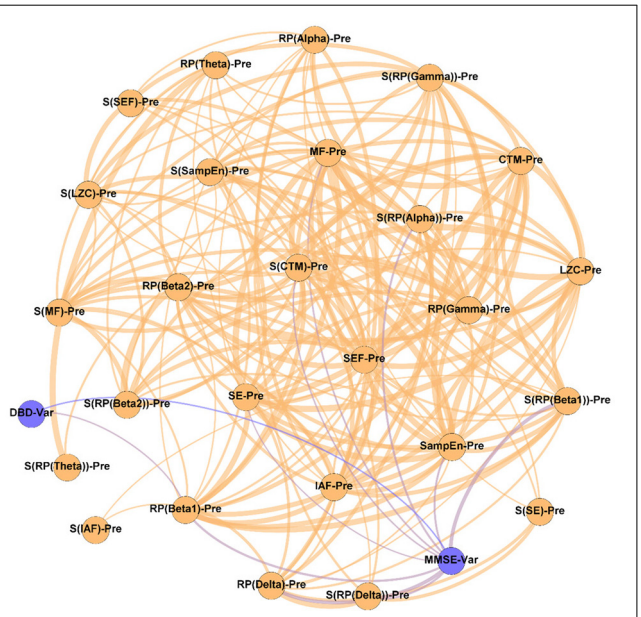

FIGURE 6 | Prediction network, showing the ability of the assessed neurophysiological parameters to predict the outcome of the NPT. The "Var" suffix, which appears associated with DBD and MMSE, means the variation of the parameters under study during the NPT (i.e., $Parameter_{Post} - Parameter_{Pre}$). Wider edges correspond with stronger associations. Nodes corresponding to cognitive and behavioral parameters are shown in blue, while nodes of neurophysiological parameters are shown in orange.

1)), S(IAF), S(SE) with DBD, and S(RP(Beta 2)) with MMSE. Besides, three associations involve beta band: RP(Beta 1), S(RP(Beta 1)), and S(RP(Beta 2)). No association involves any non-linear parameter.

Predictability of the NPT Outcome by Means of the Neurophysiological Parameters

Figure 6 contains the Prediction network. It depicts the ability of the neurophysiological parameters under study to predict the outcome of the NPT, measured by the variation of the cognitive and behavioral parameters (MMSE and DBD-13). It could be appreciated that, aside from the relationship that links cognitive and behavioral parameters, MMSE has nine significant relationships (RP(Delta), RP(Beta 1), MF, SE, SampEn, S[RP(Delta)], S[RP(Alpha)], S(RP(Beta 1)), and S(CTM)), while DBD-13 has only one (RP(Beta 1)). Of note, only two out of these 10 parameters involve non-linear parameters (MMSE-SampEn and MMSE-S(CTM)), and four of them involve spatial entropies (S[RP(Delta)], S[RP(Alpha)], S(RP(Beta 1)), and S(CTM)). **Supplementary Figure 4** depicts the stability of the network depicted in **Figure 6**.

These relationships are of great importance because, as mentioned in the Introduction section, predicting the NPT is crucial. Thus, to obtain deep insights on them, and disentangle the nature of these associations, we plotted scatterplots for every significant relationship (involving cognitive or behavioral parameters) obtained in the previous section, reporting the specific correlation values (ρ). These scatterplots are shown in **Figure 7**. Remarkably high relationships between parameters can be observed, with a mean value of 0.56. The strongest relationships can be observed for associations involving MMSE and delta and beta bands: MMSE-RP(Delta) ($\rho = -0.69$, p-value = 0.002, Spearman rank correlation), MMSE-RP(Beta 1) ($\rho = 0.57$, p-value = 0.017, Spearman rank correlation), MMSE-S(RP(Delta)) ($\rho = -0.56$, p-value = 0.019, Spearman rank correlation), and MMSE-S(RP(Beta 1)) ($\rho = 0.70$, p-value = 0.002, Spearman rank correlation).

DISCUSSION

In the present study, we have assessed the effects of an NPT in the neurophysiology of patients with AD, as well as whether its outcome is predictable by means of MEG-based parameters. Our results hold three main findings related to the three research questions posed in the introduction: (i) the NPT alters the structure of the association networks, unveiling relationships between DBD-13 and neurophysiological parameters: RP(Gamma), SE, SEF, LZC, SampEn, CTM, S(RP(Gamma)), S(SEF), S(LZC), S(SampEn), and S(CTM); (ii) the changes induced by the NPT are related to the changes in the DBD-13, suggesting an impact of the NPT in the behavioral symptoms of AD; and (iii) the value of nine neurophysiological parameters (RP(Delta), RP(Beta 1), MF, SE, SampEn, S[RP(Delta)], S[RP(Alpha)], S(RP(Beta 1)), and S(CTM)) before going through the NPT are related to the NPT outcome, suggesting a potential predictive power of the aforementioned parameters to foresee the response of the patients to the NPT.

NPT Induces Several Changes in the Structure of the Association Networks

The Pre-NPT network displayed in **Figure 2** shows that, before conducting the NPT, the neurophysiological parameters are associated with the MMSE, but not with the DBD-13. This could be explained as both tests are measuring the alterations provoked by dementia in different cognitive domains. On the one hand, DBD-13 measures strictly behavioral disturbances defined as "*the outward manifestation of some underlying cognitive, psychological, or physiological deficit—regardless of etiology—likely to cause stress to those caring for the patient*" (Baumgarten et al., 1990). On the other hand, MMSE quantifies cognitive impairment in a more global sense, by means of different cognitive dimensions, such as attention, orientation, language, perception, calculus, or the ability to follow simple instructions (Folstein et al., 1975). Therefore, these results suggest that cognitive disturbances measured in a broader sense are directly related to the neurophysiological state. Nevertheless, this is not the case for behavioral disturbances, where this relationship could be mediated or obscured by external factors, such as the environment, relationship with caregivers, or daily life habits.

It is worth mentioning that all the spectral and non-linear parameters, apart from those derived from the RP (except RP(Gamma)), show statistically significant associations with

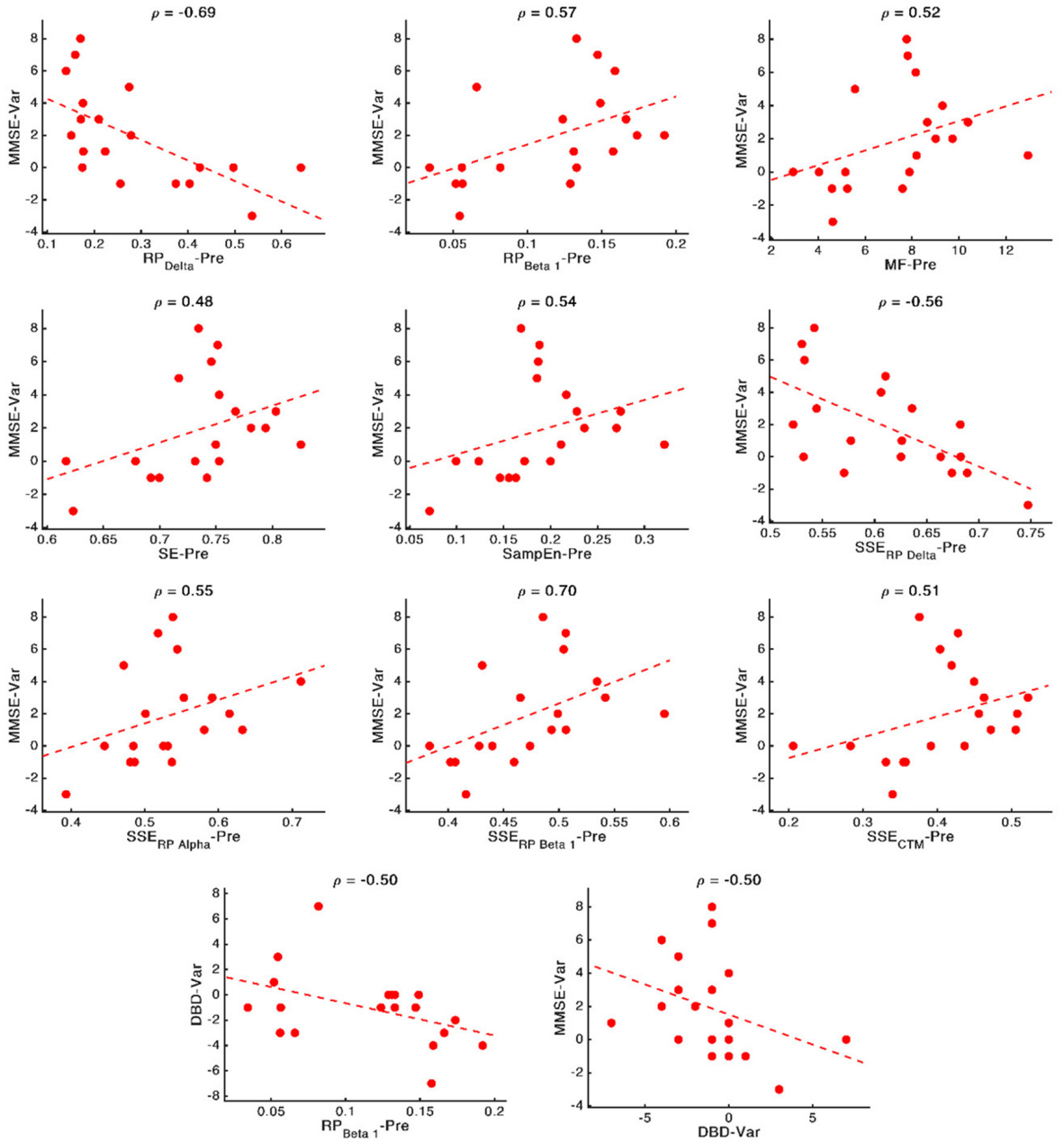

FIGURE 7 | Scatterplots representing the relationship between the neurophysiological parameters computed before applying the NPT (x-axis) and the changes in cognitive and behavioral variables after the NPT (y-axis). In the top part of each panel, the value of the Spearman rank correlation for each specific pair of parameters is plotted. Dashed lines represent the linear regression of the data.

the MMSE. RP values do not contain information about the complete oscillatory activity, but only of a certain frequency band, typically associated with a limited number of cognitive functions (Uhlhaas et al., 2008). As it is known that AD induces alterations in several cognitive domains (Alzheimer's Association, 2019; Alzheimer's Disease International, 2019), it could be hypothesized that the absence of associations between MMSE and RP could be provoked, at least partially, because they are only reflecting particular cognitive dimensions of AD disruptions. Noteworthy, associations were found for RP(Gamma), as well as for its spatial entropy. The gamma band has been proven to play an important role in several higher cognitive functions (Bartos et al., 2007; Martorell et al., 2019). Besides, this frequency band is also affected by AD neuropathology. Previous studies reported that AD patients' brain activity is associated with an enhanced gamma power (van Deursen et al., 2008; Wang et al., 2017), an increase in long distance gamma connectivity (Başar et al., 2017), and an increase

in the cross-frequency-coupling strength between gamma and low frequency bands (Wang et al., 2017).

The Post-NPT network included in **Figure 3** depicts the association network after the application of the NPT. By comparing this network with that in **Figure 2**, we can infer the influence of the NPT in the pattern of interactions between the different parameters (neurophysiological, cognitive, and behavioral) under assessment. In this regard, the Variability network (**Figure 4**) is also relevant, as it shows the 5% strongest associations with the biggest differences induced by the NPT. For MMSE, the basic structure of the network is relatively maintained, as 62% of the statistically significant associations are the same before and after conducting the NPT. Of note, the associations with RP(Gamma), as well as its spatial entropy S(RP(Gamma)), are not statistically significant; this result can be interpreted as the NPT modulating the impairment provoked by AD in the gamma band. Gamma activity is associated with gamma-aminobutyric acid (GABAergic) activity, which is the principal inhibitory neurotransmitter (Bartos et al., 2007; Porges et al., 2017). Since an increased concentration of GABA is related to superior cognitive performance, we may suggest a relationship between gamma activity and cognitive performance (Bartos et al., 2007; Porges et al., 2017; Mably and Colgin, 2018). Besides, an increase in the gamma band activity of the angular gyrus for AD patients has also been reported (Shigihara et al., 2020b). This increase was associated with the NPT inducing compensatory mechanisms against the functional deficit provoked by dementia (Shigihara et al., 2020b). Furthermore, new associations between MMSE and RP appear with the application of the NPT: RP(Delta), RP(Beta 1), RP(Beta 2), and S(RP(Beta 2)). These bands are associated with the well-documented slowing that AD elicits on oscillatory neural activity (Jeong, 2004; Dauwels et al., 2011); therefore, they are likely to be affected by the NPT. Interestingly, the association of MMSE with RP(Alpha) is missing in both networks, though it is commonly related to AD. This could be due to the fact that the alpha band is acting as a "transition" band between the decrease of power in faster bands (beta 1 and beta 2) and the increase in the slower ones (delta and theta), thus being less affected by the NPT. This result does not agree with previous findings (Shigihara et al., 2020b), where the NPT induced differences in the right temporal and right fusiform areas in the alpha band. The discrepancies could be due to the band definition (alpha band was split in alpha 1 and alpha 2) or due to the spatial dimension of the analyses conducted by Shigihara et al. (2020b).

Crucially, in **Figure 4**, it could be observed that the majority of the associations that changed the most after the NPT involve the DBD-13. This could be explained because of the environment and habits of the patients being controlled during the NPT, i.e., the therapeutic intervention would be modulating those external factors, that could, in turn, be mediating or obscuring the associations between DBD-13 and the neurophysiological parameters before the application of the NPT. Thus, we can speculate that the NPT has a direct impact on the behavioral disturbances associated with AD, unveiling their association with the neurophysiological oscillatory activity. The behavioral symptoms are common in dementia, and largely affect health and quality of life (Dyer et al., 2018). This is in line with previous studies, where NPTs showed greater effectiveness against behavioral symptoms than against cognitive symptoms (Zucchella et al., 2018). Interestingly, 55% of the associations of DBD-13 that changed the most after the NPT are spatial entropies. This suggests that the spatial patterns of the neurophysiological alterations elicited by NPT play a significant role in patients with AD. Diverse brain regions are affected differently by the NPT and, consequently, the spatial entropy of local activation parameters is able to reflect such changes. This is supported by previous studies where NPT effects were observed in specific brain regions such as the fusiform gyrus, right angular gyrus, sensorimotor area, or right temporal lobe (Zucchella et al., 2018; Shigihara et al., 2020a,b).

Relationship Between Neurophysiological, Cognitive, and Behavioral Changes

Our findings suggest that changes in RP(Beta 1) and RP(Beta 2) are related with the cognitive and behavioral changes: changes in RP(Beta 1) and S(RP(Beta 1)) are associated with changes in DBD-13, whereas changes in S(RP(Beta 2)) are related with those in MMSE. Beta activity is known to be associated with GABA transmission, somatosensory functions, and emotional processes (Jensen et al., 2005; Poil et al., 2013). Besides, beta oscillations have been linked to AD: a decrease in beta activity associated with the disease has been widely reported (Jeong, 2004; Fernández et al., 2006; Poza et al., 2007; Dauwels et al., 2011; Roh et al., 2011). Hence, its application as a clinical tool to aid in AD diagnosis and to assess neural disruption processes has been proposed (Poil et al., 2013). Likewise, it has also been linked to neuroplasticity, as well as to behavioral and psychological symptoms of dementia *via* GABAergic activity (Lanctôt et al., 2004; Griffen and Maffei, 2014). Also, in previous studies associations between RP in beta and the changes in cognition induced by an NPT has been reported (Shigihara et al., 2020a,b).

Furthermore, a remarkable number of relationships between the spatial entropies and both, cognitive and behavioral parameters can be observed. This fact reinforces the idea posed in the previous section: the NPT not only affects the global values of the parameters under study, but their spatial distribution (i.e., the changes induced by the NPT follow a specific spatial pattern). This could be explained by the NPT restoring specific cognitive domains (Zucchella et al., 2018), which are placed in specific brain regions (Augustine, 2007), and can be detected by cognitive and behavioral tests (e.g., behavior for DBD-13 or memory for MMSE; Folstein et al., 1975; Baumgarten et al., 1990). The NPT affecting different brain regions differently has been previously reported (Zucchella et al., 2018; Shigihara et al., 2020a,b).

Finally, it can also be observed that the changes in non-linear parameters are not related to the changes in cognition or behavior, indicating that the NPT does not directly affect the non-linear properties of resting-state MEG activity. It should be noted that the non-linear parameters are affected by the

NPT (as discussed in the previous section), but those changes are not related to the NPT outcome (as measured by the cognitive and behavioral tests). Thus, it is possible that non-linear parameters are affecting specific cognitive domains not measured by the tests, or that those domains are related to specific aspects of the tests, thus blurring those differences among the other dimensions. This is in line with previous studies showing that, although spectral and non-linear parameters are related (Dauwels et al., 2011), they also had remarkable differences. Furthermore, the absence of connections with non-linear parameters could be due to a decreased sensitivity of the non-linear parameters to detect the AD neurophysiological disruptions. This issue is in line with previous studies, where non-linear parameters showed reduced capabilities for AD classification compared to the spectral ones (Hornero et al., 2008; Escudero et al., 2009; Poza et al., 2012).

Potential of Neurophysiological Parameters to Predict the NPT Outcome

As stated in the Introduction section, predicting the outcome of the NPTs would be of great interest, as important differences have been found in the cognitive impact of NPT among patients; some of them showed great responsiveness to the treatment, while others were unresponsive (Shigihara et al., 2020a).

It can be observed in **Figure 6** that spectral parameters are more associated with the NPT outcome than non-linear ones: seven out of the nine local activation parameters that show statistically significant relationships are derived from the PSDn. This suggests that the NPT has a greater influence on the spectral components of the resting-state MEG activity than on its non-linear properties, which could be motivated by greater disruptions of AD in the spectral content than in the non-linear properties of the neural signals (Hornero et al., 2008; Escudero et al., 2009; Poza et al., 2012).

Associations between MMSE and RP(Delta), RP(Beta 1), and their SSEs can be appreciated, though the strongest association was obtained between DBD-13 and RP(Beta 1). These two bands are related to AD, as they measure the well-known frequency shift provoked by AD: an increase of oscillatory activity in low frequency bands and a decrease in higher ones (Jeong, 2004). Not only the beta band, as previously stated, but also the delta band is found to be associated with AD pathology. Delta has been associated with the cholinergic levels of the brain, with the current cognitive status, and also with the progression of AD. Additionally, its increased delta activity has been proposed as evidence of neural degeneration (Fernández et al., 2013; Nakamura et al., 2018; Shigihara et al., 2020a). Furthermore, the ratio between the power of neural activity in delta and beta bands has been used to reflect AD disruptions (Babiloni et al., 2004; Poza et al., 2008a; Knyazeva et al., 2010; Wang et al., 2017). In a previous study, a correlation between beta power and NPT outcome, measured by means of the MMSE, was also observed (Shigihara et al., 2020a).

It is also noteworthy that our results suggest that milder decline (measured by means of the neurophysiological deterioration, i.e., slowing, diminished variety of frequency components and irregularity loss; Jeong, 2004; Escudero et al., 2009; Dauwels et al., 2011) is related with a better NPT outcome. While AD provokes a shift to lower frequencies and a reduced SE (Poza et al., 2008b; Dauwels et al., 2011; Bruña et al., 2012), we have found that a PSDn skewed towards higher frequencies (observed in the correlations MMSE-RP(Delta), MMSE-RP(Beta 1), MMSE-MF, and DBD-13-RP(Beta 1)) and with a richer variety of frequency components (observed in the correlation MMSE-SE) predicts a better outcome of the therapy. Besides, AD is linked with more regular signals (Escudero et al., 2009; Gómez et al., 2009; Hornero et al., 2009), and we have observed that signals with higher irregularity (observed in the correlation MMSE—SampEn) predict a better response of the patient to the therapy. The correlation between DBD-13 and RP(Beta 1) is negative, whereby higher beta power is related to lower DBD-13, which indicates a better behavioral state.

Besides, the SSE of the parameters were shown to be important for predicting the NPT outcome: we found four statistically significant correlations between MMSE and S[RP(Delta)], S(RP(Beta 1)), S[RP(Alpha)], and S(CTM). Also, all the correlations apart from the one with S[RP(Delta)] are positive, which suggests that a more homogeneous spatial distribution of the corresponding local activation parameters predicts a better prognosis for the NPT. AD does not affect the whole brain simultaneously, it is a progressive process (Raji et al., 2009). Thus, a lower SSE could indicate that neural damage is focused on specific brain areas (due to the variations in the spatial pattern of the neurophysiological parameters), which the NPT is unable to recover, so yielding a worse outcome of the therapeutic intervention. Again, this idea is in line with previous findings, where the spatial dimension of the results related to the NPT is evident (Shigihara et al., 2020a,b).

The NPT significatively improved both cognition, as indicated by the MMSE, and behavior, as quantified by the DBD-13. These findings agree with previous studies where other NPTs yielded beneficial effects in dementia patients (Zucchella et al., 2018). Besides, in a previous study with the same NPT but a different sample, statistically significant improvements were observed for the MMSE but not for the DBD-13 (Shigihara et al., 2020b). The discrepancy in the DBD-13 results could be explained due to the different number of participants in the sample, or due to the different pathology of the participants; in this study, only patients with AD were included, while in the study conducted by Shigihara et al. (2020b) the sample was composed of AD and vascular dementia patients.

Limitations and Future Lines

Although this study has yielded interesting findings, there are also some methodological issues that have to be mentioned, as this is an exploratory study intended to be continued in the future.

Firstly, the sample size is limited due to the difficulty of carrying out this type of study, that requires a longitudinal follow-up. This issue impacts, in turn, the stability of the networks, probably due to the usage of bootstrapping that, with reduced sample sizes ($N = 19$ in our case), yields high variability

between iterations (Efron and Tibshirani, 1993). In order to minimize the impact on the stability of the networks, they have been generated considering only the statistically significant connections (**Supplementary Figures 1–4**). Nevertheless, we are working on incorporating new participants into the database, which could also be interesting to design a classification model useful to predict the responsiveness of a patient to the NPT.

Another limitation is that we collapsed all the ROIs, considering only the spatial dimension of the data by means of the SSE. The results obtained with the SSE-related measures support future studies that would address the role of spatial patterns in detail. By analyzing its influence in each ROI separately, deep insights on the NPT outcomes could be obtained.

We have used only two tests in the cognitive assessments. The inclusion of additional cognitive tests would be useful to increase the robustness of the results by diminishing the impact of biases and measurement errors. Besides, it would be also interesting to disaggregate the MMSE results in its different domains to assess how the NPT differently influences diverse cognitive domains.

Furthermore, we have obtained interesting findings by analyzing the association between the NPT outcome and local activation (spectral and non-linear) neurophysiological parameters. By analyzing the relationship between the NPT outcome and connectivity or graph parameters in future studies, we could potentially obtain a broader characterization of the neurophysiological patterns associated with the NPT.

Finally, we have conducted the study using resting-state MEG recordings, where the background brain activity is measured. Resting-state is a widely used paradigm, but it would be of great interest to replicate the analysis performed in this study using brain signals during sleep, as NPTs are able to ameliorate the sleep disturbances provoked by AD (Berry et al., 2012; Horvath, 2018; Zucchella et al., 2018).

CONCLUSIONS

In this study, we conducted an exploratory analysis about the associations between different local activation neurophysiological parameters (spectral and non-linear, as well their spatial counterparts) and the NPT outcome, quantified with MMSE and DBD-13 tests. Our findings suggest that the NPT modifies the association network structure, influencing the behavioral disturbances and suggesting its relationship with the neurophysiological patterns. Changes in cognition and behavior due to the NPT are related to the spectral changes in MEG activity, especially in the beta band. Furthermore, the NPT induces spatial-dependent patterns in MEG activity that are able to reflect the cognitive and behavioral changes due to the therapeutic intervention. Finally, we can conclude that the analyzed neurophysiological parameters are potential predictors of the NPT outcome; specifically, less severe neurophysiological alterations due to AD can be associated with a better prognosis of the NPT.

DATA AVAILABILITY STATEMENT

The datasets presented in this study can be found in online repositories. The names of the repository/repositories and accession number(s) can be found below: all data generated during this study are available from Rodriguez, Victor (2021), "NPT parameters," Mendeley Data, V1, doi: 10.17632/99pmshmz7m.1 (http://dx.doi.org/10.17632/99pmshmz7m.1). The raw signals analyzed during the current study are available from the authors upon reasonable request. Furthermore, the methodology is based on widespread well-documented pipelines; however, the code used in the analyses is also available from the authors under reasonable request.

ETHICS STATEMENT

The studies involving human participants were reviewed and approved by Ethics Committee of Hokuto Hospital, Hokuto Hospital, Obihiro, Japan. The patients/participants provided their written informed consent to participate in this study.

AUTHOR CONTRIBUTIONS

VR-G: managed the study, developed the software and the data visualizations, managed the data management, interpreted the results, and wrote the manuscript. CG: conceptualized the study, interpreted the results, reviewed and edited the manuscript. HH and YS: collected the data, interpreted the results, reviewed and edited the manuscript. RH: interpreted the results, reviewed and edited the manuscript. JP: managed the study, conceptualized the study, interpreted the results, reviewed and edited the manuscript. All authors contributed to the article and approved the submitted version.

FUNDING

This research was supported by "Ministerio de Ciencia e Innovación—Agencia Estatal de Investigación", "European Regional Development Fund" (FEDER), "Ministerio de Ciencia, Innovación y Universidades" under project PGC2018-098214-A-I00, the "European Commission", FEDER under project "Análisis y correlación entre la epigenética y la actividad cerebral para evaluar el riesgo de migraña crónica y episódica en mujeres" ("Cooperation Programme Interreg V-A Spain-Portugal POCTEP 2014–2020"), and by CIBER-BBN (ISCIII) co-funded with FEDER funds. V. Rodríguez-González was in receipt of a PIF-UVa grant from the "University of Valladolid."

SUPPLEMENTARY MATERIAL

The Supplementary Material for this article can be found online at: https://www.frontiersin.org/articles/10.3389/fnagi.2021.696174/full#supplementary-material.

REFERENCES

Alzheimer's Association (2019). 2019 Alzheimer's disease facts and figures. *Alzheimer's Dement.* 15, 321–387. doi: 10.1016/j.jalz.2019.01.010

Alzheimer's Disease International (2019). *World Alzheimer report 2019: Attitudes to Dementia*. London: Alzheimer's Disease International. Available online at: https://www.alzint.org/u/WorldAlzheimerReport2019.pdf.

Amjad, I., Toor, H., Niazi, I. K., Afzal, H., Jochumsen, M., Shafique, M., et al. (2019). Therapeutic effects of aerobic exercise on EEG parameters and higher cognitive functions in mild cognitive impairment patients. *Int. J. Neurosci.* 129, 551–562. doi: 10.1080/00207454.2018.1551894

Anderson, K., and Grossberg, G. T. (2014). Brain games to slow cognitive decline in Alzheimer's disease. *J. Am. Med. Dir. Assoc.* 15, 536–537. doi: 10.1016/j.jamda.2014.04.014

Augustine, J. R. (2007). *Human Neuroanatomy*, 1st Edn. Amsterdam, Netherlands: Elsevier.

Başar, E., Femir, B., Emek-Savaş, D. D., Güntekin, B., and Yener, G. G. (2017). Increased long distance event-related gamma band connectivity in Alzheimer's disease. *Neuroimage Clin.* 14, 580–590. doi: 10.1016/j.nicl.2017.02.021

Babiloni, C., Ferri, R., Moretti, D. V., Strambi, A., Binetti, G., Dal Forno, G., et al. (2004). Abnormal fronto-parietal coupling of brain rhythms in mild Alzheimer's disease: a multicentric EEG study. *Eur. J. Neurosci.* 19, 2583–2590. doi: 10.1111/j.0953-816X.2004.03333.x

Babiloni, C., Pizzella, V., Gratta, C. D., Ferretti, A., and Romani, G. L. (2009). Fundamentals of electroencefalography, magnetoencefalography and functional magnetic resonance imaging. *Int. Rev. Neurobiol.* 86, 67–80. doi: 10.1016/S0074-7742(09)86005-4

Barberán, A., Bates, S. T., Casamayor, E. O., and Fierer, N. (2012). Using network analysis to explore co-occurrence patterns in soil microbial communities. *ISME J.* 6, 343–351. doi: 10.1038/ismej.2011.119

Bartos, M., Vida, I., and Jonas, P. (2007). Synaptic mechanisms of synchronized gamma oscillations in inhibitory interneuron networks. *Nat. Rev. Neurosci.* 8, 45–56. doi: 10.1038/nrn2044

Baumgarten, M., Becker, R., and Gauthier, S. (1990). Validity and reliability of the dementia behavior disturbance scale. *J. Am. Geriatr. Soc.* 38, 221–226. doi: 10.1111/j.1532-5415.1990.tb03495.x

Berry, R. B., Budhiraja, R., Gottlieb, D. J., Gozal, D., Iber, C., Kapur, V. K., et al. (2012). Rules for scoring respiratory events in sleep: update of the 2007 AASM manual for the scoring of sleep and associated events. deliberations of the sleep apnea definitions task force of the american academy of sleep medicine. *J. Clin. Sleep Med.* 8, 597–619. doi: 10.5664/jcsm.2172

Blackman, R. B., and Tukey, J. W. (1958). The measurement of power spectra from the point of view of communications engineering. *Bell System Techn. J.* 37, 185–282.

Borsboom, D. (2017). A network theory of mental disorders. *World Psychiatry* 16, 5–13. doi: 10.1002/wps.20375

Borsboom, D., and Cramer, A. O. J. (2013). Network analysis: an integrative approach to the structure of psychopathology. *Ann. Rev. Clin. Psychol.* 9, 91–121. doi: 10.1146/annurev-clinpsy-050212-185608

Bruña, R., Poza, J., Gómez, C., García, M., Fernández, A., and Hornero, R. (2012). Analysis of spontaneous MEG activity in mild cognitive impairment and Alzheimer's disease using spectral entropies and statistical complexity measures. *J. Neural Eng.* 9:036007. doi: 10.1088/1741-2560/9/3/036007

Cotelli, M., Manenti, R., and Zanetti, O. (2012). Reminiscence therapy in dementia: a review. *Maturitas* 72, 203–205. doi: 10.1016/j.maturitas.2012.04.008

Cummings, J. L. (2003). *The Neuropsychiatry of Alzheimer's Disease and Related Dementias*, 1st Edn. Boca Raton, FL: CRC Press.

Dauwels, J., Srinivasan, K., Ramasubba Reddy, M., Musha, T., Vialatte, F.-B., Latchoumane, C., et al. (2011). Slowing and loss of complexity in Alzheimer's EEG: two sides of the same coin. *Int. J. Alzheimer's Dis.* 2011:539621. doi: 10.4061/2011/539621

Desikan, R. S., Ségonne, F., Fischl, B., Quinn, B. T., Dickerson, B. C., Blacker, D., et al. (2006). An automated labeling system for subdividing the human cerebral cortex on MRI scans into gyral based regions of interest. *Neuroimage* 31, 968–980. doi: 10.1016/j.neuroimage.2006.01.021

Douw, L., Nieboer, D., Stam, C. J., Tewarie, P., and Hillebrand, A. (2018). Consistency of magnetoencephalographic functional connectivity and network reconstruction using a template versus native MRI for co-registration. *Hum. Brain Mapp.* 39, 104–119. doi: 10.1002/hbm.23827

Dyer, S. M., Harrison, S. L., Laver, K., Whitehead, C., and Crotty, M. (2018). An overview of systematic reviews of pharmacological and non-pharmacological interventions for the treatment of behavioral and psychological symptoms of dementia. *Int. Psychogeriatr.* 30, 295–309. doi: 10.1017/S1041610217002344

Efron, B. (1992). "Bootstrap methods: another look at the jackknife," in *Breakthroughs in Statistics*, 1st edition, eds S. Kotz and N. L. Johnson (Berlin, Germany: Springer), 569–593.

Efron, B., and Tibshirani, R. J. (1993). *An Introduction to the Bootstrap*, 1st edition. Boca Raton, FL: Chapman and Hall/CRC.

Engels, M. M. A., van der Flier, W. M., Stam, C. J., Hillebrand, A., Scheltens, P., and van Straaten, E. C. W. (2017). Alzheimer's disease: the state of the art in resting-state magnetoencephalography. *Clin. Neurophysiol.* 128, 1426–1437. doi: 10.1016/j.clinph.2017.05.012

Epskamp, S., Borsboom, D., and Fried, E. I. (2018). Estimating psychological networks and their accuracy: a tutorial paper. *Behav. Res. Methods* 50, 195–212. doi: 10.3758/s13428-017-0862-1

Escudero, J., Hornero, R., Abásolo, D., and Fernández, A. (2009). Blind source separation to enhance spectral and non-linear features of magnetoencephalogram recordings. Application to Alzheimer's disease. *Med. Eng. Phys.* 31, 872–879. doi: 10.1016/j.medengphy.2009.04.003

Fernández, A., Hornero, R., Gómez, C., Turrero, A., Gil-Gregorio, P., Matías-Santos, J., et al. (2010). Complexity analysis of spontaneous brain activity in alzheimer disease and mild cognitive impairment. *Alzheimer Dis. Assoc. Disord.* 24, 182–189. doi: 10.1097/WAD.0b013e3181c727f7

Fernández, A., Hornero, R., Mayo, A., Poza, J., Gil-Gregorio, P., and Ortiz, T. (2006). MEG spectral profile in Alzheimer's disease and mild cognitive impairment. *Clin. Neurophysiol.* 117, 306–314. doi: 10.1016/j.clinph.2005.10.017

Fernández, A., Ríos-Lago, M., Abásolo, D., Hornero, R., Álvarez-Linera, J., Paul, N., et al. (2011). The correlation between white-matter microstructure and the complexity of spontaneous brain activity: a difussion tensor imaging-MEG study. *Neuroimage* 57, 1300–1307. doi: 10.1016/j.neuroimage.2011.05.079

Fernández, A., Turrero, A., Zuluaga, P., Gil-Gregorio, P., del Pozo, F., Maestu, F., et al. (2013). MEG delta mapping along the healthy aging-Alzheimer's disease continuum: diagnostic implications. *J. Alzheimer's Dis.* 35, 495–507. doi: 10.3233/JAD-121912

Folstein, M. F., Folstein, S. E., and McHugh, P. R. (1975). "Mini-mental state": a practical method for grading the cognitive state of patients for the clinician. *J. Psychiatric Res.* 12, 189–198. doi: 10.1016/0022-3956(75)90026-6

Fonov, V. S., Evans, A. C., McKinstry, R. C., Almli, C. R., and Collins, D. L. (2009). Unbiased nonlinear average age-appropriate brain templates from birth to adulthood. *NeuroImage* 47:S102. doi: 10.1016/S1053-8119(09)70884-5

Fornito, A., Zalesky, A., and Bullmore, E. T. (2016). *Fundamentals of Brain Network Analysis*, 1st Edn. Amsterdam, Netherlands: Elsevier.

Gómez, C., and Hornero, R. (2010). Entropy and complexity analyses in Alzheimer's disease: an MEG study. *Open Biomed. Eng. J.* 4, 223–235. doi: 10.2174/1874120701004010223

Gómez, C., Hornero, R., Abásolo, D., Fernández, A., and Escudero, J. (2009). Analysis of MEG background activity in Alzheimer's disease using nonlinear methods and ANFIS. *Ann. Biomed. Eng.* 37, 586–594. doi: 10.1007/s10439-008-9633-6

Gómez, C., Hornero, R., Abásolo, D., Fernández, A., and López, M. (2006). Complexity analysis of the magnetoencephalogram background activity in Alzheimer's disease patients. *Med. Eng. Phys.* 28, 851–859. doi: 10.1016/j.medengphy.2006.01.003

Gramfort, A., Papadopoulo, T., Olivi, E., and Clerc, M. (2010). OpenMEEG: opensource software for quasistatic bioelectromagnetics. *BioMed. Eng. Online* 9:45. doi: 10.1186/1475-925X-9-45

Griffen, T. C., and Maffei, A. (2014). GABAergic synapses: their plasticity and role in sensory cortex. *Front. Cell. Neurosci.* 8:91. doi: 10.3389/fncel.2014.00091

Hornero, R., Abásolo, D., Escudero, J., and Gómez, C. (2009). Nonlinear analysis of electroencephalogram and magnetoencephalogram recordings in patients with Alzheimer's disease. *Philos. Trans. A Math. Phys. Eng. Sci.* 367, 317–336. doi: 10.1098/rsta.2008.0197

Hornero, R., Escudero, J., Fernández, A., Poza, J., and Gómez, C. (2008). Spectral and nonlinear analyses of MEG background activity in patients with Alzheimer's disease. *IEEE Trans. Biomed. Eng.* 55, 1658–1665. doi: 10.1109/tbme.2008.919872

Horvath, A. (2018). EEG and ERP biomarkers of Alzheimer's disease a critical review. *Front. Biosci. (Landmark Ed)* 23, 183–220. doi: 10.2741/4587

Hsu, T.-J., Tsai, H.-T., Hwang, A.-C., Chen, L.-Y., and Chen, L.-K. (2017). Predictors of non-pharmacological intervention effect on cognitive function and behavioral and psychological symptoms of older people with dementia. *Geriatr. Gerontol. Int.* 17, 28–35. doi: 10.1111/ggi.13037

Jacomy, M., Venturini, T., Heymann, S., and Bastian, M. (2014). ForceAtlas2, a Continuous graph layout algorithm for handy network visualization designed for the gephi software. *PLoS One* 9:e98679. doi: 10.1371/journal.pone.0098679

Jensen, O., Goel, P., Kopell, N., Pohja, M., Hari, R., and Ermentrout, B. (2005). On the human sensorimotor-cortex beta rhythm: sources and modeling. *Neuroimage* 26, 347–355. doi: 10.1016/j.neuroimage.2005.02.008

Jeong, J. (2004). EEG dynamics in patients with Alzheimer's disease. *Clin. Neurophysiol.* 115, 1490–1505. doi: 10.1016/j.clinph.2004.01.001

Jimeno, N., Gomez-Pilar, J., Poza, J., Hornero, R., Vogeley, K., Meisenzahl, E., et al. (2020). Main symptomatic treatment targets in suspected and early psychosis: new insights from network analysis. *Schizophr. Bull.* 46, 884–895. doi: 10.1093/schbul/sbz140

Klimesch, W. (1999). EEG alpha and theta oscillations reflect cognitive and memory performance: a review and analysis. *Brain Res. Rev.* 29, 169–195. doi: 10.1016/s0165-0173(98)00056-3

Knyazeva, M. G., Jalili, M., Brioschi, A., Bourquin, I., Fornari, E., Hasler, M., et al. (2010). Topography of EEG multivariate phase synchronization in early Alzheimer's disease. *Neurobiol. Aging* 31, 1132–1144. doi: 10.1016/j.neurobiolaging.2008.07.019

Kurz, A. F., Leucht, S., and Lautenschlager, N. T. (2011). The clinical significance of cognition-focused interventions for cognitively impaired older adults: A systematic review of randomized controlled trials. *Int. Psychogeriatr.* 23, 1364–1375. doi: 10.1017/S1041610211001001

Lai, M., Demuru, M., Hillebrand, A., and Fraschini, M. (2018). A comparison between scalp- and source-reconstructed EEG networks. *Sci. Rep.* 8:12269. doi: 10.1038/s41598-018-30869-w

Lanctôt, K. L., Herrmann, N., Mazzotta, P., Khan, L. R., and Ingber, N. (2004). GABAergic function in Alzheimer's disease: evidence for dysfunction and potential as a therapeutic target for the treatment of behavioural and psychological symptoms of dementia. *Can. J. Psychiatry* 49, 439–453. doi: 10.1177/070674370404900705

Lempel, A., and Ziv, J. (1976). On the complexity of finite sequences. *IEEE Trans. Informat. Theory* 22, 75–81.

Lin, F.-H., Witzel, T., Hämäläinen, M. S., Dale, A. M., Belliveau, J. W., and Stufflebeam, S. M. (2004). Spectral spatiotemporal imaging of cortical oscillations and interactions in the human brain. *Neuroimage* 23, 582–595. doi: 10.1016/j.neuroimage.2004.04.027

Lu, L.-C., Lan, S.-H., Hsieh, Y.-P., Yen, Y.-Y., Chen, J.-C., and Lan, S.-J. (2020). Horticultural therapy in patients with dementia: a systematic review and meta-analysis. *Am. J. Alzheimers Dis. Other Demen.* 35:1533317519883498. doi: 10.1177/1533317519883498

Mably, A. J., and Colgin, L. L. (2018). Gamma oscillations in cognitive disorders. *Curr. Opin. Neurobiol.* 52, 182–187. doi: 10.1016/j.conb.2018.07.009

Machida, A. (2012). Estimation of the reliability and validity of the short version of the 28-item dementia behavior disturbance scale. *Nippon Ronen Igakkai Zasshi. Jpn. J. Geriatr.* 49, 463–467. doi: 10.3143/geriatrics.49.463

Mahjoory, K., Nikulin, V. V., Botrel, L., Linkenkaer-Hansen, K., Fato, M. M., and Haufe, S. (2017). Consistency of EEG source localization and connectivity estimates. *Neuroimage* 152, 590–601. doi: 10.1016/j.neuroimage.2017.02.076

Maki, Y., Sakurai, T., Okochi, J., Yamaguchi, H., and Toba, K. (2018). Rehabilitation to live better with dementia. *Geriatr. Gerontol. Int.* 18, 1529–1536. doi: 10.1111/ggi.13517

Mandal, P. K., Banerjee, A., Tripathi, M., and Sharma, A. (2018). A comprehensive review of magnetoencephalography (MEG) studies for brain functionality in healthy aging and Alzheimer's disease (AD). *Front. Computat. Neurosci.* 12:60. doi: 10.3389/fncom.2018.00060

Martorell, A. J., Paulson, A. L., Suk, H.-J., Abdurrob, F., Drummond, G. T., Guan, W., et al. (2019). Multi-sensory gamma stimulation ameliorates Alzheimer's-associated pathology and improves cognition. *Cell* 177, 256–271.e22. doi: 10.1016/j.cell.2019.02.014

McGrattan, A. M., McGuinness, B., McKinley, M. C., Kee, F., Passmore, P., Woodside, J. V., et al. (2019). Diet and inflammation in cognitive ageing and Alzheimer's disease. *Curr. Nutr. Rep.* 8, 53–65. doi: 10.1007/s13668-019-0271-4

McKhann, G. M., Knopman, D. S., Chertkow, H., Hyman, B. T., Jack, C. R., Kawas, C. H., et al. (2011). The diagnosis of dementia due to Alzheimer's disease: recommendations from the national institute on aging-Alzheimer's association workgroups on diagnostic guidelines for Alzheimer's disease. *Alzheimer's Dement.* 7, 263–269. doi: 10.1016/j.jalz.2011.03.005

Mutanen, T. P., Metsomaa, J., Liljander, S., and Ilmoniemi, R. J. (2018). Automatic and robust noise suppression in EEG and MEG: the SOUND algorithm. *Neuroimage* 166, 135–151. doi: 10.1016/j.neuroimage.2017.10.021

Nagamatsu, L. S., Handy, T. C., Hsu, C. L., Voss, M., and Liu-Ambrose, T. (2012). Resistance training promotes cognitive and functional brain plasticity in seniors with probable mild cognitive impairment. *Arch. Int. Med.* 172, 666–668. doi: 10.1001/archinternmed.2012.379

Nakamura, A., Cuesta, P., Fernández, A., Arahata, Y., Iwata, K., Kuratsubo, I., et al. (2018). Electromagnetic signatures of the preclinical and prodromal stages of Alzheimer's disease. *Brain* 141, 1470–1485. doi: 10.1093/brain/awy044

Oliveira, A. M. D., Radanovic, M., Mello, P. C. H. D., Buchain, P. C., Vizzotto, A. D. B., Celestino, D. L., et al. (2015). Nonpharmacological interventions to reduce behavioral and psychological symptoms of dementia: a systematic review. *Biomed. Res. Int.* 2015:218980. doi: 10.1155/2015/218980

Poil, S.-S., de Haan, W., van der Flier, W. M., Mansvelder, H. D., Scheltens, P., and Linkenkaer-Hansen, K. (2013). Integrative EEG biomarkers predict progression to Alzheimer's disease at the MCI stage. *Front. Aging Neurosci.* 5:58. doi: 10.3389/fnagi.2013.00058

Porges, E. C., Woods, A. J., Edden, R. A. E., Puts, N. A. J., Harris, A. D., Chen, H., et al. (2017). Frontal gamma-aminobutyric acid concentrations are associated with cognitive performance in older adults. *Biol. Psychiatry Cogn. Neurosci. Neuroimaging* 2, 38–44. doi: 10.1016/j.bpsc.2016.06.004

Poza, J., Gómez, C., Bachiller, A., and Hornero, R. (2012). Spectral and non-linear analyses of spontaneous magnetoencephalographic activity in Alzheimer's disease. *J. Healthcare Eng.* 3, 299–322. doi: 10.1260/2040-2295.3.2.299

Poza, J., Hornero, R., Abásolo, D., Fernández, A., and García, M. (2007). Extraction of spectral based measures from MEG background oscillations in Alzheimer's disease. *Med. Eng. Phys.* 29, 1073–1083. doi: 10.1016/j.medengphy.2006.11.006

Poza, J., Hornero, R., Abásolo, D., Fernández, A., and Mayo, A. (2008a). Evaluation of spectral ratio measures from spontaneous MEG recordings in patients with Alzheimer's disease. *Comput. Methods Programs Biomed.* 90, 137–147. doi: 10.1016/j.cmpb.2007.12.004

Poza, J., Hornero, R., Escudero, J., Fernández, A., and Sánchez, C. I. (2008b). Regional analysis of spontaneous MEG rhythms in patients with Alzheimer's disease using spectral entropies. *Ann. Biomed. Eng.* 36, 141–152. doi: 10.1007/s10439-007-9402-y

Qaseem, A., Snow, V., Cross, T., Forciea, M. A., Hopkins, R., Shekelle, P., et al. (2008). Current pharmacologic treatment of dementia: a clinical practice guideline from the american college of physicians and the american academy of family physicians. *Ann. Int. Med.* 148, 370–378. doi: 10.7326/0003-4819-148-5-200803040-00008

Raji, C. A., Lopez, O. L., Kuller, L. H., Carmichael, O. T., and Becker, J. T. (2009). Age, Alzheimer disease and brain structure. *Neurology* 73, 1899–1905. doi: 10.1212/WNL.0b013e3181c3f293

Rege, S., Geetha, T., Broderick, T., and Babu, J. (2016). Can diet and physical activity limit Alzheimer's disease risk. *Curr. Alzheimer Res.* 14, 76–93. doi: 10.2174/1567205013666160314145700

Rodríguez-González, V., Gómez, C., Shigihara, Y., Hoshi, H., Revilla-Vallejo, M., Hornero, R., et al. (2020). Consistency of local activation parameters at sensor- and source-level in neural signals. *J. Neural Eng.* 17:056020. doi: 10.1088/1741-2552/abb582

Rodríguez-González, V., Poza, J., Núñez, P., Gómez, C., García, M., Shigihara, Y., et al. (2019). Towards automatic artifact rejection in resting-state MEG recordings: evaluating the performance of the SOUND algorithm. *Annu. Int. Conf. IEEE Eng. Med. Biol. Soc.* 2019, 4807–4810. doi: 10.1109/EMBC.2019.8856587

Roh, J. H., Park, M. H., Ko, D., Park, K.-W., Lee, D.-H., Han, C., et al. (2011). Region and frequency specific changes of spectral power in Alzheimer's disease and mild cognitive impairment. *Clin. Neurophysiol.* 122, 2169–2176. doi: 10.1016/j.clinph.2011.03.023

Ruiz-Gómez, S., Gómez, C., Poza, J., Gutiérrez-Tobal, G., Tola-Arribas, M., Cano, M., et al. (2018). Automated multiclass classification of spontaneous EEG activity in Alzheimer's disease and mild cognitive impairment. *Entropy(Basel)* 20:35. doi: 10.3390/e20010035

Shigihara, Y., Hoshi, H., Poza, J., Rodríguez-González, V., Gómez, C., and Kanzawa, T. (2020a). Predicting the outcome of non-pharmacological treatment for patients with dementia-related mild cognitive impairment. *Aging (Albany NY)* 12, 24101–24116. doi: 10.18632/aging.202270

Shigihara, Y., Hoshi, H., Shinada, K., Okada, T., and Kamada, H. (2020b). Non-pharmacological treatment changes brain activity in patients with dementia. *Sci. Rep.* 10:6744. doi: 10.1038/s41598-020-63881-0

Stam, C. J. (2005). Nonlinear dynamical analysis of EEG and MEG: review of an emerging field. *Clin. Neurophysiol.* 116, 2266–2301. doi: 10.1016/j.clinph.2005.06.011

Stam, C. J., and van Straaten, E. C. W. (2012). The organization of physiological brain networks. *Clin. Neurophysiol.* 123, 1067–1087. doi: 10.1016/j.clinph.2012.01.011

Sugishita, M., Hemmi, I., and Iwatsubo, T. (2010). Japanese versions equivalent to original english neuropsychological tests in ADNI. *Alzheimer's Dement.* 6, S348–S348. doi: 10.1016/j.jalz.2010.05.1166

Tadel, F., Baillet, S., Mosher, J. C., Pantazis, D., and Leahy, R. M. (2011). Brainstorm: a user-friendly application for MEG/EEG analysis. *Comput. Intell. Neurosci.* 2011:879716. doi: 10.1155/2011/879716

Uhlhaas, P. J., Haenschel, C., Nikolic, D., and Singer, W. (2008). The role of oscillations and synchrony in cortical networks and their putative relevance for the pathophysiology of schizophrenia. *Schizophr. Bull.* 34, 927–943. doi: 10.1093/schbul/sbn062

van Deursen, J. A., Vuurman, E. F. P. M., Verhey, F. R. J., van Kranen-Mastenbroek, V. H. J. M., and Riedel, W. J. (2008). Increased EEG gamma band activity in Alzheimer's disease and mild cognitive impairment. *J. Neural Transm. (Vienna)* 115, 1301–1311. doi: 10.1007/s00702-008-0083-y

Wang, J., Fang, Y., Wang, X., Yang, H., Yu, X., and Wang, H. (2017). Enhanced gamma activity and cross-frequency interaction of resting-state electroencephalographic oscillations in patients with Alzheimer's disease. *Front. Aging Neurosci.* 9:243. doi: 10.3389/fnagi.2017.00243

Zhang, W. J. (2011). Constructing ecological interaction networks by correlation analysis: hints from community sampling. *Network Biol.* 1, 81–98. doi: 10.0000/issn-2220-8879-networkbiology-2011-v1-0008

Zucchella, C., Sinforiani, E., Tamburin, S., Federico, A., Mantovani, E., Bernini, S., et al. (2018). The multidisciplinary approach to Alzheimer's disease and dementia. a narrative review of non-pharmacological treatment. *Front. Neurol.* 9:1058. doi: 10.3389/fneur.2018.01058

Conflict of Interest: HH was employed by the company RICOH Company, Ltd.

The remaining authors declare that the research was conducted in the absence of any commercial or financial relationships that could be construed as a potential conflict of interest.

Publisher's Note: All claims expressed in this article are solely those of the authors and do not necessarily represent those of their affiliated organizations, or those of the publisher, the editors and the reviewers. Any product that may be evaluated in this article, or claim that may be made by its manufacturer, is not guaranteed or endorsed by the publisher.

frontiers in Aging Neuroscience

ORIGINAL RESEARCH
published: 11 August 2021
doi: 10.3389/fnagi.2021.675689

Characteristics of Resting State EEG Power in 80+-Year-Olds of Different Cognitive Status

Stephanie Fröhlich[1,2], *Dieter F. Kutz*[1,3], *Katrin Müller*[2,4] *and Claudia Voelcker-Rehage*[1,2]*

[1] Department of Neuromotor Behavior and Exercise, Institute of Sport and Exercise Sciences, Faculty of Psychology and Sport Sciences, University of Münster, Münster, Germany, [2] Department of Sports Psychology (With Focus on Prevention and Rehabilitation), Institute of Human Movement Science and Health, Faculty of Behavioural and Social Sciences, Chemnitz University of Technology, Chemnitz, Germany, [3] Institute of Human Movement Science and Health, Faculty of Behavioural and Social Sciences, Chemnitz University of Technology, Chemnitz, Germany, [4] Department of Social Science of Physical Activity and Health, Institute of Human Movement Science and Health, Faculty of Behavioural and Social Sciences, Chemnitz University of Technology, Chemnitz, Germany

Compared with healthy older adults, patients with Alzheimer's disease show decreased alpha and beta power as well as increased delta and theta power during resting state electroencephalography (rsEEG). Findings for mild cognitive impairment (MCI), a stage of increased risk of conversion to dementia, are less conclusive. Cognitive status of 213 non-demented high-agers (mean age, 82.5 years) was classified according to a neuropsychological screening and a cognitive test battery. RsEEG was measured with eyes closed and open, and absolute power in delta, theta, alpha, and beta bands were calculated for nine regions. Results indicate no rsEEG power differences between healthy individuals and those with MCI. There were also no differences present between groups in EEG reactivity, the change in power from eyes closed to eyes open, or the topographical pattern of each frequency band. Overall, EEG reactivity was preserved in 80+-year-olds without dementia, and topographical patterns were described for each frequency band. The application of rsEEG power as a marker for the early detection of dementia might be less conclusive for high-agers.

Keywords: aged 80 and over, EEG reactivity, resting state EEG, eyes open, eyes closed, mild cognitive impairment

OPEN ACCESS

Edited by:
Priyanka Shah-Basak, Medical College of Wisconsin, United States

Reviewed by:
Ute Gschwandtner, University Hospital of Basel, Switzerland
Victor Rodriguez-Gonzalez, University of Valladolid, Spain

***Correspondence:**
Claudia Voelcker-Rehage
claudia.voelcker-rehage@uni-muenster.de

Received: *03 March 2021*
Accepted: *07 July 2021*
Published: *11 August 2021*

Citation:
Fröhlich S, Kutz DF, Müller K and Voelcker-Rehage C (2021) Characteristics of Resting State EEG Power in 80+-Year-Olds of Different Cognitive Status. Front. Aging Neurosci. 13:675689. doi: 10.3389/fnagi.2021.675689

INTRODUCTION

Dementia is diagnosed due to pronounced cognitive impairments and deterioration in daily living, but pathophysiological changes in the brain usually occur before this critical stage is reached (Sperling et al., 2011). Mild cognitive impairment (MCI), which is characterized as objective cognitive deficits that are more severe than normal aging would suggest, but mild enough to not interfere with daily independence, is thought to be a precursor to dementia (Winblad et al., 2004). Older adults (OA) with MCI have a higher risk of developing dementia, particularly Alzheimer's disease (AD), compared to healthy OA (Mitchell and Shiri-Feshki, 2009) and show more brain neuropathology linked to dementia in postmortem studies (Petersen et al., 2006) and in studies with cerebrospinal fluid analysis (Visser et al., 2009). In longitudinal examinations, the development of patients with MCI is heterogeneous. For example, it was reported that 14% of MCI cases reverted back to normal cognition, 35% progressed to dementia, and 51% stayed stable at the 2-year follow-up (Pandya et al., 2017).

To further understand MCI and its progression to dementia, it is, important to study brain changes in MCI directly and to find biomarkers that better predict progression to dementia. Resting state electroencephalogram (rsEEG) measures seem to be especially suitable because they are easily obtained (non-invasive, no special stimuli necessary, short recording time) and can help to understand the connectivity of brain networks (Babiloni et al., 2019). Differences in rsEEG activity in eyes closed (EC) conditions between healthy OA and patients with AD have been shown consistently (in cross-sectional and longitudinal studies) and include decreased alpha and beta power, increased delta and theta power, and changes in coherence and other functional connectivity measures [for reviews, see Jeong (2004) and Babiloni et al. (2016)]. Similar results were reported for vascular dementia (van Straaten et al., 2012) while frontotemporal dementia does not show consistent differences in rsEEG compared with healthy OA (Nardone et al., 2018).

In contrast, only a few studies compared the rsEEG of healthy OA and OA with MCI during EC. The following studies all included the frequency bands delta, theta, alpha, and beta and reported inconsistent results. For example, in two cross-sectional studies from the same research group, MCI patients (age ∼72 years) had less alpha 1 (8–10.5 Hz) power and stronger delta power, while no changes were present in the theta and beta bands (Babiloni et al., 2006b, 2010). Others also reported higher delta power in MCI (age, 71.9 ± 7.9 years) compared to healthy individuals of the same age and no significant differences in the other frequency bands (Ya et al., 2015). Alternatively, it was reported that theta power was decreased in OA with mild cognitive deficits (age, 70.7 ± 8.8 years) and that changes in other bands were present only in further cognitively declined groups (Prichep et al., 1994). Another study with participants of similar age in the MCI group (72.5 ± 6.0 years) reported lower delta and theta band power, but no change in the faster frequency bands (Kwak, 2006). This study included comparable fewer cases of MCI ($n = 16$) than all other studies mentioned, where the sample size for MCI ranged from 40 to 155 cases. In a different sample with a similar small MCI case amount ($n = 20$, age 74 ± 5 years), no significant differences between patients with MCI and healthy OA in the theta band were detectable, although theta power of the MCI group fell in-between healthy and OA with dementia (van der Hiele et al., 2007a). In addition, it was shown that patients with MCI (mean age, 70.7 years) revealed less alpha and less beta phase-locked synchronization (measured with global field synchronization instead of power), but no changes in the slower frequency bands (Koenig et al., 2005).

Taken together, no conclusive picture for the typical delta, theta, alpha, and beta power values during rsEEG in EC condition in the presence of MCI can be obtained from these studies. It seems that the direction of changes is comparable to findings in dementia. However, which of these changes are earliest in the transition toward dementia and, therefore, most common in MCI is unclear. This might be due to the limited number of studies, including preclinical stages of dementia, small sample sizes, heterogeneity in MCI classification, and heterogeneity in the underlying cause of MCI (Yang et al., 2019).

Heterogeneity of underlying causes for MCI also means that only a certain proportion of MCI cases will progress toward dementia and, therefore, might be the only ones displaying rsEEG patterns similar to those known in dementia. Moreover, many types of dementia exist with AD being the most common cause. Longitudinal studies can take this into account and examine which EEG power parameters at the baseline best predict further cognitive decline or even progression to AD or other types of dementia in OA with MCI. For example, posterior alpha power was reported to be smaller in progressing MCI compared with stable MCI cases (age of all MCI cases at the baseline, 65.9 ± 9.6 years) and predicted worsening of cognitive function in a 1-year period with 75% positive predictive power (Luckhaus et al., 2008). For a longer follow-up period of 21 months, one study has shown that relative alpha power, relative theta power, and mean frequency at the temporo-occipital region in EC conditions at the baseline (age at baseline, 58.2 ± 5.9 years) were the best EEG predictors for conversion to AD (Jelic et al., 2000). Accuracy of prediction was raised from only 70%, which was obtained with MMSE as the only predictor, to 85% by adding EEG parameters (Jelic et al., 2000). The best choice of parameters to predict conversion from MCI (age at the baseline, 68.7 years) to AD over a 2-year follow-up period obtained by data mining from 177 EEG parameters included predominantly beta frequency parameters and reached 88% sensitivity, 82% specificity, and 64% positive predictive value (Poil et al., 2013). The classification rates in all studies so far were not sufficient enough for diagnostic application (Jelic and Kowalski, 2009; Rossini et al., 2020).

Different causes for MCI also mean that subtypes of MCI should be differentiated. Most commonly, this is done by distinguishing between amnestic (aMCI) and non-amnestic (naMCI) cognitive deficits (Petersen, 2004). The aMCI is thought to be primarily related to AD because the relative incidence of AD is significantly higher in aMCI compared with naMCI, although other outcomes, such as vascular dementia or mixed forms, are also possible (Jungwirth et al., 2012). In addition, it has been shown that the amnestic subtype of MCI differs from the non-amnestic type and shows lower central alpha and greater occipital theta power at rest compared with naMCI (Babiloni et al., 2010). Magnetic resonance imaging (MRI) results also support the notion that neuropathological changes are different in both types (Guan et al., 2017).

In addition to disease-related changes, EEG oscillations at rest are also subject to changes during healthy aging. Research on rsEEG (mostly during EC) in healthy OA consistently reveals changes in the alpha band, which are similar to changes found in AD, such as reduced power and reduced peak frequency with increasing age (Rossini et al., 2007). For delta and theta bands, decreases were mostly reported (Babiloni et al., 2006a; Gaál et al., 2010), while activity in the beta band seems to be more pronounced in OA compared with young adults (Koyama et al., 1997; Rossiter et al., 2014). Those changes in delta, theta, and beta bands are in the opposite direction of those reported due to AD. Research on healthy OA as well as MCI, however, has mainly been conducted within the age range of 60–80 years. Thus, there seem to be no detailed reports about topographical or

frequency specific EEG power characteristics in high-agers (>80 years) during rest or in comparison with younger OA.

Most studies so far only analyzed rsEEG data obtained while eyes were closed. Studying eyes open (EO) conditions seems appropriate, considering that task-related brain activity is dependent on the prior background activity (Başar and Güntekin, 2012), and cognitive tasks in everyday life are usually not solved in EC conditions. It has been shown that the classifications between healthy OA and MCI work better with data from EO than EC conditions (McBride et al., 2014). For example, alpha activity during EO was reduced in MCI compared with healthy OA, but alpha activity in EC was not able to discriminate between both groups (McBride et al., 2014). Including both conditions makes it possible to study states of low and moderate vigilance (Babiloni et al., 2019) and to differentiate between global arousal and focal activations (Barry et al., 2007). Investigating the changes from EC to EO conditions, termed EEG reactivity, might be promising as well. EEG reactivity describes the power difference in a frequency band between two distinct conditions (Klimesch, 1999). In the following, reactivity will be defined as the difference in power between EO rest and EC rest (EO-EC). Findings for reactivity are often limited to the alpha band. Synchronous alpha activity observed during EC is blocked when eyes are opened, which can be easily detected in the raw data (Berger, 1929). Healthy OA showed decreased alpha reactivity compared with young adults (Duffy et al., 1984) or a lack of reactivity at all (Gaál et al., 2010). Alpha reactivity was found to be even more decreased in patients with AD compared with healthy OA (van der Hiele et al., 2007b; Schumacher et al., 2020). In a study with small samples sizes, values of the MCI group ($n = 11$) were between the healthy ($n = 12$) and demented group ($n = 10$), but did not differ significantly from the healthy control group (van der Hiele et al., 2007b). Alpha reactivity was also found to be the best predictor of global cognitive performance, memory and language skills across all groups (van der Hiele et al., 2007b).

Recently, Barry and De Blasio (2017) have published rsEEG data for young adults (age, 20.4; range, 18.8–25.6 years) and OA (age, 68.2; range, 59.8–74.8 years), which looked in detail at the topographical characteristics of each frequency band and the changes from EC to EO conditions (reactivity) not only in the alpha frequency but also in the delta, theta, and beta bands. Across both groups, delta and theta power in EO and EC were midline dominant with a maximum at the vertex and a bias toward the right hemisphere (Barry and De Blasio, 2017). For the alpha band, the well-known posterior dominance was reported, and power in the right hemisphere was stronger compared with the left. Activation in the beta band showed centroparietal dominance. For young adults, changes from EO to EC included the overall reduction in power for delta, theta, alpha, and beta bands and a focal frontal increase in the beta frequency (Barry et al., 2007). A similar pattern was found in healthy OA, indicating that the EEG reactivity for delta, theta, alpha, and beta is maintained in healthy aging (Barry and De Blasio, 2017). No further studies exist that investigated EEG reactivity in other frequency bands than alpha in MCI or dementia.

From the current state of research, it can be concluded that further studies with adequate sample sizes are needed to better consider healthy aging as a reference point and the transition to cognitive decline (Yang et al., 2019), especially data for the oldest (>80 years) are lacking for neuropsychological as well as neurophysiological parameters (Slavin et al., 2013). Similarly, dementia research should include more of the oldest participants as they also make up the majority of the affected patients (Brayne and Davis, 2012; Richard et al., 2012).

The aim of the current study was to investigate the association of EEG activity in the delta, theta, alpha, and beta bands during different rest conditions with the cognitive status of OA, ranging from healthy to MCI (aMCI and naMCI). Since cognitive changes in the course from healthy aging to early dementia describe a continuum, the exact diagnostic classification of MCI is difficult (Petersen, 2004). This might become even more difficult with the advancing age of the sample. In order to tackle this uncertainty, we categorized OA into groups of different cognitive status, taking into consideration the level of evidence of cognitive impairments (see Methods) and using the recommendations for diagnosis of MCI in community-based samples (Petersen et al., 2018). This resulted in three groups: (1) cognitively healthy individuals (CHI) with strong evidence of no cognitive impairments, (2) possible MCI (pMCI) subjects with some evidence of cognitive impairments, and (3) MCI participants with strong evidence of cognitive impairments (Müller et al., 2020). The MCI group was further subdivided according to type of cognitive deficits in aMCI and naMCI. As the prevalence of MCI is positively correlated with age (Kryscio et al., 2006), only high agers (participants in their eighties) were included in the study to ensure a sufficient amount of MCI cases in the volunteer sample. Also, this was supposed to fill the previously identified gap for data from high-agers in the context of MCI research.

The main objective was to find out if the rsEEG of 80+-year-olds with MCI (pMCI, aMCI, and naMCI) differed significantly from healthy individuals of the same age. Therefore, differences between groups in mean absolute and mean relative power of the delta, theta, alpha, and beta bands were studied for EO, EC, and reactivity (EO–EC). It was expected that, similar to findings in younger samples of MCI and samples of patients with AD, MCI would have lower alpha and beta power and stronger delta and theta power during EC. In the EO condition, alpha power was expected to decrease in the MCI groups, while, for the other bands, no specific predictions could be made according to prior findings. Alpha reactivity was predicted to be smaller in the MCI groups, while no predictions were made for the other frequency bands.

METHODS

This study is part of the SENDA study (Sensor-based systems for early detection of dementia, registered in the German Clinical Trials Register under DRKS00013167), which was conducted at Chemnitz University of Technology, Germany. The detailed study protocol was published earlier by Müller et al. (2020). Only

TABLE 1 | Characteristics of the total sample and groups according to cognitive status.

	Total		CHI		pMCI		naMCI		aMCI		
N (in %)	213 (100)		72 (34)		80 (38)		17 (8)		44 (21)		
m/f	109/104		32/40		43/37		12/5		22/22		
Age in years *M* (*SD*)	82.5	(2.4)	82.1	(2.4)	82.5	(2.1)	83.2	(3.1)	83.0	(2.7)	
Education in years *M* (*SD*)	14.0	(3.2)	14.4	(3.4)	14.0	(3.3)	14.3	(3.2)	13.3	(2.7)	
MoCA (0–30) *M (SD)*	25.6	(2.6)	27.8	(1.2)	25.8	(2.1)	22.8	(1.6)	22.8	(1.7)	*a
Handedness (-100–100) *M (SD)*	83.3	(38.2)	89.1	(24.4)	81.9	(41.6)	78.2	(39.5)	81.5	(42.6)	
GDS Score (0–15) *M* (*SD*)	2.8	(2.0)	2.6	(1.9)	2.6	(1.8)	3.6	(2.7)	3.4	(2.1)	
NAA Score (20–60) *M* (*SD*)	26.3	(3.4)	25.3	(2.7)	25.9	(3.3)	29.5	(4.5)	27.9	(3.0)	*b

CHI, cognitively healthy individuals; pMCI, possible mild cognitive impairment; naMCI, non-amnestic MCI; aMCI, amnestic MCI; MoCA, Montreal Cognitive Assessment; GDS, Geriatric Depression Scale; NAA, Nürnberger-Alters-Alltagsaktivitätäten-Skala (Nuremberg Gerontopsychological Rating Scale for Activities of Daily Living).

*$p < 0.05$.

[a]*Post-hoc Dunn Bonferroni test showed: CHI > pMCI > naMCI = aMCI.*

[b]*Post-hoc Dunn Bonferroni test showed: CHI = pMCI< naMCI = aMCI.*

information relevant to the current research question will be described here.

Participants

The SENDA study sample included 244 participants (123 males; age, 79–93 years; $M = 82.5$; $SD = 2.5$), which were recruited from January 2018 to March 2020. Study participation required walking ability, sufficient German language skills, residence in or around Chemnitz, Germany, and self-organized means of travel to and from the laboratory. Volunteers were excluded before testing if any of the following criteria applied: (1) acute psychological disorder; (2) diagnosis of any neurocognitive or neurological disorder; (3) past traumatic head injury; (4) substance abuse; (5) participation in other clinical studies; (6) a physician-directed ban from physical activities; (7) severe restrictions due to cardiovascular, pulmonary, or orthopedic diseases; (8) or failure to reach the minimum required score of 19 during screening with the Montreal Cognitive Assessment (MoCA, Nasreddine et al., 2005). Each participant signed a written informed consent, and all study proceedings were approved by the Ethics Committee of Chemnitz University of Technology, Germany, Faculty of Behavioral and Social Sciences (V232-17-KM-SENDA-07112017, approved on 19.12.2017). Each participant received 25 € compensation for his or her participation at three appointments. This included neuropsychological testing (part of first appointment) and EEG recordings (part of the second appointment).

The analysis for this article included 213 participants. Exclusion from analysis was due to (1) dropout from the study before all needed testing was completed ($n = 17$), (2) signs of severe depressive symptoms [Geriatric Depression Scale (Gauggel and Birkner, 1999) short version > 8, $n = 9$], (3) technical issues during the EEG recording, ($n = 4$), (4) and falling asleep during EEG recording ($n = 1$). Demographic characteristics are reported in **Table 1**. In addition, the participants reported their medication regimens. Due to the old age of the participants, many of them were following a medication regimen, which most often included medication for high blood pressure, thrombosis prophylaxis, cholesterol reduction, stomach acid reduction, and thyroid function. There were 15 participants taking medication, which might have influenced EEG activity, such as tricyclic antidepressants ($n = 6$), antipsychotics ($n = 2$), Parkinson medication ($n = 2$), anti-dementia medication ($n = 2$), and benzodiazepines ($n = 5$, prescribed for sporadic, not regular use, according to medication plans). These cases were distributed across all four groups (CHI: 3, pMCI: 4, naMCI: 5, and aMCI: 3). Conducting the following analysis without these cases did not result in any differences, and we, therefore, did not remove them from the sample.

Neuropsychological Testing and MCI Classification

All the participants went through an intensive neuropsychological test battery, which was carried out from trained testing staff at the University lab. This included the German version of the MoCA (Nasreddine et al., 2005) and the German version of the Consortium to Establish a Registry for Alzheimer's Disease Neuropsychological Test Battery (Morris et al., 1989; Memory Clinic Basel, 2005; CERAD-NP). The MoCA was used to measure global cognitive functioning and to screen for MCI. It is the second most utilized geriatric cognitive screening tool after the mini mental status examination but has superior sensitivity to mild cognitive impairments (Breton et al., 2019). The CERAD-NP examines the cognitive domains memory, language, executive functions, and visuo-construction. In addition, information about the level of education (overall years of education) and handedness [a laterality quotient according to Oldfield (1971)] was obtained. The participants completed additional questionnaires at home, which included, among others, the Nürnberger-Alters-Alltagsaktivitätäten-Skala (NAA; Nuremberg Gerontopsychological Rating Scale for Activities of Daily Living; Oswald and Fleischmann, 1995) to measure basic and instrumental activities of daily living as well as the German short version of the Geriatric Depression Scale (GDS; Gauggel and Birkner, 1999) to screen for depressive symptoms. The GDS was used to exclude individuals from the analysis (GDS > 8) to prevent the inclusion of undetected cases of major depression and also as a covariate.

MCI classification was based on the recommendations of The National Institute on Aging and the Alzheimer's Association (Albert et al., 2011) and in accordance with the criteria proposed by Petersen et al. (2014). These criteria are also part of the Diagnostic and Statistical Manual of Mental Disorders (5th ed.; DSM-5; American Psychiatric Association, 2013) for the diagnosis of mild neurocognitive disorders. The criteria were: (1) self—or informant report of cognitive complaints, (2) impairments in at least one cognitive domain while taking into consideration age and education, (3) general independence in daily activities, and (4) no dementia. Cognitive complaints (criteria 1) were not included as a criterion of MCI here because there is no consensus on inclusion or operationalization (Mitchell, 2008). Subjective complaints also seem to be far less relevant for the prediction of dementia in community-based samples like ours compared with the participants in memory clinics (Snitz et al., 2018). In addition, we found subjective complaints to be very common in this age group. In a subgroup of our sample ($n = 136$), 65% of the participants reported memory complaints when asked to compare their memory performance 5 years prior.

Cognitive impairments (criteria 2) were determined according to performance in MoCA (one sum score) and CERAD-NP (nine separate test scores). The following CERAD-NP scores were used: verbal fluency (number of animals named in 1 min), Boston naming test (number of objects correctly identified), phonematic fluency (number of words named with letter "S" in 1 min), constructional praxis (number of correctly copied characteristics), word list learning (number of words correctly remembered in third trial), word list recall (savings score), word list recognition (discriminability score), constructional praxis recall (savings score), and trail making test (quotient B/A). We followed a two-step procedure that is recommended for diagnosis of MCI in the general population, which states that, first, a screening should be used, and, in case of abnormal findings, in-depth cognitive testing should follow (Petersen et al., 2018). A MoCA score below 26 points and at least one CERAD-NP performance below 1.5 standard deviations of the normative mean (taking into consideration age, sex, and education level) resulted in the classification of mild cognitive impairment (MCI). Correspondingly, the participants were classified as being healthy (CHI) if they scored 26 or more points on the MoCA and also within the normative range (no score below −1.5 SD) in all of the CERAD-NP scores. Out of the participants classified as MCI, amnestic cases (aMCI) were distinguished by deficits in at least one of the memory tests (word list learning, word list recall, word list recognition, and constructional praxis recall). Accordingly, non-amnestic cases (naMCI) presented with deficits only in the other non-memory tests. Due to the application of the two-step process, an additional class was defined for the participants who showed cognitive impairments only according to one of the two tests. They were categorized as possibly having MCI (pMCI). This group either included the participants who had deficits in one specific domain of the CERAD-NP, but, overall, cognitive functioning was normal according to MoCA or the participants that had no strong impairment in any single domain, but small deficits in different domains added up to a low MoCA score (<26). Although this group would be considered as non-MCI according to Petersen et al. (2018) as these individuals neither showed abnormal scores in the screening (MoCA > 25) nor in-depth clinical testing after abnormal testing revealed any cognitive impairments, we opted to separately analyze this group to have high discriminatory power between CHI and MCI.

General independence (criteria 3) was presumed for all the participants because we only included community-dwelling volunteers in this study. This was further confirmed by the NAA scores, which were below 39 for all individuals and fell within a normal range for this age group (Oswald and Fleischmann, 1995). No dementia (criteria 4) was also ensured due to the exclusion criteria described before.

EEG Recordings

The actiCHamp system (Brain Products GmbH, Gilching, Germany) was used to record 32 active EEG electrodes positioned according to the international 10–20 system (Fp1, Fp2, F7, F3, Fz, F4, F8, FC5, FC3, FC1, FC2, FC4, FC6, T7, C3, Cz, C4, T8, CP5, CP3, CP1, CP2, CP4, CP6, P7, P3, Pz, P4, P8, O1, Oz, and O2). The setup included a forehead ground electrode at Fpz and an online reference electrode at Fz. All data were acquired with a 500 Hz sampling rate and 24-bit resolution. The electrode-skin impedance was kept below 25 kΩ.

The EEG recording during rest only made up a small part of the complete testing on the day and always took place after gait analysis and prior to fine motor testing. Rest periods were offered during the whole procedure, and all the participants had received a short break prior to EEG recording. EEG measurements took place in an electrically shielded and darkened room. To minimize EEG artifacts and distractions for the subject, all instructions were given from an adjacent room *via* a microphone and a monitor. The participants sat relaxed, with their backs leaned against the back rest and both hands rested comfortably on the table in front of them (see **Figure 1A** for a photo of the complete setup). They looked at a white fixation cross at the center of a black screen for 4 min (condition EO) and, afterwards, closed their eyes for 2 min (condition EC). The level of consciousness the subject was monitored to annotate changes and other artifacts in the EEG protocol.

Preprocessing of EEG Data

BrainVision Analyzer 2.2 (Brain Products GmbH, Gilching, Germany) was used for all preprocessing steps. Data were filtered (phase shift-free Butterworth infinite impulse response filter, 1–70 Hz, slope 48 dB/Hz), notch filtered (50 Hz), and down sampled from 500 to 256 Hz. In addition, blink artifacts in the rest condition EO were removed *via* Independent Component Analysis (Jung et al., 1998) with Fp1 as the reference channel for vertical eye movements. Continuous EEG data were then common average re-referenced and segmented into 2-s epochs for an automatic artifact rejection. Epochs were rejected from further analysis if at least one channel included voltage steps >25 μV/ms or if the difference between minimal and maximal absolute voltage recorded exceeded 200 μV in any 200 ms interval.

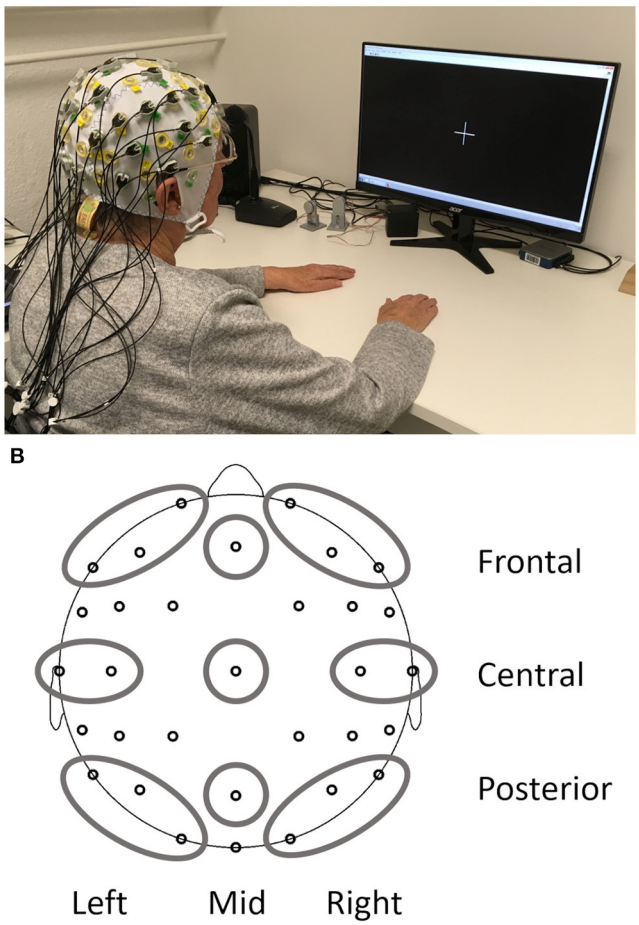

FIGURE 1 | Setup of the resting state EEG measurements **(A)** and depiction of the nine regions of interest obtained from the EEG **(B)**.

At each electrode absolute power (in μV^2) and relative power (in %, relative to the total power of the spectrum 1–24 Hz) was calculated with a Fast Fourier Transform algorithm for each 2s epoch resulting in 0.5 Hz resolution. A Hanning window (length 10%) and variance correction were applied to correct for spectral leakage. Mean absolute power and mean relative power were obtained by averaging 15 artifact-free segments for 30 s after the start of the condition. One participant did not have enough artifact free segments for the EO and another participant for the EC condition. Therefore, EO and EC analyses were carried out with $N = 212$ and the reactivity analysis with $N = 211$. Frequency bands included delta (1–3.5 Hz), theta (4–7.5 Hz), alpha (8–13 Hz), and beta (13.5–24 Hz). All data were log-transformed (base 10) to obtain normal distribution and variance homogeneity before calculation of regions of interest (ROI) based on Barry and De Blasio (2017). The combination of three sagittal planes (left, mid, and right) and three coronal planes (frontal, central, and posterior) resulted in nine different ROIs (**Figure 1B**): left frontal (Fp1, F3, and F7), mid frontal (Fz), right frontal (Fp2, F4, and F8), left central (T7 and C3), mid central (Cz), right central (T8 and C4), left posterior (P7, P3, and O1), mid posterior (Pz), and right posterior (P8, P4, and O2). Reactivity for absolute and relative power was calculated separately for each frequency band as the difference between EO and EC (log power EO- log power EC) for each ROI.

In addition, from the same spectrum (relative power, EC condition, 30 s), we also obtained the individual alpha frequency (IAF) for each person. All electrodes of the posterior region (P7, P3, O1, Pz, P8, P4, and O2) were averaged, and the frequency of the maximum value in the alpha band was extracted with the MinMax Marker Solution (BrainVision Analyzer 2.2). Six participants were not included in this analysis because they did not show clear peaks in the alpha range. This was indicated by the values of the detected peak being less than 1.96 standard deviations above the mean value of the alpha range. Visual inspection of the cases indicated either absence of a peak or a peak in the theta range.

Statistical Analysis

IBM SPSS Statistics Version 27 (IBM Corp., Armonk, NY, USA) was used for all statistical analysis. *P*-values < 0.05 were regarded as significant and *p*-values < 0.10 as a trend unless they had to be adjusted for multiple testing. Effect sizes were reported as partial eta squares (η_p^2). As variables were not normally distributed, Kruskal–Wallis tests were used to test if covariates age, education, and depressive symptoms differed between groups. A chi-square test was used to test if sex and group distributions were independent. No significant differences between groups emerged for any of the covariates, which means that potential effects of cognitive status on EEG parameters should not be due to sex, age, and education confounding with the group classification.

First, absolute power data were pre-analyzed in order to check if reactivity was still preserved in the sample of high-agers. For this purpose, a $2 \times 3 \times 3 \times 4$ mixed-design ANOVA was carried out with the three within-subject factors rest condition (EO, EC), sagittal (left, mid, and right) and coronal (frontal, central, and posterior) as well as one between-subject factor group (CHI, pMCI, naMCI, and aMCI), and the main effect of rest condition was reported for each frequency band.

All the following analyses were run with sex as covariate. Age and education in years were not included as covariates because there was no significant relationship with any of the EEG parameters, and their inclusion did not improve variance explanation. One-way analysis of covariance (ANCOVA) was used to test for differences in IAF between groups. Next, six $3 \times 3 \times 4$ mixed-design ANCOVAs were carried out with the dependent variables (1) absolute EC power, (2) absolute EC power, (3) absolute power reactivity, (4) relative EO power, (5) relative EO power, and (6) relative power reactivity, respectively. Each ANCOVA included two within-subject factors sagittal (left, mid, and right) and coronal (frontal, central, and posterior) as well as one between-subject factor group (CHI, pMCI, naMCI, and aMCI) to find differences between groups and topography. Greenhouse-Geisser adjustments were reported whenever sphericity assumptions were violated. To control for multiple testing within each frequency band (three tests for

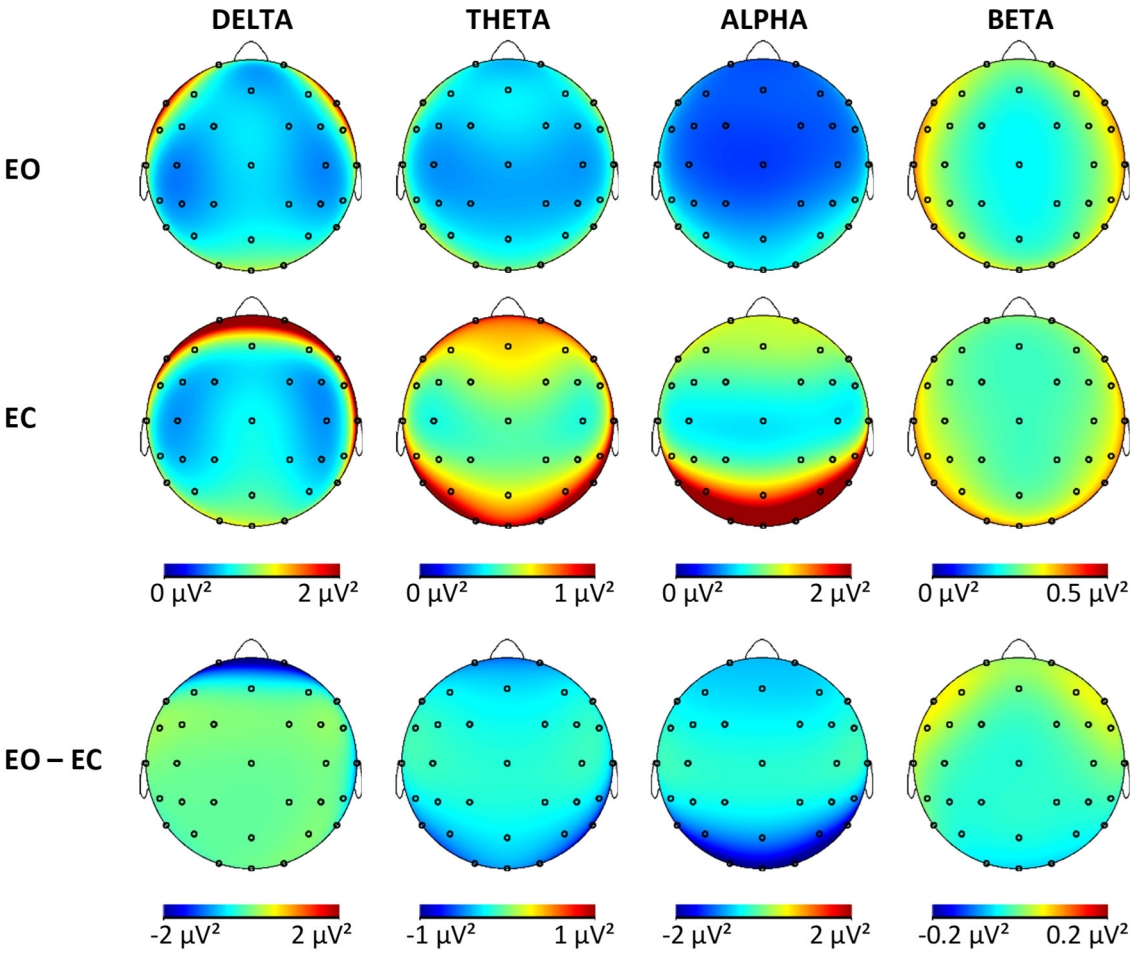

FIGURE 2 | Brain maps showing the mean absolute power in μV^2 for all frequency bands in both conditions and the difference maps. EO, eyes open; EC, eyes closed.

absolute power and three tests for relative power), the Bonferroni adjusted alpha level of 0.017 was used. Last, the directions of the significant main and interaction effects from the 3 × 3 × 4 ANCOVAs were determined *via* contrast analysis to describe the topography in more detail. For the coronal factor, two contrasts were used: comparing frontal with posterior (F – P) and comparing the mean of frontal and posterior against the central ROI (F/P – C). Similarly, two contrasts were included for the sagittal factor: comparing left with right (L – R) and comparing the mean of left and right with the mid ROI (L/R – M). Again, Bonferroni adjusted alpha levels were used to control for testing multiple contrasts within one effect (main effects: 0.025 interaction effect: 0.0125). Only significant effects are reported in the text unless stated otherwise.

RESULTS

Reactivity

Results from the 2 × 3 × 3 × 4 mixed-design ANOVA indicated a significant reduction in absolute power from EC to EO across the whole sample in delta [$F_{(1,207)} = 30$, $p < 0.001$, $\eta_p^2 = 0.13$], theta [$F_{(1,207)} = 144.4$, $p < 0.001$, $\eta_p^2 = 0.41$], alpha [$F_{(1,207)} = 275.3$, $p < 0.001$, $\eta_p^2 = 0.57$], and beta bands [$F_{(1,207)} = 6.6$, $p = 0.01$, $\eta_p^2 = 0.03$].

Cognitive Status

Classification of participants in the four groups (CHI, pMCI, aMCI, and naMCI) according to the introduced criteria resulted in 72 CHI, 80 pMCI, 17 naMCI, and 44 aMCI cases (**Table 1**). The four groups differed significantly according to problems with daily activities measured with the NAA (CHI = pMCI< aMCI = naMCI). The IAF was fastest in the healthy group ($M = 9.3$ Hz, $SD = 1.1$) compared with the groups with cognitive impairments (pMCI: $M = 9.0$ Hz, $SD = 0.8$, naMCI: $M = 9.1$ Hz, $SD = 0.8$, aMCI: $M = 9$, $SD = 0.8$). These differences were not significant [$F_{(3,206)} = 1.6$, $p = 0.19$, $\eta_p^2 = 0.02$].

Tables with log-transformed absolute power values for each frequency band, group, and ROI are available in the **Supplementary Material**. Results of the mixed ANCOVA for each frequency band for the outcome variables (power EC, power EC, and reactivity) revealed no significant group effects or interactions involving the factor group for neither absolute

nor relative power analysis. The p-values for these nonsignificant effects ranged from $p = 0.05$ to $p = 0.90$ (with effect sizes between $\eta_p^2 = 0.00$ and $\eta_p^2 = 0.04$) for absolute power and $p = 0.02$ to $p = 0.98$ (with effect sizes between $\eta_p^2 = 0.01$ and $\eta_p^2 = 0.04$) for relative power. In this sample, the rsEEG activity in the four frequency bands did not differ significantly according to the cognitive status of the participants when using absolute or relative power values. As no differences between groups were established, all the participants were pooled together to obtain brain maps from the non-transformed absolute power values (**Figure 2**) for each frequency band and condition for this sample of OA to illustrate the topographies. The maps for each group separately are available in the **Supplementary Material**. In the whole sample, the effects were significant for the sagittal factor, the coronal factor, and the interaction between sagittal and coronal for all frequency bands and absolute power outcomes. The topographical effects will be looked at in more detail in the following sections only for absolute power. Relative power values are especially useful to control for person-specific confounding variables, which are less relevant to within-subject effects. In addition, differences in relative power are less clear to interpret because they can be caused by changes in the studied frequency band or changes in any of the other bands used in normalization. The results from the topographical analysis of relative power are available in the **Supplementary Material**.

Topography During EC

The complete results of the contrast analysis can be seen in **Table 2**. For all frequency, bands activity was significantly smaller at the midline compared to hemispheres (L/R > M). There was no effect of lateralization in any of the frequency bands (L = R). Both alpha and beta were dominant in the posterior regions (F < P), while delta band was dominant in the frontal region (F > P). For the delta, theta, and alpha bands, central activity was less pronounced compared with the mean activity from frontal and posterior (F/P > C). In the delta band, the difference between midline and hemispheres was more pronounced frontally compared with the posterior regions (L/R > M × F > P). For all other bands, this was reversed with stronger differences between midline compared with L/R in the posterior regions instead of frontal regions (L/R > M × F < P). Although no global effect of lateralization was obtained in the alpha band, there was more pronounced activity in the right hemisphere of the posterior region (L < R × F < P). The smallest power values for theta and delta were obtained from the mid-central regions (L/R > M × F/P > C).

Topography During EO

The topography during the EO was very similar to EC topography (**Tables 2**, **3**). The only differences pertained to lateralization, where theta and alpha both showed greater power in the left compared with the right hemisphere (L > R) and no differences in lateralization between frontal and posterior regions.

Topography of Reactivity

Topographical differences in reactivity were apparent in the descriptive reactivity data (**Supplementary Material**) and were confirmed by the contrast analysis (**Table 4**). When interpreting the direction of effects, the sign of the reactivity values must be considered. When comparing two negative values, the smaller value is the more negative value and, therefore, indicates the larger change from EC to EO.

For the delta band, the pattern of reactivity resembled that of the EC condition, which means that the greatest changes from EC to EO were present in the areas with the most delta activity during EC [F < P; F/P < C; L/R < M × F > P; L/R < M × F/P > C]. For the theta, band reactivity was less pronounced in the central regions (F/P < C), specifically the left and right hemispheres (L/R > M × F/P < C), which were also the regions with less theta activity in EO and EC. In the alpha band, once again, reactivity was more pronounced in the right compared with the left hemisphere (L > R), which explained the change from a right hemispheric bias during EC to a significant left hemispheric bias during EO. Further considerations of interactions actually showed that this was only the case in the posterior but not the frontal region (L > R × F < P). The change from EC to EO in alpha power was greater in the midline compared with hemispheres (L/R > M), especially so in the frontal regions (L/R > M × F > P). Reactivity was strongest in the posterior region and least pronounced in the central regions (F > P, F/P < C), which reproduces the pattern of alpha activity during EC. In the beta band, reactivity was more pronounced in the midline compared with the hemisphere (L/R > M) and in the posterior compared with frontal regions (F > P). This is related to the fact that beta activity in the hemispheres is increasing in the left and right frontal regions while it is decreasing with the opening of eyes in the other regions (L/R > M × F > P). This focal frontoparietal activity with opening the eyes can also be seen in **Figure 2** (last column).

DISCUSSION

In this study, the synchronized activity at rest while eyes are open and closed in the classical broad bands delta, theta, alpha, and beta was compared between cognitively healthy OA and individuals with MCI of the same age. The sample included OA, 80 years or older, which are often not enough represented in studies on early detection of dementia. Groups were compared with respect to mean absolute power, relative power, and reactivity to eyes opening separately in each band. No significant differences between any of the groups of different cognitive status (CHI, pMCI, naMCI, and aMCI) were detected. Overall, specific topographical patterns were present, which will be compared with results from other age groups later. In addition, EEG reactivity was also present in each of the four frequency bands with overall greater power during EC compared with EO and a few focal increases in the beta band. The topography of reactivity for the most part related to the topography found in the EC condition.

TABLE 2 | Results of the contrast analysis in each frequency band for absolute power (log-transformed) at rest with eyes closed.

	Delta			Theta			Alpha			Beta		
	F	***p***	η_p^2	***F***	***p***	η_p^2	***F***	***p***	η_p^2	***F***	***p***	η_p^2
Main Effects (adj. α-level = 0.025)												
L > R	4.1	0.04	0.02	1.9	0.18	0.01	1.1	0.129	0.01	0.0	0.89	0.00
L/R > M	266.5	**<0.001**	0.56	264.4	**<0.001**	0.56	387.4	**<0.001**	0.65	141.5	**<0.001**	0.41
F > P	130.5	**<0.001**	0.39	1.1	0.29	0.01	236.4	**<0.001**	0.53	26.4	**<0.001**	0.11
F/P > C	135.7	**<0.001**	0.40	165.3	**<0.001**	0.44	115.0	**<0.001**	0.36	3.1	0.08	0.02
Interactions (adj. α-level = 0.0125)												
L > R x F > P	1.4	0.23	0.01	0.4	0.51	0.00	11.9	**0.001**	0.05	3.1	0.08	0.02
L > R x F/P > C	2.2	0.14	0.01	0.2	0.62	0.00	2.6	0.11	0.01	0.8	3.8	0.00
L/R > M x F > P	86.7	**<0.001**	0.30	4.7	0.03	0.02	81.1	**<0.001**	0.28	15.2	**<0.001**	0.07
L/R > M x F/P > C	15.9	**<0.001**	0.07	8.1	**0.005**	0.04	1.3	0.26	0.01	1.2	0.28	0.01

All test statistics are with (1, 207) degrees of freedom. Underlined effects are reversed in direction (i.e., the reversed effect from L > R × F > P is L < R × F > P). Changing the direction of both directional indicators within a single effect is equivalent (i.e., L > R × F > P is the same as L < R × F < P). L, left; R, right; M, midline; F, frontal; P, posterior; C, central. Significant results are printed in bold.

TABLE 3 | Results of the contrast analysis in each frequency band for absolute power (log-transformed) at rest with eyes open.

	Delta			Theta			Alpha			Beta		
	F	***p***	η_p^2	***F***	***p***	η_p^2	***F***	***p***	η_p^2	***F***	***p***	η_p^2
Main Effects (adj. α-level = 0.025)												
L > R	3.6	0.06	0.02	6.1	**0.02**	0.03	11.4	**0.001**	0.05	1.7	0.18	0.01
L/R > M	158.6	**<0.001**	0.43	173.7	**<0.001**	0.46	408.9	**<0.001**	0.66	143.4	**<0.001**	0.41
F > P	39.0	**<0.001**	0.16	2.9	0.09	0.01	106.1	**<0.001**	0.34			
F/P > C	50.7	**<0.001**	0.20	86.4	**<0.001**	0.29	12.0	**0.001**	0.06			
Interactions (adj. α-level = 0.0125)												
L > R x F > P	0.0	0.87	0.00	2.6	0.11	0.01	0.0	0.95	0.00	6.7	**0.01**	0.03
L > R x F/P > C	1.4	0.23	0.01	0.1	0.80	0.00	0.5	0.47	0.00	0.5	0.49	0.00
L/R > M x F > P	24.1	**<0.001**	0.10	16.5	**<0.001**	0.08	14.8	**<0.001**	0.07	0.6	0.45	0.00
L/R > M x F/P > C	1.4	0.12	0.01	0.1	0.72	0.00	45.2	**<0.001**	0.18	7.4	**0.01**	0.03

All test statistics are with (1,207) degrees of freedom. Underlined effects are reversed in direction (i.e., the reversed effect from L > R × F> P is L < R × F > P). Changing the direction of both directional indicators within a single effect is equivalent (i.e., L > R × F > P is the same as L < R × F < P). L, left; R, right; M, midline; F, frontal; P, posterior; C, central. Significant results are printed in bold.

TABLE 4 | Results of the contrast analysis in each frequency band for reactivity (difference of log-transformed absolute power).

	Delta			Theta			Alpha			Beta		
	F	***p***	η_p^2	***F***	***p***	η_p^2	***F***	***p***	η_p^2	***F***	***p***	η_p^2
Main Effects (adj. α-level = 0.025)												
L > R							21.8	**<0.001**	0.10	1.3	0.25	0.01
L/R > M							9.1	**0.003**	0.04	18.7	**<0.001**	0.08
F > P	18.0	**<0.001**	0.08	0.1	0.76	0.00	66.2	**<0.001**	0.24	29.3	**<0.001**	0.12
F/P > C	39.7	**<0.001**	0.13	25.9	**<0.001**	0.11	86.6	**<0.001**	0.30	0.5	0.48	0.00
Interactions (adj. α-level = 0.0125)												
L > R x F > P	0.6	0.43	0.00	4.5	0.04	0.02	8.5	**0.004**	0.04	2.2	0.14	0.01
L > R x F/P > C	0.1	0.76	0.00	0.1	0.80	0.00	1.0	0.33	0.01	0.1	0.77	0.00
L/R > M x F > P	11.5	**0.001**	0.05	2.83	0.09	0.00	30.6	**<0.001**	0.13	7.9	**0.01**	0.04
L/R > M x F/P > C	8.9	**0.003**	0.04	8.0	**0.01**	0.04	28.3	**<0.001**	0.12	5.5	0.02	0.03

All test statistics are with (1,206) degrees of freedom. Underlined effects are reversed in direction (i.e., the reversed effect from L > R × F > P is L < R × F > P). Changing the direction of both directional indicators within a single effect is equivalent (i.e., L > R × F > P is the same as L < R × F < P). L, left; R, right; M, midline; F, frontal; P, posterior; C, central. Significant results are printed in bold.

No significant differences between any of the groups of different cognitive status were found in IAF or resting state power in EC, and, therefore, it can be concluded that the absolute and relative power distributions were similar in each of the four groups (CHI, pMCI, naMCI, and aMCI) for this condition. Thus, the hypotheses that MCI is characterized by lower alpha and beta power as well as stronger delta and theta power during EC could not be confirmed in our sample. This is not in complete agreement with prior findings of changes in the rsEEG in patients with MCI. For the rest with EC, it was shown that alpha and beta powers were reduced and theta and delta powers were either elevated or reduced in MCI compared with healthy OA (Koenig et al., 2005; Babiloni et al., 2006b, 2010; Kwak, 2006; Ya et al., 2015). In fact, when specifying former studies, each study only showed some of the listed changes, but the overlap between results was often not great even though similar parameters were studied.

One might assume that the lack of significant differences between MCI and healthy participants in our study was caused by an unsuitable resting state measurement protocol. This seems to be rejectable as the protocol was very comparable to the ones used in other MCI and dementia studies (e.g., Alexander et al., 2006; van der Hiele et al., 2007b; Gaál et al., 2010; Toth et al., 2014).

One major difference between the current findings and that of other studies was the overall older age (mean, 82.5 years) of the participants. The average age of most study samples was ∼10–20 years below that of the present sample [e.g., 62 years (Koenig et al., 2005), 68 years (Barry and De Blasio, 2017), and 72 years (Babiloni et al., 2006b)]. In addition, the number of rsEEG studies in this age group is very limited, which means that there is limited knowledge of the typical rsEEG in MCI, but it is also unclear how the rsEEG activity of healthy high-agers looks. Some aging-related changes in the rsEEG, like the reduction in alpha power, are probably similar in the aging process and the neuropathological process of dementia (Rossini et al., 2007), and, therefore, it might be harder to differentiate between healthy but far advanced aging and early neuropathological changes. Postmortem studies also showed that dementia pathology, such as neuritic plaques, diffuse plaques, and neurofibrillary tangles can be found in healthy OA without signs of dementia or MCI during their lifetime (Bennett et al., 2006). In general, the overlap in neuropathology between healthy and individuals with dementia seems to increase with age (Richard et al., 2012). Taken all together, this suggests that the cognitive status of high-agers as determined by neuropsychological testing might not necessarily represent the underlying neurophysiological state.

For EEG measurements, it must also be considered that aging can cause anatomical changes that can dampen the measurable EEG signal. It has been shown that cortical thinning with aging results in smaller measurable EEG amplitudes and that power differences between different age groups can be explained by including cortical thickness into the analysis (Provencher et al., 2016). As a consequence, it might be statistically problematic to detect differences if the baseline level of power is very low. On average, this is not the case in the current sample. The power values at rest with EO in the present data set are comparable with values found in a prior study (Hübner et al., 2018) with younger OA (67–83 years).

The different groups of cognitive status were also compared with regard to resting state power while EO and reactivity (change from EC to EO). Although it had been shown before that EO conditions might be better suitable to detect EEG changes in MCI (McBride et al., 2014), this was not replicated here. The present results indicated no differences in resting state power with EO or reactivity according to cognitive status in any of the frequency bands. Thus, the hypothesis that MCI is characterized by reductions in alpha power during EO and reduced reactivity in the alpha band was not confirmed. In addition, for the first time, analysis of reactivity was not restricted to the alpha band and included also delta, theta, and beta bands. Group comparisons showed that reactivity in the other bands was also not related to cognitive status.

In addition, we studied the topography and reactivity of each frequency band without taking into consideration the cognitive status of the participants to generate knowledge about the rsEEG in a group of non-demented high-agers. The topography of the slower bands (delta and theta) was described with maximal power at the vertex in both rest conditions in healthy OA in prior studies (Barry and De Blasio, 2017). This topography was not replicated here, as delta power showed frontal dominance with the smallest power at the vertex. Theta power was also smallest in the central regions. It is unclear why these differences arise and if a small sample size of prior studies, EEG setup or artifacts could be the cause of this. As this pattern was especially pronounced during EC condition, which typically shows very little frontal artifacts such as blinking, this should not be the reason. Other studies with young participants actually reported a very similar pattern with prefrontal dominance of delta power (Barry et al., 2007; Chen et al., 2008).

For the alpha band, topography was similar and, as expected, showed strongest alpha power in the posterior ROI and smallest power values centrally. A right hemisphere bias was present in the alpha band during EC conditions and a left hemisphere bias in the alpha and theta bands during EO, while, for all other bands and conditions, no hemispherical differences were found. In comparison, younger adults showed a right hemisphere bias across all frequency bands during rest (EO and EC), which is assumed to arise from the dominance of the left hemisphere in right-handed participants (Simon-Dack et al., 2013; Barry and De Blasio, 2017). This difference between our sample and results from younger OA confirms many findings of age-related neural dedifferentiation (Koen and Rugg, 2019).

The changes in band power due to eyes opening, in general, resembled what has been shown in younger adults. Reactivity was present in all bands and showed the typical pattern of overall decreased power in all bands, and only focal frontal increases in the beta band in EO (Barry and De Blasio, 2017). Even in high-agers, reactivity is maintained in all frequency bands, showing intact regulation of arousal and vigilance in the different resting state conditions. The exact topographical pattern for delta, theta, and alpha bands related to the observed EC pattern in each band, meaning the difference EO – EC was the strongest in ROIs that

showed the most activity during EC (delta: frontal, theta: frontal and posterior, alpha: posterior).

Limitations

Some limitations of this study must be considered. First, all the participants were volunteers, without symptoms of dementia and no need to live in a nursing home. These constraints resulted in the sample having a bias toward comparatively healthy and well-educated individuals. Education could be an influencing factor, because it is known as a proxy of a cognitive reserve, and it can impact the relationship between brain changes and performance measured in neuropsychological testing (Liu et al., 2013). This should not influence the present results because the groups did not differ in their levels of education.

In addition, one might assume that the MCI cases found in this sample were mostly very mild and far from the progression to dementia. However, the range of MoCA scores (19–25) and the deficits found in CERAD-NP scores (<1.5 SD below age specific norms) for the MCI groups indicated that this is not the case. Although the norms of neuropsychological test batteries like the CERAD-NP can be very strict when used for individuals older than 75 years (Luck et al., 2018), this issue was resolved by using a two-step classification system to evaluate the cognitive status of the participants. This included the neuropsychological test battery (CERAD-NP) with age- and sex-corrected norm values and the MoCA. This screening tool is known to detect MCI well-compared with others like the Mini Mental Status Examination, which suffers from ceiling effects in populations with mild impairments (Larner, 2012; Breton et al., 2019). Standardized classification criteria according to recommendations of the neurotic National Institute on Aging and the Alzheimer's Association (Albert et al., 2011) were employed. This procedure is certainly comparable to the standard clinical procedure, which includes first a screening and then more extensive neuropsychological testing. In addition, this recruitment procedure was chosen to obtain a sample of OA with no or only mild cognitive deficits, as we were especially interested in those early preclinical stages of dementia. Other studies often used MCI samples that arose from memory clinics, where probably, individuals applied with complaints, indicating further progressive cognitive decline. Conversely, the present sample allowed to study the process of cognitive decline even earlier.

The prevalence of MCI obtained from this strategy was 29%, which is slightly higher than the incidence rate for community samples calculated in a recent meta-analysis (Hu et al., 2017). Considering the age of the sample, this prevalence seems well-fitting and supports the validity of the classification strategy used. In addition, the distribution from naMCI and aMCI matches with prior findings that aMCI is the most common type of MCI (Petersen et al., 2010). Unfortunately, a relatively large part of the sample was classified as pMCI, indicating the high rate of diagnostic uncertainty often apparent in the diagnosis of preclinical and early dementia (Dubois et al., 2016).

The present study only focused on a selection of EEG parameters that can be obtained from Fast Fourier transform (spectral analysis). This was done because such parameters have been shown before to differentiate between healthy and persons with mild impairment (Koenig et al., 2005; Babiloni et al., 2006b, 2010; Kwak, 2006; Ya et al., 2015). They were now applied to a high-ager sample to study their usefulness in terms of early detection of dementia in such age groups. It is possible that early changes in resting state networks are better found with other or more advanced analysis methods. For example, measures of complexity (i.e., frequency or time domain entropy) or functional connectivity (i.e., coherence, phase lag index, and synchronization likelihood, and others) are able to extract different information from the signals of resting state networks than absolute and relative power can (Babiloni et al., 2019). Signal complexity seems to be reduced in MCI compared with healthy OA, although there are only few studies, including MCI, in addition to AD cases (Sun et al., 2020). Functional connectivity in MCI has been reported both as increased or decreased compared with healthy OA (Lejko et al., 2020). This might be due to pathophysiological as well as compensational processes present in MCI (Lejko et al., 2020). Future studies should use these advanced measures in the oldest-old samples to clarify if they can add findings that spectral analysis was not able to disentangle.

Conclusion and Outlook

In this study, the rsEEG during EC and EO conditions of OA with and without cognitive impairments was studied. MCI was not related to detectable changes in EEG power during rest, neither for EC nor EO, compared with healthy individuals. Reactivity in any frequency band was also not different between groups of different cognitive status. With this sample of individuals in their 80's, it was challenging to differentiate between cognitive deficits caused by aging processes and actual pathological changes, indicating MCI. However, by including only the participants of very old age, it was possible to generate rsEEG data for an understudied age sample, which can help to establish normative data and is maybe better transferable to the clinical context, where the majority of individuals being diagnosed with MCI and dementia is rather old.

The present study results are strictly cross-sectional, and, therefore, no statements on the trajectory of neuropsychological performance and electroencephalographic parameters can be made. All the participants were part of a longitudinal study at the Chemnitz University of Technology, Germany (SENDA, sensor-based systems for early detection of dementia), and measurements were repeated up to three times in intervals of 8 months. In the future, additional data analysis will be carried out. This will have two main advantages: (1) the validity of the MCI diagnosis can be increased by including neuropsychological data of more than one time point (Albert et al., 2011) and (2) the predictive value of EEG parameters for the further cognitive decline can be studied. So far, the accuracy obtained from such studies is not high enough for clinical applications but they are more promising than cross-sectional comparisons (Yang et al., 2019).

DATA AVAILABILITY STATEMENT

The raw data supporting the conclusions of this article will be made available by the authors, without undue reservation.

Requests to access the datasets should be directed to Claudia Voelcker-Rehage, (claudia.voelcker-rehage@uni-muenster.de).

ETHICS STATEMENT

The studies involving human participants were reviewed and approved by Ethics Committee of the Chemnitz University of Technology, Faculty of Behavioral and Social Sciences (number V-232-17-KM-SENDA-07112017). The patients/participants provided their written informed consent to participate in this study.

AUTHOR CONTRIBUTIONS

SF: investigation, data curation, formal analysis, writing—original draft, and visualization. DK: conceptualization, writing review and editing, and supervision. KM: project administration, investigation, data curation, and writing review and editing. CV-R: conceptualization, funding acquisition, resources, writing review and editing, and supervision. All authors contributed to the article and approved the submitted version.

FUNDING

This work was supported by the European Social Fund for Germany and the Sächsische Aufbaubank-Förderbank (SAB) of the Free State of Saxony (Grant No. 100310502). This funding source had no role in the study design, in the collection, analysis, and interpretation of data, or in the writing of the report. We acknowledge support from the Open Access Publication Fund of the University of Münster.

SUPPLEMENTARY MATERIAL

The Supplementary Material for this article can be found online at: https://www.frontiersin.org/articles/10.3389/fnagi.2021.675689/full#supplementary-material

REFERENCES

Albert, M. S., DeKosky, S. T., Dickson, D., Dubois, B., Feldman, H. H., Fox, N. C., et al. (2011). The diagnosis of mild cognitive impairment due to Alzheimer's disease: recommendations from the National Institute on Aging-Alzheimer's Association workgroups on diagnostic guidelines for Alzheimer's disease. *Alzheimers Dement.* 7, 270–279. doi: 10.1016/j.jalz.2011.03.008

Alexander, D. M., Arns, M. W., Paul, R. H., Rowe, D. L., Cooper, N., Esser, A. H., et al. (2006). EEG markers for cognitive decline in elderly subjects with subjective memory complaints. *J. Integr. Neurosci.* 5, 49–74. doi: 10.1142/S0219635206001021

American Psychiatric Association (2013). *Diagnostic and Statistical Manual of Mental Disorders*. Washington, DC: American Psychiatric Association. doi: 10.1176/appi.books.9780890425596

Babiloni, C., Barry, R. J., Basar, E., Blinowska, K. J., Cichocki, A., Drinkenburg, W., et al. (2019). International Federation of Clinical Neurophysiology (IFCN) - EEG research workgroup: Recommendations on frequency and topographic analysis of resting state EEG rhythms. Part 1: applications in clinical research studies. *Clin. Neurophysiol.* 6:234. doi: 10.1016/j.clinph.2019.06.234

Babiloni, C., Binetti, G., Cassarino, A., Dal Forno, G., Del Percio, C., Ferreri, F., et al. (2006a). Sources of cortical rhythms in adults during physiological aging: a multicentric EEG study. *Hum. Brain Mapp.* 27, 162–172. doi: 10.1002/hbm.20175

Babiloni, C., Binetti, G., Cassetta, E., Dal Forno, G., Del Percio, C., Ferreri, F., et al. (2006b). Sources of cortical rhythms change as a function of cognitive impairment in pathological aging: a multicenter study. *Clin. Neurophysiol.* 117, 252–268. doi: 10.1016/j.clinph.2005.09.019

Babiloni, C., Lizio, R., Marzano, N., Capotosto, P., Soricelli, A., Triggiani, A. I., et al. (2016). Brain neural synchronization and functional coupling in Alzheimer's disease as revealed by resting state EEG rhythms. *Int. J. Psychophysiol.* 103, 88–102. doi: 10.1016/j.ijpsycho.2015.02.008

Babiloni, C., Visser, P. J., Frisoni, G., De Deyn, P. P., Bresciani, L., Jelic, V., et al. (2010). Cortical sources of resting EEG rhythms in mild cognitive impairment and subjective memory complaint. *Neurobiol. Aging* 31, 1787–1798. doi: 10.1016/j.neurobiolaging.2008.09.020

Barry, R. J., Clarke, A. R., Johnstone, S. J., Magee, C. A., and Rushby, J. A. (2007). EEG differences between eyes-closed and eyes-open resting conditions. *Clin. Neurophysiol.* 118, 2765–2773. doi: 10.1016/j.clinph.2007.07.028

Barry, R. J., and De Blasio, F. M. (2017). EEG differences between eyes-closed and eyes-open resting remain in healthy ageing. *Biol. Psychol.* 129, 293–304. doi: 10.1016/j.biopsycho.2017.09.010

Başar, E., and Güntekin, B. (2012). A short review of alpha activity in cognitive processes and in cognitive impairment. *Int. J. Psychophysiol.* 86, 25–38. doi: 10.1016/j.ijpsycho.2012.07.001

Bennett, D. A., Schneider, J. A., Arvanitakis, Z., Kelly, J. F., Aggarwal, N. T., Shah, R. C., et al. (2006). Neuropathology of older persons without cognitive impairment from two community-based studies. *Neurology* 66, 1837–1844. doi: 10.1212/01.wnl.0000219668.47116.e6

Berger, H. (1929). Über das Elektroenkephalogramm des Menschen. *Arch. Psychiatr. Nervenkr.* 87, 527–570. doi: 10.1007/BF01797193

Brayne, C., and Davis, D. (2012). Making Alzheimer's and dementia research fit for populations. *Lancet* 380, 1441–1443. doi: 10.1016/S0140-6736(12)61803-0

Breton, A., Casey, D., and Arnaoutoglou, N. A. (2019). Cognitive tests for the detection of mild cognitive impairment (MCI), the prodromal stage of dementia: meta-analysis of diagnostic accuracy studies. *Int. J. Geriatr. Psychiatry.* 34, 233–242. doi: 10.1002/gps.5016

Chen, A. C., Feng, W., Zhao, H., Yin, Y., and Wang, P. (2008). EEG default mode network in the human brain: spectral regional field powers. *Neuroimage* 41, 561–574. doi: 10.1016/j.neuroimage.2007.12.064

Dubois, B., Hampel, H., Feldman, H. H., Scheltens, P., Aisen, P., Andrieu, S., et al. (2016). Preclinical Alzheimer's disease: definition, natural history, and diagnostic criteria. *Alzheimers Dement.* 12, 292–323. doi: 10.1016/j.jalz.2016.02.002

Duffy, F. H., Albert, M. S., McAnulty, G., and Garvey, A. J. (1984). Age-related differences in brain electrical activity of healthy subjects. *Ann. Neurol.* 16, 430–438. doi: 10.1002/ana.410160403

Gaál, Z. A., Boha, R., Stam, C. J., and Molnár, M. (2010). Age-dependent features of EEG-reactivity–spectral, complexity, and network characteristics. *Neurosci. Lett.* 479, 79–84. doi: 10.1016/j.neulet.2010.05.037

Gauggel, S., and Birkner, B. (1999). Validität und Reliabilität einer deutschen Version der Geriatrischen Depressionsskala (GDS). *Z. Klin. Psychol. Psychother.* 28, 18–27. doi: 10.1026//0084-5345.28.1.18

Guan, H., Liu, T., Jiang, J., Tao, D., Zhang, J., Niu, H., et al. (2017). Classifying MCI subtypes in community-dwelling elderly using cross-sectional and longitudinal MRI-based biomarkers. *Front. Aging. Neurosci.* 9:309. doi: 10.3389/fnagi.2017.00309

Hu, C., Yu, D., Sun, X., Zhang, M., Wang, L., and Qin, H. (2017). The prevalence and progression of mild cognitive impairment among clinic and community populations: a systematic review and meta-analysis. *Int. Psychogeriatr.* 29, 1595–1608. doi: 10.1017/S1041610217000473

Hübner, L., Godde, B., and Voelcker-Rehage, C. (2018). Older adults reveal enhanced task-related beta power decreases during a force modulation task. *Behav. Brain Res.* 345, 104–113. doi: 10.1016/j.bbr.2018.02.028

Jelic, V., Johansson, S. E., Almkvist, O., Shigeta, M., Julin, P., Nordberg, A., et al. (2000). Quantitative electroencephalography in mild cognitive impairment: longitudinal changes and possible prediction of Alzheimer's disease. *Neurobiol. Aging* 21, 533–540. doi: 10.1016/S0197-4580(00)00153-6

Jelic, V., and Kowalski, J. (2009). Evidence-based evaluation of diagnostic accuracy of resting EEG in dementia and mild cognitive impairment. *Clin. EEG Neurosci.* 40, 129–142. doi: 10.1177/155005940904000211

Jeong, J. (2004). EEG dynamics in patients with Alzheimer's disease. *Clin. Neurophysiol.* 115, 1490–1505. doi: 10.1016/j.clinph.2004.01.001

Jung, T.-P., Humphries, C., Lee, T.-W., Makeig, S., McKeown, M. J., Iragui, V., et al. (1998). Extended ICA removes artifacts from electroencephalographic recordings. *Adv. Neural Inf. Process Syst.* 10, 894–900.

Jungwirth, S., Zehetmayer, S., Hinterberger, M., Tragl, K. H., and Fischer, P. (2012). The validity of amnestic MCI and non-amnestic MCI at age 75 in the prediction of Alzheimer's dementia and vascular dementia. *Int. Psychogeriatr.* 24, 959–966. doi: 10.1017/S1041610211002870

Klimesch, W. (1999). EEG alpha and theta oscillations reflect cognitive and memory performance: a review and analysis. *Brain Res. Rev.* 29, 169–195. doi: 10.1016/S0165-0173(98)00056-3

Koen, J. D., and Rugg, M. D. (2019). Neural dedifferentiation in the aging brain. *Trends Cogn. Sci.* 23, 547–559. doi: 10.1016/j.tics.2019.04.012

Koenig, T., Prichep, L., Dierks, T., Hubl, D., Wahlund, L. O., John, E. R., et al. (2005). Decreased EEG synchronization in Alzheimer's disease and mild cognitive impairment. *Neurobiol. Aging* 26, 165–171. doi: 10.1016/j.neurobiolaging.2004.03.008

Koyama, K., Hirasawa, H., Okubo, Y., and Karasawa, A. (1997). Quantitative EEG correlates of normal aging in the elderly. *Clin. Electroencephalogr.* 28, 160–165. doi: 10.1177/155005949702800308

Kryscio, R. J., Schmitt, F. A., Salazar, J. C., Mendiondo, M. S., and Markesbery, W. R. (2006). Risk factors for transitions from normal to mild cognitive impairment and dementia. *Neurology* 66, 828–832. doi: 10.1212/01.wnl.0000203264.71880.45

Kwak, Y. T. (2006). Quantitative EEG findings in different stages of Alzheimer's disease. *J. Clin. Neurophysiol.* 23, 456–461. doi: 10.1097/01.wnp.0000223453.47663.63

Larner, A. J. (2012). Screening utility of the Montreal Cognitive Assessment (MoCA): in place of–or as well as–the MMSE? *Int. Psychogeriatr.* 24, 391–396. doi: 10.1017/S1041610211001839

Lejko, N., Larabi, D. I., Herrmann, C. S., Aleman, A., and Curcic-Blake, B. (2020). Alpha power and functional connectivity in cognitive decline: a systematic review and meta-analysis. *J. Alzheimers. Dis.* 78, 1047–1088. doi: 10.3233/JAD-200962

Liu, Y., Cai, Z. L., Xue, S., Zhou, X., and Wu, F. (2013). Proxies of cognitive reserve and their effects on neuropsychological performance in patients with mild cognitive impairment. *J. Clin. Neurosci.* 20, 548–553. doi: 10.1016/j.jocn.2012.04.020

Luck, T., Pabst, A., Rodriguez, F. S., Schroeter, M. L., Witte, V., Hinz, A., et al. (2018). Age-, sex-, and education-specific norms for an extended CERAD Neuropsychological Assessment Battery—results from the population-based LIFE-Adult-Study. *Neuropsychology* 32:461. doi: 10.1037/neu0000440

Luckhaus, C., Grass-Kapanke, B., Blaeser, I., Ihl, R., Supprian, T., Winterer, G., et al. (2008). Quantitative EEG in progressing vs stable mild cognitive impairment (MCI): results of a 1-year follow-up study. *Int. J. Geriatr. Psychiatry* 23, 1148–1155. doi: 10.1002/gps.2042

McBride, J. C., Zhao, X., Munro, N. B., Smith, C. D., Jicha, G. A., Hively, L., et al. (2014). Spectral and complexity analysis of scalp EEG characteristics for mild cognitive impairment and early Alzheimer's disease. *Comput. Methods Programs Biomed.* 114, 153–163. doi: 10.1016/j.cmpb.2014.01.019

Memory Clinic Basel (2005). *Manual zum Auswertungsprogramm CERAD-Plus 1.0.* Basel: Memory Clinic.

Mitchell, A. J. (2008). Is it time to separate subjective cognitive complaints from the diagnosis of mild cognitive impairment? *Age Ageing* 37, 497–499. doi: 10.1093/ageing/afn147

Mitchell, A. J., and Shiri-Feshki, M. (2009). Rate of progression of mild cognitive impairment to dementia–meta-analysis of 41 robust inception cohort studies. *Acta psychiatrica Scandinavica* 119, 252–265. doi: 10.1111/j.1600-0447.2008.01326.x

Morris, J. C., Heyman, A., Mohs, R. C., Hughes, J. P., van Belle, G., Fillenbaum, G., et al. (1989). The Consortium to Establish a Registry for Alzheimer's Disease (CERAD). Part I. Clinical and neuropsychological assessment of Alzheimer's disease. *Neurology* 39, 1159–1165. doi: 10.1212/WNL.39.9.1159

Müller, K., Fröhlich, S., Germano, A. M. C., Kondragunta, J., Agoitia Hurtado, M., Rudisch, J., et al. (2020). Sensor-based systems for early detection of dementia (SENDA): a study protocol for a prospective cohort sequential study. *BMC Neurol.* 20:84. doi: 10.1186/s12883-020-01666-8

Nardone, R., Sebastianelli, L., Versace, V., Saltuari, L., Lochner, P., Frey, V., et al. (2018). Usefulness of EEG techniques in distinguishing frontotemporal dementia from Alzheimer's disease and other dementias. *Dis. Markers* 2018:6581490. doi: 10.1155/2018/6581490

Nasreddine, Z. S., Phillips, N. A., Bedirian, V., Charbonneau, S., Whitehead, V., Collin, I., et al. (2005). The Montreal Cognitive Assessment, MoCA: a brief screening tool for mild cognitive impairment. *J. Am. Geriatr. Soc.* 53, 695–699. doi: 10.1111/j.1532-5415.2005.53221.x

Oldfield, R. C. (1971). The assessment and analysis of handedness: the Edinburgh inventory. *Neuropsychologia* 9, 97–113. doi: 10.1016/0028-3932(71)90067-4

Oswald, W. D., and Fleischmann, U. M. (1995). *Nürnberger-Alters-Inventar (NAI), 3. überarbeitete Edition*. Göttingen: Hogrefe.

Pandya, S. Y., Lacritz, L. H., Weiner, M. F., Deschner, M., and Woon, F. L. (2017). Predictors of reversion from mild cognitive impairment to normal cognition. *Dement. Geriatr. Cogn. Disord.* 43, 204–214. doi: 10.1159/000456070

Petersen, R. C. (2004). Mild cognitive impairment as a diagnostic entity. *J. Intern. Med.* 256, 183–194. doi: 10.1111/j.1365-2796.2004.01388.x

Petersen, R. C., Caracciolo, B., Brayne, C., Gauthier, S., Jelic, V., and Fratiglioni, L. (2014). Mild cognitive impairment: a concept in evolution. *J. Intern. Med.* 275, 214–228. doi: 10.1111/joim.12190

Petersen, R. C., Lopez, O., Armstrong, M. J., Getchius, T. S. D., Ganguli, M., Gloss, D., et al. (2018). Practice guideline update summary: mild cognitive impairment: report of the Guideline Development, Dissemination, and Implementation Subcommittee of the American Academy of Neurology. *Neurology* 90, 126–135. doi: 10.1212/WNL.0000000000004826

Petersen, R. C., Parisi, J. E., Dickson, D. W., Johnson, K. A., Knopman, D. S., Boeve, B. F., et al. (2006). Neuropathologic Features of Amnestic Mild Cognitive Impairment. *JAMA Neurol.* 63, 665–672. doi: 10.1001/archneur.63.5.665

Petersen, R. C., Roberts, R. O., Knopman, D. S., Geda, Y. E., Cha, R. H., Pankratz, V. S., et al. (2010). Prevalence of mild cognitive impairment is higher in men. The mayo clinic study of aging. *Neurology* 75, 889–897. doi: 10.1212/WNL.0b013e3181f11d85

Poil, S. S., de Haan, W., van der Flier, W. M., Mansvelder, H. D., Scheltens, P., and Linkenkaer-Hansen, K. (2013). Integrative EEG biomarkers predict progression to Alzheimer's disease at the MCI stage. *Front. Aging Neurosci.* 5:58. doi: 10.3389/fnagi.2013.00058

Prichep, L. S., John, E. R., Ferris, S. H., Reisberg, B., Almas, M., Alper, K., et al. (1994). Quantitative EEG correlates of cognitive deterioration in the elderly. *Neurobiol. Aging* 15, 85–90. doi: 10.1016/0197-4580(94)90147-3

Provencher, D., Hennebelle, M., Cunnane, S. C., Berube-Lauziere, Y., and Whittingstall, K. (2016). Cortical thinning in healthy aging correlates with larger motor-evoked EEG desynchronization. *Front. Aging Neurosci.* 8:63. doi: 10.3389/fnagi.2016.00063

Richard, E., Schmand, B., Eikelenboom, P., Westendorp, R. G., and Van Gool, W. A. (2012). The Alzheimer myth and biomarker research in dementia. *J. Alzheimers Dis.* 31(Suppl.3), S203–209. doi: 10.3233/JAD-2012-112216

Rossini, P. M., Di Iorio, R., Vecchio, F., Anfossi, M., Babiloni, C., Bozzali, M., et al. (2020). Early diagnosis of Alzheimer's disease: the role of biomarkers including advanced EEG signal analysis. Report from the IFCN-sponsored panel of experts. *Clin. Neurophysiol.* 131, 1287–1310. doi: 10.1016/j.clinph.2020.03.003

Rossini, P. M., Rossi, S., Babiloni, C., and Polich, J. (2007). Clinical neurophysiology of aging brain: from normal aging to neurodegeneration. *Prog. Neurobiol.* 83, 375–400. doi: 10.1016/j.pneurobio.2007.07.010

Rossiter, H. E., Davis, E. M., Clark, E. V., Boudrias, M. H., and Ward, N. S. (2014). Beta oscillations reflect changes in motor cortex inhibition in healthy ageing. *Neuroimage* 91, 360–365. doi: 10.1016/j.neuroimage.2014.01.012

Schumacher, J., Thomas, A. J., Peraza, L. R., Firbank, M., Cromarty, R., Hamilton, C. A., et al. (2020). EEG alpha reactivity and cholinergic system integrity in Lewy body dementia and Alzheimer's disease. *Alzheimers Res. Ther.* 12:46. doi: 10.1186/s13195-020-00613-6

Simon-Dack, S. L., Holtgraves, T., Marsh, L. M., and Fogle, K. L. (2013). Resting electroencephalography correlates of pseudoneglect: an individual differences approach. *Neuroreport* 24, 827–830. doi: 10.1097/WNR.0b013e328364125b

Slavin, M. J., Brodaty, H., and Sachdev, P. S. (2013). Challenges of diagnosing dementia in the oldest old population. *J. Gerontol. A Biol. Sci. Med. Sci.* 68, 1103–1111. doi: 10.1093/gerona/glt051

Snitz, B. E., Wang, T., Cloonan, Y. K., Jacobsen, E., Chang, C. H., Hughes, T. F., et al. (2018). Risk of progression from subjective cognitive decline to mild cognitive impairment: the role of study setting. *Alzheimers Dement.* 14, 734–742. doi: 10.1016/j.jalz.2017.12.003

Sperling, R. A., Aisen, P. S., Beckett, L. A., Bennett, D. A., Craft, S., Fagan, A. M., et al. (2011). Toward defining the preclinical stages of Alzheimer's disease: recommendations from the National Institute on Aging-Alzheimer's Association workgroups on diagnostic guidelines for Alzheimer's disease. *Alzheimers Dement* 7, 280–292. doi: 10.1016/j.jalz.2011.03.003

Sun, J., Wang, B., Niu, Y., Tan, Y., Fan, C., Zhang, N., et al. (2020). Complexity analysis of EEG, MEG, and fMRI in mild cognitive impairment and Alzheimer's disease: a review. *Entropy* 22:e22020239. doi: 10.3390/e22020239

Toth, B., File, B., Boha, R., Kardos, Z., Hidasi, Z., Gaal, Z. A., et al. (2014). EEG network connectivity changes in mild cognitive impairment - preliminary results. *Int. J. Psychophysiol.* 92, 1–7. doi: 10.1016/j.ijpsycho.2014.02.001

van der Hiele, K., Vein, A. A., Reijntjes, R. H., Westendorp, R. G., Bollen, E. L., van Buchem, M. A., et al. (2007a). EEG correlates in the spectrum of cognitive decline. *Clin. Neurophysiol.* 118, 1931–1939. doi: 10.1016/j.clinph.2007.05.070

van der Hiele, K., Vein, A. A., van der Welle, A., van der Grond, J., Westendorp, R. G., Bollen, E. L., et al. (2007b). EEG and MRI correlates of mild cognitive impairment and Alzheimer's disease. *Neurobiol. Aging* 28, 1322–1329. doi: 10.1016/j.neurobiolaging.2006.06.006

van Straaten, E. C. W., de Haan, W., de Waal, H., Scheltens, P., van der Flier, W. M., Barkhof, F., et al. (2012). Disturbed oscillatory brain dynamics in subcortical ischemic vascular dementia. *BMC Neurosci.* 13:85. doi: 10.1186/1471-2202-13-85

Visser, P. J., Verhey, F., Knol, D. L., Scheltens, P., Wahlund, L.-O., Freund-Levi, Y., et al. (2009). Prevalence and prognostic value of CSF markers of Alzheimer's disease pathology in patients with subjective cognitive impairment or mild cognitive impairment in the DESCRIPA study: a prospective cohort study. *Lancet Neurol.* 8, 619–627. doi: 10.1016/S1474-4422(09)70139-5

Winblad, B., Palmer, K., Kivipelto, M., Jelic, V., Fratiglioni, L., Wahlund, L. O., et al. (2004). Mild cognitive impairment–beyond controversies, towards a consensus: report of the International Working Group on Mild Cognitive Impairment. *J. Intern. Med.* 256, 240–246. doi: 10.1111/j.1365-2796.2004.01380.x

Ya, M., Xun, W., Wei, L., Ting, H., Hong, Y., and Yuan, Z. (2015). Is the electroencephalogram power spectrum valuable for diagnosis of the elderly with cognitive impairment? *Int. J. Gerontol.* 9, 196–200. doi: 10.1016/j.ijge.2014.07.001

Yang, S., Bornot, J. M. S., Wong-Lin, K., and Prasad, G. (2019). M/EEG-based bio-markers to predict the MCI and Alzheimer's disease: a review from the ML perspective. *IEEE Trans. Biomed. Eng.* 66, 2924–2935. doi: 10.1109/TBME.2019.2898871

Conflict of Interest: The authors declare that the research was conducted in the absence of any commercial or financial relationships that could be construed as a potential conflict of interest.

Publisher's Note: All claims expressed in this article are solely those of the authors and do not necessarily represent those of their affiliated organizations, or those of the publisher, the editors and the reviewers. Any product that may be evaluated in this article, or claim that may be made by its manufacturer, is not guaranteed or endorsed by the publisher.

frontiers in Aging Neuroscience

ORIGINAL RESEARCH
published: 21 October 2021
doi: 10.3389/fnagi.2021.718965

Working Memory Training and Cortical Arousal in Healthy Older Adults: A Resting-State EEG Pilot Study

Chiara Spironelli[1,2]* *and Erika Borella*[1]*

[1] Department of General Psychology, University of Padova, Padova, Italy, [2] Padova Neuroscience Center, University of Padova, Padova, Italy

The current pilot study aimed to test the gains of working memory (WM) training, both at the short- and long-term, at a behavioral level, and by examining the electrophysiological changes induced by training in resting-state EEG activity among older adults. The study group included 24 older adults (from 64 to 75 years old) who were randomly assigned to a training group (TG) or an active control group (ACG) in a double-blind, repeated-measures experimental design in which open eyes, resting-state EEG recording, followed by a WM task, i.e., the Categorization Working Memory Span (CWMS) task, were collected before and after training, as well as at a 6-month follow-up session. At the behavioral level, medium to large Cohen's *d* effect sizes was found for the TG in immediate and long-term gains in the WM criterion task, as compared with small gains for the ACG. Regarding intrusion errors committed in the CWMS, an index of inhibitory control representing a transfer effect, results showed that medium to large effect sizes for immediate and long-term gains emerged for the TG, as compared to small effect sizes for the ACG. Spontaneous high-beta/alpha ratio analyses in four regions of interest (ROIs) revealed no pre-training group differences. Significantly greater TG anterior rates, particularly in the left ROI, were found after training, with frontal oscillatory responses being correlated with better post-training CWMS performance in only the TG. The follow-up analysis showed similar results, with greater anterior left high-beta/alpha rates among TG participants. Follow-up frontal high-beta/alpha rates in the right ROI were correlated with lower CWMS follow-up intrusion errors in only the TG. The present findings are further evidence of the efficacy of WM training in enhancing the cognitive functioning of older adults and their frontal oscillatory activity. Overall, these results suggested that WM training also can be a promising approach toward fostering the so-called functional cortical plasticity in aging.

Keywords: working memory, older adults, resting state, EEG, cognitive resources, transfer effects

OPEN ACCESS

Edited by:
Aneta Kielar,
University of Arizona, United States

Reviewed by:
Aneta Brzezicka,
University of Social Sciences and Humanities, Poland
Rahel Rabi,
Rotman Research Institute (RRI), Canada

***Correspondence:**
Chiara Spironelli
chiara.spironelli@unipd.it
Erika Borella
erika.borella@unipd.it

Received: *01 June 2021*
Accepted: *20 September 2021*
Published: *21 October 2021*

Citation:
Spironelli C and Borella E (2021) Working Memory Training and Cortical Arousal in Healthy Older Adults: A Resting-State EEG Pilot Study. Front. Aging Neurosci. 13:718965. doi: 10.3389/fnagi.2021.718965

INTRODUCTION

Working memory is the ability to retain and simultaneously manipulate information for use in complex cognitive tasks (Miyake and Shah, 1999), which is considered one of the core basic mechanisms of cognition (e.g., Gamboz et al., 2009). Not only it is involved in various skills, including everyday life functioning (Borella et al., 2017a), but it is also among the factors accounting

for age-related differences across the life span. Indeed, working memory (WM) has a clear and linear change. i.e., decline, with aging (e.g., Park et al., 1996, 2002; Borella et al., 2008), which is accompanied by anatomical and neuromodulatory changes, as well as alterations in functional brain activity patterns in older adults (i.e., Reuter-Lorenz, 2000; Raz, 2005; Reuter-Lorenz and Sylvester, 2005). These findings have encouraged a growing interest in developing WM training procedures to slow down or attenuate age changes in the WM performance of older adults. In particular, WM training is aimed not only at improving information-processing systems of individuals but also at inducing changes in how individuals process information, through more flexible use of their own resources (e.g., Borella et al., 2019b; Carbone et al., 2019). Therefore, not only is WM training is theoretically expected to provide benefits in the trained WM tasks (so-called specific training gains) but also to give improvements in such a core cognitive mechanism would also produce general effects in untrained cognitive abilities related to it (so-called transfer effects) (e.g., Borella et al., 2017b). According to recent reviews and meta-analyses (i.e., Karbach and Verhaeghen, 2014; Teixeira-Santos et al., 2019; Hou et al., 2020), WM training for healthy older adults has been shown to provide large (Karbach and Verhaeghen, 2014; Teixeira-Santos et al., 2019) and endurable (Hou et al., 2020) training gains in tasks similar to those trained. However, less consistent conclusions have been reported regarding the generalizability of WM training benefits: improvements to untrained tasks, i.e., transfer effects, usually are weaker than training gains are (Karbach and Verhaeghen, 2014), with mixed and less endurable effects (Teixeira-Santos et al., 2019; Hou et al., 2020), although some exceptions have been found (e.g., see Borella et al., 2017b, 2019a).

Among the different training procedures adopted with older adults, to our knowledge, the WM training program proposed in the study by Borella et al. (2010) is the only one showing promising results. Their training produced short- and long-term specific transfer benefits (see Borella et al., 2017b), even extending to tasks related to everyday life (Carretti et al., 2013; Cantarella et al., 2017; Borella et al., 2019a). Furthermore, it is one of the few procedures that other laboratories have adopted (Brum et al., 2020) and whose results have been replicated. The benefits of this WM training approach are considered to be due to: (i) the training timing (every 2 days), which provides sufficient time to consolidate the skills the participants acquired (see Borella et al., 2010); (ii) the procedure used, which is adaptive, meaning that participants are trained at a level of difficulty coming close to the limits of their own capacity; (iii) the tasks, which are always novel and challenging, thus engaging different cognitive processes and sustaining participants' interest and motivation (Borella et al., 2010, 2017b).

Despite the interest in WM training, little is known about how these WM cognitive interventions affect the structure and functioning of the older adult brain (see Nguyen et al., 2019, for a review). This is quite surprising given the well-documented association between the neurobiological and functional brain changes occurring with increasing age, particularly within the prefrontal cortex, and performance on cognitive tasks involving WM or generally the executive functions. Compared with other neuroimaging approaches, electroencephalography (EEG) is particularly suited for studying maturational brain changes because it is a non-invasive technique that can be used to directly measure the cortical functioning of a human brain (e.g., Anokhin et al., 1996; Rossini et al., 2007). EEG also provides reliable measures that are important both for assessing neural correlates of healthy aging and detecting functional neural changes from healthy to pathological aging, both at rest and when executing tasks (see Rossini et al., 2007, for a review). Changes in the frequency of resting-state brain oscillation, such as a decrease in posterior alpha power, have been associated, for instance, with altered cerebral blood flow and cognitive functioning in older adults with dementia, as compared to those with healthy aging (Rossini et al., 2007). Furthermore, both cognitive and/or physical training significantly affect neural oscillations (e.g., Styliadis et al., 2015; Klados et al., 2016; Reis et al., 2016), as well as event-related potentials (ERPs) (e.g., Spironelli et al., 2013; Zendel et al., 2016) in older adults experiencing both healthy and pathological aging. In addition, ERP modulations were reported in healthy elderly individuals after they received cognitive training, in line with neuroimaging studies showing reduced cortical activity in healthy elderly subjects after a WM training session (Brehmer et al., 2012; Heinzel et al., 2014).

Notably, to the best of our knowledge, no studies have examined resting-state EEG brain oscillation after WM training in healthy older adults. To fill this gap, we developed a 2 year research protocol to advance our understanding of the link between the cognitive and neural changes induced by WM training and, thus, on the mechanisms underlying WM cognitive training in older adults. Indeed, this latter topic is a critical aspect that is still missing from the aging literature.

The present study aimed to examine training-specific gains among healthy older adults immediately after WM training (short-term effect) and 6 months after it (long-term, follow-up, or maintenance effect). The well-validated WM training procedure in the study by Borella et al. (2010, 2017b) was conducted with a sample of healthy older adults. The specific training gains were assessed using a verbal WM criterion task closely similar to the one used in the training, which is the Categorization Working Memory Span task (CWMS; for the computerized version, see Spironelli et al., 2020). This WM task can also be used to assess intrusions errors, i.e., memory errors associated with the recall of non-target words, which represent a measure of inhibitory control failure (see Borella et al., 2007; Robert et al., 2009). Therefore, we also examined whether any transfer effect occurred for this measure.

Together with behavioral CWMS data, we analyzed a psychophysiological index of oscillatory responses, including the mean amplitude high-beta/alpha ratio, from 3 min resting-state EEG data (eyes open) collected before and after the WM training in a group of older adults, i.e., the training group (TG), and compared the data with those of a group engaged in alternative activities, i.e., the active control group (ACG), in the same period, who performed cognitive assessments. With respect to electrophysiological data, according to the study of Laufs et al. (2003), alpha activity is reduced attentively by external stimulus

TABLE 1 | Means (*M*) and standard deviations (± *SD*) of the demographic characteristics, cognitive functioning, and mood measures at pre-training for the training group vs. active control group (ACG) participants.

	Training group $N = 12$ (10 women)		Active control group $N = 12$ (9 women)		$t(22)$ tests
	M	*SD*	*M*	*SD*	
Sociodemographic characteristics					
Age (years)	68.83	±2.85	69.16	±3.18	−0.26
Education (years)	11.25	±2.14	11.00	±2.89	−0.24
Handedness (Oldfield)	99.33%	±2.31%	100.00%	±0.00%	1.00
Cognitive functioning					
Mini-Mental State Examination	27.75	±1.02	28.32	±1.15	−1.27
Vocabulary	53.92	±8.24	51.08	±11.35	0.70
Ability to Solve Problems in Everyday Life	11.95	±1.49	12.82	±1.13	−1.59
Mood					
Geriatric Depression Scale	1.75	±1.36	2.08	1.97	−0.48

processing during resting state or when one is performing intentional mental operations with high cognitive load. In detail, decreased alpha power is associated with frontal and parietal activations of cortical structures involved in goal-directed cognition and behavior. In addition, the beta band characterizes the spontaneous cognitive activation during conscious rest. In the study by Oakes et al. (2004), the cerebral activity of participants at rest was measured simultaneously with PET-FDG and EEG. Their results revealed a significant correlation between the two techniques, showing that high-frequency EEG bands, i.e., high-beta and gamma waves, were positively correlated with higher regional glucose metabolism. On the contrary, the lower alpha band (8.5–10 Hz) revealed a clear negative correlation with brain metabolism, thus supporting the traditional interpretation of alpha rhythm as a physiological index inversely related to brain activation. The authors interpreted these results as direct (high-frequency EEG bands) or inverse (lower alpha EEG band) measures of neural activation in a resting-state condition (Oakes et al., 2004). For this reason, the high-beta/alpha ratio combines both the inhibitory component measured by alpha EEG and the activation component represented by the high beta into one measure, with the further advantage of statistically normalizing these measures across participants (the ratio between the two measures within-subjects). Concerning the localization of the expected changes induced by WM training, according to a large literature base involving healthy subjects (e.g., Emch et al., 2019), the frontal lobes play an important central role in WM, together with other secondary posterior regions. In addition, patients with lesions in their prefrontal cortex typically have impaired WM (e.g., Stuss et al., 1997; Jolly et al., 2020). Therefore, we expected that when using the described high-beta/alpha EEG ratio, prefrontal EEG sites would be the main neural hubs subjected to WM-induced plastic changes.

In line with previous studies (e.g., Borella et al., 2017b), we expected both short- and long-term specific training gains in the criterion task at the behavioral level, with TG (but not ACG) improving their WM performance. We also expected WM training to produce a transfer effect in the inhibitory control index, with TG, as compared with ACG, decreasing the intrusion errors they committed in the CWMS task. At the electrophysiological level, we expected no between-group differences in spontaneous EEG oscillatory activity before the WM training but significantly greater oscillatory responses in TG rather than ACG participants after the WM training, particularly in frontal brain sites. Indeed, according to the review of Constantinidis and Klingberg (2016), WM training increases prefrontal cortex activity. Whether WM training enhances the WM performance of older adults and, simultaneously, their resting-state neural oscillations, it is associated with the support of plasticity and the coordination of both information transfer within the brain and other important cognitive functions. Thus, we hypothesized that WM training actively shapes the power of spontaneous brain oscillations.

METHODS

Participants

Healthy older adults were recruited by word of mouth and at social clubs for elderly people, according to the following inclusion criteria: (i) age between 64 and 75 years; (ii) Italian as their mother tongue; (iii) right-handed, as ascertained by the Edinburgh Handedness Inventory (Oldfield, 1971); (iv) a score of 27 or more in the Mini-Mental State Examination (MMSE; Folstein et al., 1975), which indicated a good cognitive functioning and no dementia or cognitive impairment; (v) good physical and mental health and normal or corrected-to-normal vision. Among the 24 volunteers for the study, all fulfilled the inclusion criteria.

Participants were randomized into two groups: the training group (TG), which attended the WM training, and the active control group (ACG). Six months after the training, all of the participants were called back for a follow-up session. All 24 older adults (see **Table 1** for their descriptive statistics) elected to complete the whole neuropsychological and EEG assessment, including the pre-training, post-training, and follow-up sessions. None of the 24 participants dropped out during the whole study.

All of the participants performed above the critical cut-off for their age and education in the Vocabulary test taken from

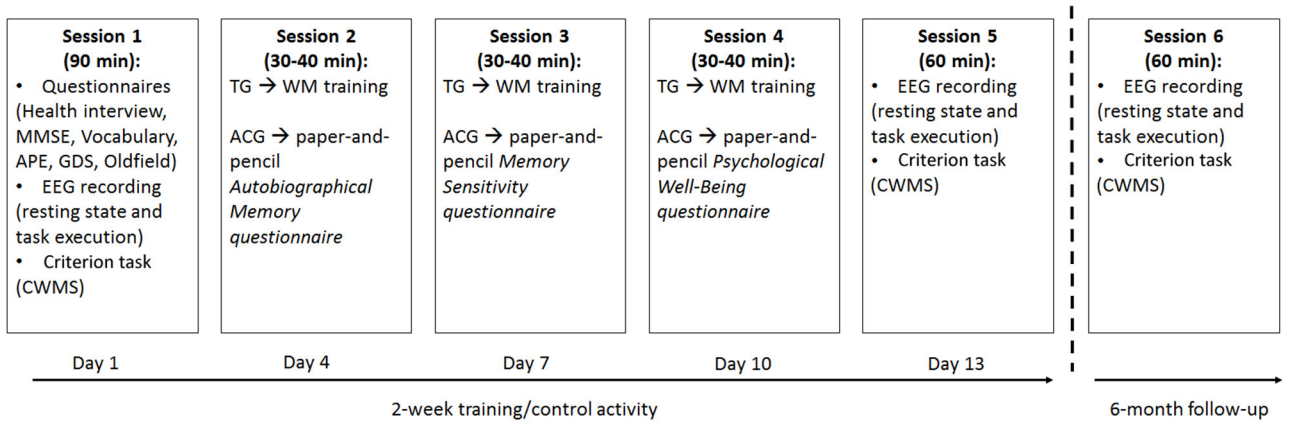

FIGURE 1 | Schematic representation of the 2-week training/alternative activity sessions assigned to the training group (TG) and active control group (ACG) participants, as well as the 6-month follow-up. TG: Trained Group; ACG: Active Control Group; MMSE: Mini Mental State Examination; GDS: Geriatric Depression Scale; CWMS: Categorisation Working Memory Span Test; APE: Ability to Solve Problems in Everyday Life test.

the Wechsler Adult Intelligence Scale-Fourth Edition (WAIS-IV) (Wechsler, 2008; Italian norms by Orsini and Pezzuti, 2013) and in an objective performance-based measure of everyday functioning, specifically the Ability to Solve Problems in Everyday Life test (APE; Italian adaptation of the Everyday Problems Test; Borella et al., 2017a). Moreover, none of them reported signs of depression, as assessed with the Geriatric Depression Scale (GDS; Yesavage et al., 1982-1983).

The present study was approved by the Ethics Committee for Psychological Research—University of Padova (protocol number 3180). All of the participants gave written informed consent to participate in the study, which was performed in accordance with the ethical standards established in the Declaration of Helsinki (World Medical Association, 2013), and they were paid back for their travel costs to attend the experiment.

Study Design

The study was conducted using a double-blind design. The assessment sessions were conducted by two experimenters, who knew that participants would have been involved in different activities and sessions, with only one group having attended WM cognitive training. They were unaware of the allocation of the participants into the training or control groups, and they did not attend any of the sessions. These two experimenters were previously trained on EEG collection and task administering. The training and alternative activity sessions for the TG and ACG, respectively, were run by a third experimenter, who previously was trained on managing the training protocol and the activities of the control group.

The participants were told about the aims of the study at the very end of the data collection (at follow-up). For ethical reasons, participants who were assigned to the control condition were offered to undergo the training program.

All participants attended six individual laboratory sessions (**Figure 1**). The first and fifth were for the pre- and post-tests, and the sixth was the 6-month follow-up.

During the three assessment sessions, lasting about 90 min (pre-test) and 60 min (post-test and follow-up), respectively, the participants completed a battery of tasks: the CWMS -criterion- task (administered during the assessment sessions) was presented via computer to allow EEG collection. The Edinburgh Handedness Inventory, Health Interview, MMSE, Vocabulary, APE, and GDS were all paper-and-pencil tests administered only at pretesting (**Figure 1**).

During the other three sessions (2–4), lasting about 30–40 min each and completed within a 2 week time frame with a fixed 2 day break between each session, the TG has given the WM training, whereas the ACG was occupied in alternative activities (**Figure 1**). The duration of the training and alternative activities as well as the amount of interaction with the experimenter were much the same for the two groups.

In the practice phase, all of the participants were asked if they could see and hear the stimuli easily. They perceived the visual stimuli adequately. The volume of training stimuli was adjusted according to the preferences of each individual, and a sound amplifier for PCs was used. Therefore, after the practice phase, all of the participants were able to see and hear all of the stimuli administered in each task.

Criterion Task (All Participants)

The computerized version of the CWMS (Spironelli et al., 2020), as in its original version (De Beni et al., 2008), consisted of 10 sets of word lists, which included 40 lists of five medium- to high-frequency words (divided into groups containing from two to six lists of words; two sets for each length). Among the total number of words in the task (200), 28% were animal words, and lists could contain zero, one, or two animal nouns, present in any position, including the last one. The participants were required to read each word appearing in the center of the computer screen and to press the spacebar whenever an animal noun appeared (processing phase). At the end of each set, when a triangle appeared in the center of the screen, the participants had to recall

the last word on each list in serial order (maintenance phase), i.e., they needed to remember from two to six words, depending on the length of the set. Two practice trials containing two words to remember were given before the experimental task started.

The participants have visually presented the words on the computer screen as follows: black words were displayed in bold Courier New font (size: 24 points) in the center of the white screen for 2,000 ms, and the interval between each trial within the same set was 2,000 ms. The end of a list was signaled by a visual triangle (shown for 1,000 ms) presented together with a 1,000 Hz sound (presented for 200 ms). The experimenter wrote down recalled words on a dedicated form. To ensure that the participants were not trading off between processing the animal nouns and remembering the last words in the lists, 85% accuracy was required on the secondary task, i.e., pressing the spacebar whenever an animal noun appeared. All of the participants satisfied this criterion.

The total number of correctly recalled words was used as the measure of WM performance (maximum score = 20), which was considered the specific training gain. The words recalled incorrectly, i.e., recall of non-target words, were also computed and used as a measure of the inhibitory control of participants over no longer relevant information in WM, which was considered a transfer effect.

Two parallel versions of this task, wherein each one including five sets of word lists (one set for each length), were created and administered, one at pretest and the other at posttest, in a counterbalanced fashion across testing sessions. The pretest version was then presented at the 6-month follow-up.

WM Training for the Training Group

The training task was presented individually in an auditory manner, adjusted to the hearing level of each participant to limit the influence of sensory variables on the outcomes. All of the verbal stimuli were presented by using a sound amplifier during the training sessions. The task consisted of a modified version of the CWMS task (see Borella et al., 2010), in which lists of audio-recorded words were presented and the participants were asked to recall target words and also to tap on the table with their hand when they heard the name of an animal.

The maintenance demand of the CWMS training task was manipulated by using an adaptive procedure in the first training session, i.e., the difficulty of the task increased based on whether a participant was successful at a given level, if not, the lowest level was presented. The demands of the task also varied and, depending on the session, could involve having to recall words proceeded by a beep (second training session) or an alternative recalling of the last or first word in each list (third training session). The processing demand (tapping on the table when an animal name was heard) was manipulated by varying the frequency of these animal words in the lists (second training session). This type of training procedure combined an adaptive procedure in the first training session with a standard one (from the easiest to the hardest trials) and was referred to as a hybrid procedure, which was considered to promote transfer effects (Borella et al., 2010).

Activities for the Active Control Group

The participants in the ACG underwent the same number of individual sessions as the TG did, but they were asked to fill in the following paper-and-pencil questionnaires. Questionnaires included the Autobiographical Memory Questionnaire (De Beni et al., 2008), which entailed remembering common events related to their childhood, adulthood, and recent events and to rate their vividness; the Memory Sensitivity Questionnaire (De Beni et al., 2008), in which participants had to rate the frequency of behaviors dedicated to saving memories of life events; the Psychological Well-Being Questionnaire (De Beni et al., 2008), to rate the personal satisfaction of the participants with their life (past, present, and future), emotional competencies (ability to understand the emotions of their own and the others), and coping strategies regarding everyday problems.

Data Recording and Analysis

The electrophysiological activity was recorded with 38 tin electrodes mounted on an elastic cap (Electro-Cap International Inc., Eaton, OH, USA) and positioned according to the International 10–20 system (Oostenveld and Praamstra, 2001). All of the cortical sites were referred to Cz during EEG acquisition and re-referenced off-line to the mean activity of the whole scalp by the average reference procedure. The data were stored using the NeuroScan software, version 4.1. The amplitude resolution was.1 μV, and the bandwidth ranged from DC to 100 Hz (6 dB per octave). The sampling rate was set at 500 Hz, and the impedance was kept below 5 KΩ (further details in Spironelli et al., 2020). After the data collection, the EEG signals were corrected for blinking and eye-movement artifacts, according to the eye movement modeling approach of Ille et al. (2002). All of the EEG data were divided into 2,048-ms time intervals. Indeed, given the constraint of the Brain Electrical Source Analysis (BESA) software to use 2^n samples, we needed to force the width of each interval to 1,024 samples, corresponding to a 2,048-ms interval. Each resting-state EEG recording, i.e., at pre-training, post-training, and follow-up at 3 min each, was divided into 2,048-ms time intervals. The continuous EEG data were transformed into the time-frequency domain using a fast Fourier transform (FFT), every task included 120 samples with.488 Hz FFT resolution. An artifact-rejection procedure was performed during each interval, with both amplitude and derivative thresholds (with respect to time) of 250 μV and 100 μV/ms, respectively. The remaining epochs were also inspected visually to remove any residual artifacts. On average, 89.93% of the epochs were accepted, equally distributed among sessions [pre-training: 88.75%, post-training: 90.94%, and follow-up 90.09%; $F_{(2,44)} = 0.55$, $p = 0.58$, $\eta_p^2 = 0.02$]. After windowing each interval with a tapered cosine, the FFT was averaged across the epochs that were finally free of residual artifacts. In the following step, the EEG amplitude was normalized within each electrode as the contribution of each band to the whole 0.488–100 Hz spectral range and expressed as a percentage. Normalization allowed us to quantify the relative contribution of each EEG band with respect to total spectral power (% value) in the two main groups (TG vs. ACG) and to compare the same scalp locations in all samples.

For statistical purposes, we calculated a new physiological index as the mean amplitude of high-beta/alpha ratio[1]. We decided to consider the ratio between the two EEG bands, rather than the alpha or high-beta rhythms separately because the high-beta/alpha ratio combines both the inhibitory component and the activation component in one measure as measured by alpha EEG and as represented by the high-beta rhythm, respectively (Oakes et al., 2004). This had the further advantage of normalizing the measures statistically across participants, i.e., the ratio between the two measures by subject.

Electrodes were grouped into four clusters with two spatial factors, consisting of two levels each, namely anterior-posterior asymmetry and laterality. Therefore, each quadrant included the average amplitude of five electrodes, including anterior left (AL: F9-F7-FT7-F3-FC3), anterior right (AR: F10-F8-FT8-F4-FC4), posterior left (PL: CP3-P3-P7-TP7-O1), and posterior right (PR: CP4-P4-P8-TP8-O2).

For the demographic and cognitive tests, separate between-groups Student's *t*-tests were carried out on age, education, handedness, MMSE, Vocabulary WAIS-IV subscale, APE, GDS, CWMS accuracy performance, and CWMS intrusion errors at the pretest to control for any difference at the pretest stage. Gender distribution was analyzed using the non-parametric χ^2 test.

Because of the small sample size, and as commonly done in cognitive training studies on aging (i.e., Borella et al., 2017a), Cohen's *d* values (1988), expressing the effect size of the comparisons, were computed within each group to better capture and assess the extent of the immediate (between the pre- and post-test sessions) and maintained (between the pre- and follow-up sessions) training gains. Values were corrected using the Hedges and Olkin (1985) correction factor to avoid the small sample bias. For the ANOVA results (see text footnote 2).

For the EEG data, we carried out an omnibus ANOVA including the between-subjects factor group (two levels, TG vs. ACG) and three within-subject factors, including session (three levels, pre-training vs. post-training vs. follow-up), region (two levels, anterior vs. posterior), and laterality (two levels, left vs. right hemisphere). Because the number of participants in each group was small ($n = 12$), we recognized that this analysis must be considered preliminary to ascertain whether the session factor showed a main effect or an interaction. Once this exploratory analysis revealed an effect of session, separate ANOVAs were carried out for each session, i.e., pre-training, post-training, and follow-up, on resting-state beta/alpha index that included the between-subjects factor group (two levels, TG vs. ACG) and two within-subject factors: region (two levels, anterior vs. posterior) and laterality (two levels, left vs. right hemisphere). Tukey's honestly significant difference (HSD) test was used to make *post hoc* comparisons ($p < 0.05$). In agreement with the behavioral data analysis, the Cohen's *d* (1988) effect sizes were also computed within each group.

In addition, Spearman's correlation analyses were carried out separately for TG and ACG participants, to ascertain whether post-training changes to the high-beta/alpha index at rest were significantly associated with better post-training performance on the CWMS task. Positive correlations marked those individuals with higher post-training scores on the CWMS task and higher post-training oscillatory responses at rest.

RESULTS

Socio-Demographical and Behavioral Data

As can be seen in **Table 1**, the two groups did not differ significantly in age, gender distribution, education level, handedness, or the general cognitive functioning (MMSE, vocabulary, APE) and mood state measures.

As for the CWMS (see **Table 2** for descriptive statistics), the groups did not differ at the pretest session in terms of either the CWMS score, representing the specific training gain, or intrusion errors, as an index of the efficiency of inhibitory control in the CWMS, representing a transfer effect [$t_{(22)} = 0.38$, $p = 0.70$ and $t_{(22)} = 0.47$, $p = 0.68$, respectively].

Concerning the Cohen's *d* effect sizes, considering the specific training gain, i.e., the CWMS performance[2], we found large to medium effect sizes immediately after the training and at the follow-up (0.80 and 0.61, respectively) for TG, whereas small effect sizes emerged for the ACG (0.27 and 0.24, respectively). Regarding the intrusion errors[2], which account for transfer effects, the medium to nearly large effect sizes immediately after the training and at the follow-up (0.68 and 0.78, respectively) was for the TG, whereas small effect sizes emerged for the ACG (0.19 and 0.13, respectively).

Electrophysiological Data

The preliminary omnibus ANOVA including all factors revealed a main effect of session [$F_{(2,44)} = 5.01$, $p < 0.05$, $\eta_p^2 = 0.19$, Cohen's $d = 0.95$], and allowed us to carry out separate ANOVAs on resting-state high-beta/alpha index for each session, i.e., pre-training, post-training, and follow-up.

The ANOVA carried out on the pre-training high-beta/alpha index revealed a significant main effect of region factor [$F_{(1,22)} = 33.53$, $p < 0.001$, $\eta_p^2 = 0.60$, Cohen's $d = 2.47$], with greater anterior than posterior oscillatory activity (**Figure 2A**). No significant main effects or interactions were found with group factor.

[1]We calculated the high-beta/alpha index as the ratio between the high-beta (20–35 Hz, effective β range 20.50–35.14 Hz) and alpha bands (8–2 Hz, effective α range 8.30–11.71 Hz).

[2]Separate ANOVAs were also carried out on CWMS performance - number of correctly recalled words- and intrusion errors. The ANOVA for the CWMS showed a main effect of the Session [$F_{(2,44)} = 6.78$, $p < 0.05$, $\eta_p^2 = 0.24$] revealing a significant improvement from the pre- to the posttest (*Mdiff.* = 1.67, $p = 0.01$) and from the pretest to follow-up (*Mdiff.* = 1.33, $p = 0.03$). The main effect of the Group factor was not significant [$F_{(1,22)} = 1.15$, $p = 0.3$], nor was the Group x Session interaction [$F_{(2,44)} < 1$]. However, the planned comparisons based on our a priori hypotheses showed that only the TG showed a significant difference between the pretest and posttest (*Mdiff.* = −2.25, $p = 0.02$) and between the pretest and follow-up (*Mdiff.* = −1.75, $p = 0.04$). These findings revealed improvements in the CWMS score at both posttest and follow-up, which did not differ from each other. No significant differences were found in the ACG.
Regarding the intrusion errors, the main effects of the Group [$F_{(1,22)} > 1$] and Session factors [$F_{(2,44)} = 1.61$, $p = 0.21$], as well as the Group x Session interaction [$F_{(2,44)} = 1.89$, $p = 0.16$] were not significant. The planned comparison did not reveal any significant differences.

TABLE 2 | Means (*M*) and standard deviations (±*SD*) of the criterion task (CWMS) and CWMS intrusion errors by group and assessment session.

	Pre-training				Post-training				6-month follow-up			
	TG		ACG		TG		ACG		TG		ACG	
CWMS	***M***	***SD***	***M***	***SD***	***M***	***SD***	***M***	***SD***	***M***	***SD***	***M***	***SD***
Accuracy	12.67	±2.96	12.08	±4.27	14.92	±2.39	13.17	±3.29	14.42	±2.53	13.00	±3.13
Intrusion errors	2.17	±1.19	1.83	±2.12	1.42	±0.90	1.50	±1.09	1.25	±1.05	2.08	±1.50

CWMS, Categorization Working Memory Span test.

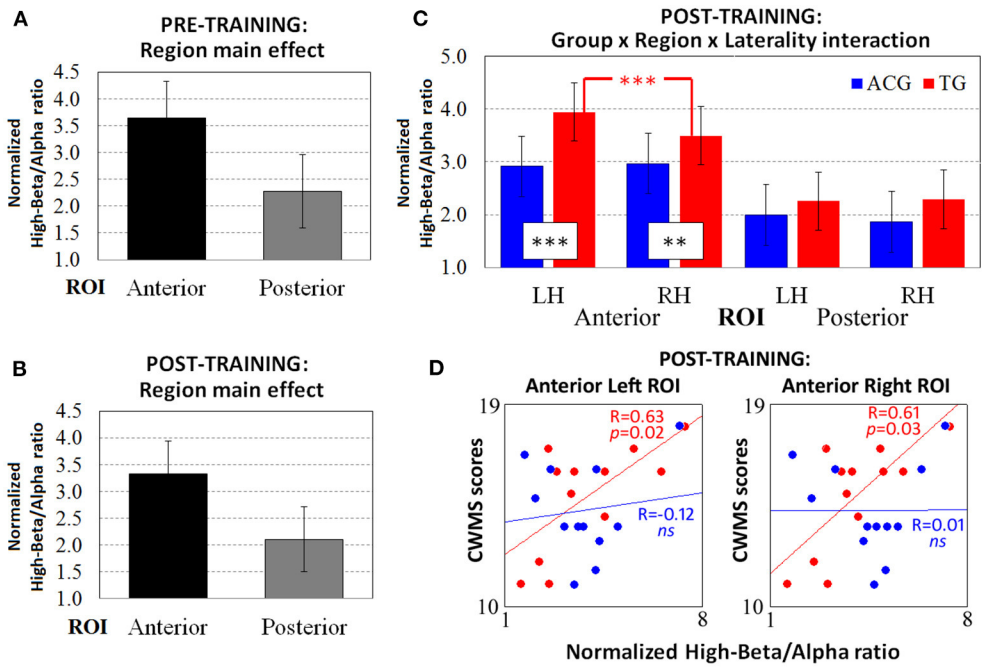

FIGURE 2 | The resting-state normalized high-beta/alpha index from the pre-training EEG data revealed only **(A)** the main effect of the region. ANOVA on the post-training EEG data showed both **(B)** the main effect of region and **(C)** the significant three-way Group × Region × Laterality interaction. The Spearman correlations between high-beta/alpha indices on both anterior ROIs and CWMS post-training performance **(D)** were significant for TG participants (red dots and lines) but not for ACG participants (blue dots and lines). ***$p < 0.001$, **$p < 0.01$ Tukey HSD *post-hoc* comparisons. TG: Trained Group; ACG: Active Control Group; LH: Left Hemisphere; RH: Right Hemisphere; CWMS: Categorisation Working Memory Span Test.

The ANOVA carried out on the post-training high-beta/alpha index revealed a significant main effect of region factor [$F_{(1,22)} = 38.86$, $p < 0.001$, $\eta^2_p = 0.63$, Cohen's $d = 2.66$], same as for the pre-training resting-state session (**Figure 2B**). However, the three-way Group × Region × Laterality interaction [$F_{(1,22)} = 7.41$, $p = 0.01$, $\eta^2_p = 0.25$, Cohen's $d = 1.16$] showed different patterns of oscillatory activity in TG vs. ACG participants. Indeed, on both anterior ROIs (all *p*s < 0.01), the TG participants had a higher high-beta/alpha index than the ACG participants did (**Figure 2C**). In addition, the TG participants showed significantly greater left vs. right high-beta/alpha ratio in anterior ROIs ($p < 0.001$), with the amplitude of left clusters being significantly increased in left vs. right sites, whereas the ACG participants exhibited a bilateral pattern of high-beta/alpha oscillatory activity.

Spearman's correlations were computed between the post-training scores achieved in the CWMS task and the high-beta/alpha ratio indices obtained at left and right anterior ROIs (**Figure 2D**). The ACG showed no significant association between left and right physiological indices and CWMS post-training scores (all *p*s > 0.05), whereas the TG showed a significant positive correlation between the scores obtained for the CWMS task and both the anterior left [$R_{(10)} = 63$, $p = 0.02$] and right [$R_{(10)} = 0.61$, $p = 0.03$] high-beta/alpha indices. This indicated that the better the performance on the CWMS task after the training, the greater the oscillatory responses in the frontal sites at rest. Regarding the effect sizes of the correlation coefficients in the anterior left and right ROIs, Cohen's *d* was 0.86 and 0.7, respectively.

The ANOVA carried out on the follow-up high-beta/alpha index revealed a significant main effect of the region factor

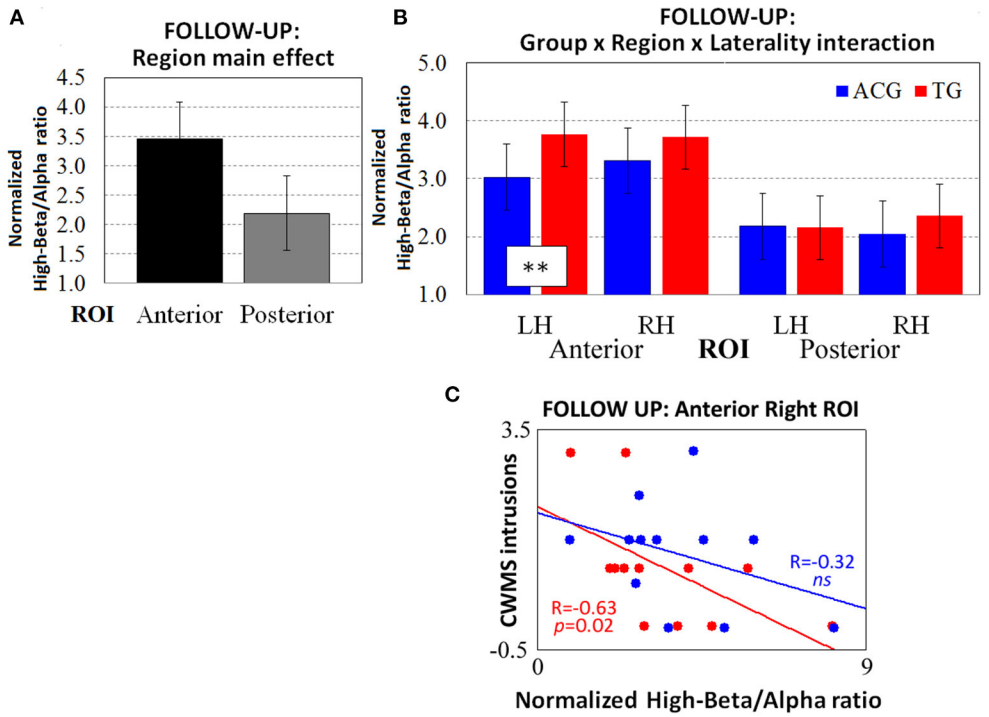

FIGURE 3 | The resting-state normalized high-beta/alpha index from the follow-up EEG data revealed **(A)** the main effect of region and **(B)** the three-way Group × Region × Laterality interaction (*tendency*). The Spearman correlations between high-beta/alpha indices on anterior right ROIs and CWMS follow-up intrusions **(C)** were significant in TG participants (red dots and lines) but not in ACG participants (blue dots and lines). $^{**}p < 0.01$ Tukey HSD *post-hoc* comparisons. TG: Trained Group; ACG: Active Control Group; LH: Left Hemisphere; RH: Right Hemisphere; CWMS: Categorisation Working Memory Span Test.

$[F_{(1,22)} = 39.21, p < 0.001, \eta_p^2 = 0.64$, Cohen's $d = 2.67]$, as it did in the previous session (**Figure 3A**). Furthermore, the three-way Group x Region x Laterality interaction was marginally significant $[F_{(1,22)} = 4.01, p = 0.05, \eta_p^2 = 0.25$, Cohen's $d = 0.85]$, revealing that, 6 months after the end of the WM training, the TG participants had higher oscillatory activity than the ACG participants on anterior left ROIs only ($p < 0.01$; **Figure 3B**).

The Spearman's correlations showed no significant association between left and right high-beta/alpha ratio indices and CWMS post-training scores in the ACG (all $ps > 0.05$), while showing a negative correlation between the follow-up intrusions of the TG in the CWMS task and the follow-up high-beta/alpha index on right anterior ROIs $[R_{(10)} = -0.63, p = 0.02)$. This indicated that the lower the number of CWMS intrusions 6 months after the training, the greater the high-beta/alpha oscillatory activity in frontal right sites at rest (**Figure 3C**). Cohen's d was 0.41 in considering the effect size of the correlation coefficients (TG vs. ACG) on anterior right ROIs.

DISCUSSION

The present pilot study was aimed at investigating the effects of WM training on behavioral and spontaneous resting-state EEG changes in healthy older adults. In particular, we examined WM-specific training gains and a transfer effect, i.e., the ability to inhibit information in WM that is no longer relevant, at both the behavioral and brain levels. Past research has revealed the efficacy of the WM training procedure used here at the behavioral level (e.g., Borella et al., 2010, 2017b), but no studies have been carried out yet considering its effects (and even the effects of WM training more generally) on spontaneous cortical functioning. Most of the past research was aimed at studying the effects of training(s) on neural activity, as collected by EEG, while participants executed training(s) (e.g., Anguera et al., 2013). Such data show how various kinds of training affect brain oscillations but provide limited information on training effects/benefits beyond the training itself. In other words, generalization, or discussion of transfer effects, is not usually seen when EEG data refer to cognitive functioning directly associated with training. Although resting-state activity might be more difficult to interpret, it offers some important advantages when the experimental design is rigorous and different groups are compared. In further detail, resting-state activity measured before and after training may better reflect the plastic neural changes occurring after training and their persistent traces across time, which is a picture that can be masked during an active task. To the best of our knowledge, no studies have examined WM training changes in older adults by analyzing EEG oscillatory activity at rest. The present study was aimed at filling this gap, by analyzing a psychophysiological index of cortical activation,

the mean amplitude high-beta/alpha ratio, in 3-min resting-state EEG data (eyes open) collected before and after WM training conducted with a group of older adults (TG) and comparing the data with an active control group engaged in cognitive assessments and alternative activities during the same period, rather than in the training, to ensure the best control sample for the TG. Finally, 6 months after the end of the WM training, all of the participants were called back for a follow-up assessment, which included electrophysiological resting-state recording. At least to our knowledge, no studies have examined maintenance effects regarding spontaneous oscillatory activity, and very few have analyzed such activity at the behavioral level.

Interestingly, in line with WM training studies in aging (Teixeira-Santos et al., 2019), the specific training gain was found only in the TG, as shown by the large effect size found for this group (as compared with the small effect size in the AG) in the criterion task, in the short term. In addition, a medium effect size was found for the specific training gains among the TG in the long term. This is in line with past studies using the same training regimen and, more in general, the very few WM training studies analyzing WM training-maintenance effects (i.e., Teixeira-Santos et al., 2019). As expected, these results confirmed the efficacy of WM training (and this specific procedure in particular) for improving the WM performance of elderly people, in both the short and long term. A transfer effect was also found regarding intrusion errors—as the index of the efficiency of inhibitory control—both at the posttest (medium effect size) and in the long-term (close to a large effect size). Such a transfer effect could be attributable to training activities that involve several processes, including the inhibition of no longer relevant information as well as attention shifting, to handle the different demands required by training tasks (see Borella et al., 2010, 2013). Notably, the larger effect sizes found in the long term, i.e., at the 6-month follow-up, as compared with the short-term ones, can indicate that more time is need for WM training to foster the ability to resist no longer relevant information. Indeed, a previous study using this same training procedure (Borella et al., 2017b) found a similar pattern of findings for intrusion errors, suggesting that certain abilities, like inhibitory abilities whose decline is particularly accentuated, thus not linear, with age take longer to benefit clearly from training activities. Notably, the ANOVA results did not show that the Group x Session interaction was significant for this measure. The divergent results between effect sizes and ANOVA may be due to the small sample size, which is one of the limits of the present study and causes the present study to be considered as a pilot one. However, the effect sizes indicating the presence of a transfer effect may subtend (a beginning of) changes that were more clearly found at the neural activity level but were still not explicit at the behavioral stage. Overall, these behavioral results both confirm that this WM training procedure fostered the specific gain and suggest the presence of a transfer effect on a mechanism (i.e., inhibition/attentional control) related to WM.

Regarding the electrophysiological data, preliminary analysis revealed the main effect of the session, allowing us to carry out a fine-grained analysis separately for the pre-training, post-training and, follow-up sessions. The analysis carried out on the normalized pre-training high-beta/alpha index revealed a main effect of region, suggesting that greater oscillatory responses appeared in frontal cortical sites, with no group differences. On the one hand, this analysis confirmed that the WM task used assesses WM and brain regions related to it (Constantinidis and Klingberg, 2016; Spironelli et al., 2020). On the other hand, it allows us to demonstrate that the training and the control group were similar, considering not only the inclusion criteria we set up a priori but also the baseline level of the cortical arousal of the participants in a resting-state condition. For this reason, post-training between-group effects reasonably could be associated with the assigned experimental condition, rather than with pre-existing differences. Greater oscillatory activity in the anterior cortical regions also was found in the post-training analysis. In addition, after the WM training, TG participants showed significantly greater oscillatory responses than ACG participants on both anterior ROIs. This result is in line with WM training studies showing that, after WM training, the regions involved in WM performance are the ones that changed (Constantinidis and Klingberg, 2016; Iordan et al., 2020). Interestingly, this increased cortical arousal was directly associated with better CWMS post-training performance: the higher the number of correct words recalled after the training, the greater the modulation of oscillatory responses in frontal sites at rest in only the TG participants. Thus, better management of WM task requests, probably due to the training activities, which led to improved WM performance, was related to greater frontal asymmetrical oscillatory activity in only the TG. This result supports the compensation hypothesis with aging (i.e., Cabeza et al., 2002), according to which aging brains recruit additional brain regions to "better" face task demands: the older adults in the TG who recruited more areas to compensate for losses had better WM performance than the ACG participants did. This pattern of findings also confirmed the role of the frontal region as an important locus for compensatory processes (Reuter-Lorenz and Park, 2014). Simultaneously, TG participants, but not ACG participants, showed higher oscillatory responses in left than in right anterior ROIs. This suggests that only the TG participants showed a shift from a more de-differentiated activity, i.e., the low specificity of processing, as shown during the pretest, to a more specific neural activity during the posttest. Therefore, the WM training could reduce the need to rely on compensatory neural mechanisms, thereby stimulating cortical efficiency. This pattern of findings is in line with other WM training studies involving older adults using fMRI (e.g., Buschkuehl et al., 2012). Indeed, laterality may serve as a marker of brain activity efficiency (Luo et al., 2016). A possible interpretation of our data could be that, because of the complexity of the WM task, a sort of over-activation compensated for age-related changes in neural efficiency during the pretest (i.e., Reuter-Lorenz and Cappell, 2008). The TG had more efficient behavioral and cortical functioning due to the training activities, as marked by greater and more specialized oscillatory activity.

Note that the leftward asymmetry found may also depend directly on the characteristics of the WM task used for training. The participants had to listen to a word list and then recall the

last word of each string in serial order (maintenance phase) and tap on the table (or press the spacebar) whenever they recognized a word depicting an animal (processing phase), regardless of its position in the word list. Therefore, the requests of the CWMS test represent a challenging and complex condition, involving an in-depth analysis of words. Because language shows left hemisphere dominance for about 95% of right-handed individuals and 70–85% of left-handers (e.g., Knecht et al., 2000; Perlaki et al., 2013), the training itself probably stimulates the linguistic network, with the frontal operculum being important not only in articulation and phonological encoding (Paulesu et al., 1993; Indefrey and Levelt, 2004) but also in the hierarchical organization of high-level linguistic processes (e.g., Bookheimer, 2002; Hagoort, 2005). In addition, this area is sensitive to age changes when verbal material is used and appears to be critical for left hemisphere functioning because the frontal operculum is also involved in high-order cognitive functions that decline with aging, such as thinking, action planning, and goal-directed behaviors (Koechlin and Jubault, 2006). In any case, these results confirm that aging is characterized by a certain degree of plasticity in terms of neural reorganization, as elicited by the WM training activities, by increasing the range of neural activity of the WM circuitry (Iordan et al., 2020).

In line with this interpretation, as compared with the ACG participants, at the 6-month follow-up, the TG participants showed significantly greater oscillatory activity in frontal left ROIs only, but no within-group frontal asymmetry appeared. Therefore, the immediately increased cortical arousal at rest in frontal sites was still present 6 months after the training ended but only in the left anterior cluster of electrodes, confirming the increased oscillatory responses among the TG compared to the ACG. Thus, it seems that the pattern found at the posttest for the TG became clearer with time. Interestingly, considering the association with a behavioral performance at follow-up, no direct link with CWMS scores was found. However, a negative correlation with intrusion errors in the CWMS emerged. Again, the greater the cortical arousal in right frontal sites, the better the performance at follow-up, as revealed by the decrease in the number of intrusion errors at the CWMS test. This result regarding electrophysiological activity levels might indicate that more general processes could be at work in the long term, particularly lessened attentional control due to the more efficient ability to inhibit information that is no longer relevant from the WM (see Buschkuehl et al., 2012). It seems that in the long term, the WM task requires less attentional control and the training results when it comes to efficient processes, probably by making one's ability to suppress no longer relevant information more efficient, which is related to a clear shift from asymmetrical oscillatory activity to a "specific" one. This pattern of relationships (and changes at the cortical level) can also account for both the larger effect sizes and the asymmetrical EEG activity found, especially in the short term, for the TG. Thus, it was presumably no longer necessary in the long term to compensate at the cortical level to improve WM performance, but rather the spontaneous oscillatory activity could remain symmetrical because of changes in how one manages their attentional control resources, as suggested by the effect sizes found for intrusion errors. Although frontal regions had similar average levels of oscillatory responses as those in ACG participants did, the link with long-lasting gains was found for TG adults only.

Despite these interesting results, our study has some main limitations. The sample size was quite small, so this study must be considered as a pilot, and the use of a unique WM task to assess training gains could be another limitation. We did not use a hearing screening task, which could be recommended for auditory cognitive training. However, some precautions were adopted, such as the use of a sound amplifier, and the participants were asked if they could easily hear the training stimuli during the experimental sessions. Furthermore, the follow-up EEG data approached statistical significance, deserving careful interpretations, and generalizations. Future studies should confirm the present results and examine whether the same brain-activation patterns are found with other WM tasks and other cognitive tasks assessing transfer effects. Regarding the modulation in oscillatory activity found, including a group of young adults would have allowed us to better specify the nature of the present results with respect to their interpretation. It would also be of interest to examine training changes at the cortical level in older adults exhibiting cognitive impairment to better capture the value of this training procedure in counteracting aging changes and examine the degree of plasticity that this training can elicit. Nonetheless, the strengths of the study include its aim, the double-blind, repeated-measures experimental design, the presence of a 6-month follow-up session (rarely used in training studies, even those focusing on the behavioral data only), and the active control group. Furthermore, as stated at the beginning of the discussion, analyzing resting-state activity may offer some important advantages. In the present study, there were no between-group differences at baseline (during the pre-training condition), but we found significantly increased oscillatory activity after this WM training in frontal sites of only the TG participants. Considering that these two samples of older adults shared similar sociodemographic characteristics as well as comparable general cognitive functioning and mood symptoms, the results support the idea that the cortical-level changes of the TG could be reasonably attributed to their WM training activity.

In conclusion, the results of the present study provided further evidence that WM training is a promising procedure with which to sustain cognitive functioning in older adults, particularly by improving their WM performance, at least in the long term and in line with past studies carried out with the same training procedure (Borella et al., 2017b). In addition, resting-state EEG analysis showed, for the first time, that the WM training procedure used in this study increased frontal oscillatory activity at rest, revealing not only short-term but also long-term training effects on the cortical arousal of the TG participants. These results were closely associated with better WM performance and a decrease in intrusion errors over the long term. No such effects appeared in the ACG participants. Overall, these findings suggested that WM training represents a scaffold with which to counter the changes in older adults both in their cognitive and brain functioning. The results also indicated that WM training is a promising approach to foster the so-called

functional cortical plasticity during aging, due to its ability to increase spontaneous oscillatory responses, particularly in frontal (left) brain regions.

DATA AVAILABILITY STATEMENT

The raw data supporting the conclusions of this article will be made available by the authors, without undue reservation.

ETHICS STATEMENT

The studies involving human participants were reviewed and approved by the Ethics Committee for Psychological Research – University of Padova (Protocol number 3180). The patients/participants provided their written informed consent to participate in this study.

AUTHOR CONTRIBUTIONS

EB selected participants according to the inclusion criteria. CS acquired and analyzed the EEG data and drafted the figures. CS and EB drafted and revised the manuscript. Both authors contributed to the conception and design of the study, approved the final version of the work, and agreed to be accountable for all aspects of the work, to ensure that questions related to the accuracy or integrity of any part of the work are investigated and resolved appropriately.

FUNDING

This work was funded by a grant from MIUR (Dipartimenti di Eccellenza DM 11/05/2017 no. 262) to the Department of General Psychology, University of Padova, and by the PRAT 2015 grant from the University of Padova, project no. CPDA152872 to CS.

REFERENCES

Anguera, J. A., Boccanfuso, J., Rintoul, J. L., Al-Hashimi, O., Faraji, F., Janowich, J., et al. (2013). Video game training enhances cognitive control in older adults. *Nature* 501, 97–103. doi: 10.1038/nature12486

Anokhin, A. P., Birbaumer, N., Lutzenberger, W., Nikolaev, A., and Vogel, F. (1996). Age increases brain complexity. *Electroenceph. Clin. Neurophysiol.* 99, 63–68. doi: 10.1016/0921-884X(96)95573-3

Bookheimer, S. (2002). Functional MRI of language: new approaches to understanding the cortical organization of semantic processing. *Annu Rev Neurosci* 25, 151–188. doi: 10.1146/annurev.neuro.25.112701.142946

Borella, E., Cantarella, A., Carretti, B., De Lucia, A., and De Beni, R. (2019a). Improving everyday functioning in the old-old with working memory training. *Am. J. Geriatr, Psychiatr.* 27, 975–983. doi: 10.1016/j.jagp.2019.01.210

Borella, E., Cantarella, A., Joly, E., Ghisletta, P., Carbone, E., Coraluppi, D., et al. (2017a). Performance-based everyday functional competence measures across the adult lifespan: the role of cognitive abilities. *Int. Psychogeriatr.* 29, 2059–2069. doi: 10.1017/S1041610217000680

Borella, E., Carbone, E., Pastore, M., De Beni, R., and Carretti, B. (2017b). Working memory training for healthy older adults: the role of individual characteristics in explaining short-and long-term gains. *Front. Hum. Neurosci.* 11:99. doi: 10.3389/fnhum.2017.00099

Borella, E., Carretti, B., Cornoldi, C., and De Beni, R. (2007). Working memory, control of interference and everyday experience of thought interference: When age makes the difference. *Aging Clin. Exp. Res.* 19, 200–206. doi: 10.1007/BF03324690

Borella, E., Carretti, B., and De Beni, R. (2008). Working memory and inhibition across the adult life-span. *Acta Psychol.* 128, 33–44. doi: 10.1016/j.actpsy.2007.09.008

Borella, E., Carretti, B., Meneghetti, C., Carbone, E., Vincenzi, M., Madonna, J. C., et al. (2019b). Is working memory training in older adults sensitive to music? *Psychol. Res.* 83, 1107–1123. doi: 10.1007/s00426-017-0961-8

Borella, E., Carretti, B., Riboldi, F., and De Beni, R. (2010). Working memory training in older adults: evidence of transfer and maintenance effects. *Psychol. Aging* 25, 767–778. doi: 10.1037/a0020683

Borella, E., Carretti, B., Zanoni, G., Zavagnin, M., and De Beni, R. (2013). Working memory training in old age: an examination of transfer and maintenance effects. *Arch. Clin. Neuropsychol.* 28, 331–347. doi: 10.1093/arclin/act020

Brehmer, Y., Westerberg, H., and Bäckman, L. (2012). Working-memory training in younger and older adults: Training gains, transfer, and maintenance. *Front. Hum. Neurosci.* 6:63. doi: 10.3389/fnhum.2012.00063

Brum, P. S., Borella, E., Carretti, B., and Sanches Yassuda, M. (2020). Verbal working memory training in older adults: an investigation of dose response. *Aging Ment. Health* 24, 81–91. doi: 10.1080/13607863.2018.1531372

Buschkuehl, M., Jaeggi, S. M., and Jonides, J. (2012). Neuronal effects following working memory training. *Develop. Cogn. Neurosci.* 2(Suppl. 1), S167–S179. doi: 10.1016/j.dcn.2011.10.001

Cabeza, R., Anderson, N. D., Locantore, J. K., and McIntosh, A. R. (2002). Aging gracefully: compensatory brain activity in high-performing older adults. *Neuroimage* 17, 1394–1402. doi: 10.1006/nimg.2002.1280

Cantarella, A., Borella, E., Carretti, B., Kliegel, M., and De Beni, R. (2017). Benefits in tasks related to everyday life competences after a working memory training in older adults. *Int. J. Geriatr. Psychiatr.* 32, 86–93. doi: 10.1002/gps.4448

Carbone, E., Vianello, E., Carretti, B., and Borella, E. (2019). Working memory training for older adults after major surgery: benefits to cognitive and emotional functioning. *Am. J. Geriatr, Psychiatr.* 27, 1219–1227. doi: 10.1016/j.jagp.2019.05.023

Carretti, B., Borella, E., Zavagnin, M., and De Beni, R. (2013). Gains in language comprehension relating to working memory training in healthy older adults. *Int. J. Geriatr. Psychiatr.* 28, 539–546. doi: 10.1002/gps.3859

Constantinidis, C., and Klingberg, T. (2016). The neuroscience of working memory capacity and training. *Nature Rev. Neurosci.* 17, 438–449. doi: 10.1038/nrn.2016.43

De Beni, R., Borella, E., Carretti, B., Marigo, C., and Nava, L. A. (2008). *Portfolio per la Valutazione del Benessere e Delle Abilità Cognitive Nell'età Adulta e Avanzata [The Assessment of Well-Being and Cognitive Abilities in Adulthood and Aging]*. Firenze: Giunti OS.

Emch, M., von Bastian, C. C., and Koch, K. (2019). Neural correlates of verbal working memory: an fMRI meta-analysis. *Front. Hum. Neurosci.* 13:180. doi: 10.3389/fnhum.2019.00180

Folstein, M. F., Folstein, S. E., and McHugh, P. R. (1975). 'Mini-Mental State': a practical method for grading the cognitive state of patients for the clinician. *J. Psychiatr. Res.* 12, 189–198. doi: 10.1016/0022-3956(75)90026-6

Gamboz, N., Borella, E., and Brandimonte, M. A. (2009). The role of switching, inhibition and working memory in older adults' performance in the Wisconsin Card Sorting Test. *Aging Neuropsychol. Cogn.* 16, 260–284. doi: 10.1080/13825580802573045

Hagoort, P. (2005). On Broca, brain, and binding: a new framework. *TRENDS Cogn. Sci.* 9, 416–423. doi: 10.1016/j.tics.2005.07.004

Hedges, L. V., and Olkin, I. (1985). *Statistical Methods for Meta-Analysis*. San Diego, CA: Academic Press.

Heinzel, S., Lorenz, R., Brockhaus, W.-R., Wüstenberg, T., Kathmann, N., Heinz, A., et al. (2014). Working memory load-dependent brain response predicts behavioral training gains in older adults. *J. Neurosci.* 34,1224–3123. doi: 10.1523/JNEUROSCI.2463-13.2014

Hou, J., Jiang, T., Fu, J., Su, B., Wu, H., Sun, R., et al. (2020). The long-term efficacy of working memory training in healthy older adults: a systematic review and meta-analysis of 22 randomized controlled trials. *J. Gerontol. B-Psychol. Sci. Soc. Sci.* 75, e174–e188. doi: 10.1093/geronb/gbaa077

Ille, N., Berg, P., and Scherg, M. (2002). Artifact correction of the ongoing EEG using spatial filters based on artifact and brain signal topographies. *J. Clin. Neurophysiol.* 19, 113–124. doi: 10.1097/00004691-200203000-00002

Indefrey, P., and Levelt, W. J. M. (2004). The spatial and temporal signatures of word production components. *Cognition* 92, 101–144. doi: 10.1016/j.cognition.2002.06.001

Iordan, A. D., Cooke, K. A., Moored, K. D., Katz, B., Buschkuehl, M., Jaeggi, S. M., et al. (2020). Neural correlates of working memory training: evidence for plasticity in older adults. *Neuroimage* 217:116887. doi: 10.1016/j.neuroimage.2020.116887

Jolly, A. E., Scott, G. T., Sharp, D. J., and Hampshire, A. H. (2020). Distinct patterns of structural damage underlie working memory and reasoning deficits after traumatic brain injury. *Brain* 143, 1158–1176. doi: 10.1093/brain/awaa067

Karbach, J., and Verhaeghen, P. (2014). Making working memory work: a meta-analysis of executive-control and working memory training in older adults. *Psychol. Sci.* 25, 2027–2037. doi: 10.1177/0956797614548725

Klados, M. A., Styliadis, C., Frantzidis, C. A., Paraskevopoulos, E., and Bamidis, P. D. (2016). Beta-band functional connectivity is reorganized in mild cognitive impairment after combined computerized physical and cognitive training. *Front. Neurosci*. 10:55. doi: 10.3389/fnins.2016.00055

Knecht, S., Dräger, B., Deppe, M., Bobe, L., Lohmann, H., Flöel, A., et al. (2000). Handedness and hemispheric language dominance in healthy humans. *Brain* 123, 2512–2518. doi: 10.1093/brain/123.12.2512

Koechlin, E., and Jubault, T. (2006). Broca's area and the hierarchical organization of human behavior. *Neuron* 50, 963–974. doi: 10.1016/j.neuron.2006.05.017

Laufs, H., Krakow, K., Sterzer, P., Eger, E., Beyerle, A., Salek-Haddadi, A., et al. (2003). Electroencephalographic signatures of attentional and cognitive default modes in spontaneous brain activity fluctuations at rest. *Proc. Natl. Acad. Sci.* 100, 11053–11058. doi: 10.1073/pnas.1831638100

Luo, C., Zhang, X., Cao, X., Gan, Y., Li, T., Cheng, Y., et al. (2016). The lateralization of intrinsic networks in the aging brain implicates the effects of cognitive training. *Front. Aging Neurosci.* 8:32. doi: 10.3389/fnagi.2016.00032

Miyake, A., and Shah, P. (1999). "Toward unified theories of working memory: Emerging general consensus, unresolved theoretical issues, and future research directions," in *Models of Working Memory: Mechanisms of Active Maintenance and Executive Control*, eds A. Miyake and P. Shah (New York, NY: Cambridge University Press), 442–481.

Nguyen, L., Murphy, K., and Andrews, G. (2019). Cognitive and neural plasticity in old age: A systematic review of evidence from executive functions cognitive training. *Ageing Res. Rev.* 53:100912. doi: 10.1016/j.arr.2019.100912

Oakes, T. R., Pizzagalli, D. A., Hendrick, A. M., Horras, K. A., Larson, C. L., Abercrombie, H. C., et al. (2004). Functional coupling of simultaneous electrical and metabolic activity in the human brain. *Hum. Brain Mapp.* 21, 257–270. doi: 10.1002/hbm.20004

Oldfield, R. C. (1971). The assessment and analysis of handedness: the Edinburgh Inventory. *Neuropsychologia* 9, 97–113. doi: 10.1016/0028-3932(71)90067-4

Oostenveld, R., and Praamstra, P. (2001). The five percent electrode system for high-resolution EEG and ERP measurements. *Clin. Neurophysiol.* 112, 713–719. doi: 10.1016/S1388-2457(00)00527-7

Orsini, A., and Pezzuti, L. (2013). *WAIS-IV. Contributo Alla Taratura Italiana [WAIS-IV. Contribution to the Italian Standardization*]. Firenze: Giunti OS.

Park, D. C., Lautenschlager, G., Hedden, T., Davidson, N., Smith, A. D., and Smith, P. K. (2002). Models of visuospatial and verbal memory across the adult life span. *Psychol. Aging* 17, 299–320. doi: 10.1037/0882-7974.17.2.299

Park, D. C., Smith, A. D., Lautenschlager, G., Earles, J. L., Frieske, D., and Zwahr, M. (1996). Mediators of long-term memory performance across the lifespan. *Psychol. Aging* 11, 621–637. doi: 10.1037/0882-7974.11.4.621

Paulesu, E., Frith, C. D., and Frackowiak, R. S. J. (1993). The neural correlates of the verbal component of working memory. *Nature* 362, 342–345. doi: 10.1038/362342a0

Perlaki, G., Horvath, R., Orsi, G., Aradi, M., Auer, T., Varga, E., et al. (2013). White-matter microstructure and language lateralization in left-handers: a whole-brain MRI analysis. *Brain Cogn.* 82, 319–328. doi: 10.1016/j.bandc.2013.05.005

Raz, N. (2005). "The aging brain observed in vivo: differential changes and their modifiers," in *Cognitive Neuroscience of Aging: Linking Cognitive and Cerebral Aging*, eds R. Cabeza, L. Nyberg, and D. C. Park (New York, NY: Oxford University Press), 19–57.

Reis, J., Portugal, A. M., Fernandes, L., Afonso, N., Pereira, M., Sousa, N., et al. (2016). An alpha and theta intensive and short neurofeedback protocol for healthy aging working-memory training. *Front. Aging Neurosci.* 8:157. doi: 10.3389/fnagi.2016.00157

Reuter-Lorenz, P. A. (2000). "Cognitive neuropsychology of the aging brain," in *Cognitive Aging: A Primer*, eds D. C. Park and N. Schwarz (Philadelphia, PA: Psychology Press), 93–114.

Reuter-Lorenz, P. A., and Cappell, K. A. (2008). Neurocognitive aging and the compensation hypothesis. *Curr. Dir. Psychol. Sci.* 17, 177–182. doi: 10.1111/j.1467-8721.2008.00570.x

Reuter-Lorenz, P. A., and Park, D. C. (2014). How does it STAC Up? Revisiting the scaffolding theory of aging and cognition. *Neuropsychol. Rev.* 24, 355–370. doi: 10.1007/s11065-014-9270-9

Reuter-Lorenz, P. A., and Sylvester, C. C. (2005). "Neuroscience of working memory and aging," in *Cognitive Neuroscience of Aging: Linking Cognitive and Cerebral Aging*, eds R. Cabeza, L. Nyberg, D.C. Park (New York, NY: Oxford University Press), 186–217.

Robert, C., Borella, E., Fagot, D., Lecerf, T., and de Ribaupierre, A. (2009). Working memory and inhibitory control across the life span: Intrusion errors in the Reading Span Task. *Mem. Cogn.* 37, 336–345. doi: 10.3758/MC.37.3.336

Rossini, P. M., Rossi, S., Babiloni, C., and Polich, J. (2007). Clinical neurophysiology of aging brain: From normal aging to neurodegeneration. *Prog. Neurobiol.* 83, 375–400. doi: 10.1016/j.pneurobio.2007.07.010

Spironelli, C., Bergamaschi, S., Mondini, S., Villani, D., and Angrilli, A. (2013). Functional plasticity in Alzheimer's disease: effect of cognitive training on language-related ERP components. *Neuropsychologia* 51, 1638–1648. doi: 10.1016/j.neuropsychologia.2013.05.007

Spironelli, C., Carbone, E., and Borella, E. (2020). Electrophysiological correlates of the Categorization Working Memory Span task in older adults. *Behav. Brain Res.* 393:112809. doi: 10.1016/j.bbr.2020.112809

Stuss, D. T., Alexander, M. P., and Benson, D. F. (1997). "Frontal lobe functions," in *Contemporary Behavioral Neurology,* eds M. R. Trimble and J. L. Cummings (Boston, MA: Butterworth-Heinemann), 169–187.

Styliadis, C., Kartsidis, P., Paraskevopoulos, E., Ioannides, A. A., and Bamidis, P. D. (2015). Neuroplastic effects of combined computerized physical and cognitive training in elderly individuals at risk for dementia: an eLORETA controlled study on resting states. *Neural Plastic.* 2015:172192. doi: 10.1155/2015/172192

Teixeira-Santos, A. C., Moreira, C. S., Magalhães, R., Magalhães, C., Pereira, D. R., Leite, J., et al. (2019). Reviewing working memory training gains in healthy older adults: A meta-analytic review of transfer for cognitive outcomes. *Neurosci. Biobehav. Rev.* 103, 163–177. doi: 10.1016/j.neubiorev.2019.05.009

Wechsler, D. (2008). *Wechsler Adult Intelligence Scale–Fourth Edition: Administration and Scoring Manual*. San Antonio, TX: NCS Pearson.

World Medical Association (2013). World Medical Association Declaration of Helsinki: ethical principles for medical research involving human subjects. *JAMA* 310, 2191–2194. doi: 10.1001/jama.2013.281053

Yesavage, J. A., Brink, T. L., Rose, T. L., Lum, O., Huang, V., Adey, M., et al. (1982-1983). Development and validation of a geriatric depression screening scale: a preliminary report. *J. Psychiatr. Res.* 17, 37–49. doi: 10.1016/0022-3956(82)90033-4

Zendel, B. R., de Boysson, C., Mellah, S., Démonet, J.-F., and Belleville, S. (2016). The impact of attentional training on event-related potentials in older adults. *Neurobiol. Aging* 47, 10–22. doi: 10.1016/j.neurobiolaging.2016.06.023

Conflict of Interest: The authors declare that the research was conducted in the absence of any commercial or financial relationships that could be construed as a potential conflict of interest.

Publisher's Note: All claims expressed in this article are solely those of the authors and do not necessarily represent those of their affiliated organizations, or those of the publisher, the editors and the reviewers. Any product that may be evaluated in this article, or claim that may be made by its manufacturer, is not guaranteed or endorsed by the publisher.

frontiers in Aging Neuroscience

ORIGINAL RESEARCH
published: 25 November 2021
doi: 10.3389/fnagi.2021.746373

Magnetoencephalography Brain Signatures Relate to Cognition and Cognitive Reserve in the Oldest-Old: The EMIF-AD 90 + Study

Alessandra Griffa[1,2,3], Nienke Legdeur[4], Maryam Badissi[4], Martijn P. van den Heuvel[5], Cornelis J. Stam[3], Pieter Jelle Visser[4,6] and Arjan Hillebrand[3]*

[1] Division of Neurology, Department of Clinical Neurosciences, Geneva University Hospitals and Faculty of Medicine, University of Geneva, Geneva, Switzerland, [2] Center of Neuroprosthetics, Institute of Bioengineering, École Polytechnique Fédérale De Lausanne (EPFL), Geneva, Switzerland, [3] Department of Clinical Neurophysiology and MEG Center, Amsterdam Neuroscience, Amsterdam UMC, Vrije Universiteit Amsterdam, Amsterdam, Netherlands, [4] Department of Neurology, Amsterdam Neuroscience, Alzheimer Center Amsterdam, Vrije Universiteit Amsterdam, Amsterdam UMC, Amsterdam, Netherlands, [5] Dutch Connectome Lab, Department of Complex Trait Genetics, Center for Neuroscience and Cognitive Research, Amsterdam Neuroscience, Vrije Universiteit Amsterdam, Amsterdam UMC, Amsterdam, Netherlands, [6] Department of Psychiatry and Neuropsychology, School for Mental Health and Neuroscience, Maastricht University, Maastricht, Netherlands

The oldest-old subjects represent the fastest growing segment of society and are at high risk for dementia with a prevalence of up to 40%. Lifestyle factors, such as lifelong participation in cognitive and leisure activities, may contribute to individual cognitive reserve and reduce the risk for cognitive impairments. However, the neural bases underlying cognitive functioning and cognitive reserve in this age range are still poorly understood. Here, we investigate spectral and functional connectivity features obtained from resting-state MEG recordings in a cohort of 35 cognitively normal (92.2 ± 1.8 years old, 19 women) and 11 cognitively impaired (90.9 ± 1.9 years old, 1 woman) oldest-old participants, in relation to cognitive traits and cognitive reserve. The latter was approximated with a self-reported scale on lifelong engagement in cognitively demanding activities. Cognitively impaired oldest-old participants had slower cortical rhythms in frontal, parietal and default mode network regions compared to the cognitively normal subjects. These alterations mainly concerned the theta and beta band and partially explained inter-subject variability of episodic memory scores. Moreover, a distinct spectral pattern characterized by higher relative power in the alpha band was specifically associated with higher cognitive reserve while taking into account the effect of age and education level. Finally, stronger functional connectivity in the alpha and beta band were weakly associated with better cognitive performances in the whole group of subjects, although functional connectivity effects were less prominent than the spectral ones. Our results shed new light on the neural underpinnings of cognitive functioning in the oldest-old population and indicate that cognitive performance and cognitive reserve may have distinct spectral electrophysiological substrates.

Keywords: cognition, functional connectivity, cognitive reserve, oldest-old, magnetoencephalography

OPEN ACCESS

Edited by:
Takako Fujioka,
Stanford University, United States

Reviewed by:
Ville Leinonen,
Kuopio University Hospital, Finland
Antonino Vallesi,
University of Padua, Italy

****Correspondence:***
Alessandra Griffa
alessandra.griffa@gmail.com

Received: *23 July 2021*
Accepted: *01 November 2021*
Published: *25 November 2021*

Citation:
Griffa A, Legdeur N, Badissi M, van den Heuvel MP, Stam CJ, Visser PJ and Hillebrand A (2021) Magnetoencephalography Brain Signatures Relate to Cognition and Cognitive Reserve in the Oldest-Old: The EMIF-AD 90 + Study. Front. Aging Neurosci. 13:746373. doi: 10.3389/fnagi.2021.746373

INTRODUCTION

The oldest-old population, including individuals aged 85–90 years and older, is the fastest growing segment of Western societies (Corrada et al., 2010; Legdeur et al., 2018). The number of oldest-old is estimated to increase fivefold in the coming decades, resulting in 77 millions of oldest-old individuals worldwide by 2050 (United Nations, Department of Economic and Social Affairs, Population Division, 2019). Many of these individuals will suffer from cognitive impairments and dementia, with a dementia prevalence of up to 40% in this age range and major implications for public health and society (Bullain and Corrada, 2013; Yang et al., 2013). The identification of dementia's neuropathological substrate becomes increasingly challenging with age (Yang et al., 2013). This is due to an increasing prevalence of Alzheimer's and cerebrovascular pathologies (the most common causes of dementia) among non-demented oldest-old individuals (Wharton et al., 2011; Paolacci et al., 2017; Legdeur et al., 2019), and to a more frequent co-occurrence of multiple dementia-related pathologies (Corrada et al., 2012; James et al., 2012). In parallel, convergent evidence suggests that different lifestyle factors may contribute to individual cognitive reserve-defined as the adaptability of functional brain processes to cope with aging or pathological processes (Stern, 2009; Stern et al., 2018)- and protect from, or delay cognitive decline and incidence of clinical dementia (Verghese et al., 2003; Pettigrew et al., 2019; Soldan et al., 2021) even in presence of extensive brain pathologies (Xu et al., 2019). Yet, the neural underpinnings of cognitive functioning and history of lifelong engagement in cognitive activities in the oldest-old population are not clear.

Few electrophysiological studies have investigated the brain functional substrate of cognitive impairments in the oldest-old population, since data for this age range are scarce (Yang et al., 2013; Legdeur et al., 2018). Studies that used electroencephalography (EEG) or magnetoencephalography (MEG) in older adults aged 65–80 years found that demented subjects and subjects at risk of developing dementia have brain functional alterations with slowing of cortical oscillations (Babiloni et al., 2006; Fernández et al., 2006; van der Hiele et al., 2007; de Haan et al., 2008), reduced functional connectivity in the higher frequency bands in posterior, parietal and limbic brain regions, and stronger functional connectivity between frontal and posterior areas (Engels et al., 2017; Miraglia et al., 2017; Maestú et al., 2019; Babiloni et al., 2020a). However, it is unknown whether comparable spectral and functional connectivity patterns are observable in cognitively impaired oldest-old compared to cognitively normal oldest-old, and how these patterns could relate to protective and cognitive reserve factors.

Little research has been done on the electrophysiological substrate of cognitive reserve (Šneidere et al., 2020; Balart-Sánchez et al., 2021). Results on resting-state data are controversial with studies reporting involvement of alpha rhythms (Babiloni et al., 2020b), gamma rhythms (Yang and Lin, 2020), or no association with cognitive reserve (López et al., 2014). One study found negative and positive associations between whole-brain EEG functional connectivity and cognitive reserve in younger and older healthy adults, respectively, suggesting possible shifts in the relationship between brain electrophysiology and cognitive reserve with aging (Fleck et al., 2017). In light of these considerations, understanding the possibly age-specific (Gonzalez-Escamilla et al., 2018) neural underpinning of cognitive impairment and cognitive reserve in the oldest-old is key to identifying protective factors for cognitive decline, testing prevention and treatment options, and monitoring dementia-related pathological evolution in this age segment.

MEG is a neuroimaging technique that allows quantifying electrophysiological patterns at the individual subject level by probing the magnetic fields associated with postsynaptic potentials by means of sensor arrays that cover the whole head (Hämäläinen et al., 1993; Stam, 2010; Hari and Puce, 2017; Gross, 2019). Signal contributions from different brain regions can be estimated from sensor-level data using source-reconstruction algorithms (Baillet et al., 2001), including beamforming techniques (Hillebrand et al., 2005), and further analyzed to elucidate spectral features of neuronal activity and functional couplings between regions (Hillebrand et al., 2012). MEG studies have revealed the functional organization of the brain across different frequency bands into large-scale systems, including the visual, sensorimotor and default mode networks (de Pasquale et al., 2010; Brookes et al., 2011; Hipp et al., 2012), and its disruption in neurodegenerative disorders (Stam, 2014) and dementia (Stam, 2010; Engels et al., 2017; Hughes et al., 2019) but have not been applied to the oldest-old. The objective of this study is to elucidate the relation between spectral and functional connectivity properties of MEG oscillations and cognitive impairments in a unique cohort of oldest-old subjects from the EMIF-AD 90 + Study (Legdeur et al., 2018), and to investigate the relationship between these neural biomarkers and lifelong engagement in cognitively demanding activity, a possible protective factor for cognitive decline and proxy for cognitive reserve (Stern, 2009; Landau et al., 2012).

MATERIALS AND METHODS

Subjects

60 subjects (91.8 ± 2.0 years of age, 37 females) were recruited at the Amsterdam University Medical Centers (Amsterdam UMC), The Netherlands, in the framework of the EMIF-AD (European Medical Information Framework for AD) 90 + Study (Legdeur et al., 2018), a case-control study with cognitively normal and impaired individuals to investigate the protective factors for cognitive impairment in the oldest-old population. In order to increase the power of our study and in agreement with others (Bullain and Corrada, 2013), we also included 4 subjects aged between 88 and 90 years. Neurological disorders (e.g., stroke or epilepsy), severe depression (Geriatric Depression Scale (GDS) > 11) (Yesavage et al., 1982) and visual or auditory impairments that made neuropsychological testing impossible, were exclusion criteria. Moreover, 14 out of 60 subjects were excluded from further analyses because of missing

MRI data, low-quality MEG recordings or poor MRI-MEG co-registration (see below), so that a restricted subset of 46 subjects (91.9 ± 1.9 years of age, 29 females) were included in the final analyses. This study was approved by the local Medical Ethics Review Committee of the Amsterdam UMC, and all subjects provided written informed consent.

Clinical and Cognitive Assessment

Each participant underwent a comprehensive neuropsychological, functional and clinical assessment. Neuropsychological and functional testing was administrated by a neuropsychologist; clinical diagnosis was made by a neurologist, geriatrician or general practitioner (McKhann et al., 1984; Petersen, 2004). Subjects were considered cognitively normal (CN) if they scored 0 points on the Clinical Dementia Rating (CDR) scale (Morris, 1993) and had no clinical diagnosis of dementia or mild cognitive impairment (35 CN, 92.2 ± 1.8 years of age, 19 females). Cognitively Impaired (CI) subjects (11 CI, 90.9 ± 1.9 years of age, 10 females) had a CDR score larger than 0 points (median CDR = 1) and a clinical diagnosis of probable Alzheimer's disease (AD, 10 subjects) or amnestic mild cognitive impairment (aMCI, 1 subject).

The overall cognitive ability of each participant was assessed with the Mini-Mental State Examination (MMSE) (Folstein et al., 1983). Executive control was tested with the letter fluency test (1 min per letter, letters D-A-T) (Tombaugh et al., 1999), the processing speed with the Trail Making Tests (TMT)-B score (Reitan, 1958; Broshek and Barth, 2000), and episodic memory with the total score of the CERAD (Consortium to Establish a Registry for Alzheimer's Disease) battery over three trials (Rossetti et al., 2010). Lifelong engagement in cognitive activities was assessed with a retrospective self-reported scale quantifying how often the participant engaged in common cognitively demanding activities that depend minimally on socioeconomic status, such as reading books or newspapers, playing games or writing letters (Wilson et al., 2003; Landau et al., 2012). Specifically, each participant was asked to rate her/his engagement in these activities at 6, 12, 18, 40, and current years of age, according to a 5-level frequency scale (once a year or never/several times a year/several times a month/several times a week/several times a day). From the questionnaire responses, two composite scores were computed: the current cognitive activity (cCAQ) (average score at current age), and the past cognitive activity (pCAQ) (average score across ages 6, 12, 18, and 40 years) (Landau et al., 2012). The lifelong engagement in leisure and cognitively stimulating activities has been associated with lower dementia risk (Verghese et al., 2003; León et al., 2014; Wang et al., 2017), slower hippocampal atrophy (Valenzuela et al., 2008) and amyloid accumulation (Landau et al., 2012) in aging, and it is considered a proxy of individual cognitive reserve.

Brain Imaging

Magnetic Resonance Imaging Acquisition and Processing

Each subject underwent an MRI session on a 3T Philips Achieva scanner equipped with an 8-channel head coil, which included a structural three-dimensional (3D) T1-weighted acquisition (sagittal gradient-echo sequence; isotropic voxel size 1 × 1 × 1 mm^3, TR 7.9 ms, TE 4.5 ms, flip angle 8°). T1-weighted volumes were skull-stripped, corrected for intensity inhomogeneity, and segmented into gray matter, white matter, and cerebrospinal fluid compartments with the Statistical Parametric Mapping (SPM) toolbox, version 8 (Penny et al., 2011). The gray matter compartment was then parcellated into 78 cortical regions of interest (ROIs) according to the Automatic Anatomical Labeling (AAL) atlas and 2 hippocampal regions (Tzourio-Mazoyer et al., 2002; Gong et al., 2009; **Supplementary Table 1**) through spatial normalization of the T1-weighted volumes to MNI space and application of the inverse MNI-to-native transform to bring the parcellation volume to native space [SPM version 8 (Penny et al., 2011)]. The correspondence between the 80 gray matter regions and the 7 resting state networks (RSNs) defined by Yeo et al. (2011) was assessed with a majority-voting procedure in MNI space (MNI-normalized atlases from the Lead-DBS database (Horn and Kühn, 2015) were used) using in-house MATLAB code (**Supplementary Table 1**).

Magnetoencephalography Recording and Preprocessing

Magnetic fields were recorded with a 306-channel whole-head MEG system (Elekta Neuromag Oy, Helsinki, Finland) inside a magnetically shielded room (Vacuumschmelze, Hanau, Germany), at a sampling frequency of 1,250 Hz. An online anti-aliasing filter of 410 Hz and a high-pass filter of 0.1 Hz were applied to sensor-level signals. The MEG protocol consisted of a 5-min eyes-closed recording in resting-state condition, during which subjects were instructed to remain awake and cognitively alert, but they were not assigned any specific task.

Sensor-level time-series were visually inspected to identify 'bad' channels (i.e., flat channels and channels affected by high-frequency noise or jump artifacts), which were excluded before applying temporal signal-space separation (tSSS) (min/median/max = 6/11/13 excluded channels per subject). Next, artifact components originating from outside the head volume, including both external noise sources and biomagnetic sources, were removed with the tSSS algorithm implemented in MaxFilter software (Elekta Neuromag Oy, version 2.2.15) (Taulu and Simola, 2006; Taulu and Hari, 2009). For the tSSS parameter setting, an automatic adjustment of the subjects' sphere center coordinates (**Supplementary Material SI.1** and **Supplementary Figures 1, 2**), a subspace correlation limit of 0.9, and a sliding window of 10 s were used.

The position of the head with respect to the MEG sensors was assessed by means of five Head Position Indicator (HPI) coils and monitored during the recording. The outline of each subject's scalp (approximatively 500 points) and the HPI coils were digitized with a 3D digitizer (Fastrak, Polhemus, Colchester, VT, United States), and registered to the MRI space using a surface-matching procedure with an approximate accuracy of 4 mm (Whalen et al., 2008). A sphere was then fitted to the outline of the scalp as obtained from the co-registered MRI, which was used as a volume conductor model for the beamformer algorithm (see next section).

Source Reconstruction

In order to obtain source-localized activity, the sensor-level preprocessed time-series were projected to 80 locations (sources) in the cortex corresponding to the centroids of the AAL and bilateral hippocampal ROIs, using a beamforming approach (Hillebrand et al., 2012, 2016). Briefly, the sensor-level data were spatially filtered to estimate the contribution to each source's time-series. For each source, the filter weights were determined from the broad-band (0.5–48 Hz) data covariance matrix and the forward solution (lead field) of the target source according to a scalar minimum variance beamformer (Hillebrand and Barnes, 2005; Hillebrand et al., 2005).

From the source-reconstructed time-series, 8 (not necessarily consecutive) epochs of 13.1 s duration (16,384 samples) were selected for each subject using an automatic procedure. Epochs possibly corrupted by artifacts or during which the subjects may have been drowsy were identified and discarded, based on the presence of extreme values in the temporal domain (indicators of artifacts such as eye movement or high frequency noise), individual peak frequency (IPF) outliers, and low alpha1 occipital power content (indicators of transition to the first stages of sleep; Hari and Puce, 2017; **Supplementary Material SI.2** and **Supplementary Figure 3**). Out of the remaining epochs, the 8 epochs with the highest individual alpha peak frequency and alpha1 occipital power content were selected for each subject, in order to include an equal amount of data for each subject while avoiding possible drowsiness biases across subjects (**Supplementary Material SI.2** and **Supplementary Figure 3**). A random subsample of the epochs selected by this automatic procedure was visually inspected to ensure data quality.

Spectral Analysis

For each selected epoch (16,384 samples), the power spectral densities (PSDs) of the source-level time-series were estimated using the periodogram method implemented in MATLAB. The IPF was computed as the frequency at which the average PSD in the occipital regions peaked (**Supplementary Table 1**), in the range 4–13 Hz. The total power (i.e., the integral of the PSD) in the frequency range 0.5–48 Hz, and the relative band power (RBP) in the delta (0.5–4 Hz), theta (4–8 Hz), alpha1 (8–10 Hz), alpha2 (10–13 Hz), beta (13–30 Hz) and gamma (30–48 Hz) band (i.e., the integral of the PSD in each frequency range, normalized by the total power) were computed for each ROI, epoch, and subject. Values were then averaged over epochs in order to obtain single values per ROI per subject.

Functional Connectivity Analysis

Single epoch MEG data were used to build 80 × 80 functional connectivity matrices for each frequency band of interest. For each epoch and subject, the source-level time-series were band-pass filtered into the six bands of interest (delta, theta, alpha1, alpha2, beta, and gamma) using a two-way least-square finite impulse response (FIR) filtering as implemented in EEGLAB (Delorme and Makeig, 2004). Band-pass filtered time-series were then pair-wised orthogonalized to correct for the effects of spatial leakage (i.e., removing zero-lag coupling components). This correction scheme was applied at the single epoch level, and in both directions (orthogonalization of a signal *i* with respect to a signal *j*, and *vice versa*). Next, orthogonalized time-series were Hilbert-transformed and their amplitude envelopes (magnitude of the analytic signal) were pair-wise correlated using the Pearson's correlation coefficient, thus computing the corrected Amplitude Envelop Correlation (AECc) (Brookes et al., 2012; Hipp et al., 2012). The AECc is a robust functional connectivity measure comprised between −1 and 1 that demonstrates high levels of within- and between-subject consistency and group-level reproducibility (Colclough et al., 2016; Sareen et al., 2021). The resulting functional connectivity matrices were then made symmetric by averaging their upper and lower triangular parts, averaged over the 8 epochs, and used to compute (i) the average functional connectivity at the whole-brain level (i.e., the average over all functional connections between the 80 cortical ROIs), and (ii) the nodal functional connectivity strength (i.e., the row-wise sum of the functional connectivity matrices) for each subject. Group-average functional connectivity matrices for the CI and CN group are shown in **Supplementary Figure 4**.

Statistical Analyses

Statistical differences between the CI and CN group were assessed with ANCOVA analyses within a general linear model (GLM) formulation. Age and gender were added as covariates in all the analyses. Considering that functional connectivity and band power content are positively related (Demuru et al., 2020), the RBP was added as covariate in supplementary analyses when comparing functional connectivity values. The effect size was quantified with the Cohen's *d* coefficient (Cohen, 2013) between GLM residual distributions, after correcting for covariates. When multiple comparisons were performed (e.g., when comparing region-wise RBP or functional connectivity strength), the false discovery rate (*FDR*) was controlled at 0.05 level with the Benjamini-Hochberg procedure (Meskaldji et al., 2013). Pair-wise associations between cognitive scores were assessed with the Spearman's rank correlation coefficient (ρ). Multivariate relationships between spectral or functional connectivity brain features and cognitive scores (including cognitive reserve indicators) were assessed with partial least square correlation (PLSC) analyses (Krishnan et al., 2011). PLSC identifies multivariate correlation patterns through singular value decomposition of the data covariance matrix. This operation results in a set of orthogonal and paired brain and cognitive saliences, each one representing a pattern of brain and cognitive features with maximum covariance. To interpret the brain and cognitive saliences, we computed the Pearson's correlation coefficient between the original data and their projection onto the respective saliences, which results in the so-called brain and cognitive loadings (Kebets et al., 2019). A large positive (or negative) loading for a particular brain (cognitive) feature indicates a greater contribution of that feature to the multivariate correlation pattern. The statistical significance of the multivariate correlation patterns was assessed with permutation testing (1,000 permutations, correlation patterns with $p < 0.05$ after *FDR* correction were deemed significant). The reliability of brain and cognitive loadings for the significant correlation patterns was assessed with bootstrapping (500 random data resamplings)

and computing standard scores with respect to the bootstrap distribution (loadings were considered reliable for absolute standard score > 3) (Krishnan et al., 2011; Zöller et al., 2019). For the PLSC analyses, missing cognitive scores were imputed using the 4-nearest-neighbor method.

All the analyses were performed with MATLAB (The MathWorks, Inc., version R2019b).

RESULTS

Subjects and Cognitive Profiles

We investigated the spectral and functional connectivity profiles of MEG data recorded in 35 CN and 11 CI oldest-old subjects. The demographic, clinical and cognitive characteristics of the two groups, and the related statistical comparisons, are reported in **Table 1**. There was a significant difference between the two groups in terms of age [Student's *t*-test, $t(44) = 2.03$, $p = 0.048$, CI < CN, difference of the means = 1.3 years] and gender [proportionally fewer women in the CI group, Chi-square test, $C^2(1, N = 46) = 4.82$, $p = 0.028$], and no significant difference in years of education or GDS TOTAL score. By definition CI subjects had significantly lower MMSE total [$F(1, 42) = 60.73$, $p < 10^{-9}$] and CERAD total [$F(1, 42) = 19.15$, $p = 0.000073$] scores, indicating overall cognitive impairment and reduced episodic memory performances compared to CNs, when taking into account the effects of age and gender. There were no differences between CNs and CIs with respect to letter fluency and TMT-B scores. At the time of this study, CI subjects engaged less frequently in cognitively demanding activity compared to CN subjects [cCAQ, $F(1, 40) = 5.03$, $p = 0.030$]. CN and CI oldest-old subjects did not differ in terms of cognitive reserve (i.e., there was no difference between CNs and CIs with respect to pCAQ scores). The rank correlations between age, years of education, cognition, and cognitive reserve scores in the whole groups of subjects are reported in **Figure 1**. There were statistically significant ($FDR < 0.05$) positive correlations between education level and pCAQ [$(44) = 0.54$, $p = 0.0010$]; verbal fluency and MMSE [$(44) = 0.70$, $p < e^{-7}$]; verbal fluency and cCAQ [$\rho(44) = 0.45$, $p = 0.0016$]; CERAD total and MMSE [$\rho(44) = 0.40$, $p = 0.0062$]. The pCAQ score was also positively correlated with the verbal fluency [$(44) = 0.36$, $p = 0.020$], but this association did not survive multiple comparison correction.

Spectral Features in the Theta and Beta Bands Are Altered in Cognitively Impaired Oldest-Old Subjects

Spectral features of the CN and CI MEG were quantified with the IPF and the relative band power (RBP) in six frequency bands, both at the whole-brain and regional levels. Before computing IPF and RBP values, we verified that there was no significant difference in global power (i.e., average over all the 80 brain regions; [$F(1, 42) = 0.06$, $p = 0.81$] or total power estimated over the occipital regions only [$F(1, 42) = 1.27$, $p = 0.27$, **Supplementary Table 1**] between the CN and CI groups.

On average, CI subjects had lower IPF than CN subjects, but this difference did not reach statistical significance (mean ± std IPF: CN = 9.1 ± 0.8 Hz, CI = 8.7 ± 0.3 Hz; [$F(1, 42) = 2.44$, $p = 0.13$]. We found significantly higher whole-brain theta RBP [$F(1, 42) = 14.54$, $p = 0.00044$, $d = 1.15$] and lower beta RBP [$F(1, 42) = 16.82$, $p = 0.00018$, $d = -1.23$] in CI compared to CN subjects (**Figure 2**). Moreover, the individual theta and beta RBP values were strongly negatively correlated across subjects [linear correlation coefficient $r(44) = -0.79$, $p <$ e-10], suggesting an overall shift of the average MEG spectrum toward the lower frequencies in CI subjects. This effect is qualitatively illustrated by the group-average power spectral density curves in **Figure 2A**. There was also a significant decrease of whole-brain gamma RBP in CI compared to CN subjects, but this effect had smaller effect size than was the case for the theta and beta bands [$F(1, 42) = 4.19$, $p = 0.047$, $d = -0.63$]. No significant CI-CN whole-brain RBP differences were found in the delta, alpha1 or alpha2 frequency band.

Next, we investigated the spectral properties of CN and CI time-series at the level of the individual cortical regions. We found spatially diffuse CI-CN RBP alterations in the theta and beta band with 73 and 77 regions surviving multiple comparison correction, respectively ($FDR < 0.05$). In the theta band, RBP was higher in CI compared to CN subjects in the frontal lobe, including superior frontal and anterior cingulate cortices, in the primary and association somatosensory cortices, and, to a lesser extent, in the parietal and temporal lobes (no region showed lower theta RBP) (**Figure 3A**). In the beta band, RBP was lower

TABLE 1 | Demographic and cognitive characteristics.

	CN ($n = 35$)	CI ($n = 11$)	*p*-values
Demographic and clinical indicators			
Age, years	92.2 (1.8)	90.9 (1.9)	0.048*
Gender, F/M	19/16	1/10	0.028*
Education, years	12.5 (4.7)	12.4 (4.2)	0.94
GDS TOTAL	1.7 (1.6)	3.0 (2.3)	0.057
Cognition			
MMSE, points	28.3 (1.1)	23.2 (3.4)	<e-9**
DAT fluency, number	28.2 (7.9)	23.0 (10.9)	0.090
TMT-B, seconds	268 (125)	217 (105)	0.15
CERAD TOTAL, words	16.6 (3.5)	11.4 (3.4)	0.000073**
Cognitive engagement			
cCAQ, points	3.2 (0.6)	2.6 (1.0)	0.03*
pCAQ, points	2.5 (0.6)	2.8 (0.6)	0.49

Column 1: demographic, clinical and cognitive indicators. Columns 2 and 3: group-mean (standard deviation) values for continuous variables for the 35 cognitively normal (CN) and 11 cognitively impaired (CI) subjects. Column 4: p-values for statistical comparisons between CN and CI groups (one-way ANOVA for continuous and interval variables; chi-square test for categorical variables).

**p < 0.05; **p < 0.001. GDS TOTAL score was missing for 1 CI subject; TMT-B for 8 CN and 5 CI subjects; pCAQ for 1 CN and 1 CI subject; cCAQ for 1 CN and 1 CI subject. Reported statistics are based on available data. GDS, Geriatric Depression Scale; MMSE, Mini-Mental State Examination; CERAD, total score of the Consortium to Establish Registry for Alzheimer's Disease; DAT, letters D-A-T fluency test; TMT-B, Trail Making Tests B score; cCAQ, current engagement in cognitively demanding activities; pCAQ, past engagement in cognitively demanding activities.*

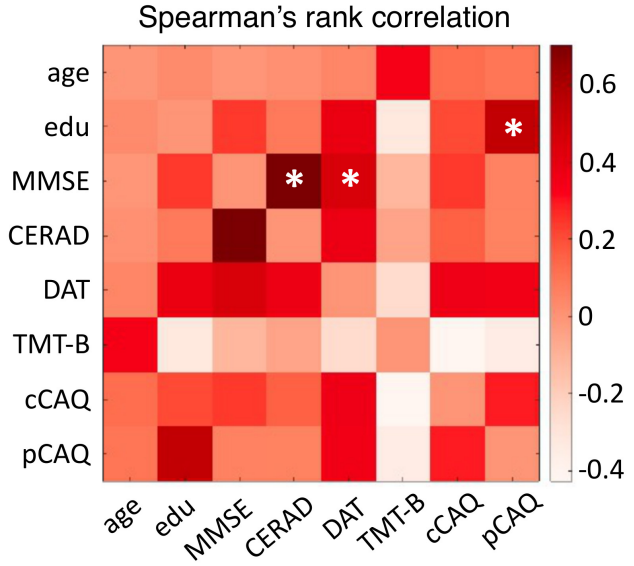

FIGURE 1 | Relationships between cognitive and cognitive reserve scores. The matrix entries represent the Spearman's rank correlation coefficient between cognitive performances, cognitive reserve, age and education level. Correlations surviving multiple comparison correction (*FDR* < 0.05) are indicated with an asterisk. Edu, education level; MMSE, Mini-Mental State Examination; CERAD, total score of the Consortium to Establish Registry for Alzheimer's Disease; DAT, letters D-A-T fluency test; TMT-B, Trail Making Tests B score; cCAQ, current engagement in cognitively demanding activities; pCAQ, past engagement in cognitively demanding activities.

in CI compared to CN subjects in superior parietal regions (including the postcentral gyrus), posterior cingulate/precuneus, dorsolateral prefrontal, and anterior cingulate cortices (no region showed higher beta RBP) (**Figure 3A**). Globally, these spectral alterations mainly involved the default mode network and, to a lesser extent, the limbic, somatomotor, and fronto-parietal resting state networks, in both the theta and beta band (**Figure 3B**). The visual cortex was spared in the theta bands but partially affected in the beta band.

Functional Connectivity Is Similar Between Cognitively Normal and Impaired Subjects

We investigated possible CI-CN group-differences of functional connectivity values at whole-brain and cortical region level. At the whole-brain level, the average functional connectivity in the alpha2 band was decreased in CI compared to CN, with small effect size [$F(1, 42) = 4.28$, $p = 0.045$, $d = -0.64$; $F(1, 42) = 2.36$, $p = 0.13$, $d = -0.47$ when also covarying for the alpha2 RBP]. There was no CI-CN difference of average functional connectivity in the other frequency bands. Similarly, no CI-CN comparison of functional connectivity at the level of single brain regions survived multiple comparison correction ($FDR < 0.05$) in any frequency band.

Magnetoencephalography Brain Features Relate to Cognition and Cognitive Reserve in Oldest-Old Subjects

The cognitive profile of individual subjects was characterized in terms of overall cognitive ability (MMSE score), executive control (letter fluency), processing speed (TMT-B score) and episodic memory (CERAD total score). Moreover, we considered the lifelong engagement in cognitively demanding activity as possible protective factors for cognitive impairment and proxy for subjects' cognitive reserve. We investigated multivariate linear relationships between whole-brain spectral or functional

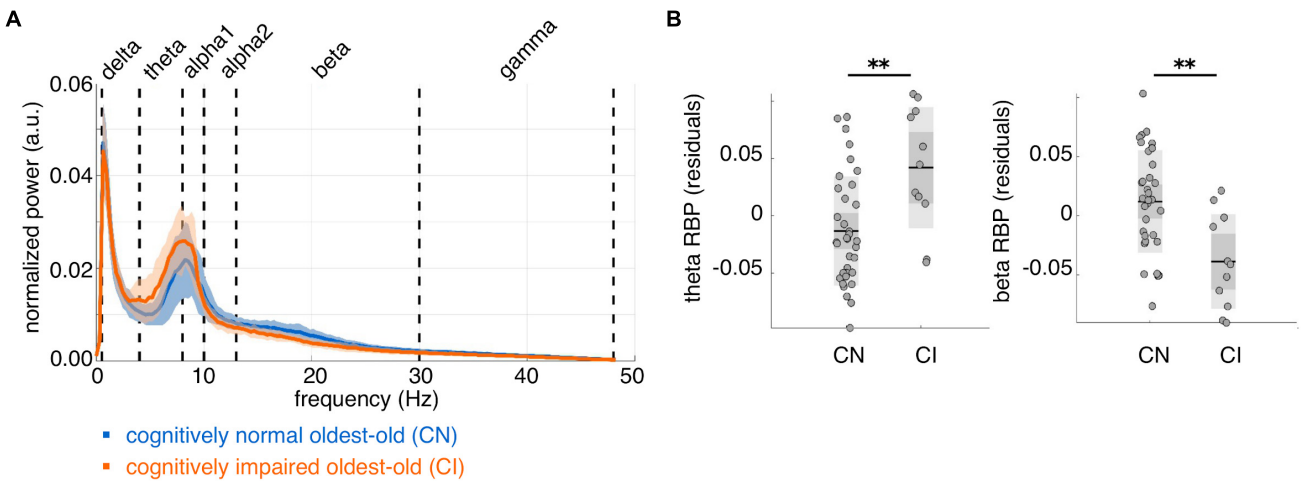

FIGURE 2 | Whole-brain average spectral properties of cognitively normal and impaired oldest-old subjects. **(A)** Group-average power spectral density curves over 80 cortical regions of interest, for cognitively normal ($n = 35$, blue curve) and cognitively impaired ($n = 11$, orange curve) subjects. Solid lines represent the group means; shaded areas represent ± 1 standard deviation interval. **(B)** Distributions of whole-brain relative band power (RBP) in the theta and beta band, after correction for age and gender. $^{**}p < 0.001$ for CI-CN comparison.

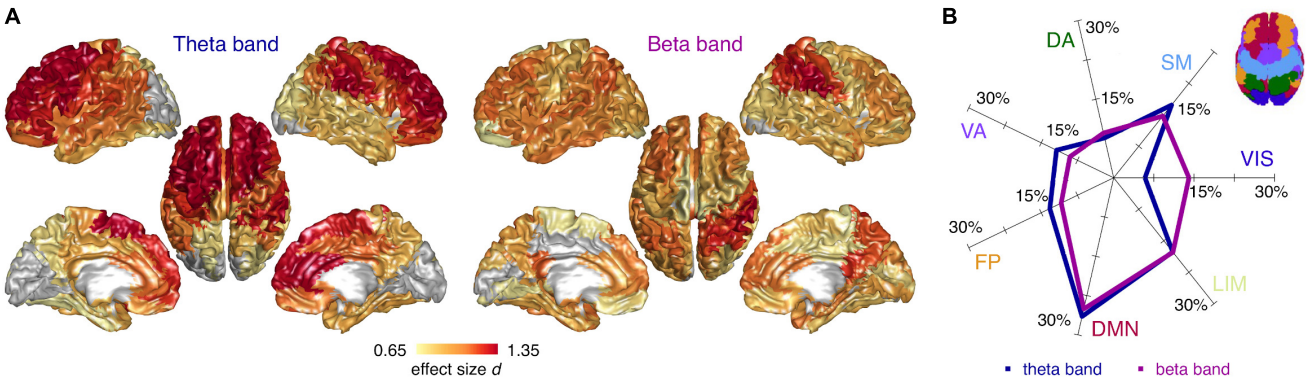

FIGURE 3 | Cortical distribution of spectral differences between cognitively normal and impaired subjects. **(A)** Cortical surface plots of local effect size (Cohen's *d*) for statistically significant (*FDR* < 0.05) CI-CN comparisons of source relative band power (RBP), in the theta and beta frequency band (ANCOVA analyses including age and gender covariates). Cortical regions not surviving multiple comparison correction are represented in gray. **(B)** Percentage effect size contributions in the 7 RSNs, for the theta and beta RBP. The percentage effect size contribution for each RSN was assessed by normalizing the effect size sum over the regions belonging to each RSNs by the sum of all regions' effect size, and considering only the regions significantly different between cognitively normal and impaired subjects. Inset: schematic representation of the 7 RSNs on the cortical surface. VIS, visual; SM, sensorimotor; DA, dorsal attention; VA, ventral attention; FP, fronto-parietal; DMN, default mode; LIM, limbic network.

connectivity features, and cognition, cognitive reserve, education level and age with two PLSC analyses. The analyses were performed on the whole group of 46 subjects (i.e., considering both CI and CN subjects) and replicated in the CN group (we did not repeat the analyses in the CI group given the small sample size).

Concerning the spectral features, the PLSC analysis extracted by construction 7 multivariate correlation patterns, one of which was statistically significant ($p = 0.0010$; $FDR < 0.05$). On an exploratory basis, we also report a second multivariate correlation pattern with $p = 0.68$. The brain and cognitive loadings associated with the two patterns are shown in **Figures 4A,B**, with loadings that were reliably different from zero highlighted in yellow. The first multivariate pattern shows an association between higher cognitive reserve (larger pCAQ score and education level, while taking into account the age) and processing speed, and a spectral signature characterized by less power in the delta and gamma band and more power in the alpha band (**Figure 4A**). The second multivariate pattern mirrors the CI-CN differences reported above (**Figure 2**) and suggests an association between poorer cognitive performances (including lesser current involvement in cognitively demanding activities, i.e., lower cCAQ) and slowing down of brain oscillations, particularly involving the beta and theta band (**Figure 4B**).

Concerning the functional connectivity features, none of the multivariate correlation patterns survived multiple comparison correction. However, we report on an exploratory basis the correlation pattern with the smallest *p*-value ($p = 0.087$), which suggests a possible relationship between better cognitive performance and stronger functional connectivity in the alpha and beta band (**Figure 4C**). All PLSC results were consistent when analyses were performed on CN participants only (**Supplementary Figure 5**), suggesting that the brain-cognition associations reflect a continuum over cognitive decline stages and are not driven by just the cognitively impaired individuals.

DISCUSSION

This study represents the first characterization of neuronal oscillations' spectral features and amplitude coupling with respect to cognition and lifelong engagement in cognitive activity in oldest-old participants using MEG. Compared to cognitively normal subjects, those with cognitive impairments showed extended alterations of relative power in the theta and beta band, indicating a global slowing of cortical oscillations. The source-level power alterations heavily involved the frontal lobe in the theta band and extended to fronto-parietal and visual areas in the beta band, with an overall predominant involvement of the default mode network. Spectral and, to a lesser extent, functional connectivity features related to cognitive traits. In the spectral domain, two multivariate correlation patterns were discussed, one mirroring the spectral changes observed in cognitively impaired participants with lower (higher) power content in the theta (beta) band associated with better cognitive performances (trend-level, $p = 0.068$). The main multivariate correlation pattern ($p = 0.0010$) revealed an association between spectral content in the delta, alpha, and gamma band, and cognitive reserve approximated with the lifelong (past) engagement in cognitively demanding activity. Finally, better cognitive performances were marginally associated with overall stronger functional connectivity in the alpha and beta band.

Our finding of higher theta and lower beta power in cognitively impaired oldest-old subjects suggests that the association between electrophysiological changes and cognitive impairment is substantially similar in oldest-old participants and individuals younger than 85 years.

Younger old-adults with prodromal AD, early onset AD or typical-onset AD show widespread power increases of electrophysiological signals in lower frequency bands (delta and theta band) and power decreases in higher frequency bands (alpha and beta band) compared to normal aging adults,

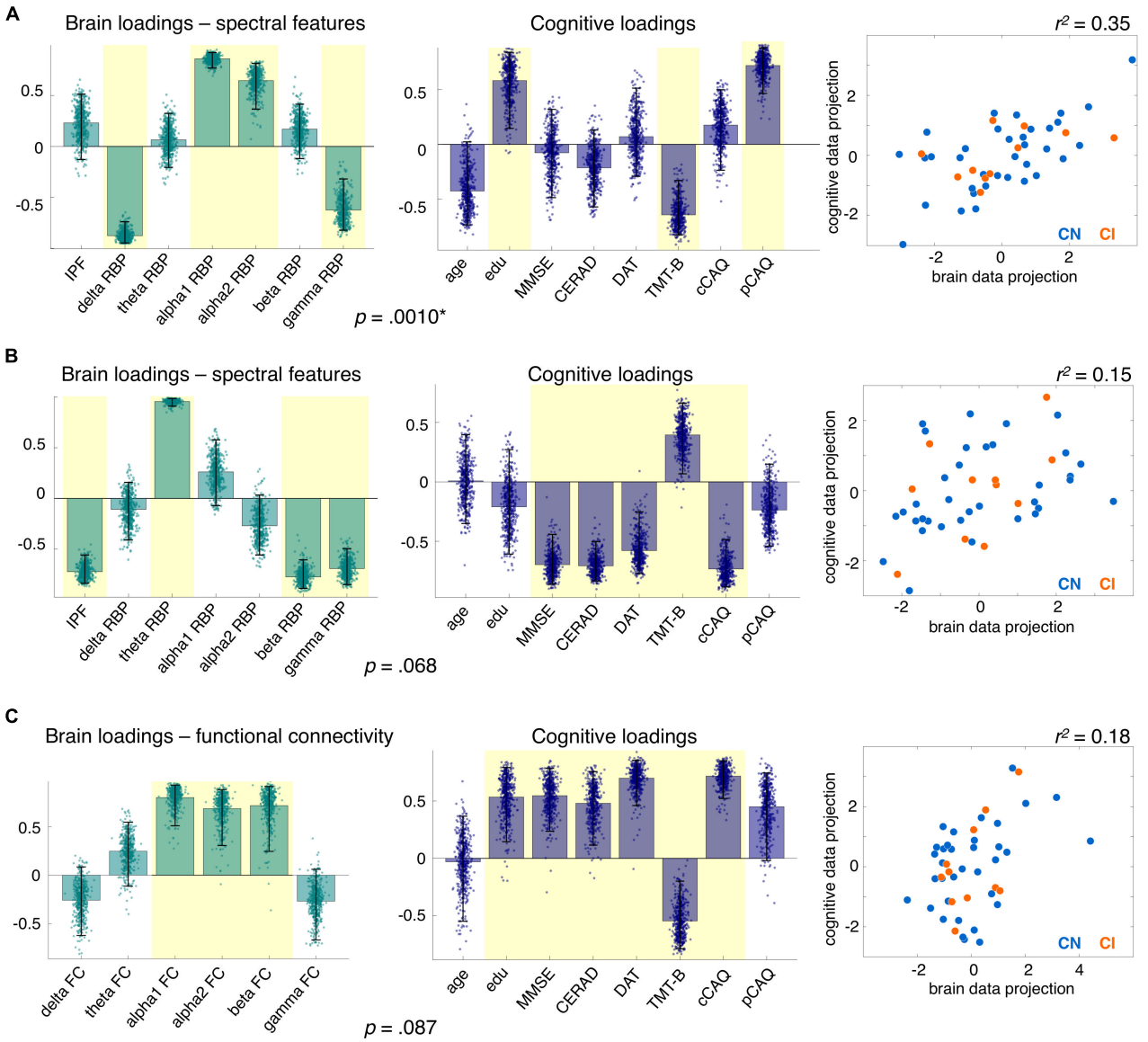

FIGURE 4 | Multivariate correlation patterns between electrophysiological and cognitive features. Each panel represents, from left to right: (i) the brain loadings, (ii) the cognitive loadings, and (iii) the data projection onto the brain and cognitive saliences for the first **(A)** and second **(B)** significant multivariate correlation patterns between spectral and cognitive features, and for the multivariate pattern between functional connectivity and cognitive features **(C)** from partial least square correlation (PLSC) analyses. In the loading plots, bars and dots represent the average and dispersion of brain and cognitive loadings over 500 bootstraps; loadings reliably different from zero are shaded in yellow. *P*-values for the multivariate correlation patterns are reported below the loading bar plots (* indicates pattern surviving multiple comparison correction at *FDR* < 0.05). In the scatter plots on the right, each dot represents brain and cognitive data of a single subject projected onto the corresponding PLSC saliences, with cognitively normal (CN) and impaired (CI) subjects represented in light blue and orange, respectively. The r-squared between the brain and cognitive data projection onto the PLSC saliences is reported above each scatter plot and quantifies the amount of cognitive scores' variance explained by the spectral or functional connectivity features.

indicating a global slowing of resting-state activity (Dauwels et al., 2010; Micanovic and Pal, 2014; Engels et al., 2016, 2017; Gouw et al., 2017; Babiloni et al., 2020a). This finding is highly consistent in literature, and it is here extended to cognitively impaired oldest-old with probable late-onset AD or aMCI. It should be noted, however, that the slowing of cortical oscillations is observed not only in AD, but also in multiple pre-dementia and dementia forms (notably, dementia with Levy Bodies) (Dauwan et al., 2016; van der Zande et al., 2020), as well as in normal aging (Knyazeva et al., 2018). In our sample, there was a small but significant age difference between cognitively normal and cognitively impaired subjects, but the latter were on average younger than the former. It is therefore unlikely that the slowing down of cortical rhythms observed in our cognitively impaired sample was due to physiological aging rather than neurodegenerative processes. In further support

of this interpretation, lower IPF, larger relative power in the theta band and lower power in higher frequency bands (beta, gamma) were weakly associated with worse overall cognitive performances, memory, executive control, processing speed, and current engagement in cognitively demanding activity both in the whole sample and in the cognitively normal group only, suggesting a relationship between cortical slowing and cognition that is independent from clinical classification. This is consistent with previous findings that have linked increased theta power with decreased cognitive functioning in healthy older adults (Mitchell et al., 2008; Stomrud et al., 2010; Finnigan and Robertson, 2011). Moreover, baseline theta power predicts longitudinal cognitive decline and conversion to dementia in younger old-adults (Prichep et al., 2006; Gouw et al., 2017; Rossini et al., 2020). Finally, previous works have associated theta (but also delta and alpha) power with clinical symptoms and global cognitive status in AD patients (Engels et al., 2016; Gouw et al., 2017). In our study, it was not possible to investigate associations between electrophysiological and cognitive features specifically in the AD/aMCI group given the small sample size (only 11 out of 46 subjects were cognitively impaired). Therefore, it remains to be further investigated in a larger cohort whether the relationships between spectral features and cognition in this age range are diagnosis-dependent (Vlahou et al., 2014; Benwell et al., 2020) or reflect more generic neurodegenerative processes that lead to cognitive decline.

The cortical distributions of the theta and beta changes in cognitively impaired oldest-old participants largely overlapped in the frontal lobe with involvement of the default mode network, but showed distinct spatial patterns in posterior cortices.

Theta alterations were widespread and mainly involved the frontal lobe, while beta alterations extended to more posterior areas, including the visual cortices and showing relatively large effects in the precuneus and posterior cingulate regions. The superior parietal cortex was affected in both bands, in agreement with MEG findings in younger AD patients (Berendse et al., 2000; Engels et al., 2016, 2017). Globally, the power changes involved the default mode network, a brain system that includes medial (medial prefrontal and precuneus/posterior cingulate cortices), hippocampal and parietal regions (Raichle et al., 2001; Greicius et al., 2003; Andrews-Hanna et al., 2014; Raichle, 2015). Functional connectivity in the default mode network predicts cognitive abilities in healthy adults (Van Den Heuvel et al., 2009) and is strongly implicated in the pathophysiology of AD (Agosta et al., 2012). In AD and preclinical AD, default mode regions show early accumulation of amyloid-β and early neurodegeneration (Palmqvist et al., 2017; Sepulcre et al., 2017), possibly driven by high baseline activity levels (Buckner et al., 2009). Default mode regions in AD also show decreased synchronization of hemodynamic signals (weakened functional connectivity) as assessed with resting-state functional magnetic resonance imaging (rfMRI) (Myers et al., 2014; Pasquini et al., 2017). Interestingly, simultaneous EEG-rfMRI studies in healthy subjects specifically associate the amplitude of neuronal oscillations in the theta and beta frequency band to default mode network hemodynamic activity (Laufs et al., 2003; Scheeringa et al., 2008; Hlinka et al., 2010). Alterations of default mode hemodynamic activity and widespread changes of theta and beta rhythms could therefore be the manifestations of the same pathophysiological mechanisms, such as activity-dependent neurodegeneration (Buckner et al., 2009; Griffa and van den Heuvel, 2018; de Lange et al., 2019). Moreover, computational models demonstrate that activity-dependent degeneration of default mode regions can reproduce AD-like changes such as oscillatory slowing and loss of spectral power (de Haan et al., 2012). Yet, the subdivision of cortical regions into RSNs that we used in this work was derived from fMRI data (Yeo et al., 2011). It is not yet clear whether MEG functional activity shows the same RSNs (de Pasquale et al., 2010), especially in this age group, which deserves further investigation.

Previous studies on AD patients also report slower rhythms in the occipital lobe and visual areas in the alpha band (Engels et al., 2017; Babiloni et al., 2020a), which was not the case for our cohort. However, the alpha band was involved in terms of functional connectivity, with cognitively impaired oldest-old participants having lower alpha2 amplitude coupling at the whole-brain network level. This CI-CN difference partially related to the power content in the two groups, since covarying by the alpha2 band power decreased the effect size. Nonetheless, the functional-connectivity group-effect should not be disregarded because of the power contribution. Signal power is necessary to get functional connectivity, especially when connectivity is based on amplitude coupling, and the relationship between the two dimensions is non-trivial and may reflect underlying mechanisms (Tewarie et al., 2019). In addition, the PLSC analysis suggested a relationship between stronger functional connectivity in the alpha and beta band, and preserved cognitive performances, particularly in the executive domain. These results in oldest-old participants are in line with MEG literature showing decreased functional connectivity in AD (Berendse et al., 2000; Stam et al., 2002, 2006, 2009; Yu et al., 2017), but they remain preliminary considering the limited power of the study in relation to the small effects detected in the functional connectivity domain. Indeed, it should be noted that the effect sizes of the CI-CN group-differences and the linear associations with cognitive traits were more prominent in the spectral domain, highlighting the relevance of relatively simple electrophysiological measures in a clinical setting. Functional connectivity analyses on larger cohorts may nonetheless contribute to the understanding of neural mechanisms associated with specific cognitive dysfunctions -such as impairments in executive functioning- that strongly rely on network-level integration processes.

Participants underwent an interview reporting how often they engaged in common cognitively demanding activities that depend minimally on socioeconomic status (Landau et al., 2012). Lifestyle factors are considered as a proxy for cognitive reserve, defined as the adaptability of functional brain processes to cope with aging, brain insults or pathological processes (Stern, 2009; Stern et al., 2018). In particular, frequency of past and present engagement in cognitively demanding activities has been associated with lower amyloid-β accumulation in brain tissues (Landau et al., 2012), less hippocampal atrophy (Valenzuela et al., 2008), and lower dementia incidence

(Valenzuela and Sachdev, 2006; Xu et al., 2019) in healthy older adults. However, in subjects aged 85 years or older, education, occupational complexity and engagement in cognitive and leisure activities do not predict cognitive decline nor the risk of 5-year incident dementia (Lavrencic et al., 2018; Hakiki et al., 2020), suggesting that cognitive reserve mechanisms may be age-dependent and become less effective in counterbalancing neurodegenerative processes (Nelson et al., 2019). In line with these observations, past engagement in cognitively demanding activities (pCAQ score) did not differ between cognitively normal and impaired oldest-old participants in our study, although higher pCAQ scores were weakly associated with better executive performances at the whole-group level. As expected, higher pCAQ (but not cCAQ) scores were also associated with higher educational level, a component of the cognitive reserve construct (Nucci et al., 2012). On the contrary, cognitively impaired participants tended to engage less frequently in cognitive activities than cognitively normal ones at the time of the study. The frequency of current engagement in cognitively demanding activities may therefore better reflect the present cognitive status rather than cumulate cognitive reserve. Our and literature findings converge on the hypothesis that education and sociobehavioral lifestyle habits including lifelong (past) engagement in cognitively demanding activities may serve as protective factors for cognitive decline in younger-old, but that this beneficial effect may be progressively less prominent in oldest-old subjects who, possibly, face distinct or more severe pathophysiological mechanisms.

In support of this hypothesis, we found that cognitive reserve in oldest-old participants was associated with a specific spectral signature involving delta, alpha and gamma band, in contrast to the spectral changes associated with cognitive performances, which mainly involved the theta and beta band. In particular, higher cognitive reserve (higher pCAQ scores and education level while accounting for age) related to lower (higher) cortical oscillation power in the delta (alpha) band, combined with lower power in the gamma band. This finding nicely corroborates a recent sensor-level EEG study that identified higher alpha amplitudes in (amyloid negative) older adults (mean age 75 years) with subjective cognitive complaints and higher educational level compared to those with lower education level (Babiloni et al., 2020b). It is well known that posterior resting-state alpha is progressively reduced with aging, which may partially be linked to a deterioration of the cholinergic system (Wan et al., 2019). Our results suggest that lifestyle factors may compensate this process, even at advanced age, resulting in stronger alpha activity at rest. However, we have also shown that the relationship between cognitive reserve and spectral features is independent from memory and executive control performance, which was taken into account through the multivariate nature of our analyses and replication of results in the cognitively normal group. Yet, the spectral signature of cognitive reserve might change as a function of the pathological substrate underlying cognitive decline (Babiloni et al., 2021). Considering the small size of the CI group, it was not possible to perform reliable correlation analyses within this group. Further research is needed to elucidate the interplay between the distinct electrophysiological mechanisms reflecting cognitive reserve, cognitive decline, and pathological load, particularly in an age segment - the oldest-old- for which dementia risk and protective factors identified in younger subjects may not be valid. Taken together, our results indicate that functional adaptability mechanisms associated with cognitive reserve (lifelong engagement in cognitive activity) are present in the oldest-old and expressed in specific electrophysiological signatures, but that they are less effective in limiting cognitive decline.

This study has some limitations that should be noted. First, the sample size is relatively small and absence of statistically significant findings might relate to limited statistical power. However, one should consider that the recruitment of oldest-old subjects in research programs is challenging and few neuroimaging data are available for oldest-old participants (Legdeur et al., 2018). Second, in this study measures of brain pathology, such as biomarkers for amyloid, tau, and cerebrovascular pathologies, were not taken into account. Third, the subjects' cognitive profile was condensed in few cognitive scores probing executive control, processing speed and episodic memory, mainly to accommodate the limited statistical power linked to the small sample size. However, further analyses are needed to fully explore the relationship between cognitive dimensions and MEG features. For example, executive control is a complex construct that is only partially captured by the phonemic verbal fluency (DAT scores) (Jurado and Rosselli, 2007; Friedman and Miyake, 2017; Vallesi, 2021). Finally, individual levels of cognitive reserve were approximated with a self-reported questionnaire on past engagement in cognitively demanding activities. Self-reporting may be poorly reliable, particularly in the oldest-old age range, and additional sociobehavioral proxies of cognitive reserve could be used in future studies (Stern et al., 2018).

To conclude, in this work we have shown that cognitive impairments in oldest-old subjects are associated with a slowing of theta/beta oscillatory brain activity converging onto the default mode network. In the same subjects, a distinct spectral signature involving the delta, alpha and gamma band is associated with cognitive reserve mechanisms, which, however, may be ineffective in preserving cognitive performances in this age range. Future studies should further investigate how these brain functional changes relate to underlying neuropathological factors and to functional adaptive mechanisms that are possibly specific to this age range.

DATA AVAILABILITY STATEMENT

The datasets presented in this article are not readily available because they are already part of the EMIF-AD 90 + study. Requests to access the datasets should be directed to AH.

ETHICS STATEMENT

The studies involving human participants were reviewed and approved by the local Medical Ethics Review Committee of

the Amsterdam UMC. The patients/participants provided their written informed consent to participate in this study.

AUTHOR CONTRIBUTIONS

AG, AH, CS, and PV co-designed the study. AG performed the analyses and wrote the first version of the manuscript. NL and MB took care of data curation and EMIF-AD 90 + database. AH, CS, PV, MH, AG, and NL were involved in the interpretation and discussion of results. All authors contributed to manuscript revision, read, and approved the submitted version.

FUNDING

This study was supported by the Swiss National Science Foundation (SNSF grant #P2ELP3_172087). The research leading to these results has received support from the Innovative Medicines Initiative Joint Undertaking under EMIF grant agreement n° 115372, resources of which are composed of financial contribution from the European Union's Seventh Framework Programme (FP7/2007-2013) and EFPIA companies' in kind contribution.

ACKNOWLEDGMENTS

We would like to thank all subjects for their participation in this study, and Prof. Gilles Allali and Dr. Valeria Kebets for insightful comments on this work.

SUPPLEMENTARY MATERIAL

The Supplementary Material for this article can be found online at: https://www.frontiersin.org/articles/10.3389/fnagi.2021.746373/full#supplementary-material

REFERENCES

Agosta, F., Pievani, M., Geroldi, C., Copetti, M., Frisoni, G. B., and Filippi, M. (2012). Resting state fMRI in Alzheimer's disease: beyond the default mode network. *Neurobiol. Aging* 33, 1564–1578. doi: 10.1016/j.neurobiolaging.2011.06.007

Andrews-Hanna, J. R., Smallwood, J., and Spreng, R. N. (2014). The default network and self-generated thought: component processes, dynamic control, and clinical relevance. *Ann. N. Y. Acad. Sci.* 1316, 29–52. doi: 10.1111/nyas.12360

Babiloni, C., Binetti, G., Cassetta, E., Forno, G. D., Percio, C. D., Ferreri, F., et al. (2006). Sources of cortical rhythms change as a function of cognitive impairment in pathological aging: a multicenter study. *Clin. Neurophysiol.* 117, 252–268. doi: 10.1016/j.clinph.2005.09.019

Babiloni, C., Blinowska, K., Bonanni, L., Cichocki, A., De Haan, W., Del Percio, C., et al. (2020a). What electrophysiology tells us about Alzheimer's disease: a window into the synchronization and connectivity of brain neurons. *Neurobiol. Aging* 85, 58–73. doi: 10.1016/j.neurobiolaging.2019.09.008

Babiloni, C., Lopez, S., Del Percio, C., Noce, G., Pascarelli, M. T., Lizio, R., et al. (2020b). Resting-state posterior alpha rhythms are abnormal in subjective memory complaint seniors with preclinical Alzheimer's neuropathology and high education level: the INSIGHT-preAD study. *Neurobiol. Aging* 90, 43–59. doi: 10.1016/j.neurobiolaging.2020.01.012

Babiloni, C., Ferri, R., Noce, G., Lizio, R., Lopez, S., Lorenzo, I., et al. (2021). Abnormalities of Cortical Sources of Resting State Alpha Electroencephalographic Rhythms are Related to Education Attainment in Cognitively Unimpaired Seniors and Patients with Alzheimer's Disease and Amnesic Mild Cognitive Impairment. *Cereb. Cortex* 31, 2220–2237. doi: 10.1093/cercor/bhaa356

Baillet, S., Mosher, J. C., and Leahy, R. M. (2001). Electromagnetic brain mapping. *IEEE Signal Process. Mag.* 18, 14–30. doi: 10.1109/79.962275

Balart-Sánchez, S. A., Bittencourt-Villalpando, M., van der Naalt, J., and Maurits, N. M. (2021). Electroencephalography, Magnetoencephalography, and Cognitive Reserve: a Systematic Review. *Arch. Clin. Neuropsychol.* 36, 1374–1391. doi: 10.1093/arclin/acaa132

Benwell, C. S. Y., Davila-Pérez, P., Fried, P. J., Jones, R. N., Travison, T. G., Santarnecchi, E., et al. (2020). EEG spectral power abnormalities and their relationship with cognitive dysfunction in patients with Alzheimer's disease and type 2 diabetes. *Neurobiol. Aging* 85, 83–95. doi: 10.1016/j.neurobiolaging.2019.10.004

Berendse, H. W., Verbunt, J. P. A., Scheltens, P., van Dijk, B. W., and Jonkman, E. J. (2000). Magnetoencephalographic analysis of cortical activity in Alzheimer's disease: a pilot study. *Clin. Neurophysiol.* 111, 604–612. doi: 10.1016/S1388-2457(99)00309-0

Brookes, M. J., Hale, J. R., Zumer, J. M., Stevenson, C. M., Francis, S. T., Barnes, G. R., et al. (2011). Measuring functional connectivity using MEG: methodology and comparison with fcMRI. *NeuroImage* 56, 1082–1104. doi: 10.1016/j.neuroimage.2011.02.054

Brookes, M. J., Woolrich, M. W., and Barnes, G. R. (2012). Measuring functional connectivity in MEG: a multivariate approach insensitive to linear source leakage. *NeuroImage* 63, 910–920. doi: 10.1016/j.neuroimage.2012.03.048

Broshek, D. K., and Barth, J. T. (2000). "The Halstead-Reitan Neuropsychological Test Battery," in *Neuropsychological assessment in clinical practice: a guide to test interpretation and integration*, ed G. Groth-Marnat (Hoboken, NJ, US: John Wiley & Sons Inc), 223–262.

Buckner, R. L., Sepulcre, J., Talukdar, T., Krienen, F. M., Liu, H., Hedden, T., et al. (2009). Cortical Hubs Revealed by Intrinsic Functional Connectivity: mapping, Assessment of Stability, and Relation to Alzheimer's Disease. *J. Neurosci.* 29, 1860–1873. doi: 10.1523/JNEUROSCI.5062-08.2009

Bullain, S. S., and Corrada, M. M. (2013). Dementia in the Oldest Old. *Contin. Lifelong Learn. Neurol.* 19, 457–469. doi: 10.1212/01.CON.0000429172.27815.3f

Cohen, J. (2013). *Statistical Power Analysis for the Behavioral Sciences*. Cambridge, Massachusetts: Academic Press.

Colclough, G. L., Woolrich, M. W., Tewarie, P. K., Brookes, M. J., Quinn, A. J., and Smith, S. M. (2016). How reliable are MEG resting-state connectivity metrics? *NeuroImage* 138, 284–293. doi: 10.1016/j.neuroimage.2016.05.070

Corrada, M., Berlau, D., and Kawas, C. (2012). A Population-Based Clinicopathological Study in the Oldest-Old: the 90+ Study. *Curr. Alzheimer Res.* 9, 709–717. doi: 10.2174/156720512801322537

Corrada, M. M., Brookmeyer, R., Paganini-Hill, A., Berlau, D., and Kawas, C. H. (2010). Dementia incidence continues to increase with age in the oldest old: the 90+ study. *Ann. Neurol.* 67, 114–121. doi: 10.1002/ana.21915

Dauwan, M., van der Zande, J. J., van Dellen, E., Sommer, I. E. C., Scheltens, P., Lemstra, A. W., et al. (2016). Random forest to differentiate dementia with Lewy bodies from Alzheimer's disease. *Alzheimers Dement. Diagn. Assess. Dis. Monit.* 4, 99–106. doi: 10.1016/j.dadm.2016.07.003

Dauwels, J., Vialatte, F., and Cichocki, A. (2010). Diagnosis of Alzheimer's Disease from EEG Signals: where Are We Standing? *Curr. Alzheimer Res.* 7, 487–505. doi: 10.2174/156720510792231720

de Haan, W., Mott, K., van Straaten, E. C., Scheltens, P., and Stam, C. J. (2012). Activity Dependent Degeneration Explains Hub Vulnerability in Alzheimer's Disease. *PLoS Comput. Biol.* 8:e1002582. doi: 10.1371/journal.pcbi.1002582

de Haan, W., Stam, C. J., Jones, B. F., Zuiderwijk, I. M., van Dijk, B. W., and Scheltens, P. (2008). Resting-State Oscillatory Brain Dynamics in

Alzheimer Disease. *J. Clin. Neurophysiol.* 25, 187–193. doi: 10.1097/WNP.0b013e31817da184

de Lange, S. C., Scholtens, L. H., van den Berg, L. H., Boks, M. P., Bozzali, M., Cahn, W., et al. (2019). Shared vulnerability for connectome alterations across psychiatric and neurological brain disorders. *Nat. Hum. Behav.* 3, 988–998. doi: 10.1038/s41562-019-0659-6

de Pasquale, F., Penna, S. D., Snyder, A. Z., Lewis, C., Mantini, D., Marzetti, L., et al. (2010). Temporal dynamics of spontaneous MEG activity in brain networks. *Proc. Natl. Acad. Sci. U. S. A.* 107, 6040–6045. doi: 10.1073/pnas.0913863107

Delorme, A., and Makeig, S. (2004). EEGLAB: an open source toolbox for analysis of single-trial EEG dynamics including independent component analysis. *J. Neurosci. Methods* 134, 9–21. doi: 10.1016/j.jneumeth.2003.10.009

Demuru, M., La Cava, S. M., Pani, S. M., and Fraschini, M. (2020). A comparison between power spectral density and network metrics: an EEG study. *Biomed. Signal Process. Control* 57:101760. doi: 10.1016/j.bspc.2019.101760

Engels, M. M. A., Hillebrand, A., van der Flier, W. M., Stam, C. J., Scheltens, P., and van Straaten, E. C. W. (2016). Slowing of Hippocampal Activity Correlates with Cognitive Decline in Early Onset Alzheimer's Disease. An MEG Study with Virtual Electrodes. *Front. Hum. Neurosci.* 10:238. doi: 10.3389/fnhum.2016.00238

Engels, M. M. A., van der Flier, W. M., Stam, C. J., Hillebrand, A., Scheltens, Ph, and van Straaten, E. C. W. (2017). Alzheimer's disease: the state of the art in resting-state magnetoencephalography. *Clin. Neurophysiol.* 128, 1426–1437. doi: 10.1016/j.clinph.2017.05.012

Fernández, A., Hornero, R., Mayo, A., Poza, J., Gil-Gregorio, P., and Ortiz, T. (2006). MEG spectral profile in Alzheimer's disease and mild cognitive impairment. *Clin. Neurophysiol.* 117, 306–314. doi: 10.1016/j.clinph.2005.10.017

Finnigan, S., and Robertson, I. H. (2011). Resting EEG theta power correlates with cognitive performance in healthy older adults. *Psychophysiology* 48, 1083–1087. doi: 10.1111/j.1469-8986.2010.01173.x

Fleck, J. I., Kuti, J., Mercurio, J., Mullen, S., Austin, K., and Pereira, O. (2017). The Impact of Age and Cognitive Reserve on Resting-State Brain Connectivity. *Front. Aging Neurosci.* 9:392. doi: 10.3389/fnagi.2017.00392

Folstein, M. F., Robins, L. N., and Helzer, J. E. (1983). The Mini-Mental State Examination. *Arch. Gen. Psychiatry* 40, 812–812. doi: 10.1001/archpsyc.1983.01790060110016

Friedman, N. P., and Miyake, A. (2017). Unity and diversity of executive functions: individual differences as a window on cognitive structure. *Cortex* 86, 186–204. doi: 10.1016/j.cortex.2016.04.023

Gong, G., He, Y., Concha, L., Lebel, C., Gross, D. W., Evans, A. C., et al. (2009). Mapping Anatomical Connectivity Patterns of Human Cerebral Cortex Using In Vivo Diffusion Tensor Imaging Tractography. *Cereb. Cortex* 19, 524–536. doi: 10.1093/cercor/bhn102

Gonzalez-Escamilla, G., Muthuraman, M., Chirumamilla, V. C., Vogt, J., and Groppa, S. (2018). Brain Networks Reorganization During Maturation and Healthy Aging-Emphases for Resilience. *Front. Psychiatry* 9:601. doi: 10.3389/fpsyt.2018.00601

Gouw, A. A., Alsema, A. M., Tijms, B. M., Borta, A., Scheltens, P., Stam, C. J., et al. (2017). EEG spectral analysis as a putative early prognostic biomarker in nondemented, amyloid positive subjects. *Neurobiol. Aging* 57, 133–142. doi: 10.1016/j.neurobiolaging.2017.05.017

Greicius, M. D., Krasnow, B., Reiss, A. L., and Menon, V. (2003). Functional connectivity in the resting brain: a network analysis of the default mode hypothesis. *Proc. Natl. Acad. Sci. U. S. A.* 100, 253–258. doi: 10.1073/pnas.0135058100

Griffa, A., and van den Heuvel, M. P. (2018). Rich-club neurocircuitry: function, evolution, and vulnerability. *Dialogues Clin. Neurosci.* 20, 121–132.

Gross, J. (2019). Magnetoencephalography in Cognitive Neuroscience: a Primer. *Neuron* 104, 189–204. doi: 10.1016/j.neuron.2019.07.001

Hakiki, B., Pancani, S., Portaccio, E., Molino-Lova, R., Sofi, F., Macchi, C., et al. (2020). Impact of occupational complexity on cognitive decline in the oldest-old. *Aging Ment. Health* 25, 1630–1635. doi: 10.1080/13607863.2020.1746739

Hämäläinen, M., Hari, R., Ilmoniemi, R. J., Knuutila, J., and Lounasmaa, O. V. (1993). Magnetoencephalography—theory, instrumentation, and applications to noninvasive studies of the working human brain. *Rev. Mod. Phys.* 65, 413–497. doi: 10.1103/RevModPhys.65.413

Hari, R., and Puce, A. (2017). *MEG-EEG Primer*. Oxford, New York: Oxford University Press.

Hillebrand, A., and Barnes, G. R. (2005). Beamformer Analysis of MEG Data. *Int. Rev. Neurobiol.* 68, 149–171. doi: 10.1016/S0074-7742(05)68006-3

Hillebrand, A., Barnes, G. R., Bosboom, J. L., Berendse, H. W., and Stam, C. J. (2012). Frequency-dependent functional connectivity within resting-state networks: an atlas-based MEG beamformer solution. *NeuroImage* 59, 3909–3921. doi: 10.1016/j.neuroimage.2011.11.005

Hillebrand, A., Singh, K. D., Holliday, I. E., Furlong, P. L., and Barnes, G. R. (2005). A new approach to neuroimaging with magnetoencephalography. *Hum. Brain Mapp.* 25, 199–211. doi: 10.1002/hbm.20102

Hillebrand, A., Tewarie, P., van Dellen, E., Yu, M., Carbo, E. W. S., Douw, L., et al. (2016). Direction of information flow in large-scale resting-state networks is frequency-dependent. *Proc. Natl. Acad. Sci. U. S. A.* 113, 3867–3872. doi: 10.1073/pnas.1515657113

Hipp, J. F., Hawellek, D. J., Corbetta, M., Siegel, M., and Engel, A. K. (2012). Large-scale cortical correlation structure of spontaneous oscillatory activity. *Nat. Neurosci.* 15, 884–890. doi: 10.1038/nn.3101

Hlinka, J., Alexakis, C., Diukova, A., Liddle, P. F., and Auer, D. P. (2010). Slow EEG pattern predicts reduced intrinsic functional connectivity in the default mode network: an inter-subject analysis. *NeuroImage* 53, 239–246. doi: 10.1016/j.neuroimage.2010.06.002

Horn, A., and Kühn, A. A. (2015). Lead-DBS: a toolbox for deep brain stimulation electrode localizations and visualizations. *NeuroImage* 107, 127–135. doi: 10.1016/j.neuroimage.2014.12.002

Hughes, L. E., Henson, R. N., Pereda, E., Bruña, R., López-Sanz, D., Quinn, A. J., et al. (2019). Biomagnetic biomarkers for dementia: a pilot multicentre study with a recommended methodological framework for magnetoencephalography. *Alzheimers Dement. Diagn. Assess. Dis. Monit.* 11, 450–462. doi: 10.1016/j.dadm.2019.04.009

James, B. D., Bennett, D. A., Boyle, P. A., Leurgans, S., and Schneider, J. A. (2012). Dementia From Alzheimer Disease and Mixed Pathologies in the Oldest Old. *JAMA* 307, 1798–1800. doi: 10.1001/jama.2012.3556

Jurado, M. B., and Rosselli, M. (2007). The Elusive Nature of Executive Functions: a Review of our Current Understanding. *Neuropsychol. Rev.* 17, 213–233. doi: 10.1007/s11065-007-9040-z

Kebets, V., Holmes, A. J., Orban, C., Tang, S., Li, J., Sun, N., et al. (2019). Somatosensory-Motor Dysconnectivity Spans Multiple Transdiagnostic Dimensions of Psychopathology. *Biol. Psychiatry* 86, 779–791. doi: 10.1016/j.biopsych.2019.06.013

Knyazeva, M. G., Barzegaran, E., Vildavski, V. Y., and Demonet, J.-F. (2018). Aging of human alpha rhythm. *Neurobiol. Aging* 69, 261–273. doi: 10.1016/j.neurobiolaging.2018.05.018

Krishnan, A., Williams, L. J., McIntosh, A. R., and Abdi, H. (2011). Partial Least Squares (PLS) methods for neuroimaging: a tutorial and review. *NeuroImage* 56, 455–475. doi: 10.1016/j.neuroimage.2010.07.034

Landau, S. M., Marks, S. M., Mormino, E. C., Rabinovici, G. D., Oh, H., O'Neil, J. P., et al. (2012). Association of Lifetime Cognitive Engagement and Low β-Amyloid Deposition. *Arch. Neurol.* 69, 623–629. doi: 10.1001/archneurol.2011.2748

Laufs, H., Krakow, K., Sterzer, P., Eger, E., Beyerle, A., Salek-Haddadi, A., et al. (2003). Electroencephalographic signatures of attentional and cognitive default modes in spontaneous brain activity fluctuations at rest. *Proc. Natl. Acad. Sci. U. S. A.* 100, 11053–11058. doi: 10.1073/pnas.1831638100

Lavrencic, L. M., Richardson, C., Harrison, S. L., Muniz-Terrera, G., Keage, H. A. D., Brittain, K., et al. (2018). Is There a Link Between Cognitive Reserve and Cognitive Function in the Oldest-Old? *J. Gerontol. A Biol. Sci. Med. Sci.* 73, 499–505. doi: 10.1093/gerona/glx140

Legdeur, N., Badissi, M., Carter, S. F., de Crom, S., van de Kreeke, A., Vreeswijk, R., et al. (2018). Resilience to cognitive impairment in the oldest-old: design of the EMIF-AD 90+ study. *BMC Geriatr.* 18:289. doi: 10.1186/s12877-018-0984-z

Legdeur, N., Visser, P. J., Woodworth, D. C., Muller, M., Fletcher, E., Maillard, P., et al. (2019). White Matter Hyperintensities and Hippocampal Atrophy in Relation to Cognition: the 90+ Study. *J. Am. Geriatr. Soc.* 67, 1827–1834. doi: 10.1111/jgs.15990

León, I., García-García, J., and Roldán-Tapia, L. (2014). Estimating Cognitive Reserve in Healthy Adults Using the Cognitive Reserve Scale. *PLoS One* 9:e102632. doi: 10.1371/journal.pone.0102632

López, M. E., Aurtenetxe, S., Pereda, E., Cuesta, P., Castellanos, N. P., Bruña, R., et al. (2014). Cognitive reserve is associated with the functional organization of the brain in healthy aging: a MEG study. *Front. Aging Neurosci.* 6:125. doi: 10.3389/fnagi.2014.00125

Maestú, F., Cuesta, P., Hasan, O., Fernandéz, A., Funke, M., and Schulz, P. E. (2019). The Importance of the Validation of M/EEG With Current Biomarkers in Alzheimer's Disease. *Front. Hum. Neurosci.* 13:17. doi: 10.3389/fnhum.2019.00017

McKhann, G., Drachman, D., Folstein, M., Katzman, R., Price, D., and Stadlan, E. M. (1984). Clinical diagnosis of Alzheimer's disease: report of the NINCDS-ADRDA Work Group under the auspices of Department of Health and Human Services Task Force on Alzheimer's Disease. *Neurology* 34, 939–944. doi: 10.1212/wnl.34.7.939

Meskaldji, D. E., Fischi-Gomez, E., Griffa, A., Hagmann, P., Morgenthaler, S., and Thiran, J.-P. (2013). Comparing connectomes across subjects and populations at different scales. *NeuroImage* 80, 416–425. doi: 10.1016/j.neuroimage.2013.04.084

Micanovic, C., and Pal, S. (2014). The diagnostic utility of EEG in early-onset dementia: a systematic review of the literature with narrative analysis. *J. Neural Transm.* 121, 59–69. doi: 10.1007/s00702-013-1070-5

Miraglia, F., Vecchio, F., and Rossini, P. M. (2017). Searching for signs of aging and dementia in EEG through network analysis. *Behav. Brain Res.* 317, 292–300. doi: 10.1016/j.bbr.2016.09.057

Mitchell, D. J., McNaughton, N., Flanagan, D., and Kirk, I. J. (2008). Frontal-midline theta from the perspective of hippocampal "theta.". *Prog. Neurobiol.* 86, 156–185. doi: 10.1016/j.pneurobio.2008.09.005

Morris, J. C. (1993). The Clinical Dementia Rating (CDR): current version and scoring rules. *Neurology* 43, 2412–2412. doi: 10.1212/WNL.43.11.2412-a

Myers, N., Pasquini, L., Göttler, J., Grimmer, T., Koch, K., Ortner, M., et al. (2014). Within-patient correspondence of amyloid-β and intrinsic network connectivity in Alzheimer's disease. *Brain* 137, 2052–2064. doi: 10.1093/brain/awu103

Nelson, P. T., Dickson, D. W., Trojanowski, J. Q., Jack, C. R., Boyle, P. A., Arfanakis, K., et al. (2019). Limbic-predominant age-related TDP-43 encephalopathy (LATE): consensus working group report. *Brain J. Neurol.* 142, 1503–1527. doi: 10.1093/brain/awz099

Nucci, M., Mapelli, D., and Mondini, S. (2012). Cognitive Reserve Index questionnaire (CRIq): a new instrument for measuring cognitive reserve. *Aging Clin. Exp. Res.* 24, 218–226. doi: 10.3275/7800

Palmqvist, S., Schöll, M., Strandberg, O., Mattsson, N., Stomrud, E., Zetterberg, H., et al. (2017). Earliest accumulation of β-amyloid occurs within the default-mode network and concurrently affects brain connectivity. *Nat. Commun.* 8:1214. doi: 10.1038/s41467-017-01150-x

Paolacci, L., Giannandrea, D., Mecocci, P., and Parnetti, L. (2017). Biomarkers for Early Diagnosis of Alzheimer's Disease in the Oldest Old: yes or No? *J. Alzheimers Dis.* 58, 323–335. doi: 10.3233/JAD-161127

Pasquini, L., Benson, G., Grothe, M. J., Utz, L., Myers, N. E., Yakushev, I., et al. (2017). Individual Correspondence of Amyloid-β and Intrinsic Connectivity in the Posterior Default Mode Network Across Stages of Alzheimer's Disease. *J. Alzheimers Dis.* 58, 763–773. doi: 10.3233/JAD-170096

Penny, W. D., Friston, K. J., Ashburner, J. T., Kiebel, S. J., and Nichols, T. E. (2011). *Statistical Parametric Mapping: the Analysis of Functional Brain Images*. Amsterdam: Elsevier.

Petersen, R. C. (2004). Mild cognitive impairment as a diagnostic entity. *J. Intern. Med.* 256, 183–194. doi: 10.1111/j.1365-2796.2004.01388.x

Pettigrew, C., Shao, Y., Zhu, Y., Grega, M., Brichko, R., Wang, M.-C., et al. (2019). Self-reported lifestyle activities in relation to longitudinal cognitive trajectories. *Alzheimer Dis. Assoc. Disord.* 33, 21–28. doi: 10.1097/WAD.0000000000000281

Prichep, L. S., John, E. R., Ferris, S. H., Rausch, L., Fang, Z., Cancro, R., et al. (2006). Prediction of longitudinal cognitive decline in normal elderly with subjective complaints using electrophysiological imaging. *Neurobiol. Aging* 27, 471–481. doi: 10.1016/j.neurobiolaging.2005.07.021

Raichle, M. E. (2015). The Brain's Default Mode Network. *Annu. Rev. Neurosci.* 38, 433–447. doi: 10.1146/annurev-neuro-071013-014030

Raichle, M. E., MacLeod, A. M., Snyder, A. Z., Powers, W. J., Gusnard, D. A., and Shulman, G. L. (2001). A default mode of brain function. *Proc. Natl. Acad. Sci. U. S. A.* 98, 676–682. doi: 10.1073/pnas.98.2.676

Reitan, R. M. (1958). Validity of the Trail Making Test as an Indicator of Organic Brain Damage. *Percept. Mot. Skills* 8, 271–276.

Rossetti, H. C., Munro Cullum, C., Hynan, L. S., and Lacritz, L. (2010). The CERAD Neuropsychological Battery Total Score and the Progression of Alzheimer's Disease. *Alzheimer Dis. Assoc. Disord.* 24, 138–142. doi: 10.1097/WAD.0b013e3181b76415

Rossini, P. M., Di Iorio, R., Vecchio, F., Anfossi, M., Babiloni, C., Bozzali, M., et al. (2020). Early diagnosis of Alzheimer's disease: the role of biomarkers including advanced EEG signal analysis. Report from the IFCN-sponsored panel of experts. *Clin. Neurophysiol.* 131, 1287–1310. doi: 10.1016/j.clinph.2020.03.003

Sareen, E., Zahar, S., Ville, D. V. D., Gupta, A., Griffa, A., and Amico, E. (2021). Exploring MEG brain fingerprints: evaluation, pitfalls, and interpretations. *NeuroImage* 240:118331. doi: 10.1016/j.neuroimage.2021.118331

Scheeringa, R., Bastiaansen, M. C. M., Petersson, K. M., Oostenveld, R., Norris, D. G., and Hagoort, P. (2008). Frontal theta EEG activity correlates negatively with the default mode network in resting state. *Int. J. Psychophysiol.* 67, 242–251. doi: 10.1016/j.ijpsycho.2007.05.017

Sepulcre, J., Sabuncu, M. R., Li, Q., El Fakhri, G., Sperling, R., and Johnson, K. A. (2017). Tau and amyloid β proteins distinctively associate to functional network changes in the aging brain. *Alzheimers Dement.* 13, 1261–1269. doi: 10.1016/j.jalz.2017.02.011

Šneidere, K., Mondini, S., and Stepens, A. (2020). Role of EEG in Measuring Cognitive Reserve: a Rapid Review. *Front. Aging Neurosci.* 12:249. doi: 10.3389/fnagi.2020.00249

Soldan, A., Pettigrew, C., Zhu, Y., Wang, M.-C., Bilgel, M., Hou, X., et al. (2021). Association of Lifestyle Activities with Functional Brain Connectivity and Relationship to Cognitive Decline among Older Adults. *Cereb. Cortex* 2021:bhab187. doi: 10.1093/cercor/bhab187

Stam, C. J. (2010). Use of magnetoencephalography (MEG) to study functional brain networks in neurodegenerative disorders. *J. Neurol. Sci.* 289, 128–134. doi: 10.1016/j.jns.2009.08.028

Stam, C. J. (2014). Modern network science of neurological disorders. *Nat. Rev. Neurosci.* 15, 683–695. doi: 10.1038/nrn3801

Stam, C. J., de Haan, W., Daffertshofer, A., Jones, B. F., Manshanden, I., van Cappellen van Walsum, A. M., et al. (2009). Graph theoretical analysis of magnetoencephalographic functional connectivity in Alzheimer's disease. *Brain* 132, 213–224. doi: 10.1093/brain/awn262

Stam, C. J., Jones, B. F., Manshanden, I., van Cappellen van Walsum, A. M., Montez, T., Verbunt, J. P. A., et al. (2006). Magnetoencephalographic evaluation of resting-state functional connectivity in Alzheimer's disease. *NeuroImage* 32, 1335–1344. doi: 10.1016/j.neuroimage.2006.05.033

Stam, C. J., van Cappellen van Walsum, A. M., Pijnenburg, Y. A. L., Berendse, H. W., de Munck, J. C., Scheltens, P., et al. (2002). Generalized Synchronization of MEG Recordings in Alzheimer's Disease: evidence for Involvement of the Gamma Band. *J. Clin. Neurophysiol.* 19, 562–574.

Stern, Y. (2009). Cognitive reserve. *Neuropsychologia* 47, 2015–2028. doi: 10.1016/j.neuropsychologia.2009.03.004

Stern, Y., Arenaza-Urquijo, E. M., Bartrés-Faz, D., Belleville, S., Cantilon, M., Chetelat, G., et al. (2018). Whitepaper: defining and investigating cognitive reserve, brain reserve, and brain maintenance. *Alzheimers Dement.* 16, 1305–1311. doi: 10.1016/j.jalz.2018.07.219

Stomrud, E., Hansson, O., Minthon, L., Blennow, K., Rosén, I., and Londos, E. (2010). Slowing of EEG correlates with CSF biomarkers and reduced cognitive speed in elderly with normal cognition over 4 years. *Neurobiol. Aging* 31, 215–223. doi: 10.1016/j.neurobiolaging.2008.03.025

Taulu, S., and Hari, R. (2009). Removal of magnetoencephalographic artifacts with temporal signal-space separation: demonstration with single-trial auditory-evoked responses. *Hum. Brain Mapp.* 30, 1524–1534. doi: 10.1002/hbm.20627

Taulu, S., and Simola, J. (2006). Spatiotemporal signal space separation method for rejecting nearby interference in MEG measurements. *Phys. Med. Biol.* 51, 1759–1768. doi: 10.1088/0031-9155/51/7/008

Tewarie, P., Hunt, B. A. E., O'Neill, G. C., Byrne, A., Aquino, K., Bauer, M., et al. (2019). Relationships Between Neuronal Oscillatory Amplitude and Dynamic Functional Connectivity. *Cereb. Cortex* 29, 2668–2681. doi: 10.1093/cercor/bhy136

Tombaugh, T. N., Kozak, J., and Rees, L. (1999). Normative Data Stratified by Age and Education for Two Measures of Verbal Fluency: FAS and Animal Naming. *Arch. Clin. Neuropsychol.* 14, 167–177. doi: 10.1093/arclin/14.2.167

Tzourio-Mazoyer, N., Landeau, B., Papathanassiou, D., Crivello, F., Etard, O., Delcroix, N., et al. (2002). Automated Anatomical Labeling of Activations in SPM Using a Macroscopic Anatomical Parcellation of the MNI MRI Single-Subject Brain. *NeuroImage* 15, 273–289. doi: 10.1006/nimg.2001.0978

United Nations, Department of Economic and Social Affairs, Population Division (2019). *World population prospects Highlights, 2019 revision*. New York: United Nations

Valenzuela, M. J., and Sachdev, P. (2006). Brain reserve and dementia: a systematic review. *Psychol. Med.* 36, 441–454. doi: 10.1017/S0033291705006264

Valenzuela, M. J., Sachdev, P., Wen, W., Chen, X., and Brodaty, H. (2008). Lifespan Mental Activity Predicts Diminished Rate of Hippocampal Atrophy. *PLoS One* 3:e2598. doi: 10.1371/journal.pone.0002598

Vallesi, A. (2021). The Quest for Hemispheric Asymmetries Supporting and Predicting Executive Functioning. *J. Cogn. Neurosci.* 33, 1679–1697. doi: 10.1162/jocn_a_01646

Van Den Heuvel, M. P., Stam, C. J., Kahn, R. S., and Pol, H. E. H. (2009). Efficiency of Functional Brain Networks and Intellectual Performance. *J. Neurosci.* 29, 7619–7624. doi: 10.1523/JNEUROSCI.1443-09.2009

van der Hiele, K., Vein, A. A., Reijntjes, R. H. A. M., Westendorp, R. G. J., Bollen, E. L. E. M., van Buchem, M. A., et al. (2007). EEG correlates in the spectrum of cognitive decline. *Clin. Neurophysiol.* 118, 1931–1939. doi: 10.1016/j.clinph.2007.05.070

van der Zande, J., Gouw, A., van Steenoven, I., van de Beek, M., Scheltens, P., Stam, C., et al. (2020). Diagnostic and prognostic value of EEG in prodromal dementia with Lewy bodies. *Neurology* 95, e662–e670. doi: 10.1212/WNL.0000000000009977

Verghese, J., Lipton, R. B., Katz, M. J., Hall, C. B., Derby, C. A., Kuslansky, G., et al. (2003). Leisure Activities and the Risk of Dementia in the Elderly. *N. Engl. J. Med.* 348, 2508–2516. doi: 10.1056/NEJMoa022252

Vlahou, E. L., Thurm, F., Kolassa, I.-T., and Schlee, W. (2014). Resting-state slow wave power, healthy aging and cognitive performance. *Sci. Rep.* 4:5101. doi: 10.1038/srep05101

Wan, L., Huang, H., Schwab, N., Tanner, J., Rajan, A., Lam, N. B., et al. (2019). From eyes-closed to eyes-open: role of cholinergic projections in EC-to-EO alpha reactivity revealed by combining EEG and MRI. *Hum. Brain Mapp.* 40, 566–577. doi: 10.1002/hbm.24395

Wang, H.-X., MacDonald, S. W. S., Dekhtyar, S., and Fratiglioni, L. (2017). Association of lifelong exposure to cognitive reserve-enhancing factors with dementia risk: a community-based cohort study. *PLoS Med.* 14:e1002251. doi: 10.1371/journal.pmed.1002251

Whalen, C., Maclin, E. L., Fabiani, M., and Gratton, G. (2008). Validation of a method for coregistering scalp recording locations with 3D structural MR images. *Hum. Brain Mapp.* 29, 1288–1301. doi: 10.1002/hbm.20465

Wharton, S. B., Brayne, C., Savva, G. M., Matthews, F. E., Forster, G., Simpson, J., et al. (2011). Epidemiological Neuropathology: the MRC Cognitive Function and Aging Study Experience. *J. Alzheimers Dis.* 25, 359–372. doi: 10.3233/JAD-2011-091402

Wilson, R. S., Barnes, L. L., and Bennett, D. A. (2003). Assessment of Lifetime Participation in Cognitively Stimulating Activities. *J. Clin. Exp. Neuropsychol.* 25, 634–642. doi: 10.1076/jcen.25.5.634.14572

Xu, H., Yang, R., Qi, X., Dintica, C., Song, R., Bennett, D. A., et al. (2019). Association of Lifespan Cognitive Reserve Indicator With Dementia Risk in the Presence of Brain Pathologies. *JAMA Neurol.* 76:1184–1191. doi: 10.1001/jamaneurol.2019.2455

Yang, C.-Y., and Lin, C.-P. (2020). Classification of cognitive reserve in healthy older adults based on brain activity using support vector machine. *Physiol. Meas.* 41:065009. doi: 10.1088/1361-6579/ab979e

Yang, Z., Slavin, M. J., and Sachdev, P. S. (2013). Dementia in the oldest old. *Nat. Rev. Neurol.* 9, 382–393. doi: 10.1038/nrneurol.2013.105

Yeo, B. T., Krienen, F. M., Sepulcre, J., Sabuncu, M. R., Lashkari, D., Hollinshead, M., et al. (2011). The organization of the human cerebral cortex estimated by intrinsic functional connectivity. *J. Neurophysiol.* 106, 1125–1165. doi: 10.1152/jn.00338.2011

Yesavage, J. A., Brink, T. L., Rose, T. L., Lum, O., Huang, V., Adey, M., et al. (1982). Development and validation of a geriatric depression screening scale: a preliminary report. *J. Psychiatr. Res.* 17, 37–49. doi: 10.1016/0022-3956(82)90033-4

Yu, M., Engels, M. M. A., Hillebrand, A., van Straaten, E. C. W., Gouw, A. A., Teunissen, C., et al. (2017). Selective impairment of hippocampus and posterior hub areas in Alzheimer's disease: an MEG-based multiplex network study. *Brain* 140, 1466–1485. doi: 10.1093/brain/awx050

Zöller, D., Sandini, C., Karahanoğlu, F. I., Padula, M. C., Schaer, M., Eliez, S., et al. (2019). Large-Scale Brain Network Dynamics Provide a Measure of Psychosis and Anxiety in 22q11.2 Deletion Syndrome. *Biol. Psychiatry Cogn. Neurosci. Neuroimaging* 4, 881–892.doi: 10.1016/j.bpsc.2019.04.004

Conflict of Interest: The authors declare that the research was conducted in the absence of any commercial or financial relationships that could be construed as a potential conflict of interest.

Publisher's Note: All claims expressed in this article are solely those of the authors and do not necessarily represent those of their affiliated organizations, or those of the publisher, the editors and the reviewers. Any product that may be evaluated in this article, or claim that may be made by its manufacturer, is not guaranteed or endorsed by the publisher.

frontiers | Frontiers in Aging Neuroscience

ORIGINAL RESEARCH
published: 08 April 2022
doi: 10.3389/fnagi.2022.755454

Decreased EEG Field Synchronization in Slow-Frequency Bands Characterizes Synaptic Dysfunction in Amnestic Subtypes of Mild Cognitive Impairment

*Una Smailovic[1,2], Daniel Ferreira[1,3], Birgitta Ausén[1,4,5], Nicholas James Ashton[6,7,8,9,10], Thomas Koenig[11], Henrik Zetterberg[6,7,12,13,14], Kaj Blennow[6,7] and Vesna Jelic[1,4]**

[1] Division of Clinical Geriatrics, Center for Alzheimer Research, Department of Neurobiology, Care Sciences and Society, Karolinska Institutet, Huddinge, Sweden, [2] Department of Clinical Neurophysiology, Karolinska University Hospital, Stockholm, Sweden, [3] Department of Radiology, Mayo Clinic, Rochester, MN, United States, [4] Clinic for Cognitive Disorders, Karolinska University Hospital-Huddinge, Stockholm, Sweden, [5] Women's Health and Allied Health Professionals Theme, Medical Unit Medical Psychology, Karolinska University Hospital, Huddinge, Sweden, [6] Department of Psychiatry and Neurochemistry, Institute of Neuroscience and Physiology, The Sahlgrenska Academy at the University of Gothenburg, Mölndal, Sweden, [7] Clinical Neurochemistry Laboratory, Sahlgrenska University Hospital, Mölndal, Sweden, [8] Wallenberg Centre for Molecular and Translational Medicine, University of Gothenburg, Gothenburg, Sweden, [9] King's College London, Institute of Psychiatry, Psychology and Neuroscience, Maurice Wohl Institute Clinical Neuroscience Institute, London, United Kingdom, [10] NIHR Biomedical Research Centre for Mental Health and Biomedical Research Unit for Dementia at South London and Maudsley NHS Foundation, London, United Kingdom, [11] Psychiatric Electrophysiology Unit, Translational Research Center, University Hospital of Psychiatry, Bern, Switzerland, [12] Department of Neurodegenerative Disease, UCL Queen Square Institute of Neurology, London, United Kingdom, [13] UK Dementia Research Institute at UCL, London, United Kingdom, [14] Hong Kong Center for Neurodegenerative Diseases, Hong Kong, Hong Kong SAR, China

OPEN ACCESS

Edited by:
Aneta Kielar,
The University of Arizona, United States

Reviewed by:
Lucie Bréchet, University of Geneva, Switzerland
András Horváth, National Institute of Clinical Neurosciences (NICN), Hungary

***Correspondence:**
Vesna Jelic
vesna.jelic@ki.se

Specialty section:
This article was submitted to Alzheimer's Disease and Related Dementias, a section of the journal Frontiers in Aging Neuroscience

Received: *08 August 2021*
Accepted: *17 January 2022*
Published: *08 April 2022*

Citation:
Smailovic U, Ferreira D, Ausén B, Ashton NJ, Koenig T, Zetterberg H, Blennow K and Jelic V (2022) Decreased EEG Field Synchronization in Slow-Frequency Bands Characterizes Synaptic Dysfunction in Amnestic Subtypes of Mild Cognitive Impairment. Front. Aging Neurosci. 14:755454. doi: 10.3389/fnagi.2022.755454

Background: Mild cognitive impairment (MCI) is highly prevalent in a memory clinic setting and is heterogeneous regarding its clinical presentation, underlying pathophysiology, and prognosis. The most prevalent subtypes are single-domain amnestic MCI (sd-aMCI), considered to be a prodromal phase of Alzheimer's disease (AD), and multidomain amnestic MCI (md-aMCI), which is associated with multiple etiologies. Since synaptic loss and dysfunction are the closest pathoanatomical correlates of AD-related cognitive impairment, we aimed to characterize it in patients with sd-aMCI and md-aMCI by means of resting-state electroencephalography (EEG) global field power (GFP), global field synchronization (GFS), and novel cerebrospinal fluid (CSF) synaptic biomarkers.

Methods: We included 52 patients with sd-aMCI (66.9 ± 7.3 years, 52% women) and 30 with md-aMCI (63.1 ± 7.1 years, 53% women). All patients underwent a detailed clinical assessment, resting-state EEG recordings and quantitative analysis (GFP and GFS in delta, theta, alpha, and beta bands), and analysis of CSF biomarkers of synaptic dysfunction, neurodegeneration, and AD-related pathology. Cognitive subtyping was based on a comprehensive neuropsychological examination. The Mini-Mental State Examination (MMSE) was used as an estimation of global cognitive performance. EEG and CSF biomarkers were included in a multivariate model together with MMSE and demographic variables, to investigate differences between sd-aMCI and md-aMCI.

Results: Patients with sd-aMCI had higher CSF phosphorylated tau, total tau and neurogranin levels, and lower values in GFS delta and theta. No differences were observed in GFP. The multivariate model showed that the most important synaptic measures for group separation were GFS theta, followed by GFS delta, GFP theta, CSF neurogranin, and GFP beta.

Conclusion: Patients with sd-aMCI when compared with those with md-aMCI have a neurophysiological and biochemical profile of synaptic damage, neurodegeneration, and amyloid pathology closer to that described in patients with AD. The most prominent signature in sd-aMCI was a decreased global synchronization in slow-frequency bands indicating that functional connectivity in slow frequencies is more specifically related to early effects of AD-specific molecular pathology.

Keywords: electroencephalography, synaptic dysfunction, amnestic mild cognitive impairment (aMCI), Alzheimer's disease, EEG power, global field synchronization (GFS)

INTRODUCTION

Mild cognitive impairment (MCI) is an intermediate stage between cognitively healthy brain aging and dementia (Winblad et al., 2004) and is one of the most common diagnoses in memory clinic (Wahlund et al., 2003). It represents a risk condition for future development of dementia, with an annual conversion rate ranging from 5 to 15% (Bruscoli and Lovestone, 2004; Farias et al., 2009). The risk of progression to dementia is even higher among patients with MCI from the specialized memory clinics than community-based populations, emphasizing the need for improved clinical phenotyping of patients with objectively evident cognitive impairment (Mitchell and Shiri-Feshki, 2009). Several diagnostic criteria for MCI have been proposed so far (Petersen, 2004; Winblad et al., 2004; Albert et al., 2011), all of which highlight the heterogeneity of this condition in terms of its clinical and etiological presentation. MCI is typically classified as amnestic or non-amnestic, depending on whether there is an objectively evident impairment in the memory domain (Petersen, 2004, 2016; Winblad et al., 2004). Amnestic MCI (aMCI) is considered to clinically correspond to the prodromal stage of typical Alzheimer's disease (AD) (Dubois et al., 2014; Petersen, 2016) and has been linked to the AD biomarker profile including positive markers for amyloid and tau pathology (Visser et al., 2009; Wolk et al., 2009). MCI can be additionally classified as a single or multiple domain based on the number of affected cognitive domains, with the latter including deficits in memory, language, attention, executive function, and visuospatial skills (Petersen, 2004; Albert et al., 2011). Objectively verified impairment in multiple cognitive domains seems to be related to the faster progression to dementia, including dementia due to AD, Lewy bodies (DLB), and cerebrovascular disease (Petersen, 2004; Hughes et al., 2011).

Cognitive subtypes of MCI still exhibit variability in terms of disease etiology and prognosis, emphasizing the role of biomarkers in delineating more homogeneous subgroups of patients with objective cognitive impairment. Recent studies have shown that markers of synaptic degeneration and dysfunction are closely related to cognitive impairment (Scheff et al., 2006, 2007; Headley et al., 2018) and future cognitive deterioration in patients with MCI (Poil et al., 2013; Kvartsberg et al., 2015a), supporting their role in characterizing subgroups of patients with cognitive impairment.

Electroencephalography (EEG) is a neurophysiological method that can detect real-time changes in the brain synaptic activity associated with different vigilance states, cognitive load, and pathological brain disorders. Its clinical use spans across a spectrum of brain disorders with underlying synaptic pathology that causes cortical hypo- and hyperexcitability, focal, or more generalized cerebral dysfunction (Schomer and Lopes da Silva, 2015). The nature of cortical and subcortical synaptic degeneration and loss in patients with cognitive impairment therefore suggest EEG as a candidate neurophysiological marker of impaired cerebral activity. So far, most of the research studies have emphasized the advantage of quantitative EEG (qEEG) that offers objective, comprehensive, and more generalizable interpretation of EEG analyses (Smailovic and Jelic, 2019). The quantitative resting-state EEG analysis commonly assesses the power and synchronization of EEG oscillations across four conventional frequency bands that are also routinely described during visual EEG assessments (Schomer and Lopes da Silva, 2015). The most common qEEG finding in patients with cognitive impairment includes the increase in power in slow-frequency bands (i.e., delta and theta) and decrease in power in fast-frequency bands (i.e., alpha and beta) (Smailovic and Jelic, 2019). At the same time, the decrease in global EEG synchronization has also been reported in patients with cognitive impairment, noted as early as in patients with subjective cognitive decline (SCD) (Koenig et al., 2005). In the context of MCI subtypes, different qEEG changes have been reported in relation to the underlying neurodegenerative or cerebrovascular pathology (Moretti et al., 2012; Schumacher et al., 2020) and duration of disease symptoms (Moretti et al., 2010).

Synaptic dysfunction in patients with cognitive impairment can be further assessed by changes in molecular markers available from cerebrospinal fluid (CSF) that are thought to reflect degeneration and loss of pre- or postsynaptic compartments in the central nervous system. Recent studies support neurogranin,

a postsynaptic neuron-specific protein, as a CSF marker of synaptic degeneration in AD (Kvartsberg et al., 2015b; Portelius et al., 2018). Neurogranin is mainly expressed in the cortical and hippocampal neurons and has an important role in regulating synaptic plasticity (Bogdanovic et al., 2002; Zhong et al., 2009; Zhong and Gerges, 2012). Previous studies have shown that increased neurogranin levels in the CSF correlate with poor memory scores and aMCI presentation (Lista et al., 2016; Headley et al., 2018) as well as progression to AD dementia in patients with MCI (Kvartsberg et al., 2015a).

Despite the close relationship between synaptic markers and measures of cognitive impairment, their role in characterizing heterogeneous clinical presentation of the mild neurocognitive disorders is yet to be fully elucidated. The main aim of this study was to investigate whether EEG power and synchronization and novel CSF synaptic marker neurogranin, in addition to the conventional CSF markers of amyloid and tau pathology, differentiate subtypes of aMCI based on the single- vs. multidomain cognitive profile. We hypothesized that neurophysiological and molecular markers of synaptic dysfunction have added value to conventional AD biomarkers in characterizing aMCI subtypes.

MATERIALS AND METHODS

Study Population

The study included 82 patients from memory clinic recruited at Karolinska University Hospital and diagnosed with MCI based on the clinical criteria by Winblad et al. (2004). Our comprehensive clinical assessment included clinical interviews with the patient and informant, blood testing, lumbar puncture, screening for depression, and somatic and neurological examinations. MCI of the amnestic type has been defined during a discussion on the consensus diagnostic round and was based on the clinical observation and summarized neuropsychological test profile. Patients with an amnestic profile of MCI were further clinically subtyped into a single domain (sd-aMCI; n = 52) and multiple-domain amnestic MCI (md-aMCI: n = 30) based on the standard neuropsychological examination including tests of language, visuospatial ability, executive functions, and memory (**Table 1**; Ekman et al., 2020). Impairment in memory and/or any other cognitive domain was standardized by z-transformation of test results, using age- and education-adjusted Swedish norms and references (Arnáiz and Almkvist, 2003; Wechsler, 2003, 2010). Clinical Dementia Rating (CDR) scale was used to assess the level of disease severity. The CDR global score was 0 or 0.5 with no major difficulties in performing independent activities of daily living. Global cognitive performance was estimated by means of the Mini-Mental State Examination (MMSE) (Folstein et al., 1975).

All patients underwent lumbar puncture and CSF conventional (i.e., Aβ42, p-tau, and t-tau) and synaptic (i.e., neurogranin) biomarker analysis and resting-state EEG recording at the baseline. The exclusion criteria involved patients younger than 50 years, presence of any major psychiatric or neurological disorder, brain trauma, psychotropic medication, and the time gap between the EEG recording and lumbar puncture longer than 6 months. Demographics and clinical data in the whole MCI cohort as well as in sd-aMCI and md-aMCI subgroups are presented in **Table 2**. We also presented descriptive data for a selection of neuropsychological tests within different cognitive domains to illustrate the differences between the sd-aMCI and md-aMCI groups (**Table 3**). The study was approved by the Local Ethical Committee of the Karolinska Hospital and Regional Ethical Review Board in Stockholm (Dnr: 2020-00678, 2011/1978-31/4).

TABLE 1 | Cognitive tests used for subtyping of MCI patients into sd-aMCI and md-aMCI groups in the current study.

Cognitive domains	Neuropsychological tests
Language	WAIS-IV: Similarities; BNT; Letter Fluency (F-A-S); Semantic Fluency (animals)
Visuospatial	WAIS-IV: Block Design; RCFT; Copying Geometric Shapes; Clock Drawing/Reading Test
Executive	WAIS-IV: Digit Symbol; Trail-Making Test A&B; D-KEFS: Trail-Making Test 1–5
Attention/Working memory	WAIS-IV: Digit span and Arithmetic; RCFT; WMS-III: Logical Memory
Semantic/Episodic memory	WAIS-IV: Information; RAVLT; RCFT; WMS-III: Logical Memory

BNT, Boston Naming Test; D-KEFS, Delis-Kaplan Executive System; MCI, mild cognitive impairment; RCFT, Rey-Osterrieth Complex Figure Test; WAIS-IV, Wechsler Adult Intelligence Scale 4th edition; WMS-III, Wechsler Memory Scale 3rd edition; md-aMCI, multidomain amnestic MCI; sd-aMCI, single-domain amnestic MCI.

Cerebrospinal Fluid Sampling and Analysis

All CSF samples were collected according to the standard lumbar puncture procedure (Engelborghs et al., 2017). Conventional markers of AD (i.e., Aβ42, t-tau, and p-tau) were analyzed using the xMAP technology and INNO-BIA AlzBio3 kit (Innogenetics) (Olsson et al., 2005). The clinical cutoff value for amyloid positivity according to the CSF Aβ42 levels was < 550 ng/L. Neurogranin concentrations in the CSF were analyzed using the in-house-developed ELISA assay as described previously in detail by Kvartsberg et al. (2019).

TABLE 2 | Demographics and clinical characteristics in the whole MCI cohort and sd-aMCI and md-aMCI subgroups.

Variables	Whole cohort (N = 82)	sd-aMCI (n = 52)	md-aMCI (n = 30)	Effect size (η^2)	p-value
Age, years	65.49 (7.42)	66.85 (7.31)	63.13 (7.12)	0.059	**0.028**
Sex, women (%)	52%	52%	53%	0.001	0.999
Education, years	12.58 (3.94)	12.18 (3.31)	13.27 (4.83)	0.018	0.281
MMSE	27.31 (1.94)	27.65 (1.67)	26.73 (2.24)	0.053	**0.040**

Data presented as mean and standard deviation except for sex, where percentage of women is presented. p-values were obtained using t-tests (or ANCOVA when including age as a covariate) for all the variables except for sex, where the chi-square test was used. MMSE, Mini-Mental State Examination. sd-aMCI, single-domain amnestic MCI; md-aMCI, multidomain amnestic MCI.
Significant p-values are written in bold text.

TABLE 3 | Neuropsychological test results in *z*-scores for subtyping of MCI patients into sd-aMCI and md-aMCI groups.

Cognitive domains/ Neuropsychological tests	sd-aMCI (*n* = 52)	md-aMCI (*n* = 30)
Language		
Similarities	0.23 (0.89)	−0.28 (0.79)
Visuospatial		
W: Block Design	0.24 (1.05)	−0.63 (0.80)
RCFT, copy	−0.69 (0.97)	−1.83 (2.14)
Executive		
W: Digit symbol	−0.52 (0.89)	−1.02 (0.87)
Attention/Working memory		
Digit span	−0,32 (0.85)	−0.94 (0.64)
Episodic memory		
RAVLT, total learning	−1.37 (0.84)	−1.32 (0.96)
RAVLT, delayed recall	−1.71 (0.86)	−1.87 (0.81)
RCFT, immediate recall	−0.88 (1.16)	−1.24 (1.03)

Data presented as mean and standard deviation. RAVLT, Rey Auditory Verbal Learning Test; W, Wechsler Adult Intelligence Scale (WAIS) 3rd and 4th edition.

Electroencephalography Recordings and Analysis

All MCI patients underwent resting-state EEG recording within 6 months of lumbar puncture and CSF sampling. Resting-state EEGs were recorded as a standard clinical procedure for 15–20 min on the nervous system at the Department of Clinical Neurophysiology at Karolinska University Hospital (NicoletOne EEG Reader v5.93.0.424, Natus NicoletOne, Pleasanton, CA) using the standard placement of 21 scalp electrodes according to the 10/20 system. Trained biomedical engineers were noting any changes in the vigilance states and alarming patients in the case of drowsiness during EEG recording. The standard recording setup was described previously in detail by Smailovic et al. (2018).

All EEGs were exported in the common average reference montage and preprocessed following the same procedure. All exceptional events during the resting-state eyes-closed recording, such as periods of eyes opening, drowsiness, alarming of the patient, movements, and other non-physiological and physiological artifacts, were removed by visual inspection and manual artifact rejection. Ocular artifacts were additionally removed by using electrooculogram (EOG) and semi-automated independent component algorithm (ICA). Preprocessed EEGs were analyzed in frequency-transformed artifact-free 2 s EEG epochs and averaged within subjects. The qEEG analysis involved two complementary and comprehensive EEG measures of global field power (GFP) and global field synchronization (GFS). GFP reduces and summarizes data across multiple EEG channels to a single measure of generalized EEG amplitude. Specifically, in the context of this study, GFP corresponds to the root mean of spectral amplitudes across all EEG channels (Huang et al., 2000; Michel, 2009). GFS, in contrast, reflects, for a particular frequency, the amount of the EEG activity that can be explained by a common phase across all EEG electrodes (Koenig et al., 2001). The computation of GFS measure has been introduced and described in detail in Koenig et al. (2001). GFP and GFS measures were averaged in predefined conventional frequency bands defined within the frequencies as follows: delta (1–3.5 Hz), theta (4–7.5 Hz), alpha (8–11.5 Hz), and beta (12–19.5 Hz). The beta frequency range was defined between 12 and 20 Hz since EEG frequencies above 20 Hz may be contaminated with muscle artifacts (Goncharova et al., 2003; Whitham et al., 2007).

Statistical Analysis

We compared sd-aMCI and md-aMCI groups with *t*-tests when the dependent variables were continuous and chi-square tests when the dependent variables were categorical. We applied the Mann-Whitney *U*-test for group differences when continuous variables were not normally distributed. We also used analysis of variance (ANCOVA) to compare sd-aMCI and md-aMCI groups in MMSE scores while controlling for the effect of age as a covariate. Effect sizes are reported as eta squared (η^2) and interpreted per convention: small = 0.01, medium = 0.06, and large = 0.14. We further wanted to compare EEG measures with CSF biomarkers and key clinical measures, such as MMSE, in their capacity to differentiate sd-aMCI from md-aMCI. For this analysis, we used MMSE instead of the comprehensive neuropsychological protocol to avoid circularity, since the MCI subtype was based on the neuropsychological protocol. Age, sex, and education were also included to assess their role in the model. Given the nature of our variables, the multicollinearity between several of the variables, and the sample size, we chose to apply a classification random forest model, which is superior to the general linear model and other statistical methods in such a scenario (Breiman, 2001; Machado et al., 2018). Random forest is an ensemble method in machine learning based on growing of multiple decision trees *via* bootstrap aggregation (i.e., bagging). Each tree predicts a classification independently and votes for the corresponding class. The best model for each outcome variable is chosen from the majority of votes. The combination of bootstrap aggregation (Breiman, 1996) with random feature selection (Amit and Geman, 1997) in a random forest is important to prevent data overfitting and increase the prediction power. Our random forest model included 5,000 trees, providing an accurate estimation of the importance of variables without introducing too much noise in the model due to the addition of redundant trees. Each of the trees was trained on randomly selected 70% of the data and subsequently tested on the unseen 30% of the data. A total of three variables were randomly selected and tested at each split, where the number of variables was defined by the square root of the total number of predictors in the model. The maximum depth of each tree was determined by the maximum number of nodes in each tree, ensuring at least one observation per node (i.e., trees were not truncated at a given depth). We conducted a random forest classification model (Liaw and Wiener, 2002), with the MCI subtype (i.e., sd-aMCI vs. md-aMCI) treated as the outcome variable, and age, sex, education, MMSE, CSF amyloid-beta 42, CSF p-tau, CSF t-tau, CSF neurogranin, and the four GFP and four GFS qEEG measures included as the predictors. We accounted for the fact that the outcome variable presented with an unbalanced number of cases in its two levels (i.e., sd-aMCI n = 52 and md-aMCI n = 30). When the groups are not balanced in size, the

probability of taking observations from the larger group is higher, which could affect the performance of the model. Therefore, we *a priori* fixed our model to select random samples of the two MCI groups that were 50/50 in proportion. We reported the classification error as a measure of goodness of the model (i.e., out-of-the-bag estimated error rate, OOB-EER) (Breiman, 2001). When outcome variables are dichotomous, as it is our case, the error by chance is 50%. Therefore, a classification error below 50% is better than chance, with values closest to 0% denoting better classification performance, hence, good reliability of the model. We also reported the importance of the predictors as a measure of their contribution toward differentiating the sd-aMCI and md-aMCI groups. Higher important values denote a stronger contribution to the prediction. The random forest model was further complemented with the Pearson correlation coefficients (or point biserial correlation in the case of categorical variables, which were coded as dummy variables), to present the magnitude and direction of the association between variables (i.e., bivariate association). All the analyses were performed using the R[1] version 3.2.4 software, with a p-value $\leq$ 0.05 deemed significant.

RESULTS

Demographics and Clinical Characteristics

With respect to the demographical characteristics, patients in the md-aMCI group were significantly younger (63.1 $\pm$ 7.1 years) than patients in the sd-aMCI group (66.9 $\pm$ 7.3 years). There were no statistically significant differences in the distribution of sex and years of education between the two groups. However, patients in the md-aMCI group obtained significantly lower MMSE scores (26.7 $\pm$ 2.2) than patients in the sd-aMCI group (27.7 $\pm$ 1.7) (p = 0.040) (**Table 2**). ANCOVA showed that group differences in MMSE scores remained significant when including age as a covariate (p = 0.040). The differences in age and MMSE were, however, small, with effect sizes (η^2) below 0.06. Results of the neuropsychological test presented in z-scores for patients with sd-aMCI and md-aMCI are presented in **Table 3**.

Conventional and Synaptic Cerebrospinal Fluid Biomarkers

The analysis of conventional AD CSF biomarkers revealed that patients from the sd-aMCI group had higher CSF t-tau (p = 0.009) and p-tau levels (p = 0.031) than patients from the md-aMCI group. Even though the sd-aMCI group exhibited lower CSF Aβ42 levels and included a higher percentage of patients with CSF amyloid positive than those in the md-aMCI group, the difference was not statistically significant in the patient cohort of this study. In contrast, neurogranin levels were significantly increased in the CSF of patients with sd-aMCI compared with those with md-aMCI (p = 0.044) (**Table 4**).

[1]www.R-project.org

TABLE 4 | Conventional and synaptic CSF biomarkers in the whole MCI cohort and sd-aMCI and md-aMCI subgroups.

Variables	Whole cohort (*N* = 82)	sd-aMCI (*n* = 52)	md-aMCI (*n* = 30)	Effect size (η^2)	*p*-value
CSF amyloid-beta 42 (ng/L)	697 (255.6)	673 (249.7)	738 (264.8)	0.015	0.273
CSF amyloid-beta 42, abnormal (% positive)	33%	35%	30%	0.002	0.854
CSF t-tau (ng/L)	397 (212.7)	443 (231.9)	317 (145.9)	0.082	**0.009**
CSF p-tau (ng/L)	66 (25.3)	70 (26.5)	58 (21.4)	0.057	**0.031**
CSF neurogranin (ng/L)	204 (75.1)	217 (80.3)	182 (60.2)	0.050	**0.044**

Data presented as mean and standard deviation except for CSF amyloid-beta 42, abnormal where percentage of a positive biomarker is presented. p-values were obtained using t-tests for all the variables except for CSF amyloid-beta 42, abnormal, where the chi-square test was used. The cutoff value for CSF Aβ42 positivity < 550 ng/L. CSF, cerebrospinal fluid. sd-aMCI, single-domain amnestic MCI; md-aMCI, multidomain amnestic MCI.
Significant p-values are written in bold text.

TABLE 5 | qEEG measures of global field power (GFP) and synchronization (GFS) in four conventional frequency bands in the whole MCI cohort and sd-aMCI and md-aMCI subgroups.

Variables	Whole cohort (*N* = 82)	sd-aMCI (*n* = 52)	md-aMCI (*n* = 30)	Effect size (η^2)	*p*-value
GFP delta	0.102 (0.051)	0.098 (0.048)	0.109 (0.056)	0.010	0.367
GFP theta	0.055 (0.044)	0.054 (0.044)	0.058 (0.046)	0.002	0.717
GFP alpha	0.157 (0.120)	0.164 (0.135)	0.144 (0.090)	0.007	0.468
GFP beta	0.036 (0.029)	0.039 (0.032)	0.030 (0.023)	0.025	0.180
GFS delta	0.550 (0.026)	0.545 (0.022)	0.558 (0.030)	0.059	**0.029**
GFS theta	0.554 (0.026)	0.549 (0.024)	0.563 (0.027)	0.063	**0.023**
GFS alpha	0.576 (0.036)	0.575 (0.032)	0.578 (0.043)	0.002	0.719
GFS beta	0.516 (0.022)	0.516 (0.022)	0.518 (0.022)	0.002	0.720

Data presented as mean and standard deviation. p-values were obtained using t-tests for all the variables.
GFP, global field power; GFS, global field synchronization. sd-aMCI, single-domain amnestic MCI; md-aMCI, multidomain amnestic MCI.
Significant p-values are written in bold text.

Quantitative Electroencephalography Parameters in Single-Domain Amnestic Mild Cognitive Impairment and Multidomain Amnestic Mild Cognitive Impairment

The qEEG analysis showed that the sd-aMCI group had a statistically significant lower GFS delta (p = 0.029) and theta (0.023) compared with that of the md-aMCI group. There were no statistically significant differences in the EEG measure of

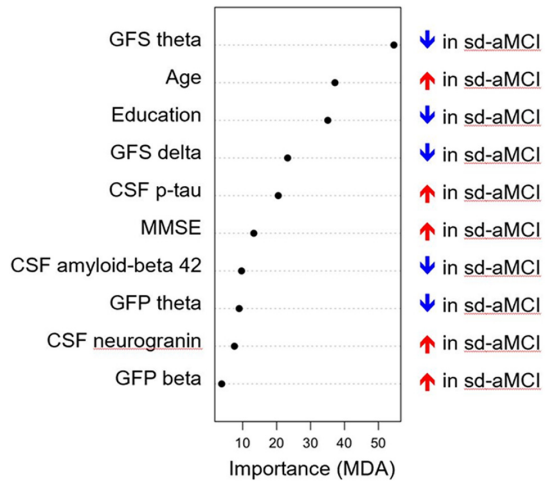

FIGURE 1 | Classification model for differentiating sd-aMCI and md-aMCI. The *x*-axis displays the importance of the variables in the differentiation between sd-aMCI and md-aMCI, with higher values (i.e., dots to the right side) indicating a greater importance. MDA, mean decrease accuracy; GFP, global field power; GFS, global field synchronization; MMSE, Mini-Mental State Examination; MCI, mild cognitive impairment; md-aMCI, multidomain amnestic MCI; sd-aMCI, single domain amnestic MCI.

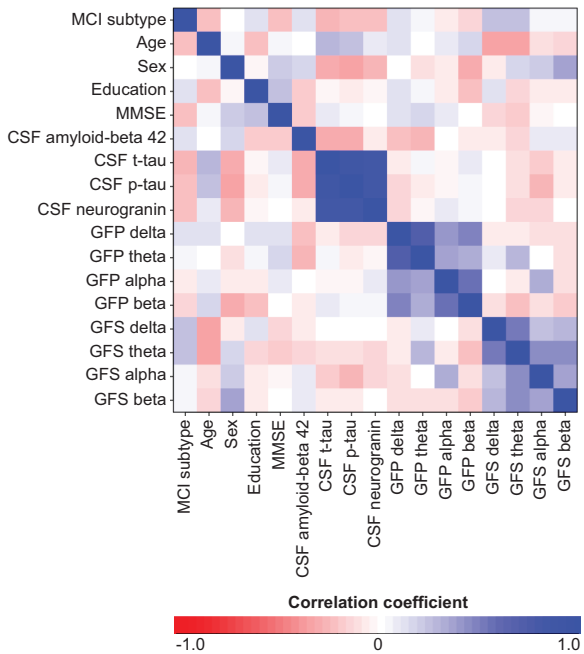

FIGURE 2 | Correlation matrix between all predictors and outcome variable of the random forest model. MCI subtype was coded as sd-aMCI = 0 and md-aMCI = 1. Sex was coded as women = 0 and men = 1. GFP, global field power; GFS, global field synchronization; MMSE, Mini-Mental State Examination; CSF, cerebrospinal fluid.

global power (i.e., GFP) between the two groups, in any of the conventional frequency bands (**Table 5**).

Classification Model for Differentiating Single-Domain Amnestic Mild Cognitive Impairment and Multidomain Amnestic Mild Cognitive Impairment

The multivariate model showed a good performance (out-of-the-bag error = 35.5%). **Figure 1** shows that several EEG measures had an important contribution toward discriminating the sd-aMCI and md-aMCI groups, including GFS theta and delta and GFP theta and beta. This contribution was beyond the differences in age and MMSE between the two MCI groups. Other measures that were important to differentiate sd-aMCI from md-aMCI were age, education, CSF p-tau, MMSE, CSF Aβ42, and neurogranin. Regarding the direction of these measures, lower GFS theta and delta, lower GFP theta, higher GFP beta, lower education, older age, higher MMSE scores, higher CSF p-tau and neurogranin, and lower CSF amyloid-beta 42 were almost always related to sd-aMCI (17.0% of classification error), while the opposite was not always true for md-aMCI (65.5% of classification error). **Figure 2** shows the correlation matrix between all predictors and the outcome variable in our random forest model.

DISCUSSION

This study reports that the qEEG measure of global synchrony (i.e., GFS) in slow frequencies, in particular in the theta band, is the strongest discriminator between the two most common clinical subtypes of aMCI: single-domain (sd-aMCI) and multi-domain amnestic MCI (md-aMCI). The GFS in theta-frequency band was significantly lower in the sd-aMCI group than that of the md-aMCI group, followed by lower GFS in the delta band. These differences and the capacity of qEEG measures to discriminate between MCI groups were above and beyond group differences in MMSE and age. Patients with single-domain aMCI in this study, in accordance with the literature and the common clinical experience, had more pathological changes in CSF biomarkers of amyloid pathology and neurodegeneration (Visser et al., 2009; Damian et al., 2013). Interestingly, a previous study by Koenig et al. (2005) on GFS alterations on the clinical continuum of AD showed that the decrease in the alpha-frequency band was more pronounced than in other frequency bands, with a gradient mode of decrease across the severity of the functional decline. This might not be at odds with our findings in this study since patients with early AD and dementia show a shift of alpha power peak toward lower frequencies in the theta range (Samson-Dollfus et al., 1997; Moretti et al., 2004). It would have been of interest to subdivide alpha frequencies in slow and fast alpha bands since they could have different functional significance as suggested previously (Schomer and Lopes da Silva, 2015).

In the study by Koenig et al. (2005), 2-center large data sets from cognitively healthy subjects and patients ranging from subjective and MCI to the most severe stages of AD dementia were included although not with a balanced number of cases in different diagnostic categories. Thus, there was a noteworthy

heterogeneity of the contrast groups phenotyped only by the clinical assessment and not by additional consideration of disease biomarkers. Furthermore, the inclusion of a considerable number of healthy subjects might have introduced a bias toward alpha frequencies, since the GFS in the alpha band was strongest in the healthy controls thus increasing contrast toward other groups.

Another EEG study that explored changes in global EEG synchronization in AD showed a decrease in GFS in beta-frequency band in patients with AD with more severe disease stages when compared with those in healthy controls (Ma et al., 2014). However, only GFS in the slow delta band correlated significantly with a CDR scale, a measure of clinical disease severity, which was also found in an earlier study by Park et al. (2008). Increased synchronization within and between frontal and parietal areas in the delta band has been further associated with better visual episodic memory performance (Tóth et al., 2012), while the overall increase in the EEG delta activity was observed during the performance of arithmetic tasks (Dimitriadis et al., 2010). Delta synchronization has been additionally related to the object maintenance in short-term memory in experiments involving primates (Siegel et al., 2009). These findings highlight the functional importance of slow-frequency synchronization for maintaining healthy cognitive performance.

Our findings are further supported by a plausible conceptual background. Amnestic syndrome in AD is driven by hippocampal dysfunction (Dubois et al., 2014), and it was shown that the source of theta activity originates in the hippocampus and entorhinal cortex (Schomer and Lopes da Silva, 2015). It is plausible that cortico-cortical disconnection in the limbic system is an early event in the pathophysiology of the amnestic syndrome. Although intraoperative recordings, as well as magnetoencephalography (MEG) studies, have confirmed the existence of hippocampal theta activity in human subjects (de Araújo et al., 2002; Jacobs and Kahana, 2010), it is still speculative to conclude that theta activity in our patient population has an exclusive hippocampal origin without in-parallel application of source imaging. Studies performed in rodents have shown that theta oscillations seem to coordinate the activity of widespread neural networks, such as prefrontal, somatosensory, and entorhinal cortices (Chrobak and Buzsáki, 1998; Siapas et al., 2005; Sirota et al., 2008). Thus, alterations in the scalp-recorded theta activity are possibly a result of a more complex neuronal network dysfunction. Additionally, both theta and delta activities were shown to reflect EEG slowing due to cholinergic deafferentation of the cortex that is a major neurotransmitter failure in AD and occurs already at the MCI stage of the disease (Spehlmann and Norcross, 1982; Whitehouse et al., 1982; Riekkinen et al., 1990; Lee et al., 1994; Haense et al., 2012).

Interestingly, some neuropsychiatric diseases that could also cause memory impairment in a cluster of other clinical features have shown similar alteration in the GFS. For example, in obsessive-compulsive disorder, a decreased GFS in delta, theta, and the slow alpha band was reported (Özçoban et al., 2018). Decreased GFS in theta-frequency band was also reported in first-episode, neuroleptic-naïve patients with schizophrenia (Koenig et al., 2001). In healthy subjects, a simple working memory activation paradigm increases the activity in the theta band (Gevins et al., 1997). Decreased functional synchrony in the theta band in resting-state EEG of cognitively impaired subjects might therefore reflect disease-induced desynchronization of neuronal networks that are necessary for successful performance of the working memory task. In addition, a number of other studies showed that scalp-recorded theta power and synchronization in humans correlated with cognitive processing involved in encoding and retrieving verbal stimuli (Kahana, 2006).

In contrast, neither of the spectral power-related EEG measures played any significant role in discriminating the two amnestic subtypes of MCI. In previous publications, a temporal pattern of changes in EEG power spectra has been repeatedly confirmed on a continuum of AD, including MCI. The temporal dynamics of EEG power alterations during the course of the disease include an early increase in theta and decrease in beta power, followed by a decrease in alpha and an increase in delta power (Coben et al., 1985; Dierks et al., 1991; Prichep et al., 1994). Interestingly, the recent MEG study by López et al. (2014) showed an increase in delta and theta and a decrease in alpha and beta power in patients with md-aMCI compared with those with sd-aMCI; however, it involved relative power measures on topographical clusters of sensors, thus presenting with some key methodological differences. In addition, Moretti et al. (2009) showed a correlation between the increase of the relative theta/gamma power ratio and performance on memory tests in subjects with MCI. Another study that assessed changes in topographical resting-state EEG sources between different MCI subtypes showed increased occipital theta and decreased centro-parieto-occipital alpha activity in amnestic compared with non-amnestic MCI. The same study observed a positive correlation between central-parietal alpha and a negative correlation between frontal delta sources and scores on cognitive tests assessing attention, episodic memory, and executive functions (Babiloni et al., 2010).

However, it may not be surprising that global spectral power parameters do not play a role in discriminating the two clinical entities with amnestic profiles and similar low grades of functional impairment since our study did not include cognitively healthy individuals or patients with more severe stages of AD as contrast groups. Rather, our study included patients with MCI at an intermediate cognitive level of impairment, with minimal differences in global cognition (MMSE) between MCI groups, despite showing different cognitive profiles (i.e., single- vs. multiple-domain impairments). This is supported by the low importance of MMSE to discriminate the two MCI groups in our multivariate analysis. In addition, inclusion of the local relative EEG power measures instead of the global parameters that summarize the amplitude/power across all EEG channels may be more sensitive to the fine EEG power changes between MCI subtypes as indicated by some of the previous studies (Moretti et al., 2009; López et al., 2014). Thus, in contrast to GFS that seems to be a trait marker of AD-related early functional disconnection of neuronal networks, differential alterations in global EEG power frequency spectra seem to be a state marker of disease progression.

It is interesting that a novel CSF molecular marker of synaptic pathology, i.e., neurogranin, did not considerately contribute to discriminating the two MCI groups in our multivariate model. This implies that changes in neurophysiological

markers of synaptic dysfunction in sd-aMCI, a group that represents prodromal AD, may precede changes in markers of molecular synaptic pathology. Another explanation could be that neurogranin is associated with conditions with memory-related deficits irrespective of AD pathology as was suggested in a study that found that this synaptic marker is also sensitive to age-related cognitive performance on memory tests in neurologically healthy older adults (Casaletto et al., 2017). However, this was contradicted by studies suggesting that the CSF neurogranin is specific to AD-type synaptic dysfunction (Wellington et al., 2016; Portelius et al., 2018).

It is interesting that the biological profile of clinically defined sd-aMCI in this study is closer to the biological profile of AD in contrast to the empirically data-driven classification of sd-aMCI recently published by Edmonds et al. (2021). This discrepancy emphasizes a need for validation of different diagnostic criteria in diverse clinical populations. It is of utmost importance to characterize this prodromal AD stage as early and as accurately as possible to convey the risk and likelihood of developing AD dementia to patients (Frederiksen et al., 2021).

A limitation of our multivariate model is the small groups size, especially for the patients with md-aMCI (n = 30) when the cohort is split in 70% for training and 30% for testing of model performance. However, the multivariate model in this study was designed as an extension of the univariate tests for group differences, to investigate EEG measures and CSF biomarkers in the context of age, sex, education, and MMSE measures. Both set of analyses converged in the findings, validating the results from the multivariate model despite the small group size for the test set. Another limitation is that the non-memory cognitive domains affected in the md-aMCI group may vary from patient to patient. Hence, our current results could be expanded in future studies with a larger md-aMCI group, by analyzing associations of different non-memory cognitive domains with qEEG and CSF biomarkers. Importantly, the inclusion of the control group in such comparisons may extend the panel of relevant qEEG and CSF biomarkers for contrasting different cognitive subtypes and considerably add to the interpretation of the results when it comes to the expected direction of change from the cognitively healthy state. Furthermore, the analysis of GFS measure over full EEG frequency spectra instead of averaging across standard frequency bands, or a local topographical parcellation of synchronization patterns, may provide more detailed and physiologically meaningful results in this patient group. Addition of the analysis in the gamma-frequency range while addressing high-frequency artifact contamination would be of further interest since gamma oscillations have been associated with different cognitive processes and were shown to be impaired in AD (Herrmann and Demiralp, 2005; van Deursen et al., 2008; Zheng et al., 2016; Etter et al., 2019).

In conclusion, our study suggests that measures of global EEG synchronization could contribute to the characterization of synaptic dysfunction in different MCI cognitive subtypes. Future studies are required to address and further explore some of the limitations of this study by including other clinical and etiological subtypes of MCI as well as cognitively healthy subjects.

DATA AVAILABILITY STATEMENT

The original contributions presented in the study are included in the article, further inquiries can be directed to the corresponding author.

ETHICS STATEMENT

This study was approved by the Local Ethical Committee of the Karolinska Hospital and Regional Ethical Review Board in Stockholm (Dnr: 2020-00678, 2011/1978-31/4). Written informed consent for participation was not required for this study in accordance with the national legislation and the institutional requirements.

AUTHOR CONTRIBUTIONS

US, DF, and VJ: conceptualization. US, DF, BA, TK, NA, HZ, KB, and VJ: methodology. US, DF, and BA: formal analysis. US, BA, and VJ: investigation. VJ and US: resources, writing—original draft preparation, and funding acquisition. US, DF, BA, NA, HZ, and VJ: writing—review and editing. US and DF: visualization. VJ: supervision. All authors have read and agreed to the published version of the manuscript.

FUNDING

This work was supported by the European Union's Horizon 2020 Research and Innovation Program under the Marie Skłodowska-Curie grant agreement number 676144 (Synaptic Dysfunction in Alzheimer's Disease, SyDAD) (US and VJ), Gun and Bertil Stohne's Research Scholarship (US), Gamla Tjänarinnor grant (US and VJ), and Swedish State Support for Clinical Research (#ALF–591660) (VJ). DF was supported by the Center for Innovative Medicine (CIMED), the ALF–agreement (#FoUI–962240), Hjärnfonden, Alzheimerfonden, Neurofonden, and Gamla Tjänarinnor grant. HZ is a Wallenberg Scholar supported by grants from the Swedish Research Council (#2018–02532), the European Research Council (#681712), Swedish State Support for Clinical Research (#ALFGBG–720931), the Alzheimer Drug Discovery Foundation (ADDF), United States (#201809-2016862), and the UK Dementia Research Institute at UCL. KB was supported by the Swedish Research Council (#2017-00915), the Alzheimer Drug Discovery Foundation (ADDF), United States (#RDAPB-201809-2016615), the Swedish Alzheimer Foundation (#AF-742881), Hjärnfonden, Sweden (#FO2017-0243), the Swedish state under the agreement between the Swedish Government and the County Councils, the ALF-agreement (#ALFGBG-715986), and European Union Joint Program for Neurodegenerative Disorders (JPND2019-466-236).

REFERENCES

Albert, M. S., DeKosky, S. T., Dickson, D., Dubois, B., Feldman, H. H., and Fox, N. C. (2011). The diagnosis of mild cognitive impairment due to Alzheimer's disease: recommendations from the National Institute on Aging-Alzheimer's Association workgroups on diagnostic guidelines for Alzheimer's disease. *Alzheimers Dement.* 7, 270–279. doi: 10.1016/j.jalz.2011.03.008

Amit, Y., and Geman, D. (1997). Shape quantization and recognition with randomized trees. *Neural Comput.* 9, 1545–1588. doi: 10.1162/neco.1997.9.7.1545

Arnáiz, E., and Almkvist, O. (2003). Neuropsychological features of mild cognitive impairment and preclinical Alzheimer's disease. *Acta Neurol. Scand. Suppl.* 179, 34–41. doi: 10.1034/j.1600-0404.107.s179.7.x

Babiloni, C., Visser, P. J., Frisoni, G., De Deyn, P. P., Bresciani, L., Jelic, V., et al. (2010). Cortical sources of resting EEG rhythms in mild cognitive impairment and subjective memory complaint. *Neurobiol. Aging.* 31, 1787–1798. doi: 10.1016/j.neurobiolaging.2008.09.020

Bogdanovic, N. D., Gottfries, J., Volkman, I., Winblad, B., and Blennow, K. (2002). Regional and Cellular Distribution of Synaptic Proteins in the Normal Human Brain. *Brain Aging* 2, 18–30.

Breiman, L. (1996). Bagging predictors. *Machine Learn.* 24, 123–140. doi: 10.1007/bf00058655

Breiman, L. (2001). Random Forests. *Machine Learn.* 45, 5–32.

Bruscoli, M., and Lovestone, S. (2004). Is MCI really just early dementia? A systematic review of conversion studies. *Int. Psychogeriatr.* 16, 129–140. doi: 10.1017/s1041610204000092

Casaletto, K. B., Elahi, F. M., Bettcher, B. M., Neuhaus, J., Bendlin, B. B., Asthana, S., et al. (2017). Neurogranin, a synaptic protein, is associated with memory independent of Alzheimer biomarkers. *Neurology* 89, 1782–1788. doi: 10.1212/WNL.0000000000004569

Chrobak, J. J., and Buzsáki, G. (1998). Gamma Oscillations in the Entorhinal Cortex of the Freely Behaving Rat. *J. Neurosci.* 18, 388–398. doi: 10.1523/JNEUROSCI.18-01-00388.1998

Coben, L. A., Danziger, W., and Storandt, M. A. (1985). longitudinal EEG study of mild senile dementia of Alzheimer type: changes at 1 year and at 2.5 years. *Electroencephalogr. Clin. Neurophysiol.* 61, 101–112. doi: 10.1016/0013-4694(85)91048-x

Damian, M., Hausner, L., Jekel, K., Richter, M., Froelich, L., Almkvist, O., et al. (2013). Single-domain amnestic mild cognitive impairment identified by cluster analysis predicts Alzheimer's disease in the european prospective DESCRIPA study. *Dement. Geriatr. Cogn. Disord.* 36, 1–19. doi: 10.1159/000348354

de Araújo, D. B., Baffa, O., and Wakai, R. T. (2002). Theta oscillations and human navigation: a magnetoencephalography study. *J. Cognit. Neurosci.* 14, 70–78. doi: 10.1162/089892902317205339

Dierks, T., Perisic, I., Frolich, L., Ihl, R., and Maurer, K. (1991). Topography of the quantitative electroencephalogram in dementia of the Alzheimer type: relation to severity of dementia. *Psychiatry Res.* 40, 181–194. doi: 10.1016/0925-4927(91)90009-f

Dimitriadis, S. I., Laskaris, N. A., Tsirka, V., Vourkas, M., and Micheloyannis, S. (2010). What does delta band tell us about cognitive processes: A mental calculation study. *Neurosci. Lett.* 483, 11–15. doi: 10.1016/j.neulet.2010.07.034

Dubois, B., Feldman, H. H., Jacova, C., Hampel, H., Molinuevo, J. L., and Blennow, K. (2014). Position Paper Advancing research diagnostic criteria for Alzheimer's disease: the IWG-2 criteria. *Lancet Neurol.* 13, 614–629. doi: 10.1016/S1474-4422(14)70090-0

Edmonds, E. C., Smirnov, D. S., Thomas, K. R., Graves, L. V., Bangen, K. J., Delano-Wood, L., et al. (2021). Data-Driven vs Consensus Diagnosis of MCI. *Enhanced Sensitiv. Detect. Clin. Biomark. Neuropathol. Outcomes* 97, e1288–e1299. doi: 10.1212/WNL.0000000000012600

Ekman, U., Ferreira, D., Muehlboeck, J. S., Wallert, J., Rennie, A., Eriksdotter, M., et al. (2020). The MemClin project: a prospective multi memory clinics study targeting early stages of cognitive impairment. *BMC Geriatrics* 20:93. doi: 10.1186/s12877-020-1478-3

Engelborghs, S., Niemantsverdriet, E., Struyfs, H., Blennow, K., Brouns, R., Comabella, M., et al. (2017). Consensus guidelines for lumbar puncture in patients with neurological diseases. *Alzheimer's Dement.* 8, 111–126. doi: 10.1016/j.dadm.2017.04.007

Etter, G., van der Veldt, S., Manseau, F., Zarrinkoub, I., Trillaud-Doppia, E., and Williams, S. (2019). Optogenetic gamma stimulation rescues memory impairments in an Alzheimer's disease mouse model. *Nat. Commun.* 10:5322. doi: 10.1038/s41467-019-13260-9

Farias, S. T., Mungas, D., Reed, B. R., Harvey, D., and DeCarli, C. (2009). Progression of mild cognitive impairment to dementia in clinic- vs community-based cohorts. *Arch. Neurol.* 66, 1151–1157. doi: 10.1001/archneurol.2009.106

Folstein, M. F., Folstein, S. E., and McHugh, P. R. (1975). "Mini-mental state". A practical method for grading the cognitive state of patients for the clinician. *J. Psychiatr. Res.* 12, 189–198.

Frederiksen, K. S., Nielsen, T. R., Winblad, B., Schmidt, R., Kramberger, M. G., Jones, R. W., et al. (2021). European Academy of Neurology/European Alzheimer's Disease Consortium position statement on diagnostic disclosure, biomarker counseling, and management of patients with mild cognitive impairment. *Eur. J. Neurol.* 28, 2147–2155. doi: 10.1111/ene.14668

Gevins, A., Smith, M. E., McEvoy, L., and Yu, D. (1997). High-resolution EEG mapping of cortical activation related to working memory: effects of task difficulty, type of processing, and practice. *Cereb. Cortex* 7, 374–385. doi: 10.1093/cercor/7.4.374

Goncharova, I. I., McFarland, D. J., Vaughan, T. M., and Wolpaw, J. R. (2003). EMG contamination of EEG: spectral and topographical characteristics. *Clin. Neurophysiol.* 114, 1580–1593. doi: 10.1016/s1388-2457(03)00093-2

Haense, C., Kalbe, E., Herholz, K., Hohmann, C., Neumaier, B., Krais, R., et al. (2012). Cholinergic system function and cognition in mild cognitive impairment. *Neurobiol. Aging* 33, 867–877. doi: 10.1016/j.neurobiolaging.2010.08.015

Headley, A., De Leon-Benedetti, A., Dong, C., Levin, B., Loewenstein, D., Camargo, C., et al. (2018). Neurogranin as a predictor of memory and executive function decline in MCI patients. *Neurology* 90, e887–e895. doi: 10.1212/WNL.0000000000005057

Herrmann, C. S., and Demiralp, T. (2005). Human EEG gamma oscillations in neuropsychiatric disorders. *Clin. Neurophysiol.* 116, 2719–2733. doi: 10.1016/j.clinph.2005.07.007

Huang, C., Wahlund, L., Dierks, T., Julin, P., Winblad, B., and Jelic, V. (2000). Discrimination of Alzheimer's disease and mild cognitive impairment by equivalent EEG sources: a cross-sectional and longitudinal study. *Clin. Neurophysiol.* 111, 1961–1967. doi: 10.1016/s1388-2457(00)00454-5

Hughes, T. F., Snitz, B. E., and Ganguli, M. (2011). Should mild cognitive impairment be subtyped? *Curr. Opin. Psychiatry* 24, 237–242. doi: 10.1097/YCO.0b013e328344696b

Jacobs, J., and Kahana, M. J. (2010). Direct brain recordings fuel advances in cognitive electrophysiology. *Trends Cognit. Sci.* 14, 162–171. doi: 10.1016/j.tics.2010.01.005

Kahana, M. J. (2006). The Cognitive Correlates of Human Brain Oscillations. *J. Neurosci.* 26, 1669–1672. doi: 10.1523/JNEUROSCI.3737-05c.2006

Koenig, T., Lehmann, D., Saito, N., Kuginuki, T., Kinoshita, T., and Koukkou, M. (2001). Decreased functional connectivity of EEG theta-frequency activity in first-episode, neuroleptic-naive patients with schizophrenia: preliminary results. *Schizophr. Res.* 50, 55–60. doi: 10.1016/s0920-9964(00)00154-7

Koenig, T., Prichep, L., Dierks, T., Hubl, D., Wahlund, L. O., John, E. R., et al. (2005). Decreased EEG synchronization in Alzheimer's disease and mild cognitive impairment. *Neurobiol. Aging* 26, 165–171. doi: 10.1016/j.neurobiolaging.2004.03.008

Kvartsberg, H., Duits, F. H., Ingelsson, M., Andreasen, N., Ohrfelt, A., Andersson, K., et al. (2015a). Cerebrospinal fluid levels of the synaptic protein neurogranin correlates with cognitive decline in prodromal Alzheimer's disease. *Alzheimers Dement.* 11, 1180–1190. doi: 10.1016/j.jalz.2014.10.009

Kvartsberg, H., Lashley, T., Murray, C. E., Brinkmalm, G., Cullen, N. C., Hoglund, K., et al. (2019). The intact postsynaptic protein neurogranin is reduced in brain tissue from patients with familial and sporadic Alzheimer's disease. *Acta Neuropathol.* 137, 89–102. doi: 10.1007/s00401-018-1910-3

Kvartsberg, H., Portelius, E., Andreasson, U., Brinkmalm, G., Hellwig, K., Lelental, N., et al. (2015b). Characterization of the postsynaptic protein neurogranin in paired cerebrospinal fluid and plasma samples from Alzheimer's disease patients and healthy controls. *Alzheimers Res. Ther.* 7:40. doi: 10.1186/s13195-015-0124-3

Lee, M. G., Chrobak, J. J., Sik, A., Wiley, R. G., and Buzsáki, G. (1994). Hippocampal theta activity following selective lesion of the septal cholinergic system. *Neuroscience* 62, 1033–1047. doi: 10.1016/0306-4522(94)90341-7

Liaw, A., and Wiener, M. (2002). Classification and regression by random forest. *R News* 2, 18–22.

Lista, S., Toschi, N., Garaci, F., Blennow, K., Zetterberg, H., Teipel, S., et al. (2016). ADDED DIAGNOSTIC VALUE OF CEREBROSPINAL FLUID NEUROGRANIN IN THE CLASSIFICATION OF PRODROMAL AND ALZHEIMER'S DISEASE DEMENTIA. *Alzheimer's Dement.* 12:468.

López, M. E., Cuesta, P., Garcés, P., Castellanos, P. N., Aurtenetxe, S., Bajo, R., et al. (2014). MEG spectral analysis in subtypes of mild cognitive impairment. *Age* 36:9624. doi: 10.1007/s11357-014-9624-5

Ma, C. C., Liu, A. J., Liu, A. H., Zhou, X. Y., and Zhou, S. N. (2014). Electroencephalogram global field synchronization analysis: a new method for assessing the progress of cognitive decline in Alzheimer's disease. *Clin. EEG Neurosci.* 45, 98–103. doi: 10.1177/1550059413489669

Machado, A., Barroso, J., Molina, Y., Nieto, A., Díaz-Flores, L., Westman, E., et al. (2018). Proposal for a hierarchical, multidimensional, and multivariate approach to investigate cognitive aging. *Neurobiol. Aging* 71, 179–188. doi: 10.1016/j.neurobiolaging.2018.07.017

Michel, C. M. (2009). *Electrical neuroimaging*. Cambridge: Cambridge University Press, 238.

Mitchell, A. J., and Shiri-Feshki, M. (2009). Rate of progression of mild cognitive impairment to dementia–meta-analysis of 41 robust inception cohort studies. *Acta Psychiatr. Scand.* 119, 252–265. doi: 10.1111/j.1600-0447.2008.01326.x

Moretti, D. V., Babiloni, C., Binetti, G., Cassetta, E., Dal Forno, G., Ferreric, F., et al. (2004). Individual analysis of EEG frequency and band power in mild Alzheimer's disease. *Clin. Neurophysiol.* 115, 299–308. doi: 10.1016/s1388-2457(03)00345-6

Moretti, D. V., Fracassi, C., Pievani, M., Geroldi, C., Binetti, G., Zanetti, O., et al. (2009). Increase of theta/gamma ratio is associated with memory impairment. *Clin. Neurophysiol.* 120, 295–303. doi: 10.1016/j.clinph.2008.11.012

Moretti, D. V., Pievani, M., Geroldi, C., Binetti, G., Zanetti, O., Rossini, P. M., et al. (2010). EEG markers discriminate among different subgroup of patients with mild cognitive impairment. *Am. J. Alzheimer's Dis. Dement.* 25, 58–73. doi: 10.1177/1533317508329814

Moretti, D. V., Zanetti, O., Binetti, G., and Frisoni, G. B. (2012). Quantitative EEG Markers in Mild Cognitive Impairment: Degenerative versus Vascular Brain Impairment. *Int. J. Alzheimer's Dis.* 2012:917537. doi: 10.1155/2012/917537

Olsson, A., Vanderstichele, H., Andreasen, N., De Meyer, G., Wallin, A., Holmberg, B., et al. (2005). Simultaneous measurement of beta-amyloid(1-42), total tau, and phosphorylated tau (Thr181) in cerebrospinal fluid by the xMAP technology. *Clin. Chem.* 51, 336–345. doi: 10.1373/clinchem.2004.039347

Özçoban, M. A., Tan, O., Aydin, S., and Akan, A. (2018). Decreased global field synchronization of multichannel frontal EEG measurements in obsessive-compulsive disorders. *Med. Biol. Enginee. Comput.* 56, 331–338. doi: 10.1007/s11517-017-1689-8

Park, Y.-M., Che, H.-J., Im, C.-H., Jung, H.-T., Bae, S.-M., and Lee, S.-H. (2008). Decreased EEG synchronization and its correlation with symptom severity in Alzheimer's disease. *Neurosci. Res.* 62, 112–117. doi: 10.1016/j.neures.2008.06.009

Petersen, R. C. (2004). Mild cognitive impairment as a diagnostic entity. *J. Intern. Med.* 256, 183–194. doi: 10.1111/j.1365-2796.2004.01388.x

Petersen, R. C. (2016). Mild Cognitive Impairment. *Continuum* 22, 404–418.

Poil, S. S., de Haan, W., van der Flier, W. M., Mansvelder, H. D., Scheltens, P., and Linkenkaer-Hansen, K. (2013). Integrative EEG biomarkers predict progression to Alzheimer's disease at the MCI stage. *Front. Aging Neurosci.* 5:58. doi: 10.3389/fnagi.2013.00058

Portelius, E., Olsson, B., Hoglund, K., Cullen, N. C., Kvartsberg, H., Andreasson, U., et al. (2018). Cerebrospinal fluid neurogranin concentration in neurodegeneration: relation to clinical phenotypes and neuropathology. *Acta Neuropathol.* 136, 363–376. doi: 10.1007/s00401-018-1851-x

Prichep, L. S., John, E. R., Ferris, S. H., Reisberg, B., Almas, M., Alper, K., et al. (1994). Quantitative EEG correlates of cognitive deterioration in the elderly. *Neurobiol. Aging* 15, 85–90. doi: 10.1016/0197-4580(94)90147-3

Riekkinen, P. Jr., Sirvio, J., and Riekkinen, P. (1990). Relationship between the cortical choline acetyltransferase content and EEG delta-power. *Neurosci. Res.* 8, 12–20. doi: 10.1016/0168-0102(90)90052-g

Samson-Dollfus, D., Delapierre, G., Do Marcolino, C., and Blondeau, C. (1997). Normal and pathological changes in alpha rhythms. *Int. J. Psychophysiol.* 26, 395–409. doi: 10.1016/s0167-8760(97)00778-2

Scheff, S. W., Price, D. A., Schmitt, F. A., and Mufson, E. J. (2006). Hippocampal synaptic loss in early Alzheimer's disease and mild cognitive impairment. *Neurobiol. Aging* 27, 1372–1384. doi: 10.1016/j.neurobiolaging.2005.09.012

Scheff, S. W., Price, D. A., Schmitt, F. A., DeKosky, S. T., and Mufson, E. J. (2007). Synaptic alterations in CA1 in mild Alzheimer disease and mild cognitive impairment. *Neurology* 68, 1501–1508. doi: 10.1212/01.wnl.0000260698.46517.8f

Schomer, D. L., and Lopes da Silva, F. (2015). *Niedermeyer's Electroencephalography: Basic Principles, Clinical Applications, and Related Fields*. Philadelphia: LWW.

Schumacher, J., Taylor, J.-P., Hamilton, C. A., Firbank, M., Cromarty, R. A., Donaghy, P. C., et al. (2020). Quantitative EEG as a biomarker in mild cognitive impairment with Lewy bodies. *Alzheimer's Res. Therapy* 12:82. doi: 10.1186/s13195-020-00650-1

Siapas, A. G., Lubenov, E. V., and Wilson, M. A. (2005). Prefrontal Phase Locking to Hippocampal Theta Oscillations. *Neuron* 46, 141–151. doi: 10.1016/j.neuron.2005.02.028

Siegel, M., Warden, M. R., and Miller, E. K. (2009). Phase-dependent neuronal coding of objects in short-term memory. *Proc. Natl. Acad. Sci. U S A.* 106, 21341–21346. doi: 10.1073/pnas.0908193106

Sirota, A., Montgomery, S., Fujisawa, S., Isomura, Y., Zugaro, M., and Buzsáki, G. (2008). Entrainment of neocortical neurons and gamma oscillations by the hippocampal theta rhythm. *Neuron* 60, 683–697. doi: 10.1016/j.neuron.2008.09.014

Smailovic, U., and Jelic, V. (2019). Neurophysiological Markers of Alzheimer's Disease: Quantitative EEG Approach. *Neurol. Ther.* 8(Suppl. 2), 37–55. doi: 10.1007/s40120-019-00169-0

Smailovic, U., Koenig, T., Kåreholt, I., Andersson, T., Kramberger, M. G., Winblad, B., et al. (2018). Quantitative EEG power and synchronization correlate with Alzheimer's disease CSF biomarkers. *Neurobiol. Aging* 63, 88–95.

Spehlmann, R., and Norcross, K. (1982). Cholinergic mechanisms in the production of focal cortical slow waves. *Experientia* 38, 109–111. doi: 10.1007/BF01944557

Tóth, B., Boha, R., Pósfai, M., Gaál, Z. A., Kónya, A., Stam, C. J., et al. (2012). EEG synchronization characteristics of functional connectivity and complex network properties of memory maintenance in the delta and theta frequency bands. *Int. J. Psychophysiol.* 83, 399–402. doi: 10.1016/j.ijpsycho.2011.11.017

van Deursen, J. A., Vuurman, E. F. P. M., Verhey, F. R. J., van Kranen-Mastenbroek, V. H. J. M., and Riedel, W. J. (2008). Increased EEG gamma band activity in Alzheimer's disease and mild cognitive impairment. *J. Neural Transmiss.* 115, 1301–1311. doi: 10.1007/s00702-008-0083-y

Visser, P. J., Verhey, F., Knol, D. L., Scheltens, P., Wahlund, L.-O., Freund-Levi, Y., et al. (2009). Prevalence and prognostic value of CSF markers of Alzheimer's disease pathology in patients with subjective cognitive impairment or mild cognitive impairment in the DESCRIPA study: a prospective cohort study. *Lancet Neurol.* 8, 619–627. doi: 10.1016/S1474-4422(09)70139-5

Wahlund, L. O., Pihlstrand, E., and Jönhagen, M. E. (2003). Mild cognitive impairment: experience from a memory clinic. *Acta Neurol. Scand. Suppl.* 179, 21–24. doi: 10.1034/j.1600-0404.107.s179.3.x

Wechsler, D. (2003). *WAIS III: Wechsler Adult Intelligence Scale – Third Edition. Svensk version*. Bloomington, MN: NCS Pearson Inc.

Wechsler, D. (2010). *WAIS IV: Wechsler Adult Intelligence Scale - Fourth Edition. Swedish version*. Bloomington, MN: NCS Pearson Inc.

Wellington, H., Paterson, R. W., Portelius, E., Tornqvist, U., Magdalinou, N., Fox, N. C., et al. (2016). Increased CSF neurogranin concentration is specific to Alzheimer disease. *Neurology* 86, 829–835. doi: 10.1212/WNL.0000000000002423

Whitehouse, P. J., Price, D. L., Struble, R. G., Clark, A. W., Coyle, J. T., and Delon, M. R. (1982). Alzheimer's disease and senile dementia: loss of neurons in the basal forebrain. *Science* 215, 1237–1239. doi: 10.1126/science.7058341

Whitham, E. M., Pope, K. J., Fitzgibbon, S. P., Lewis, T., Clark, C. R., Loveless, S., et al. (2007). Scalp electrical recording during paralysis: quantitative evidence that EEG frequencies above 20 Hz are contaminated by EMG. *Clin. Neurophysiol.* 118, 1877–1888. doi: 10.1016/j.clinph.2007.04.027

Winblad, B., Palmer, K., Kivipelto, M., Jelic, V., Fratiglioni, L., Wahlund, L. O., et al. (2004). Mild cognitive impairment–beyond controversies, towards a consensus: report of the International Working Group on Mild Cognitive Impairment. *J. Internal Med.* 256, 240–246. doi: 10.1111/j.1365-2796.2004.01380.x

Wolk, D. A., Price, J. C., Saxton, J. A., Snitz, B. E., James, J. A., Lopez, O. L., et al. (2009). Amyloid imaging in mild cognitive impairment subtypes. *Ann. Neurol.* 65, 557–568. doi: 10.1002/ana.21598

Zheng, C., Bieri, K. W., Hsiao, Y. T., and Colgin, L. L. (2016). Spatial Sequence Coding Differs during Slow and Fast Gamma Rhythms in the Hippocampus. *Neuron* 89, 398–408. doi: 10.1016/j.neuron.2015.12.005

Zhong, L., and Gerges, N. Z. (2012). Neurogranin targets calmodulin and lowers the threshold for the induction of long-term potentiation. *PLoS One* 7:e41275. doi: 10.1371/journal.pone.0041275

Zhong, L., Cherry, T., Bies, C. E., Florence, M. A., and Gerges, N. Z. (2009). Neurogranin enhances synaptic strength through its interaction with calmodulin. *EMBO J.* 28, 3027–3039. doi: 10.1038/emboj.2009.236

Conflict of Interest: The authors declare that the research was conducted in the absence of any commercial or financial relationships that could be construed as a potential conflict of interest.

frontiers | Frontiers in Aging Neuroscience

ORIGINAL RESEARCH
published: 25 April 2022
doi: 10.3389/fnagi.2022.756687

Fast Alpha Activity in EEG of Patients With Alzheimer's Disease Is Paralleled by Changes in Cognition and Cholinergic Markers During Encapsulated Cell Biodelivery of Nerve Growth Factor

*Helga Eyjolfsdottir[1,2], Thomas Koenig[3], Azadeh Karami[1], Per Almqvist[4,5], Göran Lind[4,5], Bengt Linderoth[4,5], Lars Wahlberg[6], Åke Seiger[7], Taher Darreh-Shori[1], Maria Eriksdotter[1,2] and Vesna Jelic[1,2]**

[1] Department of Neurobiology, Care Science and Society, Karolinska Institutet, Solna, Sweden, [2] Theme Inflammation and Aging, Karolinska University, Stockholm, Sweden, [3] Translational Research Center, University Hospital of Psychiatry, University of Bern, Bern, Switzerland, [4] Department of Clinical Neuroscience, Stockholm, Sweden, [5] Department of Neurosurgery, Theme Neuro, Karolinska University, Stockholm, Sweden, [6] NsGene Inc., Providence, RI, United States, [7] Stiftelsen Stockholms Sjukhem, Stockholm, Sweden

OPEN ACCESS

Edited by:
Takako Fujioka,
Stanford University, United States

Reviewed by:
Grace M. Clements,
University of Illinois at Urbana-Champaign, United States
Daniel Dautan,
Italian Institute of Technology (IIT), Italy
Vinay V. Parikh,
Temple University, United States

***Correspondence:**
Vesna Jelic
vesna.jelic@ki.se

Specialty section:
This article was submitted to Alzheimer's Disease and Related Dementias, a section of the journal Frontiers in Aging Neuroscience

Received: 10 August 2021
Accepted: 10 March 2022
Published: 25 April 2022

Citation:
Eyjolfsdottir H, Koenig T, Karami A, Almqvist P, Lind G, Linderoth B, Wahlberg L, Seiger Å, Darreh-Shori T, Eriksdotter M and Jelic V (2022) Fast Alpha Activity in EEG of Patients With Alzheimer's Disease Is Paralleled by Changes in Cognition and Cholinergic Markers During Encapsulated Cell Biodelivery of Nerve Growth Factor. Front. Aging Neurosci. 14:756687. doi: 10.3389/fnagi.2022.756687

Background: Basal forebrain cholinergic neurons are dependent on nerve growth factor (NGF) for growth and survival and these cells are among the first to degenerate in Alzheimer's disease (AD). Targeted delivery of NGF has been suggested as a potential therapy for AD. This hypothesis was tested in a clinical trial with encapsulated cell biodelivery of NGF (NGF-ECB) in AD patients. Three of six patients showed improved biomarkers for cognition by the end of the study. Here, we report on the effects of targeted delivery of NGF on human resting EEG.

Materials and methods: NGF-ECB implants were implanted bilaterally in the basal forebrain of six AD patients for 12 months. EEG recordings and quantitative analysis were performed at baseline, 3 and 12 months of NGF delivery, and analyzed for correlation with changes in Mini-mental state examination (MMSE) and levels of the cholinergic marker choline acetyltransferase (ChAT) in cerebrospinal fluid (CSF).

Results: We found significant correlations between the topographic variance of EEG spectral power at the three study points (baseline, 3 and 12 months) and changes in MMSE and CSF ChAT. This possible effect of NGF was identified in a narrow window of alpha frequency 10–11.5 Hz, where a stabilization in MMSE score during treatment was related to an increase in EEG alpha power. A similar relation was observed between the alpha power and ChAT. More theta power at 6.5 Hz was on the contrary associated with a decrease in CSF ChAT during the trial period.

Conclusion: In this exploratory study, there was a positive correlative pattern between physiological high-frequency alpha activity and stabilization in MMSE and increase in CSF ChAT in AD patients receiving targeted delivery of NGF to the cholinergic basal forebrain.

Keywords: EEG, EEG alpha activity, Alzheimer's disease, nerve growth factor, encapsulated cell biodelivery, choline acetyltransferase

INTRODUCTION

Resting-state quantitative EEG (qEEG) is a good candidate marker for intervention clinical trials in Alzheimer's disease (AD) since it has shown good discriminatory power between AD patients and healthy aging in several studies (Brenner et al., 1988; Lehmann et al., 2007; Jelic and Kowalski, 2009; Babiloni et al., 2021). These studies report on an increase in the slow frequency activities including early changes in theta range and the later stage of the disease alterations in the delta range, in parallel with a decrease in the faster alpha and beta frequencies.

Already at the very beginning of acetylcholine esterase inhibitor (ChEI) treatment for AD, it was reported that chronic treatment with cholinergic drugs induces a specific pattern of electrical brain activity corresponding to both the treatment response and early decline in treatment efficacy (Jelic et al., 1998).

It has been shown repeatedly that the ChEI treatment increases the physiological alpha rhythm oscillations in EEG, particularly in the posterior regions (Jelic et al., 1998; Moretti, 2014). Furthermore, these positive effects on the resting EEG spectral alpha power induced by ChEIs, correlated well with improved cognitive function as measured by significant changes in Mini-mental state examination (MMSE) scores (Moretti, 2014). Recently an EEG-based acetylcholine (ACh) index has been developed using data from a scopolamine challenge study showing a reduced ACh index even in prodromal AD (Johannsson et al., 2015). Interestingly, even cholinergic stimulation of healthy subjects with the ChEI galantamine showed an effect on the alpha power and working memory performance (Eckart et al., 2016).

The symptomatic cholinergic treatment approach to AD is based on findings that Nucleus Basalis of Meynert (NBM) is a major source of cholinergic projections to the cortex (Mesulam and Geula, 1988) and reductions in levels of the cholinergic markers acetylcholinesterase (AChE) and choline acetyltransferase (ChAT) reflects the loss of cholinergic innervation that have been reported in the AD brain (Giacobini, 2003). Traditionally, ChAT activity is used as a marker of cholinergic neuronal loss in lesion studies (Wenk et al., 1994; Rossner et al., 1995). It has been shown that NBM lesions in animal models decrease cortical ChAT activity and modulate event-related oscillations in EEG by increasing power in low and decreasing power in high frequencies (Sanchez-Alavez et al., 2014).

Nerve growth factor (NGF) has emerged as a potential therapeutic agent in Alzheimer's disease (AD) due to its regenerative effects on basal forebrain cholinergic neurons (Williams et al., 2006; Mufson et al., 2008). Exogenous NGF delivered to the cholinergic basal forebrain has shown regenerative effects correlating with improved cognition in animal models of AD (Hefti and Mash, 1989; Olson et al., 1992). Since NGF does not cross the blood-brain barrier, administration to the brain provides a challenge.

Nerve growth factor administration to the brain has previously been tested in clinical studies of AD patients. A first trial was performed in three AD patients where NGF was delivered by intracerebroventricular infusion (Eriksdotter Jönhagen et al., 1998). The results indicated an up-regulation of nicotinic receptors and glucose metabolism on positron emission tomography (PET), as well as a normalization of the electroencephalography (EEG) pattern. However, adverse effects of NGF (neuropathic pain being the most prominent), made this route of administration unacceptable for routine treatment. In a clinical trial using genetically modified fibroblasts secreting NGF injected into the basal forebrain in AD patients, Tuszynski et al. (2005) demonstrated the feasibility of an *ex vivo* gene therapy approach with results indicating a slowing of disease progression. Our group has shown that targeted delivery of NGF through encapsulated cell biodelivery (NGF-ECB) into the basal forebrain is safe and well-tolerated (Eriksdotter-Jönhagen et al., 2012; Wahlberg et al., 2012). Three of the six patients responded to the NGF-delivery with a decrease in brain atrophy (Ferreira et al., 2015), and an increase in cholinergic markers in cerebrospinal fluid (CSF), correlating with improved cognition and brain glucose metabolism (Karami et al., 2015). Importantly, the activity of the acetylcholine synthesizing enzyme, ChAT in CSF showed a significant increase in patients with stable cognition during the 12-month NGF delivery (responders), compared to those patients who declined cognitively (non-responders) (Koenig et al., 2011).

The present report aimed to explore the potential effects of NGF-ECB administration on qEEG parameters during a 12-month exploratory study in a small, but unique sample of AD patients that have undergone this advanced experimental treatment. Our findings corroborate the previously reported changes in the rate of brain atrophy (Ferreira et al., 2015) and cholinergic markers in CSF (Karami et al., 2015) and further investigate changes in the functional measure of synaptic brain activity such as EEG. Moreover, we wanted to investigate whether qEEG changes were related to the global measures of cognitive

stabilization and the levels of cholinergic markers in the CSF by using an advanced statistical method to analyze multichannel EEG data.

SUBJECTS AND METHODS

Participants, Clinical Assessments, Procedures, and Ethics

The details of the NGF-ECB study as well as patient demographic and clinical data have been previously reported (Eriksdotter-Jönhagen et al., 2012; Wahlberg et al., 2012). In brief, six patients with mild to moderate AD, the median age of 62 years (range 55–73), and a median MMSE score of 23 (range 19–24) were enrolled and completed the study. They were all on stable ChEI treatment at baseline (median of 12 months, range 8–26 months) and throughout the study.

Before enrollment, the patients underwent a comprehensive medical evaluation, including medical history, somatic assessment and cognitive screening with MMSE (Folstein et al., 1975), lumbar puncture for CSF analyses, computerized tomography (CT) or magnetic resonance imaging (MRI), psychometric testing of cognition, EEG and routine blood sampling. All mentioned procedures were repeated within 1 week at 3 and 12 months follow-up. AD diagnosis was confirmed histopathologically on a cortical biopsy from surgical implantation (Vijayaraghavan et al., 2013).

The NGF-ECB implant is a catheter-like device containing a human retinal epithelial cell line, genetically modified to secrete NGF. All six patients received bilateral single implants in the Ch4 region in the basal forebrain and the last three patients also received additional bilateral implants in the Ch2 region as previously described (Rosengren et al., 1996; Vijayaraghavan et al., 2013). None of the patients suffered complications related to the neurosurgery or the device, and the post-operative courses were mainly uneventful (Rosengren et al., 1996; Vijayaraghavan et al., 2013). All patients completed the study, including the removal of all implants after the 12-month study period.

The patients were monitored primarily for safety and tolerability. Secondary outcome measures included effects on cognition, imaging, and quantitative EEG (qEEG) parameters, the latter being an additional exploratory outcome.

The study was conducted according to the Helsinki Declaration and was approved by the Swedish Medical Products Agency. Ethical approval was obtained from the Regional Human Ethics Committee of Stockholm. Both patients and caregivers gave written informed consent before study entry.

EEG Recordings

All spontaneous EEGs were recorded in a resting awake condition during the morning between 8 and 12 p.m. using the Nervus digital recording system (Natus Medical/NicoletOne). Electrodes were placed according to the standard 10/20 system, the reference electrode was placed in the midline between Fz and Cz, and the ground electrode between Cz and Pz. Horizontal and vertical eye movements and blinking were monitored by an EOG channel. Electrode impedance was below 5 kΩ. Initial filter settings were: low pass online filter 70 Hz to de-noise various types of interferences during the recording and sampling rate 256 Hz. The patients were seated in a slightly reclined chair in a sound-attenuated, normally lit room and after completion of the EEG set-up were instructed to remain relaxed, yet alert and awake during recording. Trained biomedical engineers were continuously monitoring the level of consciousness and used acoustic stimulation (noise or calling a patient's name) to keep the patients awake during the recording. Duration of resting-state eyes-closed EEG recording was 15 min with intermittent 5 s eyes open intervals during the first 10 min of recording, followed by 5 min eyes closed recording.

Quantitative EEG Analysis

EEGs were exported in an average reference mode into an EDF-file format and computerized EEG analysis was performed offline using the commercially available software, Brain Vision Analyzer, version 2.1 (Brain Products GmbH, Gilching, Germany). Non-physiological and physiological artifacts due to eye movements, contamination with muscle activity, and episodes with drowsiness were removed after visual inspection of the recording, and only segments with the awake eyes-closed state during the recording were included in the analyses. Ocular artifacts were additionally removed from all channels by using EOG and additionally semi-automated independent component (ICA) algorithm. Drowsiness during EEG recording was defined by transients of slow rolling eye movements (SREM) and concomitant attenuation of posterior alpha rhythm or occurrence of frontocentral theta activity. The preprocessed EEG data were segmented in 2-s epochs, frequency transformed at all electrodes using Fast Fourier Transform (FFT) algorithm with a Hanning window which is an in-built solution in the Brain Vision Analyzer software used to smooth out the endpoints of the data before applying FFT and thus reduce spectral leakage. All frequency transformed epochs were thereafter averaged to yield one amplitude/power spectrum per patient.

Cerebrospinal Fluid Biomarkers

Cerebrospinal fluid samples were collected by lumbar puncture before implantation (at baseline), 3 and 12 months after implantation. The samples were aliquoted and kept in polypropylene tubes at −80°C until analyzed. CSF ChAT activity was measured by a colorimetric assay as previously described (Vijayaraghavan et al., 2013). CSF levels of neurofilament light chain protein (NFL) were analyzed using a previously described enzyme-linked immunosorbent assay (ELISA) method (Rosengren et al., 1996).

Statistical Analyses

The analysis of treatment effects on the frequency domain EEG scalp distribution was based on topographical analyses of covariance (TANCOVAs) (Koenig et al., 2008), testing whether

a statistically significant amount of topographic variance can be accounted for by the linear contribution of an individual external predictor that may vary by condition, and there the significance of such accounts is assessed globally across all electrodes using a randomization test. For the testing of EEG associations with an external predictor that interacts with some condition, first, electrode-wise regression maps with the external regressor are computed. The difference of these regression maps is then globally quantified by first subtracting, from all regression maps the mean regression map, and then computing the overall mean square of the residual. To estimate the distribution of this RMS measure under the null hypothesis, the procedure is then also applied to data where the condition and subject labels have been randomly permutated. The statistical significance is given by the percent rank of the original measure in comparison to the estimated distribution under the null hypothesis. TANCOVAs have the advantage that they do not require any *a priori* hypothesis about a particular spatial distribution of some effect, which limits type I errors, but need, for a given frequency, only one test for the entire set of electrodes, which strongly reduces type II errors. This is particularly useful in the current context, where a larger number of subjects, and thus more statistical power, is not possible due to the costs and the invasive nature of the study. For the computation of the TANCOVAs and the visualization of the results, we used a Matlab-based program, Ragu (Randomization Graphical User interface) (Koenig et al., 2011), and estimated null-hypothesis based on 1,000 randomization runs. TANCOVA uses non-parametric randomization statistics that do not require a Gaussian distribution of the variable values across subjects.

No correction for multiple comparisons was used since randomization tests use global measures of effect size and therefore "downsize" a large amount of data by using a single measure of effect size which makes it suitable for this type of exploratory analysis. This results in a significant reduction of the tests needed for comparisons which in return, avoids correction of the results for multiple comparisons (Gudmundsson et al., 2007).

In the present analysis, MMSE and ChAT were considered as external predictors and the EEG spectral power maps at baseline, after 3 and 12 months of NGF delivery were considered as repeated measures. As this was an interventional study, we were primarily interested in systematic EEG covariates of the interaction of clinical measures with time after the intervention, which was computed for each frequency bin in the range from 1 to 30 Hz. Frequency bins are intervals between points in frequency-transformed data and thus bins refer to each 0.5 Hz frequency point computed separately for 1–30 Hz spectral range.

RESULTS

Six patients were enrolled in the study, two men and four women, implanted with NGF-ECB implants in the basal forebrain for 12 months, when the implants were removed uneventfully. All six patients were treated with ChEI as concomitant medication for a median duration of 12 months (range 8–26) before enrollment and continued this therapy throughout the study (**Table 1**).

Association Between EEG Spectral Power and Cognitive Stabilization During Nerve Growth Factor Delivery

We tested the data for significant changes in EEG spectral power in the frequency range from 1 to 30 Hz and if there were associations found with MMSE change at 12 months of NGF delivery against a baseline, as a function of time of the EEG recording (baseline, 3 months or 12 months). **Figure 1** illustrates change in averaged power spectra, baseline vs. 12 months, per individual subject.

The interaction between EEG frequency spectra across the three recordings and two groups, based on above or below the mean change in MMSE (12 months minus baseline), for the six patients showed a significant association at around 11 Hz (10–11.5 Hz), $p = 0.042$, **Figure 2**. *Post hoc* tests: baseline against 3 months $p = 0.059$, the baseline against 12 months $p = 0.033$, the baseline against merged 3 and 12 months $p = 0.023$, 3 months against 12 months, $p = 0.56$. This suggests a correlation between change in MMSE and EEG activity in the narrow window of the upper alpha band that was marginally significant at 3-months and significant at 12-months of NGF delivery. The fact that there was no significant correlation between the 3

TABLE 1 | Demographic data on enrolled patients.

	Patients
Gender, *n* (M/F)	4 M/2 F
Age, median (range)	62 (55–73)
Memory problems (y), median (range)	4 (1–6)
AD diagnosis (y), median (range)	1.5 (1–3)
Duration of ChEI (m), median (range)	12 (8–26)
MMSE score at baseline, median (range)	23 (19–24)
• Non-responders	23 (19–24)
• Responders	23 (21–23)
MMSE score at end of study, median (range)	18 (14–27)
• Non-responders	15 (14–16)
• Responders	21 (21–27)
CSF ChAT activity (nmol/min/ml), baseline, median (range)	2.6 (2.0–3.7)
• Non-responders	2.7 (2.0–3.4)
• Responders	2.6 (2.6–3.7)
CSF ChAT activity (nmol/min/ml), 3 months, median (range)	2.7 (2.3–3.1)
• Non-responders	2.7 (2.3–2.7)
• Responders	3.1 (2.5–3.1)
CSF ChAT activity (nmol/min/ml), 12 months, median (range)	3.0 (2.0–4.3)
• Non-responders	2.9 (2.0–3.0)
• Responders	3.7 (3.0–4.3)
CSF NFL (ng/L), baseline, median (range)	157.5 (125–360)
CSF NFL (ng/L), 12 months, median (range)	260 (125–420)

AD, Alzheimer's disease, ChAT, choline acetyltransferase, ChEI, cholinesterase inhibitors, CSF, cerebrospinal fluid, F, female, M, male, MMSE, Mini-mental state examination, NFL, neurofilament light protein.

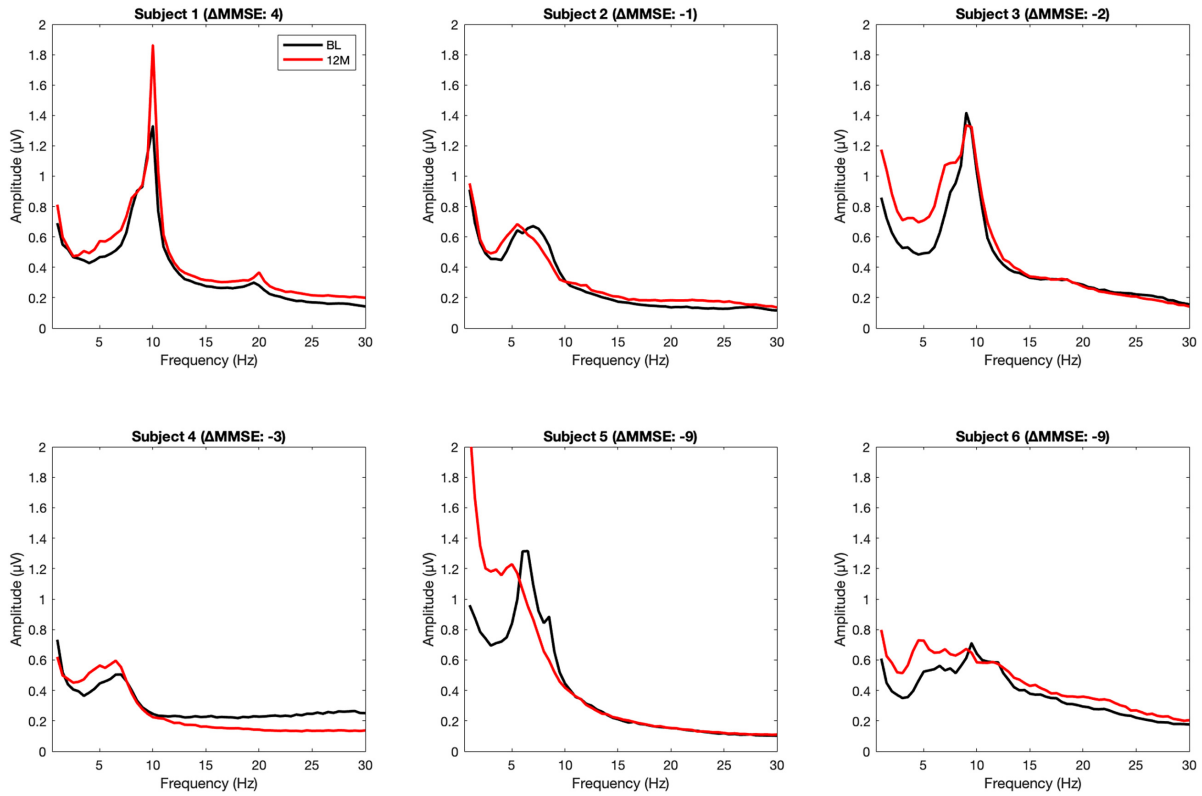

FIGURE 1 | Averaged power spectra, baseline vs. 12 months, per individual subject. The upper row shows the power spectra of responders, the lower row of the non-responders.

and 12 months implicates that most clinically detectable change happens in the first 3 months of treatment. The effect remains sustained during the treatment, although no further increase is detectable between the 3 and 12 months. No significant effects were observed when the data were merged across all observational points.

Association Between Changes in Cerebrospinal Fluid Choline Acetyltransferase Activity and EEG Spectral Power

TANCOVA correlations between EEG frequency spectra across the three recording occasions, dividing the six patients into two groups according to a change in CSF ChAT activity, below or above the mean change (12 months minus baseline), showed a marginally significant correlation in the frequency of around 6.0–6.5 Hz, **Figure 3**. This indicates that the more power in the theta frequency band, the less the change in CSF ChAT activity, $p = 0.058$ (**Figure 3**a). *Post hoc* tests: baseline vs. 3 months ($p = 0.09$), baseline vs. 12 months ($p = 0.06$), 3 months vs. 12 months ($p = 0.29$), baseline vs. 3 and 12 months merged ($p = 0.023$). The results suggest that the relationship between a reduction in CSF ChAT activity and EEG slowing in a narrow theta frequency range was mostly detectable at 3 months.

We also found a significant correlation between time vs. change in ChAT activity at 11–11.5 Hz ($p = 0.025$), **Figure 3**b. The interaction was mainly accounted for by the difference between baseline and 3 months, indicating that at 3 months of NGF delivery, the patients showed more alpha power correlating to positive changes in CSF ChAT activity, compared to baseline. Hence, the increase in ChAT seems to predict an increase in fast alpha activity up to 3 months of treatment. *Post hoc* tests: baseline vs. 3 months ($p = 0.042$), baseline vs. 12 months ($p = 0.21$), 3 months against 12 months ($p = 0.12$), baseline against merged 3 and 12 months ($p = 0.056$).

Association Between Changes in Cerebrospinal Fluid Nerve Growth Factor and EEG Spectral Power

There was no correlation between changes in NFL and EEG at any time point, and no significant interaction with time, MMSE, and ChAT.

DISCUSSION

This exploratory study is the first to report a correlation between the cholinergic marker ChAT in CSF and EEG oscillations in the alpha and theta frequency range during encapsulated NGF

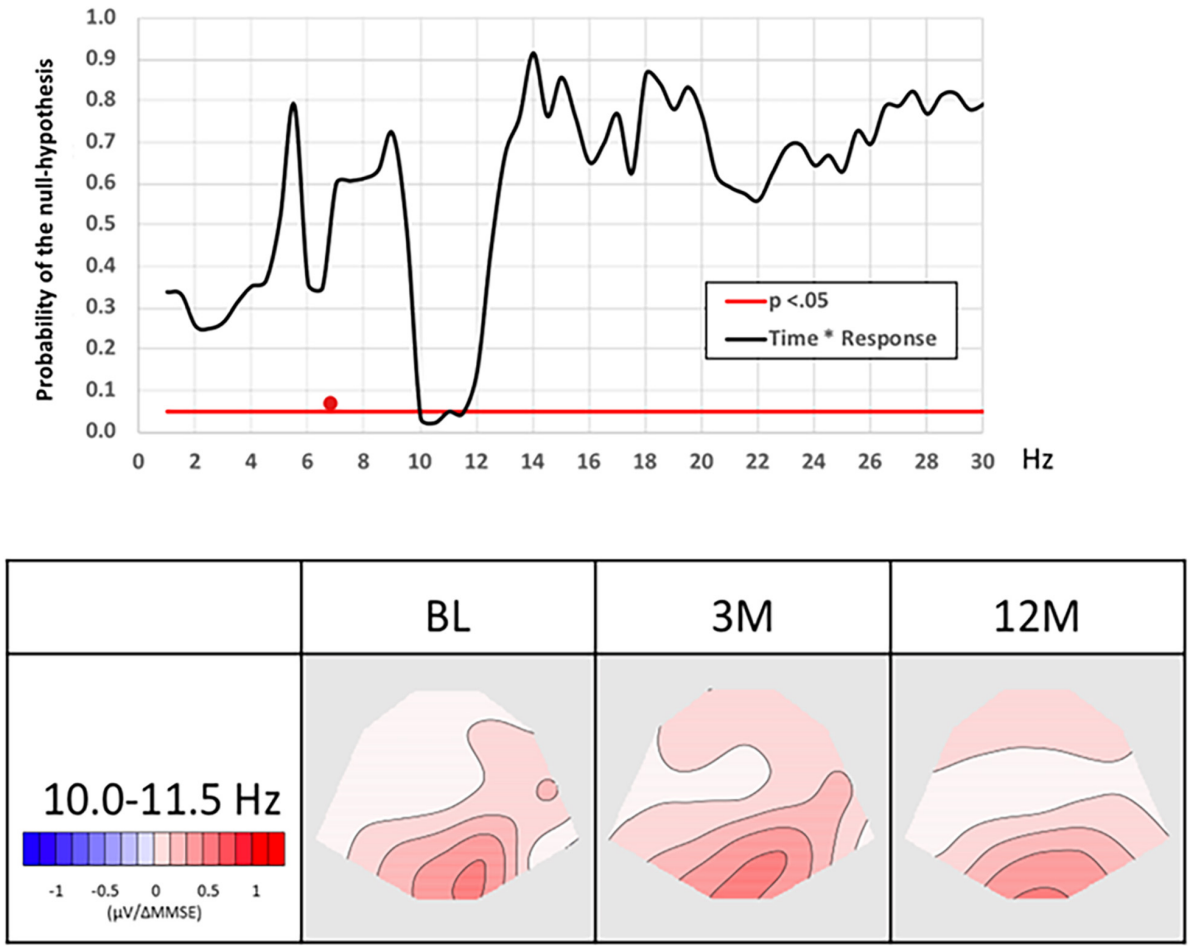

FIGURE 2 | Association between MMSE and EEG spectral power as a function of time. The graph on the left the probability (p) of the null hypothesis (*y*-axis) for the TANCOVA interaction between time and MMSE change as a function of frequency in Hz (*x*-axis). Significant ($p < 0.05$) frequency range is marked by a white line shows. The red cursor marks the frequency range represented by the covariance maps. Topographic maps display topographic covariance of the EEG spectral power correlating to MMSE changes at the **frequency range 10–11.5 Hz** for the three EEG recording occasions. Red maps show were less than the average change in MMSE score related to an increase in alpha frequency. BL, baseline; EEG, electroencephalography; MMSE, mini-mental state examination; TANCOVA, topographic analysis of covariance, 3 m: 3 months, 12 m: 12 months.

delivery to patients with a definite AD diagnosis as confirmed by a cortical biopsy (Eriksdotter-Jönhagen et al., 2012). Associations between changes in ChAT activity and EEG in narrow windows of both the theta and alpha frequency bands were mainly observed during the first 3 months of NGF delivery and do not seem to increase further thereafter. These limited effects could be explained by the fact that all the patients already were on a stable long-term treatment with ChEI which is a requirement for all clinical trials with new experimental treatments.

This was also the first cohort of patients who received NGF delivery *via* the NGF-ECB implants, with safety and tolerability as primary endpoints. However, at implant retrieval at 12 months, the NGF release was low (Eriksdotter-Jönhagen et al., 2012). It would be of interest to study the delivery of NGF with NGF-ECB implants for a longer duration than 12 months at sustained NGF dose level, to see if there are similar or even more pronounced effects on EEG, cholinergic biomarkers, and cognition.

In our study, a cognitive stabilization in some patients, as measured by an increased or stable MMSE score during the NGF delivery was related to a significant effect in a narrow frequency of the fast alpha band 10–11.5 Hz. Although such a narrow window of significant correlations might be the result of small sample size and could be questioned as physiologically relevant, an alternative explanation for the selective effect on the fast alpha frequencies may be the different functional significance of slow and fast alpha oscillations (Klimesch, 2012). It has been suggested that activities in the lower alpha bands (slower alpha oscillatory frequencies) are related to attentional processes and that those of the higher alpha bands (faster alpha oscillatory frequencies) are related to retrieval from the long-term memory (Klimesch, 1996). Although this knowledge is generated in EEG studies during a cognitive activation paradigm, we could speculate that it could be extrapolated to the resting EEG during stimulation of the cholinergic system, which may

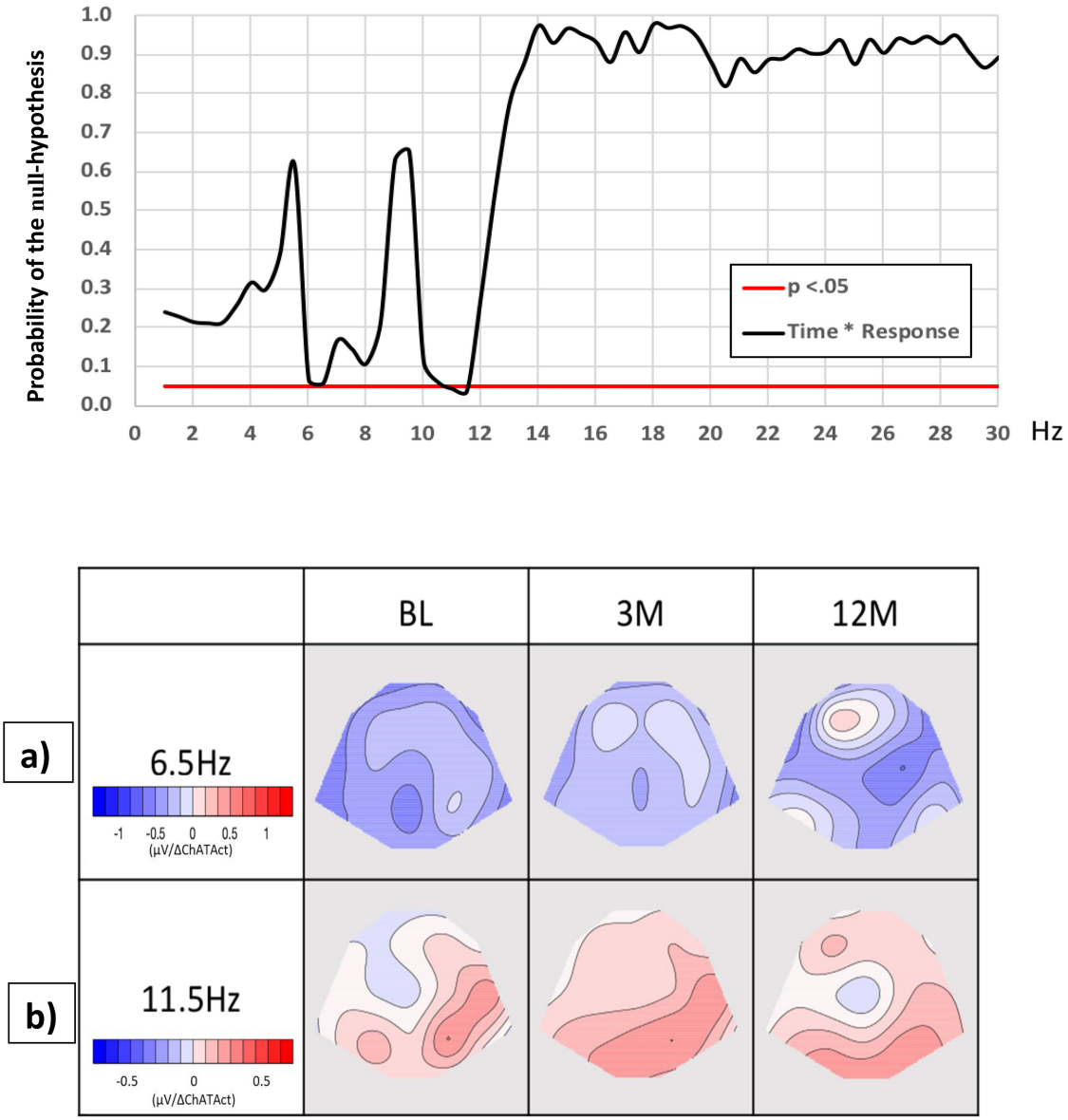

FIGURE 3 | Associations between CSF ChAT activity and EEG spectral power as a function of time during the NGF delivery. The graph shows the probability (p) of the null hypothesis (*y*-axis) for the TANCOVA interaction between time and change in CSF ChAT activity, as a function of EEG frequency in Hz. The significant ($p < 0.05$) frequency range is marked by a white line. The red cursor marks the frequency range represented by the covariance maps. Maps display topographic covariance of the EEG spectral power correlating to changes in ChAT activity at the frequency ranges: (a) **6.0–6.5** for the three EEG recording occasions. The blue maps show where lower than the average difference in CSF ChAT values correlated with an increase in the theta frequency, (b) **11.0–11.5 Hz** for the three EEG recording occasions. The red maps indicate where a higher than average difference in CSF ChAT activity (12 months vs. baseline) is related to an increase in upper alpha frequency. BL, baseline; ChAT, choline acetyltransferase; CSF, cerebrospinal fluid; EEG, electroencephalography; TANCOVA, topographic analysis of covariance, 3 m: 3 months, 12 m: 12 months.

preferentially activate neuronal networks involved in selective cognitive processes.

An alternative explanation may be that both thalamocortical and cortico-cortical networks are responsible for the generation of rhythmic alpha oscillations, assuming that the balance with other neurotransmitter systems during the disease process in AD affects the profile of EEG changes and cognitive response (Dringenberg, 2000).

While our earlier study showed that treatment with ChEI gave limited improvements of qEEG parameters up to 6 months (Jelic et al., 1998), this study showed a sustained association between positive changes in qEEG profile in the patients who showed clinical stabilization as suggested by MMSE change after a 12 month NGF delivery. The narrow windows of correlations between the EEG frequency spectra and cognitive and biochemical markers of cognitive deterioration and

biological activity of the disease during the NGF-ECB treatment should be interpreted with a reservation as a converging pattern in the context of current knowledge.

There was no strong consistent relation with theta power and the MMSE change as was shown for alpha power. Theta activity is known to increase early during AD and reaches a plateau during the disease course (Musaeus et al., 2018). Thus, theta power may not be a single sensitive electrophysiological state marker for monitoring disease activity and effects of therapeutic stimulation of the cholinergic system but can rather be considered an indicator of the baseline disease severity and could therefore be a basis for the selection of patients for clinical trials.

One limitation of this study is the small number of patients, which increases the variance of the data and puts limits to the use of conventional statistics. We propose here the use of the Ragu program which by using assumption-free randomization statistics computes significance as a function of frequency, controls for type 2 error, and displays results in a user-friendly visual format with EEG spectral power covariance maps (Gudmundsson et al., 2007).

Another limitation is the invasiveness of the treatment method which induces a minor brain lesion during implantation of the NGF-releasing implants. This is reflected in the temporary increase in the CSF neurofilament light chain (NFL) protein at the 3-month follow-up, returning to baseline levels when measured at 12 months (Eriksdotter-Jönhagen et al., 2012). However, there was no correlation between the qEEG parameters and CSF NFL levels and no significant interaction with time, MMSE, or ChAT.

A possible confounding placebo effect of the implantation procedure is less likely but since it could not be ruled out future investigation requires a cross-validation design.

We have employed only selected conventional EEG parameters that have shown in previous studies reliable test-retest reliability (Gudmundsson et al., 2007; Näpflin et al., 2007) at the individual level, which was important for the present study with the limited number of patients. Since the molecular family of NGFs plays an important role in synaptic plasticity (Liu et al., 2014; Numakawa and Odaka, 2021) it would be of interest to further explore on a larger sample size EEG connectivity measures that are more closely related to the efficacy of neuronal networks.

Although this study is exploratory, the results give further support for the qEEG method as a possible marker of disease activity. Furthermore, it is a desirable outcome measure in clinical trials monitoring treatment efficacy over time since it does not put limits on serial recordings. As with many other treatment strategies in AD, there will probably always be responders and non-responders to therapy and the corresponding need to define these patients with an objective and validated functional measures. The present results motivate the use of qEEG as one of the outcome measures in the clinical trials of novel potential therapeutics in AD. However, future validation studies with different treatment approaches on a larger sample of patients are further warranted.

DATA AVAILABILITY STATEMENT

The raw data supporting the conclusions of this article will be made available by the authors, without undue reservation, upon request.

ETHICS STATEMENT

Ethical approval was obtained from the Regional Human Ethics Committee of Stockholm. The patients/participants provided their written informed consent to participate in this study.

AUTHOR CONTRIBUTIONS

HE, ME, and VJ: conceptualization. TK, PA, BL, GL, LW, TD-S, and VJ: methodology. HE, TK, and VJ: formal analysis. HE, AK, and ME: investigation. HE, ÅS, ME, and VJ: resources. HE and VJ: writing—original draft preparation. TK and VJ: visualisation. ÅS, ME, and VJ: supervision. ME: funding acquisition. All authors have been engaged in review and editing and have read and agreed to the published version of the manuscript.

FUNDING

This study was supported by grants from the Regional agreement on medical training and clinical research (ALF) between Stockholm County Council and the Karolinska Institute, the Swedish medical research council (#2016-02317), Gustaf V and Queen Victorias Freemason Foundation, the Swedish Brain Power Consortium, KI Foundations, and Odd Fellow Memorial Foundation.

ACKNOWLEDGMENTS

We wish to thank the patients and their families and acknowledge the excellent assistance by the research nurse, Ann-Christine Tysen-Bäckström.

REFERENCES

Babiloni, C., Arakaki, X., Azami, H., Bennys, K., Blinowska, K., Bonanni, L., et al. (2021). Measures of resting-state EEG rhythms for clinical trials in Alzheimer's disease: recommendations of an expert panel. *Alzheimers Dement.* 17, 1528–1553. doi: 10.1002/alz.12311

Brenner, R. P., Reynolds, C. F. III, and Ulrich, R. F. (1988). Diagnostic efficacy of computerized spectral versus visual EEG analysis in elderly normal, demented, and depressed subjects. *Electroencephalogr. Clin. Neurophysiol.* 69, 110–117. doi: 10.1016/0013-4694(88)90206-4

Dringenberg, H. C. (2000). Alzheimer's disease: more than a 'cholinergic disorder' - evidence that cholinergic-monoaminergic interactions contribute to EEG slowing and dementia. *Behav. Brain Res.* 115, 235–249. doi: 10.1016/s0166-4328(00)00261-8

Eckart, C., Woźniak-Kwaśniewska, A., Herweg, N. A., Fuentemilla, L., and Bunzeck, N. (2016). Acetylcholine modulates human working memory and

subsequent familiarity based recognition via alpha oscillations. *Neuroimage* 137, 61–69. doi: 10.1016/j.neuroimage.2016.05.049

Eriksdotter Jönhagen, M., Nordberg, A., Amberla, K., Bäckman, L., Ebendal, T., Meyerson, B., et al. (1998). Intracerebroventricular infusion of nerve growth factor in three patients with Alzheimer's disease. *Dement. Geriatr. Cogn. Disord.* 9, 246–257. doi: 10.1159/000017069

Eriksdotter-Jönhagen, M., Linderoth, B., Lind, G., Aladellie, L., Almkvist, O., Andreasen, N., et al. (2012). Encapsulated cell biodelivery of nerve growth factor to the basal forebrain in patients with Alzheimer's disease. *Dement. Geriatr. Cogn. Disord.* 33, 18–28. doi: 10.1159/000336051

Ferreira, D., Westman, E., Eyjolfsdottir, H., Almqvist, P., Lind, G., Linderoth, B., et al. (2015). Brain changes in Alzheimer's disease patients with implanted encapsulated cells releasing nerve growth factor. *J. Alzheimers Dis.* 43, 1059–1072. doi: 10.3233/JAD-141068

Folstein, M. F., Folstein, S. E., and McHugh, P. R. (1975). Mini-mental state". A practical method for grading the cognitive state of patients for the clinician. *J. Psychiatric Res.* 12, 189–198.

Giacobini, E. (2003). Cholinergic function and Alzheimer's disease. *Int. J. Geriatr. Psychiatry* 18, S1–S5.

Gudmundsson, S., Runarsson, T. P., Sigurdsson, S., Eiriksdottir, G., and Johnsen, K. (2007). Reliability of quantitative EEG features. *Clin. Neurophysiol.* 118, 2162–2171. doi: 10.1016/j.clinph.2007.06.018

Hefti, F., and Mash, D. C. (1989). Localization of nerve growth factor receptors in the normal human brain and Alzheimer's disease. *Neurobiol. Aging.* 10, 75–87. doi: 10.1016/s0197-4580(89)80014-4

Jelic, V., and Kowalski, J. (2009). Evidence-based evaluation of diagnostic accuracy of resting EEG in dementia and mild cognitive impairment. *Clin. EEG Neurosci.* 40, 129–142. doi: 10.1177/155005940904000211

Jelic, V., Dierks, T., Amberla, K., Almkvist, O., Winblad, B., and Nordberg, A. (1998). Longitudinal changes in quantitative EEG during long-term tacrine treatment of patients with Alzheimer's disease. *Neurosci. Lett.* 254, 85–88. doi: 10.1016/s0304-3940(98)00669-7

Johannsson, M., Snaedal, J., Johannesson, G. H., Gudmundsson, T. E., and Johnsen, K. (2015). The acetylcholine index: an electroencephalographic marker of cholinergic activity in the living human brain applied to Alzheimer's disease and other dementias. *Dement. Geriatr. Cogn. Disord.* 39, 132–142. doi: 10.1159/000367889

Karami, A., Eyjolfsdottir, H., Vijayaraghavan, S., Lind, G., Almqvist, P., Kadir, A., et al. (2015). Changes in CSF cholinergic biomarkers in response to cell therapy with NGF in patients with Alzheimer's disease. *Alzheimers. Dement.* 11, 1316–1328. doi: 10.1016/j.jalz.2014.11.008

Klimesch, W. (1996). Memory processes, brain oscillations and EEG synchronization. *Int. J. Psychophysiol.* 24, 61–100. doi: 10.1016/s0167-8760(96)00057-8

Klimesch, W. (2012). alpha-band oscillations, attention, and controlled access to stored information. *Trends Cogn. Sci.* 16, 606–617. doi: 10.1016/j.tics.2012.10.007

Koenig, T., Kottlow, M., Stein, M., and Melie-García, L. (2011). Ragu: a free tool for the analysis of EEG and MEG event-related scalp field data using global randomization statistics. *Comput. Intell. Neurosci.* 2011:938925. doi: 10.1155/2011/938925

Koenig, T., Melie-García, L., Stein, M., Strik, W., and Lehmann, C. (2008). Establishing correlations of scalp field maps with other experimental variables using covariance analysis and resampling methods. *Clin. Neurophysiol.* 119, 1262–1270. doi: 10.1016/j.clinph.2007.12.023

Lehmann, C., Koenig, T., Jelic, V., Prichep, L., John, R. E., Wahlund, L. O., et al. (2007). Application and comparison of classification algorithms for recognition of Alzheimer's disease in electrical brain activity (EEG). *J. Neurosci. Methods* 161, 342–350. doi: 10.1016/j.jneumeth.2006.10.023

Liu, F., Xuan, A., Chen, Y., Zhang, J., Xu, L., Yan, Q., et al. (2014). Combined effect of nerve growth factor and brain-derived neurotrophic factor on neuronal differentiation of neural stem cells and the potential molecular mechanisms. *Mol. Med. Rep.* 10, 1739–1745. doi: 10.3892/mmr.2014.2393

Mesulam, M. M., and Geula, C. (1988). Nucleus basalis (Ch4) and cortical cholinergic innervation in the human brain: observations based on the distribution of acetylcholinesterase and choline acetyltransferase. *J. Compar. Neurol.* 275, 216–240. doi: 10.1002/cne.902750205

Moretti, D. V. (2014). Alpha rhythm oscillations and MMSE scores are differently modified by transdermal or oral rivastigmine in patients with Alzheimer's disease. *Am. J Neurodegener. Dis.* 3, 72–83.

Mufson, E. J., Counts, S. E., Perez, S. E., and Ginsberg, S. D. (2008). Cholinergic system during the progression of Alzheimer's disease: therapeutic implications. *Expert Rev. Neurotherapeut.* 8, 1703–1718. doi: 10.1586/14737175.8.11.1703

Musaeus, C. S., Engedal, K., Hogh, P., Jelic, V., Morup, M., Naik, M., et al. (2018). EEG Theta Power Is an Early Marker of Cognitive Decline in Dementia due to Alzheimer's Disease. *J. Alzheimers. Dis.* 64, 1359–1371. doi: 10.3233/JAD-180300

Näpflin, M., Wildi, M., and Sarnthein, J. (2007). Test–retest reliability of resting EEG spectra validates a statistical signature of persons. *Clin. Neurophysiol.* 118, 2519–2524. doi: 10.1016/j.clinph.2007.07.022

Numakawa, T., and Odaka, H. (2021). Brain-Derived Neurotrophic Factor Signaling in the Pathophysiology of Alzheimer's Disease: beneficial Effects of Flavonoids for Neuroprotection. *Int. J Mol. Sci.* 22:5719. doi: 10.3390/ijms22115719

Olson, L., Nordberg, A., von Holst, H., Bäckman, L., Ebendal, T., Alafuzoff, I., et al. (1992). Nerve growth factor affects 11C-nicotine binding, blood flow, EEG, and verbal episodic memory in an Alzheimer patient (case report). *J. Neural Trans. Parkinson's Dis. Dement. Sect.* 4, 79–95. doi: 10.1007/BF02257624

Rosengren, L. E., Karlsson, J. E., Karlsson, J. O., Persson, L. I., and Wikkelso, C. (1996). Patients with amyotrophic lateral sclerosis and other neurodegenerative diseases have increased levels of neurofilament protein in CSF. *J. Neurochem.* 67, 2013–2018. doi: 10.1046/j.1471-4159.1996.67052013.x

Rossner, S., Schliebs, R., Härtig, W., and Bigl, V. (1995). 192IGG-saporin-induced selective lesion of cholinergic basal forebrain system: neurochemical effects on cholinergic neurotransmission in rat cerebral cortex and hippocampus. *Brain Res. Bull.* 38, 371–381. doi: 10.1016/0361-9230(95)02002-9

Sanchez-Alavez, M., Robledo, P., Wills, D. N., Havstad, J., and Ehlers, C. L. (2014). Cholinergic modulation of event-related oscillations (ERO). *Brain Res.* 1559, 11–25. doi: 10.1016/j.brainres.2014.02.043

Tuszynski, M. H., Thal, L., Pay, M., Salmon, D. P., Hs, U., Bakay, R., et al. (2005). A phase 1 clinical trial of nerve growth factor gene therapy for Alzheimer disease. *Nat. Med.* 11, 551–555. doi: 10.1038/nm1239

Vijayaraghavan, S., Karami, A., Aeinehband, S., Behbahani, H., Grandien, A., Nilsson, B., et al. (2013). Regulated Extracellular Choline Acetyltransferase Activity- The Plausible Missing Link of the Distant Action of Acetylcholine in the Cholinergic Anti-Inflammatory Pathway. *PLoS One* 8:e65936. doi: 10.1371/journal.pone.0065936

Wahlberg, L. U., Lind, G., Almqvist, P. M., Kusk, P., Tornoe, J., Juliusson, B., et al. (2012). Targeted delivery of nerve growth factor via encapsulated cell biodelivery in Alzheimer disease: a technology platform for restorative neurosurgery. *J. Neurosurg.* 117, 340–347. doi: 10.3171/2012.2.JNS11714

Wenk, G. L., Stoehr, J. D., Quintana, G., Mobley, S., and Wiley, R. G. (1994). Behavioral, biochemical, histological, and electrophysiological effects of 192 IgG-saporin injections into the basal forebrain of rats. *J. Neurosci.* 14, 5986–5995. doi: 10.1523/JNEUROSCI.14-10-05986.1994

Williams, B. J., Eriksdotter-Jonhagen, M., and Granholm, A. C. (2006). Nerve growth factor in treatment and pathogenesis of Alzheimer's disease. *Progress Neurobiol.* 80, 114–128. doi: 10.1016/j.pneurobio.2006.09.001

Conflict of Interest: LW is an employee of NsGene and owns shares in the company.

The remaining authors declare that the research was conducted in the absence of any commercial or financial relationships that could be construed as a potential conflict of interest.

Publisher's Note: All claims expressed in this article are solely those of the authors and do not necessarily represent those of their affiliated organizations, or those of the publisher, the editors and the reviewers. Any product that may be evaluated in this article, or claim that may be made by its manufacturer, is not guaranteed or endorsed by the publisher.

frontiers | Frontiers in Aging Neuroscience

ORIGINAL RESEARCH
published: 29 April 2022
doi: 10.3389/fnagi.2022.846017

Dopaminergic Modulation of Local Non-oscillatory Activity and Global-Network Properties in Parkinson's Disease: An EEG Study

Juanli Zhang[1,2], Arno Villringer[1,3] and Vadim V. Nikulin[1,4]**

[1] Department of Neurology, Max Planck Institute for Human Cognitive and Brain Sciences, Leipzig, Germany, [2] Department of Neurology, Charité – Universitätsmedizin Berlin, Berlin, Germany, [3] Department of Cognitive Neurology, University Hospital Leipzig, Leipzig, Germany, [4] Neurophysics Group, Department of Neurology, Charité – Universitätsmedizin Berlin, Berlin, Germany

OPEN ACCESS

Edited by:
Aneta Kielar,
University of Arizona, United States

Reviewed by:
Eugenia Fatima Hesse Rizzi, Universidad de San Andrés, Argentina
Shivakumar Viswanathan, Institute of Neuroscience and Medicine, Julich Research Center, Helmholtz Association of German Research Centres (HZ), Germany

***Correspondence:**
Juanli Zhang
juanlizhang@cbs.mpg.de
Vadim V. Nikulin
nikulin@cbs.mpg.de

Specialty section:
This article was submitted to Parkinson's Disease and Aging-related Movement Disorders, a section of the journal Frontiers in Aging Neuroscience

Received: *30 December 2021*
Accepted: *31 March 2022*
Published: *29 April 2022*

Citation:
Zhang J, Villringer A and Nikulin VV (2022) Dopaminergic Modulation of Local Non-oscillatory Activity and Global-Network Properties in Parkinson's Disease: An EEG Study. Front. Aging Neurosci. 14:846017. doi: 10.3389/fnagi.2022.846017

Dopaminergic medication for Parkinson's disease (PD) modulates neuronal oscillations and functional connectivity (FC) across the basal ganglia-thalamic-cortical circuit. However, the non-oscillatory component of the neuronal activity, potentially indicating a state of excitation/inhibition balance, has not yet been investigated and previous studies have shown inconsistent changes of cortico-cortical connectivity as a response to dopaminergic medication. To further elucidate changes of regional non-oscillatory component of the neuronal power spectra, FC, and to determine which aspects of network organization obtained with graph theory respond to dopaminergic medication, we analyzed a resting-state electroencephalography (EEG) dataset including 15 PD patients during OFF and ON medication conditions. We found that the spectral slope, typically used to quantify the broadband non-oscillatory component of power spectra, steepened particularly in the left central region in the ON compared to OFF condition. In addition, using lagged coherence as a FC measure, we found that the FC in the beta frequency range between centro-parietal and frontal regions was enhanced in the ON compared to the OFF condition. After applying graph theory analysis, we observed that at the lower level of topology the node degree was increased, particularly in the centro-parietal area. Yet, results showed no significant difference in global topological organization between the two conditions: either in global efficiency or clustering coefficient for measuring global and local integration, respectively. Interestingly, we found a close association between local/global spectral slope and functional network global efficiency in the OFF condition, suggesting a crucial role of local non-oscillatory dynamics in forming the functional global integration which characterizes PD. These results provide further evidence and a more complete picture for the engagement of multiple cortical regions at various levels in response to dopaminergic medication in PD.

Keywords: Parkinson's disease, dopaminergic medication, spectral slope, functional connectivity, graph theory

INTRODUCTION

Parkinson's disease (PD) is the second most common neural degenerative disorder characterized by massive degeneration of dopaminergic neurons in the nigrostriatal dopamine system (Olanow et al., 2009). It has been increasingly recognized that PD is accompanied by functional disturbances both at subcortical and cortical levels (Braak et al., 2003; Boon et al., 2019). Clinically, dopamine loss is managed *via* dopaminergic therapy (DT). The dopaminergic system has been shown to have considerable and widespread modulatory influences on many brain structures including the cortex (Steiner and Kitai, 2001). While dopamine replacement therapy is efficient for improving the motor symptoms, the neural mechanisms of dopaminergic medication are not yet fully understood (Schapira, 2005).

In PD, it has been repeatedly reported that it is characterized by abnormal oscillatory synchrony in the basal ganglia-thalamus-cortical (BGTC) network in the beta frequency band (13–30 Hz) that could be modulated by dopaminergic medications and deep brain stimulation (DBS) (Brown, 2003; Wingeier et al., 2006; Kühn et al., 2009; De Hemptinne et al., 2015; Müller and Robinson, 2018). In the frequency domain, electrophysiological brain signals typically consist of a power-law 1/f component and periodic oscillatory activities. While a majority of studies have so far been dedicated to the oscillatory activity, increasing evidence shows that non-oscillatory (aperiodic) activity also provides information about the intricate neuronal dynamics unfolding at different temporal scales (He et al., 2010; Voytek et al., 2015). A broadband aperiodic component of the spectrum is often represented by the slope of the fitted line in log-log space (known as spectral slope). The changes in spectral slope have been associated with neural development, healthy aging, and performance in working memory tasks (Voytek et al., 2015; Donoghue et al., 2020). In addition, previous studies have reported that it is altered in different pathologies, such as schizophrenia (Peterson et al., 2017; Molina et al., 2020) and ADHD (attention deficit/hyperactivity disorder) (Robertson et al., 2019). Importantly, it has also been demonstrated that the spectral slope is a potential indicator of the local excitation/inhibition balance (Gao et al., 2017; Colombo et al., 2019). In addition, TMS (transcranial magnetic stimulation) studies, which can directly probe the changes in excitation and inhibition, have shown that PD is accompanied by changes in cortical excitability (Ridding et al., 1995; Hanajima et al., 1996; Cantello, 2002). Thus, it would be important to test whether and how this measure is altered in PD, in particular with dopaminergic medication.

While regional changes could provide comprehensive understanding of the underlying local circuitry, the brain rather functions as a distributed network. Functional connectivity (FC) analysis allows us to understand how distinct regions interact, and graph-theory based approach enables a macroscopic perspective of brain connections on the regional and whole-brain network level. Many previous studies showed that network architecture is related to brain function or dysfunction (Bassett and Bullmore, 2009; Bullmore and Sporns, 2009). Using resting state fMRI (functional magnetic resonance imaging), it has been intensively investigated how dopaminergic medication modulates brain FC in the BGTC network (Tahmasian et al., 2015). The most consistent finding across different rs-fMRI studies revealed decreased connectivity within the posterior putamen in PD (Tessitore et al., 2019), and that its cortical projections are modulated by dopaminergic medication (Herz et al., 2014). To date, few fMRI studies have adopted graph theoretical approach in PD, and the reported findings have been inconsistent. Specifically, compared to healthy controls, PD patients showed lower global efficiency (GE) (Sang et al., 2015), while no abnormalities in topographical property at the global level were observed in PD (Berman et al., 2016; Hou et al., 2018; Ruan et al., 2020). Both increase (Sang et al., 2015) and decrease (Hou et al., 2018) in nodal centrality have been observed in PD compared to healthy controls. In addition, it was found that levodopa administration significantly decreased local efficiency of the network (Berman et al., 2016), and conversely resulted in an increase in eigenvector centrality of cerebellum and brainstem in PD (Jech et al., 2013).

As for the EEG/MEG (electro- and magnetoencephalography) studies, compared to healthy controls, increased cortico-cortical FC in PD has been found primarily in alpha and beta frequency ranges, and cortico-cortical coherence was linked to the severity of the clinical symptoms (Silberstein et al., 2005; Stoffers et al., 2007, 2008; Bosboom et al., 2009; George et al., 2013; Miller et al., 2019). Dopaminergic medication induced changes in cortical synchronization have also been investigated by computing pair-wise coherence across the entire montage using multi-channel EEG/MEG. However, both reduction of FC after dopamine medication (Silberstein et al., 2005; George et al., 2013; Heinrichs-Graham et al., 2014) and the absence of connectivity modulation were previously reported (Miller et al., 2019). Very recently, using advanced modeling analysis, in response to dopaminergic medication, increased cortico-cortical synchronization in beta band has been detected by taking into account the contribution from other sub-networks (Sharma et al., 2021). To capture the changes across the whole cortex, through the application of graph theoretical measures in EEG/MEG, previous studies have demonstrated abnormalities in topographical organizations of functional network in PD compared to healthy controls, suggesting that the interactions between cortical areas become abnormal and contribute to PD symptoms at various stages (Utianski et al., 2016). Furthermore, the alterations in network attributes were linked to both motor and cognitive dysfunctions (Olde Dubbelink et al., 2014; Boon et al., 2017). However, how the topological organization of the cortical functional network changes after dopaminergic administration remains rather elusive. To address this issue, we applied graph theory-based network analysis to investigate further changes in cortical connectivity in patients with PD after the administration of dopaminergic medication. Besides, previous studies have suggested a close link between the local excitation/inhibition balance and information transmission locally and globally (Deco et al., 2014), and the network's organizational structure (Zhou et al., 2021). Therefore, we asked whether and how the spectral slope, as a proxy of the local E/I ratio, would relate to the network-wise activity in the context of PD.

To further characterize the regional and functional network changes due to dopaminergic medication, we address the following questions. Regarding local properties: (1) How does the aperiodic property of the electrophysiological brain signal change in response to dopaminergic medication administration? With respect to cross-area interactions: (2) What is the effect of dopaminergic medication on functional connectivity? (3) Does dopaminergic medication induce alterations in the lower and/or higher level of the network architectures? (4) Do local changes in non-oscillatory component of neural activity influence functional network topology/organization? To answer these questions, we analyzed a publicly available dataset including EEG data of PD patients from ON and OFF dopaminergic medication conditions (George et al., 2013; Rockhill et al., 2020).

MATERIALS AND METHODS

Participants

The data analyzed in this study is open-source data (George et al., 2013; Swann et al., 2015; Jackson et al., 2019). This dataset includes resting state EEG data with a duration of around 3 min. Data were collected from 15 PD patients (8 female, average age = 63.2 ± 8.2 years, mild to moderate disease with average disease duration of 4.5 ± 3.5 years) during OFF and ON dopaminergic medication sessions. All participants were right-handed and provided written consent in accordance with the Institutional Review Board of the University of California, San Diego and the Declaration of Helsinki. For more information you may refer to George et al. (2013).

Data Collection

EEG of patients with PD were recorded on two different days for ON and OFF medication sessions which were counterbalanced across subjects. For the OFF medication session, patients were requested to withdraw from their medication at least 12 h prior to the EEG recording. For the ON medication session, subjects took their medication as usual. A 32-channel EEG cap with BioSemi ActiveTwo system was used to acquire the EEG data with a sampling rate of 512 Hz. Two additional electrodes were placed over the left and right mastoids used for reference. During the EEG recording, participants were instructed to sit comfortably and fixate on a cross presented on the screen. Each recording session lasted at least 3 min. In addition, participants completed a few clinical assessments which were previously reported in George et al. (2013). In this study, we did not link the clinical scores of patients to the EEG measures as the authors of the original paper mentioned some uncertainty about these scores. Yet, to assure these two conditions represent two distinct parkinsonian states, we examined the change in the motor section of unifined Parkinson's disease rating scale (UPDRS III) scores between the two conditions. Statistical analysis showed that there was a significant reduction of the clinical scores in ON condition (mean ± SD: 32.67 ± 10.42) compared to that in OFF condition (mean ± SD: 39.27 ± 9.71). Note, that in this dataset a healthy control group was also included. However, we focused on the comparison of data between ON and OFF conditions which is also a standard study setup for differential parkinsonian states induced by medication in PD (Tinkhauser et al., 2017; Sharma et al., 2021).

Data Pre-processing

EEG data were analyzed using EEGLAB (version 14.1.2; Delorme and Makeig, 2004) and FieldTrip toolboxes, together with customized scripts in Matlab (The MathWorks Inc., Natick, MA, United States). First, a high-pass filter at 1 Hz was applied to remove low frequency drifts (two-way FIR filter, order = 1,536, eegfilt.m from EEGLab). Subsequently, independent component analysis (ICA – infomax algorithm implemented in EEGLab) was used to remove artifactual sources of cardiographic components, eye movements and blinks, and muscle activity in the data. Further, channels with inadequate quality were rejected by visually inspecting whether their spectra demonstrated residual EMG at higher frequency ranges [on average 5.4 ± 3.1 for OFF and 5.2 ± 2.8 for ON, no difference between conditions (p = 0.6606)]. Bad channels were interpolated with neighboring electrodes using a method of spherical splines (EEGLab function "*eeg_interp*"). Next, data were examined visually for the presence of residual artifacts and segments contaminated by gross artifacts and these events were marked and then excluded from further analysis [on average 172.5 ± 22.7 s in OFF and 165.5 ± 33.6 s in the ON condition remained, no difference in the number of rejected data points (p = 0.3591)]. Subsequently, data were re-referenced to the common average.

DATA ANALYSIS

Power Spectral Density

Power spectral density (PSD) was calculated using the function "*pwelch*" in MATLAB, with a Hamming window of 512 samples (i.e., 1 s) and a 50% overlap. Beta band power was estimated as the averaged PSD in the beta frequency range (13–30 Hz). In addition, in line with a previous study (Donoghue et al., 2020), we utilized another way of estimating the oscillatory beta power by accounting for the overall spectral slope. For this purpose, we subtracted the spectral slope (measured by a fitted line in a log-log space) and estimated the beta power on the residuals of the PSD.

Power Spectral Density Slope

To reduce contamination from high frequency non-neuronal noise, we estimated the slope of the PSD in a frequency range of 2–45 Hz. A three-step robust regression method was used to estimate the slope based on the computed PSD. This method was proposed and applied by Colombo et al. (2019). First, a least-squares linear line was fitted to the raw PSD using the function "*robustfit*" in MATLAB in the log frequency-log PSD space. Second, frequency points with larger than 1 median absolute deviations of the PSD residuals were identified as oscillatory peaks. Continuous frequency bins surrounding these peak frequencies were considered as the base of the oscillatory peaks and were also excluded for the further step. Last, a second least-squares fit was performed on the rest of the frequency ranges. We took the slope (with the sign) of the second fitted

line as the final spectral slope of the PSD. Thus, a more negative slope demonstrates a steeper decay, while a less negative slope represents a flatter one. One advantage of this method is that it considers the potential bias resulting from linearly spaced frequency bins being estimated with a logarithmic scale. Therefore, before the regression procedure, the PSD curve was up-sampled with logarithmically distributed frequency bins. For more details, please refer to the study by Colombo et al. (2019).

Functional Network Analysis

A network is constructed by a collection of nodes and links between pairs of nodes. In this study, we defined each node as a brain region approximately represented by each channel, while links represent the connectivity between pairs of channels. FC between the brain areas was determined by computing the lagged coherence which accounts for the volume conduction issue. Each network can be represented by a symmetrical 32 × 32 adjacency matrix.

Functional Connectivity

Functional connectivity measure was quantified by the lagged coherence between all the channel pairs in a frequency range of 1–35 Hz with resolution of 1 Hz. This metric quantifies the strength of phase coupling between two signals by eliminating the effects of volume conduction (Pascual-Marqui, 2007; Pascual-Marqui et al., 2011), and it has been shown to be even more suitable than phase lag index for the application of connectivity estimation when using EEG and MEG (Hindriks, 2021). Its value ranges between [0, 1]: "0" stands for no coupling, and "1" represents perfect coupling. This measure has been utilized in earlier EEG studies (Milz et al., 2014; Vecchio et al., 2021). FC in an oscillatory frequency band was acquired by averaging the FC values over the respective frequency range (for instance beta band FC was obtained by averaging the FC values over 13–30 and 8–12 Hz for the alpha band). To investigate whether medication could result in changes in FC in oscillatory frequency band across the whole brain (neighboring areas and remote regions), we applied a seed-based connectivity comparison approach. This means that the connectivity was calculated between a given electrode (seed) and all other electrodes for each subject. Then, whole-head connectivity was compared between conditions using a cluster-based permutation test to account for multiple comparisons.

Network Measure

We estimated the brain network metrics based on the scalp sensor-based EEG connectivity matrix. Although often performed in source space, due to a small number of channels (Lantz et al., 2003) we did it rather in sensor space similar to previous studies (Stam et al., 2007; Zeng et al., 2015; Chai et al., 2019; Sun et al., 2019; Mitsis et al., 2020; Smith et al., 2021). In the discussion, we mention and discuss limitations associated with the estimation of graph metrics in sensor space.

Node Degree

Node degree estimates the number of edges connected to each node. To estimate the importance of each node (each channel in our case), node degree centrality weighted by edge importance (the connection is stronger, edge weights are larger) was utilized for this purpose. Specifically, we used the function "*Centrality*" implemented in Matlab for this measure (parameter "*importance*" specified by edge weights).

Graph Theory Based Complex Network Measures

Overall Functional Connectivity. For each individual FC matrix, the overall FC was obtained by averaging all the connectivity values across all the pairs of the connection in a matrix.

Proportional Thresholding. Proportional thresholding is a commonly applied approach to remove connections with lower strength and to obtain a sparse connectivity matrix for computing the network properties based on graph theory. Here, we applied a proportional threshold to keep a consistent density of the connections across individuals (Bassett and Bullmore, 2009; van den Heuvel et al., 2017). If a proportional threshold (PT%) is applied to a functional network, all the strongest PT% of the connections are preserved and set to 1; the other connections are set to 0. As suggested by Rubinov and Sporns (2010), networks should be ideally characterized and show consistent patterns across a broad range of thresholds. These threshold values are often determined differently across studies. Therefore, in this study we examined a wide range of thresholds ranging from 36 to 4% (resulting in networks with around 20–200 links) in steps of 2%, similar to a previous study (van den Heuvel et al., 2017). To show how the network looks like, in **Figure 1**, we plotted the grand mean networks within each group at differential thresholding values (20, 10, and 2%).

Graph Metrics. Various measures characterize a network's structure. Two fundamental ones are included here: clustering coefficient (CC) and global efficiency (GE). These two basic graph metrics were computed as implemented in the Brain Connectivity Toolbox (Rubinov and Sporns, 2010). Clustering coefficient is a commonly used measure to quantify the functional network segregation. It is defined as the fraction of triangles (ratio of the present and total possible number of connected triangles) around an individual node and is equivalent to the fraction of a node's neighbors that are neighbors of each other (Watts and Strogatz, 1998). The clustering coefficient of a network CC is the average clustering coefficient across all the nodes in the network. It reflects the prevalence of clustered connectivity around individual nodes (Rubinov and Sporns, 2010): the larger the CC, the greater the degree of functional segregation.

The other metric, GE, was used to quantify the functional network integration. This is based on a basis measure – shortest characteristic path length. Paths are sequences of distinct nodes and links, with shortest paths between two nodes defined as the path with the fewest edges in a network (the sum of the number of its constituent edges is minimized). GE for a network, obtained by the average inverse shortest path length between all the pairs, is a measure of functional network integration: the larger the GE, the greater the degree of global integration. All these measures

were computed with an open source Matlab toolbox (Rubinov and Sporns, 2010).[1]

Statistical Tests

Non-parametric Wilcoxon signed rank test was performed for the comparisons of measures in PD OFF and ON states. Spearman's correlation coefficients were calculated to estimate the relations between different measures. We applied the false discovery rate (FDR) procedure (Benjamini and Hochberg, 1995) to correct for multiple tests (correlation calculation) across channels. Significance is reported when FDR-corrected p-values are below 0.05.

To account for multiple comparisons of metrics across all channels, we performed a channel space cluster-based permutation test using the "*Monte Carlo*" method, as implemented in FieldTrip (Oostenveld et al., 2011). At sample level (each channel in this case), a dependent t-test was utilized to estimate the effect. A total of 1,000 randomizations were performed across groups (ON and OFF conditions) and for each permutation. Additionally, the single sample t-values are thresholded at the 95th quantile, and cluster-level statistics (sum of t-values within each cluster) were computed and the largest cluster statistic was taken to build a null distribution. We then compared the observed cluster-level statistic from the empirical data against the null distribution derived from the permutation procedure. p-Values below 0.05 (two-tailed) were considered significant. A positive or negative cluster demonstrates a significant difference between two conditions (OFF > ON) or (OFF < ON).

RESULTS

Spatial Specificity and Effects of Medication on Spectral Slope

The grand mean of PSD averaged from all channels across subjects in each group is shown in **Figure 2A**. One can observe that the PSD decay in PD OFF was shallower compared to the PSD decay in PD in the ON condition. The spectral slope was computed for each channel and each subject. **Figure 2B** shows the topography of the grand mean of the spectral slope across all subjects within each group (upper panel for OFF and lower panel for ON condition). As shown in **Figure 2B**, for both groups, spectral slopes were more negative (steeper slopes) along the fronto-central-parietal midline of the brain and flatter in the other regions. In general, the ON condition was characterized by a more negative slope than that in the OFF condition.

We investigated the difference between the two conditions for all channels. As described in section "Materials and Methods," we applied a non-parametric cluster-based permutation test to correct for multiple comparisons in the channel space. When comparing slope values in PD OFF with those of PD ON, a significant positive cluster (p = 0.0220) indicated an increased slope (flatter) in PD OFF. This difference demonstrated a lateralized pattern covering mostly left central region (**Figure 2C**).

No Beta Power Difference Between Conditions Before and After Correcting for the Slope Effect

Previous studies have demonstrated inconsistent changes in cortical beta power: an increase of beta power after dopaminergic medication (Melgari et al., 2014) and insignificant cortical beta power changes after DT in PD (George et al., 2013; Miller et al., 2019). Since we showed that the background slope was significantly modulated by dopaminergic medication (significantly steepened by the medication), we assumed that insignificant beta power reports might partly be attributed to the overall broadband slope changes. To test this assumption, we first applied a traditional approach to estimate the beta band power on the raw PSD. We computed the mean PSD value in the beta frequency range (13–30 Hz) for each channel and each subject in each group. Cluster-based permutation tests in channel space showed no significant difference in beta power between conditions (**Figure 3A**). Next, to address whether this finding might be due to a flattened background spectral slope (as observed in the PD OFF vs. ON comparison) on the top of which oscillations were present, we used a second approach controlling for the spectral slope to estimate beta-oscillation power for each channel and subject. **Figure 3B** shows the grand mean of the residuals of the PSD across all channels after accounting for spectral slope. By averaging the PSD values in the same frequency range of 13–30 Hz, beta band power for each channel and each subject was re-calculated. Cluster-based permutation tests identified two non-significant negative clusters (OFF-ON) (p = 0.0739, 0.0939), mainly localized in bilateral centro-parietal regions (CP5, CP1 and C4, CP6, **Figure 3C**). This demonstrates that even after accounting for the background slope effect, there were no significant beta power changes between the two medication conditions.

Functional Connectivity in Beta Band Is Increased After Medication

First, we predominantly focused on the sensorimotor seed-based connectivity changes, which typically include C3 and C4 electrodes (Swann et al., 2015; Miller et al., 2019). The upper panel of **Figure 4A** depicts the FC between C3 and one of the representative channels from the parietal region (Pz) along a wide frequency range (1–35 Hz). One can observe clear peaks around the alpha and beta frequency bands for both the ON and OFF conditions. Next, we averaged the connectivity values in the beta frequency range (13–30 Hz) as a measure of beta band FC. As described above, C3 seed-based beta band connectivity was compared between medication conditions. A negative cluster localized in the parieto-occipital region (OFF < ON, p = 0.007) was identified as shown in the upper panel of **Figure 4B**, demonstrating a lower connectivity between C3 and parieto-occipital regions in the OFF compared to the ON conditions. However, there was no significant difference in the comparison of C4 seed-based connectivity between conditions.

[1] http://www.brain-connectivity-toolbox.net

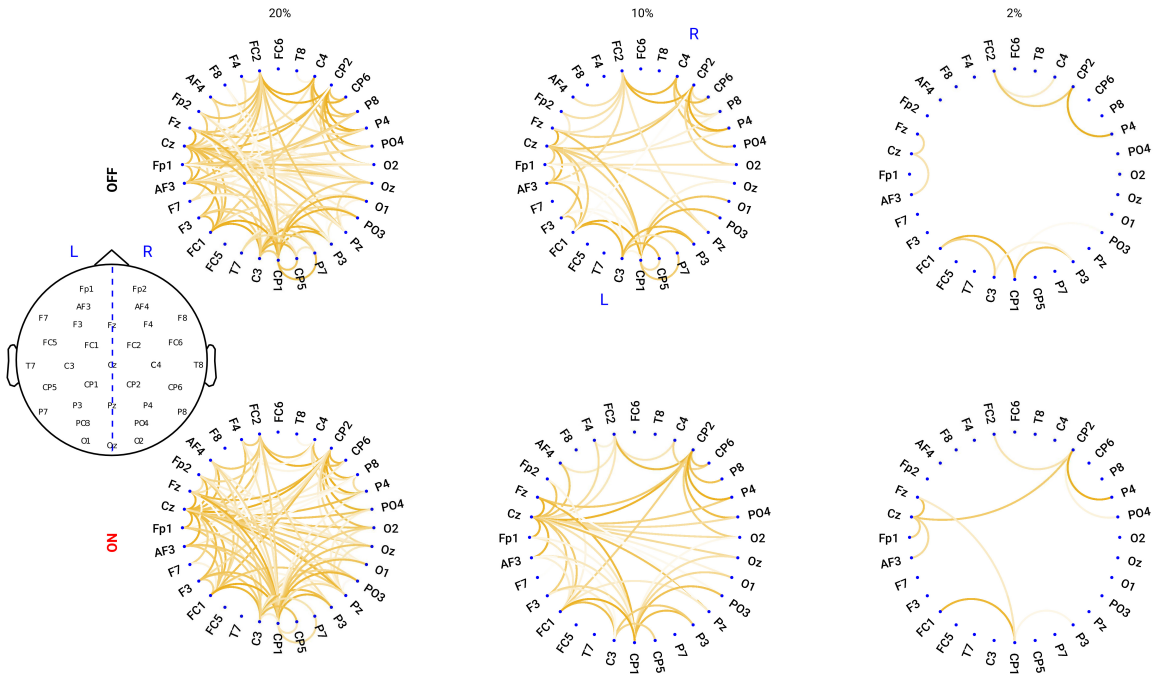

FIGURE 1 | Circular graph plot for the grand mean networks within each group under different PT%. Upper panel: in OFF condition, the networks under the thresholding values of 20, 10, and 2%. Lower panel: in ON condition, the networks under the thresholding values of 20, 10, and 2%. The degree of transparency represents how relatively strong the connection is within the network: the less transparency, the stronger the connection is.

Furthermore, to investigate whether the frontal region showed altered synchronization with other regions, we chose one of the representative channels in the frontal area [Fz, which is typically within the cluster of electrodes near the supplementary motor area (Casarotto et al., 2019)] and performed the same analysis as for electrode C3. As shown in the lower panel of **Figure 4A**, there were obvious peaks in the broad oscillatory frequency range (alpha and beta) for both conditions. The lower panel of **Figure 4B** shows the topographical pattern for the comparison between OFF and ON conditions, and a significant negative cluster (p = 0.0250) localized primarily in the parietal region. This demonstrated that the synchronization between Fz and parietal regions in the beta band was significantly enhanced in the ON compared to OFF condition in PD. Finally, we performed the same analysis for the other channels to demonstrate whole-head comparisons in a head-in-head plot (**Figure 4C**). As in C3 and Fz seed-based connectivity comparisons, the other channels in seed-based connectivity also showed significant increase in ON compared to OFF conditions. Significant clusters ($p < 0.05$) are marked by warm color. In general, the topographies showed significant alterations in synchronization between frontal, central, and parieto-occipital regions. To show that these connectivity effects are not mainly driven by the power of the beta oscillation itself, we also examined the PSD and connectivity profiles and found that in the beta band the peaks of the connectivity between the two channels do not coincide with the peaks of the power from either of the relevant channels (see **Supplementary Figure 1**). Therefore, we conclude that the connectivity effect estimated from the lagged coherence is not driven by the power and rather reflects phase-driven interaction. In addition, due to presence of peaks of the FC in the alpha band, we used the same approach to explore the FC changes in alpha band (8–12 Hz). Yet, there was no significant cluster detected for all the possible seeds when comparing the two conditions. Due to our predominant interest in the beta frequency range and pronounced effects observed in this frequency band, in the rest of the study we focus on the measures from the beta band.

Node Degree in Centro-Parietal Region in Beta Band Is Increased After Medication

Next, we tested whether the local level of a network feature, namely the node degree, was modulated by the medication effect. For this purpose, we calculated the node degree (from the connectivity in the beta band) for each channel and each subject. **Figure 5A** shows the topographical maps of the grand mean of the node degree across subjects within each group. As can be seen from **Figure 5A**, both groups showed a spatial specificity regarding the degree distribution (left for OFF and right for ON conditions): a higher level of the node degree in central areas than in other regions. This demonstrates that the central region might, in general, interact more with other regions in the whole brain network. Next, we compared the node degree between conditions for all channels using a cluster-based permutation test. **Figure 5B** shows the spatial difference pattern – a significant negative cluster was detected (p = 0.0140, OFF vs. ON, shown by labels)

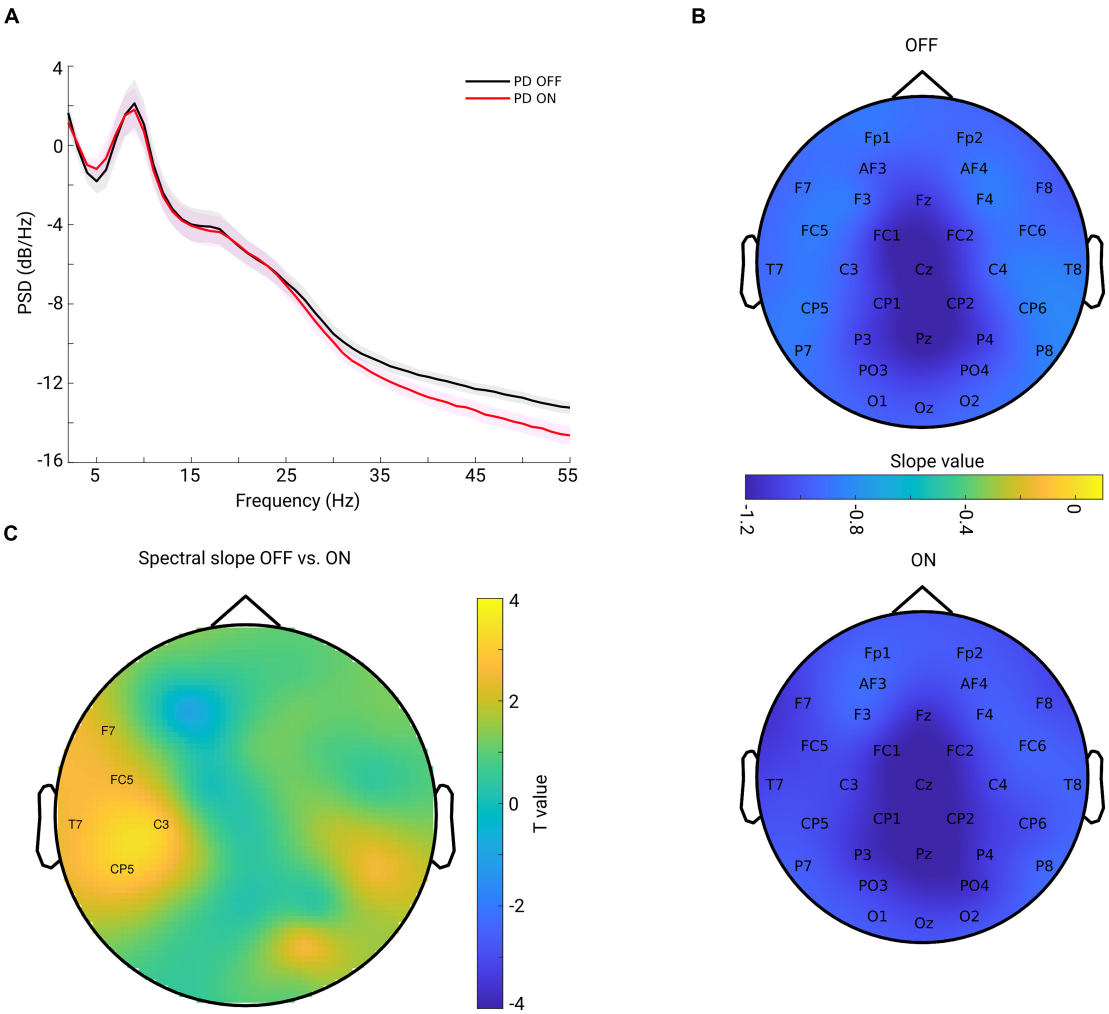

FIGURE 2 | (A) Grand mean of PSD across all channels and subjects within each group [OFF in black and ON in red, and the shaded area indicates the standard error of the mean (SEM)]. **(B)** Grand mean spatial distribution of spectral slope estimated from power spectra over 2–45 Hz across subjects within each group (upper panel for OFF, lower panel for ON condition). Color bar indicates the slope value. **(C)** Spatial-difference pattern of spectral slope between OFF and ON (OFF-ON) condition (cluster-based permutation test, $p = 0.0220$). Significant positive clusters are labeled. Color bar indicates the statistical *t*-value.

mainly in the centro-parietal region, suggesting that medication modulated the node degree of the beta band functional network in a way that the connectivity of the centro-parietal region became more pronounced in the whole network. Thus, this analysis further confirmed our findings obtained from seed-based connectivity analyses, revealing that synchronization was up-regulated by medication specifically between the centro-parietal region and other regions.

No Significant Change in the Global Network Topology: Either in Network Segregation or Network Integration Measure

To answer the question whether the global network structure is modulated by medication, we estimated the two fundamental features of a network: the GE for measuring functional network integration and the CC for measuring network functional segregation. We report the comparison results for both of the measures across a wide range of proportional thresholding values (36–4%, with a step of 2%) between the two conditions. Since it has been shown that differences in overall FC could have predictable consequences for between-group differences in network topology (van den Heuvel et al., 2017), we here first checked whether in our data there could be a possible bias for the comparison. However, no significant difference in overall FC between condition comparisons was found (Wilcoxon signed rank test, two-tailed, $p = 0.1514$). Thus, the overall FC is probably not a significant bias in the comparisons we performed as shown below. As seen in **Figure 6A**, across the whole range of thresholding (36–4%), the mean GE across subjects in the OFF condition (in black) almost overlapped with that from the ON condition (in red). As for clustering coefficient, the grand mean of CC in the OFF condition (black line) showed higher values

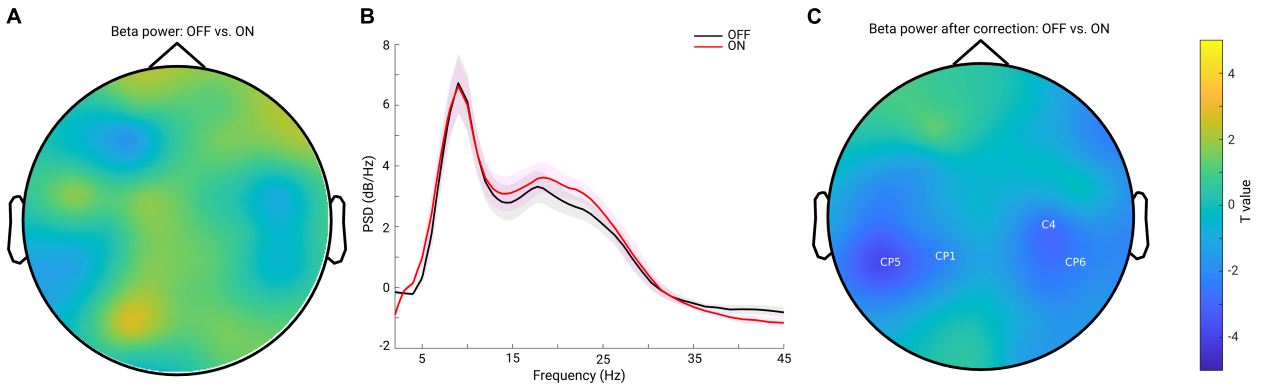

FIGURE 3 | (A) Topography for the comparison of beta band power between PD OFF and ON conditions estimated from the raw power spectra. No significant cluster was detected for the comparison. **(B)** Mean of the residuals of PSD (across all channels and subjects within each group, OFF in black and ON in red, and the shaded area indicates the SEM) after subtracting the spectral slope. Oscillatory peaks are present in alpha and beta bands in both groups. **(C)** Topography for the comparison of oscillatory beta band power between PD OFF vs. ON conditions after accounting for the background spectral slope. Two negative clusters were identified as shown by the labels, but none of them reached significance (p = 0.0739, 0.0939). Color bar indicates the statistical t-value.

than those in the ON condition (red line) across all thresholding values (**Figure 6B**). However, the statistical comparison did not indicate a significant difference in GE ($p > 0.05$, p-values shown in dashed orange line, right y-axis), or in CC between the two conditions ($p > 0.05$, p-values shown in dashed orange line, right y-axis). Thus, controlling for the overall FC values and across a wide range of thresholding values, we were not able to demonstrate a significant impact of medication on global network configuration.

Spectral Slope (Local and Global) Predicts the Network Global Efficiency in OFF Medication

Next, we asked how the spectral slope, as a proxy of measuring local E/I balance, would relate to the brain functional network; thus, we investigated a possible relationship between spectral slope and network topology. First, we averaged the spectral slope across all channels to represent an overall slope (referred to as global slope) for each subject. Spearman's correlation was performed between global slope and network metrics (GE and CC) derived under an exemplary thresholding value at 20% in both groups. As shown in the scatter plot in **Figure 7A**, GE negatively correlated with global slope (Rho = −0.7643, $p < 0.001$) in the OFF condition. In contrast, no such association was observed in the ON condition (Rho = −0.1036, $p = 0.7144$). Next, we performed a correlation analysis for the channel-wise slope (referred to as local slope) and network GE in the OFF condition. This analysis revealed a significant negative relationship between local slope values and network GE as shown in the topographical map (channels demonstrating significance are highlighted by label, FDR-corrected) in **Figure 7B**, and this relationship was most pronounced in the left centro-parietal area. There was no significant relationship between local slopes and GE in the ON condition. In addition, we examined if the relationship we observed at the 20% thresholding could be obtained regardless of the specific thresholding value. We performed the correlation analyses between global slope and network GE across the whole range of thresholding values (36–4% with a step of 2%) in the OFF group. As shown in **Figure 7C**, almost across all PT%, the negative association between global slope and network GE was present consistently ($p < 0.05$, p-values shown in dashed orange line, right y-axis), except under an extreme thresholding value of 4%. The spatial correlation pattern between local slope and network GE was also examined under the same range of thresholding values, and consistently negative relations between local slope from the centro-parietal region and network GE were observed (see **Supplementary Figure 4**). These results showed that global slope negatively correlated with network GE across a wide range of thresholding values, and a further topographical correlation map between local slope and network GE demonstrated a region-specific pattern.

Control for the Discontinuity in the Data

To assure that the estimation of the metrics is not affected by signal discontinuity introduced by removing the artifacts, we additionally performed the main analyses respecting the cutting borders. Consistently, we obtained very similar results with respect to spectral slope and lagged coherence. The differences between the two medication conditions remained unchanged. A detailed report can be found in **Supplementary Figures 2, 3**.

DISCUSSION

In this study, we investigated local and global changes induced by dopaminergic medication in a cohort of PD patients using non-oscillatory spectral slope measure and connectivity analysis in resting state EEG. Locally, we estimated the slope of the non-oscillatory wideband background activity and showed that the left central region had a significantly decreased (steeper) spectral slope during the ON compared to OFF medication state. In addition, in ON compared to OFF, we observed an increase in the FC in the beta band, mainly between centro-parietal and

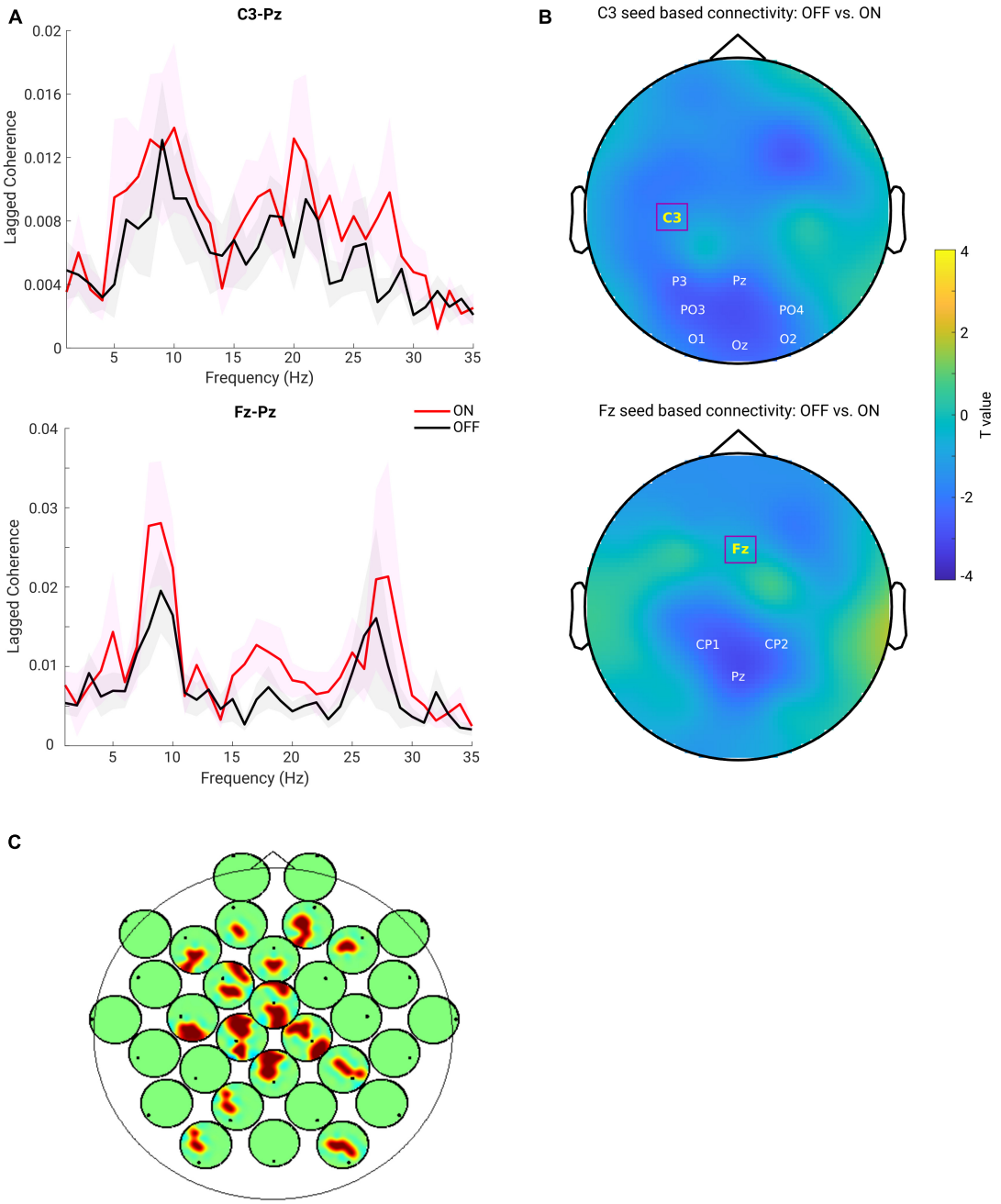

FIGURE 4 | (A) Lagged coherence plot over a frequency range of 1–35 Hz. Upper panel shows the mean connectivity (measured by lagged coherence) estimated from C3 and Pz, while the lower panel shows the connectivity estimated from Fz and Pz, across the subjects within each group (OFF in black and ON in red, and the shaded area indicates the SEM). **(B)** Upper panel: topography for C3 seed-based connectivity (lagged coherence in beta band) comparison between OFF vs. ON condition (channel-space cluster-based permutation test). The significant cluster is highlighted by the labels in white, while the seed channel C3 is marked in yellow and outlined by a square box. Lower panel: the same analysis performed for the seed channel Fz, and a significant negative cluster (OFF < ON) was detected ($p = 0.0250$). Color bar indicates the statistical t-value. **(C)** Head-in-head plot for the seed-based connectivity (lagged coherence in beta band) comparison for all channels. At each channel, the head plot shows the topography for comparison of connectivity between this channel and all other channels using cluster-based permutation test. Only the significant clusters ($p < 0.05$) are shown by warm color.

frontal regions. Further, graph theory-based analysis showed an enhanced node centrality in particular in the centro-parietal regions but no significant alteration in the complex level of network topology (GE or CC). Lastly, we found a strong negative relationship between spectral slope (locally and globally) and network's GE in the OFF condition, where a flatter slope was associated with a smaller degree of GE of the functional network. These findings provide further evidence for the engagement of

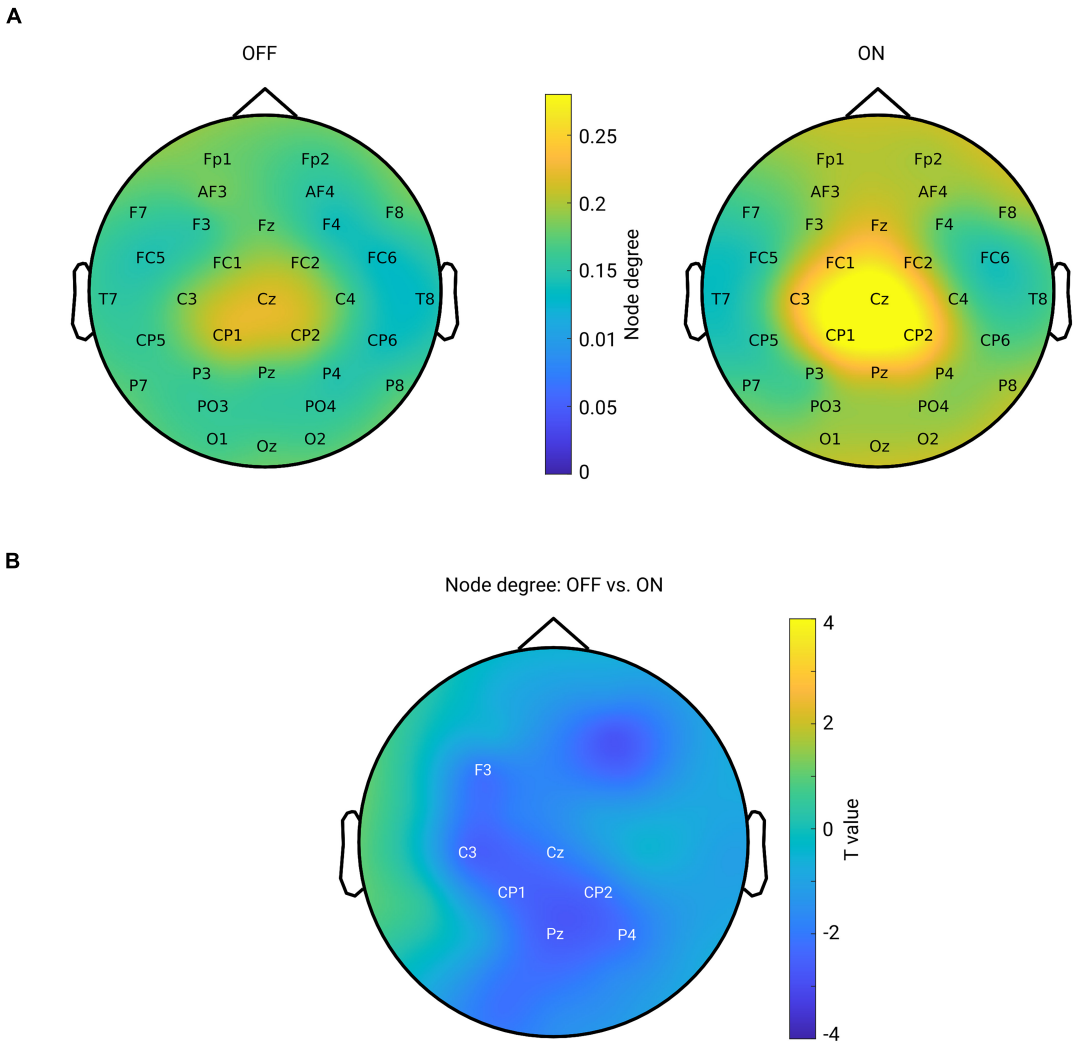

FIGURE 5 | (A) Mean spatial distribution of node degree calculated from the beta band functional connectivity for each group: left for OFF and right for ON condition. For both groups, the electrodes in the central area have a higher level of node degree than that of other regions. Color bar indicates the magnitude of node degree. **(B)** Spatial difference pattern for comparison of node degree between two conditions (OFF vs. ON). The labeled channels show the identified significant negative cluster (OFF < ON, $p = 0.0140$) using cluster-based permutation test. Color bar indicates the statistical *t*-value.

multiple cortical regions in response to dopaminergic medication in PD, which in turn may indicate that the therapeutic efficacy of dopaminergic medication may relate to both regional and global changes in cortical activity.

Non-oscillatory Background Spectral Slope

Using multi-channel resting state EEG, we observed that patients with PD in the medication OFF condition had an increased (flatter) spectral slope compared to medication ON condition. This effect was found to be spatially specific to the left central region. The spectral slope, a metric to quantify this background power spectrum, has been reported to be altered in the first year of development, healthy aging and in mental disorder such as schizophrenia (Peterson et al., 2017; Donoghue et al., 2020; Molina et al., 2020; Schaworonkow and Voytek, 2021), and could also predict the dynamic behavioral outcome in working memory tasks (Voytek et al., 2015; Donoghue et al., 2020). In our study, we observed that the spectral slope steepened in ON compared to OFF conditions. Given that previous studies demonstrated that healthy aging is accompanied by flattening of the spectral slope (Voytek et al., 2015; Cesnaite et al., 2021) and that neural electrophysiological biomarkers associated with PD are already present in the apparently healthy aging brain (Zhang et al., 2021), one can speculate that PD might be accompanied by a flattening of the power spectra and that dopaminergic medication might reverse this flattening effect. The effect was found most pronounced in the left central area (strongest at C3 electrode in the detected cluster), which might indicate a modification over the sensorimotor area by the medication. The broadband spectral slope underlying the dopamine medication modulation effect

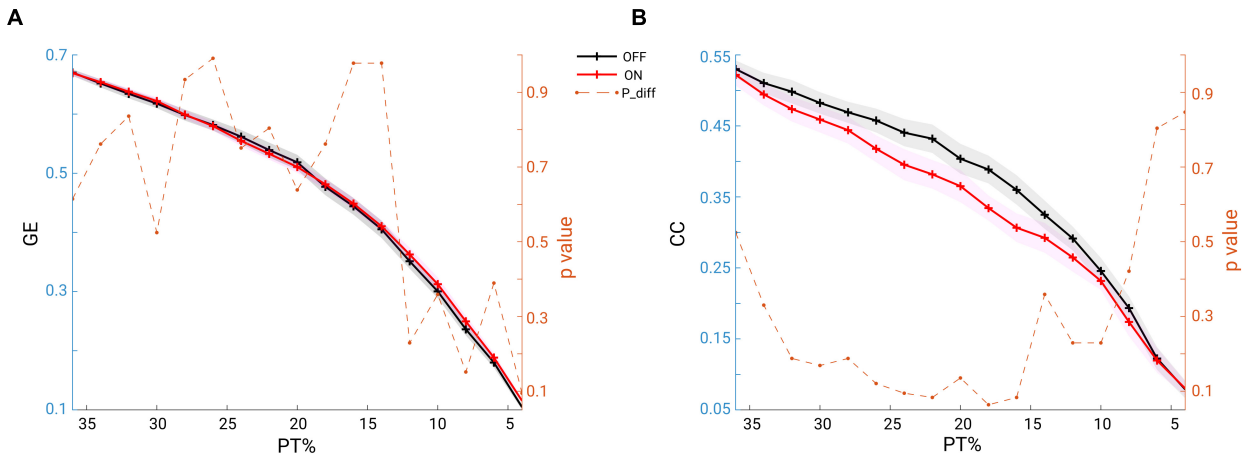

FIGURE 6 | (A) Mean GE estimated from beta band functional connectivity across subjects within each group (OFF in black and ON in red, and the shaded area indicates the SEM) across a wide range of thresholding values (36–4% in step of 2%). The dashed orange line represents the *p*-values (right *y*-axis) for the comparisons: none are below 0.05. **(B)** Same analysis, but for CC: across a wide range of thresholding values no significant difference was observed between the conditions (OFF vs. ON).

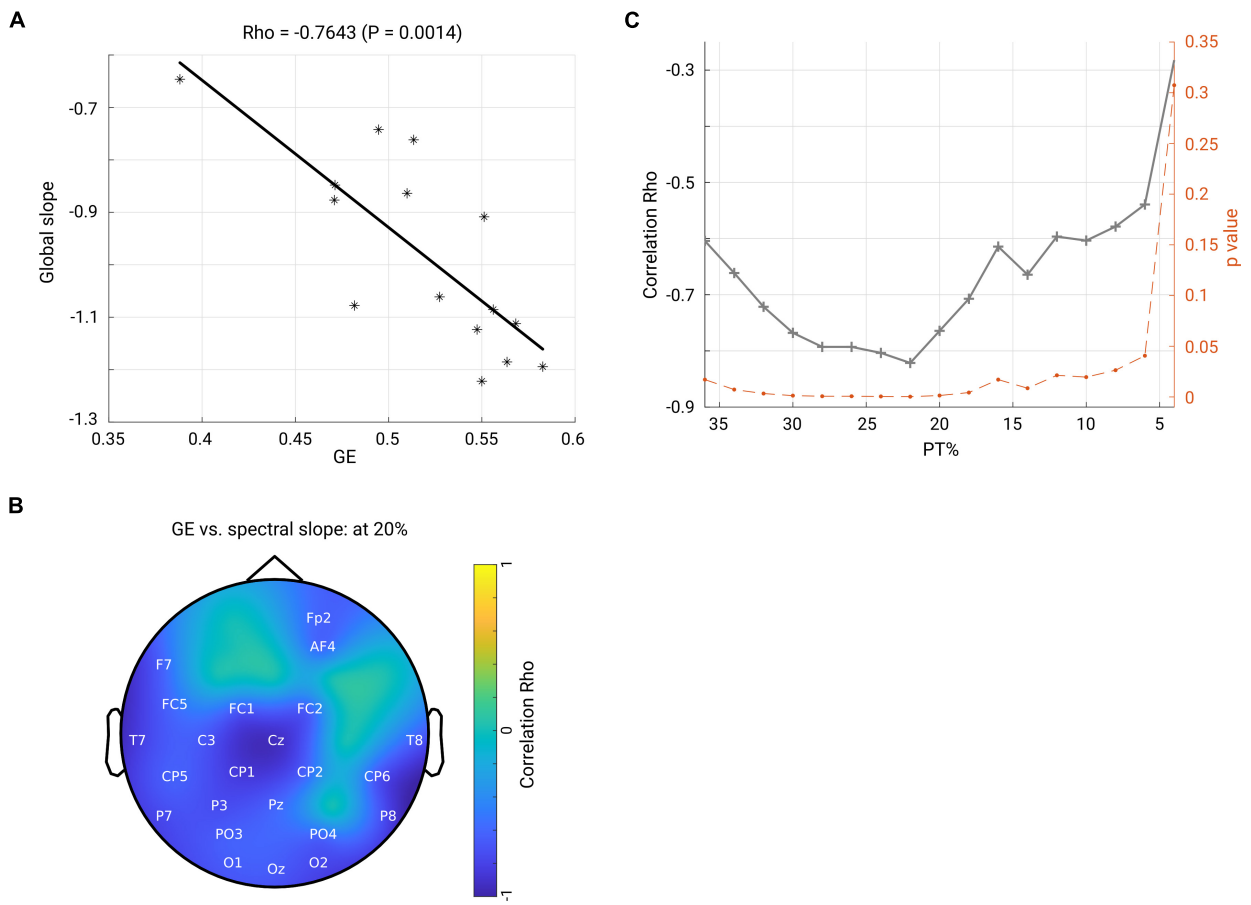

FIGURE 7 | (A) Scatter plot shows that global efficiency for the beta band network (under thresholding value 20%) negatively correlates with the global slope (averaged slope across the whole head) in the OFF condition. Each asterisk represents one subject. **(B)** Spatial pattern for the correlation between local slope and global efficiency (beta network and under 20% thresholding). The channels highlighted by label indicate significant correlation after FDR correction. Color bar indicates the correlation coefficient value. **(C)** Through a family of thresholding values (36–6%, with a step of 2%), there was a significantly negative relationship ($p < 0.05$, *p*-values shown in dashed orange line, right *y*-axis) between global efficiency and global slope.

in patients with PD may thus potentially serve as a biomarker sensitive to dopamine replacement therapy. At the same time, even though we carefully cleaned the data and removed artifacts which might contribute to the estimation of spectral slope, we could not completely rule out this confounder. However, we would like to emphasize that this is unlikely to drive the effect of spectral slope we observed, otherwise one would expect a spatial pattern which shows strongest difference over the frontal or temporal areas (which cover large muscle groups and prone to be contaminated by the muscle activity). Additionally, as we mentioned before, the spectral slope has been shown to index the E/I balance, and we will discuss the implication of this finding below (see section "Spectral Slope and Network Global Efficiency: Local E/I Balance and Global Network").

Power of Beta Oscillation

Previous studies have demonstrated an increase in cortical beta-band power in PD compared to healthy controls and alleviated beta band synchrony after medication administration (Stanzione et al., 1996) and attenuation by DBS (Whitmer et al., 2012). On the other hand, other studies have also reported an opposite effect—an increase of beta band power after dopaminergic medication (Melgari et al., 2014). In addition, some studies demonstrated that dopaminergic medication did not have any effect on cortical beta power (Stoffers et al., 2007; George et al., 2013; Swann et al., 2015; Miller et al., 2019). Importantly, all previous PD studies on this topic have only considered total power of beta without separating it into oscillatory and 1/f aperiodic components. In the present study, we tested the impact of the removal of the aperiodic part of the spectrum on the estimation of oscillatory power. We found that a conventional approach to estimate oscillatory power based on the raw PSD resulted in a non-significant difference in beta band in the PD OFF compared to ON state. After accounting for the spectral slope changes, a marginal increase of beta power was detected in the centro-parietal regions in the comparison between the ON and OFF conditions, yet this difference failed to reach significance. Our data thus suggests that even though the beta-band power estimation by the conventional approach might be partly affected by the background wideband PSD spectra, correcting the effect still does not yield a clear and statistically significant difference between the ON and OFF conditions. Thus, in line with some previous studies (George et al., 2013; Swann et al., 2015; Miller et al., 2019), we further confirm that with and without considering the background slope effect, there was no difference in beta power between the medication conditions. In addition, we discuss a possible relation of our findings to prior studies which were based on the same dataset. The only intersecting aspect across all these prior studies and ours is the investigation of beta-band power change during resting state. Consistently with what have been reported by George et al. (2013) and Swann et al. (2015), our study demonstrated there was no beta power change between the two medication states. Importantly, in our study, we have examined a possible bias from the overall PSD slope effect and showed that even when considering it there was no spectral power change in beta frequency range between the two conditions. Yet, we suggest that future studies should take into account the effect of the aperiodic spectral component for the comprehensive evaluation of oscillatory power changes in PD.

Functional Connectivity

We observed a significant increase in FC of beta oscillations in the ON compared to OFF condition, in particular between the centro-parietal regions with frontal regions. Previous studies have demonstrated a presence of beta-band coherence between STN (subthalamic nucleus) and multiple cortical regions, including sensorimotor (Hirschmann et al., 2011, 2013; Litvak et al., 2011), parietal and frontal areas (Litvak et al., 2011) in the OFF medication condition in patients with PD. Dopaminergic medication can also alter the beta-band connectivity between STN and cortical regions (Stoffers et al., 2008; Litvak et al., 2011; Hirschmann et al., 2013; van Wijk et al., 2016). As for the cortico-cortical connectivity, dopaminergic medication administration was shown to either reduce interactions between cortical areas (Silberstein et al., 2005; George et al., 2013; Pollok et al., 2013; Heinrichs-Graham et al., 2014) or not to produce any significant changes (Miller et al., 2019). In a very recent study using combined STN-LFP (local field potential) and MEG recordings, the authors discovered differential effects of dopaminergic medication in different levels of networks (Sharma et al., 2021). Specifically, in the cortico-cortical network, sensorimotor-cortical connectivity across multiple regions was enhanced in the beta band during the ON medication state. Therefore, our observations of the enhancement of such a coherent fronto-parietal motor network in the ON condition is consistent with this recent report. Such enhancement of FC is partially in agreement with another study which employed simultaneous fMRI/EEG recordings and showed that a higher dose of dopaminergic medication increased FC between motor areas and the default mode network in fMRI, whereas EEG connectivity remained unaffected (Evangelisti et al., 2019). In general, the dopaminergic effect over the cortico-cortical motor network might relate to the motor decision-making associated network, which has been shown to involve cortical fronto-parietal regions (Siegel et al., 2015), or it might relate to the default-mode network changes associated with non-motor symptoms in PD as suggested by other fMRI studies (Gao and Wu, 2016). Notably, a recent EEG study in PD using source localization demonstrated the presence of strong phase-amplitude coupling between the phase of beta and the amplitude of broadband gamma oscillations in a variety of cortical regions (including sensorimotor, somatosensory, and prefrontal areas) involved in motor and executive control (Gong et al., 2021). In line with this study, our findings of increased connectivity between centroparietal-frontal regions after dopaminergic medication further emphasize the importance of cortico-cortical connections in PD. These electrophysiological findings are consistent with previous fMRI studies suggesting a critical role of motor circuitry in PD in response to dopamine administration (Shen et al., 2020).

Global and Local Network Organization

Using graph theory, we demonstrated that in the ON condition, there was a significant increase in node degree in centro-parietal

regions implying that these regions became more influential in the communication within the network. However, the network topology does not seem to undergo a major re-configuration as we did not identify significant changes in GE or CC in the brain network. This seems consistent with findings of previous studies in which PD patients were compared to healthy controls and no differences in topographical properties were found at the global level either in fMRI (Ruan et al., 2020) or in EEG in all frequency bands (Hassan et al., 2017). Another previous study also investigated the topographical structure of functional network using graph analysis based on MEG of patients with PD (Olde Dubbelink et al., 2013). Compared to healthy controls, their longitudinal study revealed a tendency toward a more random brain functional organization which was associated with lower local integration in multiple frequency bands and lower GE in the upper alpha band. However, another study using EEG found an increase in local integration and a decrease in GE across all the frequency bands in PD compared to healthy subjects (Utianski et al., 2016). In the present study, we explored the alterations in a functional spectral network using graph metrics and showed that dopaminergic medication intake did not significantly alter the brain network organization but did exert a significant enhancement in node degree of some particular regions within the network. The absence of significant changes in global integration and segregation of the functional network might suggest that dopaminergic medication does not re-configure the network at a global organizational level. Instead, these observations appear to imply that the brain network as a whole does not respond to medication at the complex (global integration and segregation) but rather at the low-level network topology (local node). It would be interesting for future studies to test whether this relates to the clinical improvement of symptoms and whether it is possible to significantly alter the network organization through different therapeutic interventions based on brain stimulation.

Spectral Slope and Network Global Efficiency: Local E/I Balance and Global Network

A steeper spectral slope after dopaminergic medication intake was evident in PD. As proposed by previous computational work, the scaling property of the power spectrum of the membrane potentials and EEG could be due to the frequency attenuation of the extracellular medium itself (Bédard et al., 2006), or the intrinsic low-pass filtering effect of the electrical properties of the neural dendrites (Lindén et al., 2010; Einevoll et al., 2013). Alternatively, steepening of the slope could be a consequence of dampened activity propagation (Freeman and Zhai, 2009). More recently, by applying a realistic computational model, it has been demonstrated that stronger inhibitory activity results in steeper spectral decay compared to a situation with a stronger excitatory drive and thus the spectral slope value can be linked to the local excitation/inhibition ratio (Gao et al., 2017). Importantly, this spectral slope derived from ECoG recording dynamically reflects the effects of anesthesia induced by propofol. Furthermore, other pharmacological studies on resting state EEG confirmed further that spectral slope can differentiate the states of wakefulness compared to a reduction or a complete loss of consciousness induced in the anesthesia (Colombo et al., 2019). Even though an exact generative mechanism of the 1/f shaped arrhythmic brain activity is still unclear (He, 2014), these recent prior work from simulations and experiments with the recordings across different spatial scales have indicated that the spectral slope could be a sensitive marker of the E/I dynamics. Following the E/I balance hypothesis of the spectral slope, a steeper slope after medication, observed in this study, may indicate that dopamine induced a state characterized by stronger inhibition over excitation. This line of interpretation agrees with previous TMS studies reporting a reduction of intracortical inhibition at rest in PD OFF medication (Ridding et al., 1995; Hanajima et al., 1996; Cantello, 2002) and an enhancement of evoked inhibitory activity (reflected in late TMS-evoked activity and beta TMS-evoked oscillations) after dopaminergic medication intake (Casula et al., 2017).

In addition, we found a close relationship between broadband non-oscillatory background activity measured by the spectral slope and the beta-band GE of the functional network. Global network efficiency represents the ability of integration of activity of widely distributed regions within a network, impacting information transmission and communication (Bullmore and Sporns, 2012). Notably, a previous simulation work demonstrated that synaptic E/I balance is crucial for efficient neural coding (Zhou and Yu, 2018), and the local E/I ratio plays a role in information transmission at large scale brain level (Deco et al., 2014). This theory concurs with our findings: the local and global spectral slope, reflecting the local and global tune of E/I balance, is closely associated with the functional network global integration property. The negative relationship between them implies that more excitation over inhibition corresponds to a lower level of functional network integration. Consistently, a recent study from both fMRI recording and simulation data showed that the local E/I ratio could have a significant impact on the organization of whole brain functional networks: GE of the functional network is an inverted-U shaped function of local E/I ratio and the more deviation from the balanced E/I state (in either direction), the lower GE of the whole functional network (Zhou et al., 2021). Our observation about the relationship between local and global slopes with the global network integration property can potentially be explained by this model: in OFF medication, an imbalanced E/I state (indexed by flatter slope) deviating from balanced E/I ratio exerts a monotonous negative relation with functional network GE. A presence of a negative relation between the spectral slope and GE might indicate that the network in PD OFF state resides within the left part of the inverted-U shaped function [GE vs. E/I ratio, refer to the Figure 8A of the study (Zhou et al., 2021)] where a monotonous correlation can be expected. Such a close association did not hold for the medication ON group. We assume that the medication moves the network back closer to a more balanced state, reflected in a steeper spectral slope (steepening of the flattened slope in OFF state); thus, functional network organization was no longer closely related to the E/I, since in a close-to balanced E/I state the GE would rather remain

stable (i.e., it reaches a maximum at the optimal E/I state). Our data did not show a difference in the network's GE property and in contrast did demonstrate a difference in E/I dynamics (reflected by the spectral slope) between the two conditions, thus actually providing a possibility which allows us to more specifically identify a position of the network in the OFF state. One intriguing explanation would be that GE changes rather slowly for quickly changing E/I ratio; therefore, the network in OFF condition stays relatively close to the one in ON condition along the GE axis, and along the E/I axis the networks from two conditions stay further apart.

The spatial distribution of local slope and GE demonstrated a specific pattern where the slope from the centro-parietal regions showed strongest relations with the GE of the brain network. In line with previous fMRI studies demonstrating that the nodal property of the parietal cortex is closely associated with motor outcome and decreased with progressing disease stage (Hoehn and Yahr stage) in PD (Sang et al., 2015; Fang et al., 2017; Suo et al., 2017), we assume that centro-parietal regions play an important role in orchestrating the whole global network organization. This is congruent with the finding that the connectivity patterns in these cortical regions are also affected by dopaminergic medication, as discussed above.

LIMITATIONS

The first limitation of this study is that due to a rather low density of electrodes, we performed all connectivity analysis in sensor space. Thus, we refrain from making any conclusions about the specific structure of the networks (e.g., small-world and scale-free networks) as is also suggested in a critical study on the application of graph measures in EEG/MEG (Kaminski and Blinowska, 2018). It should also be noted that even if the analysis were to be conducted in source space, the volume conduction issue may still be present. Importantly, we applied a connectivity measure that is specifically used to overcome the volume conduction issue. Moreover, we were able to show that our findings remained consistent for a wide range of thresholds for the networks' properties.

Another limitation of our study is that clinical measures were not available and therefore, we could not associate EEG measures with the severity of clinical symptoms. We acknowledge this and suggest that future studies could include such a design so that the link between EEG parameters and clinical phenotypes can be explored. Future work should test whether and how local and global EEG parameters relate to clinical symptoms.

Lastly, due to the lack of EEG comparison with the healthy control group and the possibility to link the observed effects to differential components of the clinical symptoms in PD, we are rather restricted in our interpretation of the neuronal effects due to dopaminergic modulation. In particular, significant modulation of the spectral slopes and connectivity in some specific regions might potentially indicate a successful improvement associated with particular motor aspects (for instance bradykinesia), while non-significant changes might indicate the absence of such modulation for other motor components such as internal motor control as shown in a recent study (Michely et al., 2015). Alternatively, the absence of neuronal changes in some regions might imply a co-existence of possible non-dopaminergic alterations (for instance serotonergic dysfunction) that could also become present in the course of PD and are not modulated by dopaminergic medication (Politis and Niccolini, 2015).

CONCLUSION

Using multi-channel resting EEG recordings in PD patients, we showed differential effects of dopaminergic medication on local non-oscillatory components and connectivity parameters. Both from the local-level and brain-network perspective, the centro-parietal area was identified as the region where significant alterations in non-oscillatory wideband activity, measured by spectral slope and node centrality within the spectral functional network in the beta band, occurred. However, the network's global topologies, namely global integration (measured by GE) and global segregation (measured by CC) remained unaffected by the dopaminergic medication. Furthermore, during the OFF state, a close association between the spectral slopes (local and global) and network global integration was observed. These findings align with the theory that local E/I balance impacts global network structure, which might in turn demonstrate a crucial role of local non-oscillatory dynamics in forming the functional global integration in PD.

DATA AVAILABILITY STATEMENT

Publicly available datasets were analyzed in this study. This data can be found here: https://openneuro.org/datasets/ds002778.

ETHICS STATEMENT

The studies involving human participants were reviewed and approved by the Institutional Review Board Protocol at the University of California, San Diego. The patients/participants provided their written informed consent to participate in this study.

AUTHOR CONTRIBUTIONS

JZ: conceptualization, methodology, software, formal analysis, data curation, writing—original draft, writing—review and editing, visualization, and project administration. AV: writing—review and editing, and supervision. VN: conceptualization, methodology, writing—original draft, writing—review and editing, project administration, and supervision. All authors contributed to the article and approved the submitted version.

FUNDING

This work was supported by Deutsche Forschungsgemeinschaft (German Research Foundation) (Project ID: 424778381 TRR 295).

ACKNOWLEDGMENTS

We thank Tilman Stephani for valuable discussions on the manuscript.

SUPPLEMENTARY MATERIAL

The Supplementary Material for this article can be found online at: https://www.frontiersin.org/articles/10.3389/fnagi.2022.846017/full#supplementary-material

Supplementary Figure 1 | Normalized PSDs and connectivity profiles in OFF and ON conditions. In the upper panel: in OFF state, blue lines show the PSD profiles and black lines show the connectivity (left for C3-Pz and right for Fz-Pz). In the lower panel: in ON state, blue lines show the PSD profiles and red lines show the connectivity (left for C3-Pz and right for Fz-Pz).

Supplementary Figure 2 | Spectral slope effect remains the same after taking care of the cutting borders. **(A)** Left panel: grand mean PSD plot in PD ON condition before and after respecting the cutting borders (original PSD estimation in magenta and PSD estimation with taking care of the cutting borders in light blue). Two lines almost completely overlap across all the frequencies. Right panel: histograms of the estimated spectral slope values across all the channels and all the subjects within PD ON group with original approach in magenta and new approach (considering the borders) in light blue. **(B)** Topographical pattern of the comparison of the spectral slope between two conditions based on the estimations considering the cutting borders (OFF vs. ON, $p = 0.0240$). This topography is consistent with the **Figure 2C** of the main manuscript.

Supplementary Figure 3 | Functional connectivity effects remain unchanged after taking care of the borders introduced by removing the artifactual segments. **(A)** Left panel: averaged functional connectivity between Fz-Pz channels in PD OFF condition before and after considering the cutting borders (original and new estimation in magenta and light blue color, respectively). Two approaches give rise to very similar estimation values. Right panel: same analysis but in the PD ON condition. **(B)** Topographical pattern of the comparison of the Fz-seed based functional connectivity between two conditions (OFF vs. ON, $p = 0.028$). The significant cluster is highlighted by the labels in white, while the seed channel Fz is marked in yellow outlined by a square box. This spatial difference pattern is very consistent with the lower panel of **Figure 4B** of the main manuscript.

Supplementary Figure 4 | Spatial patterns for the correlation between local slope and global efficiency (beta network and under a variety of thresholding values). Significant channels are shown in labels ($p < 0.05$) after FDR correction. Color bar indicates the correlation coefficient value. The spatial specificity over the centro-parietal region is generally consistent across a family of thresholding values (36–18%). At the PT% of 14%, a significant negative relationship is still present. For the higher PT% values, no significant correlation remains after multiple testing correction.

REFERENCES

Bassett, D. S., and Bullmore, E. T. (2009). Human brain networks in health and disease. *Curr. Opin. Neurol.* 22, 340–347. doi: 10.1097/WCO.0b013e32832d93dd

Bédard, C., Kröger, H., and Destexhe, A. (2006). Does the 1/f frequency scaling of brain signals reflect self-organized critical states? *Phys. Rev. Lett.* 97:118102. doi: 10.1103/PhysRevLett.97.118102

Benjamini, Y., and Hochberg, Y. (1995). Controlling the false discovery rate: a practical and powerful approach to multiple testing. *J. R. Stat. Soc. Lond. B Methodol.)* 57, 289–300.

Berman, B. D., Smucny, J., Wylie, K. P., Shelton, E., Kronberg, E., Leehey, M., et al. (2016). Levodopa modulates small-world architecture of functional brain networks in Parkinson's disease. *Mov. Disord.* 31, 1676–1684. doi: 10.1002/mds.26713

Boon, L. I., Geraedts, V. J., Hillebrand, A., Tannemaat, M. R., Contarino, M. F., Stam, C. J., et al. (2019). A systematic review of MEG-based studies in Parkinson's disease: the motor system and beyond. *Hum. Brain Mapping.* 40, 2827–2848. doi: 10.1002/hbm.24562

Boon, L. I., Hillebrand, A., Olde Dubbelink, K. T. E., Stam, C. J., and Berendse, H. W. (2017). Changes in resting-state directed connectivity in cortico-subcortical networks correlate with cognitive function in Parkinson's disease. *Clin. Neurophysiol.* 128, 1319–1326. doi: 10.1016/j.clinph.2017.04.024

Bosboom, J. L. W., Stoffers, D., Wolters, E. C., Stam, C. J., and Berendse, H. W. (2009). MEG resting state functional connectivity in Parkinson's disease related dementia. *J. Neural Trans.* 116, 193–202. doi: 10.1007/s00702-008-0132-6

Braak, H., Del Tredici, K., Rüb, U., De Vos, R. A. I., Jansen Steur, E. N. H., and Braak, E. (2003). Staging of brain pathology related to sporadic Parkinson's disease. *Neurobiol. Aging* 24, 197–211. doi: 10.1016/S0197-4580(02)00065-9

Brown, P. (2003). Oscillatory nature of human basal ganglia activity: relationship to the pathophysiology of parkinson's disease. *Mov. Disord.* 18, 357–363. doi: 10.1002/mds.10358

Bullmore, E., and Sporns, O. (2009). Complex brain networks: graph theoretical analysis of structural and functional systems. *Nat. Rev. Neurosci.* 10, 186–198. doi: 10.1038/nrn2575

Bullmore, E., and Sporns, O. (2012). The economy of brain network organization. *Nat. Rev. Neurosci.* 13, 336–349. doi: 10.1038/nrn3214

Cantello, R. (2002). Applications of transcranial magnetic stimulation in movement disorders. *J. Clin. Neurophysiol.* 19, 272–293. doi: 10.1097/00004691-200208000-00003

Casarotto, S., Turco, F., Comanducci, A., Perretti, A., Marotta, G., Pezzoli, G., et al. (2019). Excitability of the supplementary motor area in Parkinson's disease depends on subcortical damage. *Brain Stimul.* 12, 152–160. doi: 10.1016/j.brs.2018.10.011

Casula, E. P., Stampanoni Bassi, M., Pellicciari, M. C., Ponzo, V., Veniero, D., Peppe, A., et al. (2017). Subthalamic stimulation and levodopa modulate cortical reactivity in Parkinson's patients. *Park. Relat. Disord.* 34, 31–37. doi: 10.1016/j.parkreldis.2016.10.009

Cesnaite, E., Steinfath, P., Idaji, M. J., Stephani, T., Haufe, S., Sander, C., et al. (2021). Alterations in rhythmic and non-rhythmic resting-state EEG activity and their link to cognition in older age. *bioRxiv* [Preprint] 1–34. doi: 10.1101/2021.08.26.457768

Chai, M. T., Amin, H. U., Izhar, L. I., Saad, M. N. M., Abdul Rahman, M., Malik, A. S., et al. (2019). Exploring EEG effective connectivity network in estimating influence of color on emotion and memory. *Front. Neuroinform.* 13:66. doi: 10.3389/fninf.2019.00066

Colombo, M. A., Napolitani, M., Boly, M., Gosseries, O., Casarotto, S., Rosanova, M., et al. (2019). The spectral exponent of the resting EEG indexes the presence of consciousness during unresponsiveness induced by propofol, xenon, and ketamine. *NeuroImage* 189, 631–644. doi: 10.1016/j.neuroimage.2019.01.024

De Hemptinne, C., Swann, N. C., Ostrem, J. L., Ryapolova-Webb, E. S., San Luciano, M., Galifianakis, N. B., et al. (2015). Therapeutic deep brain stimulation reduces cortical phase-amplitude coupling in Parkinson's disease. *Nat. Neurosci.* 18, 779–786. doi: 10.1038/nn.3997

Deco, G., Ponce-Alvarez, A., Hagmann, P., Romani, G. L., Mantini, D., and Corbetta, M. (2014). How local excitation-inhibition ratio impacts the whole brain dynamics. *J. Neurosci.* 34, 7886–7898. doi: 10.1523/JNEUROSCI.5068-13.2014

Delorme, A., and Makeig, S. (2004). EEGLAB: an open source toolbox for analysis of single-trial EEG dynamics including independent component analysis. *J. Neurosci. Methods* 134, 9–21. doi: 10.1016/j.jneumeth.2003.10.009

Donoghue, T., Haller, M., Peterson, E. J., Varma, P., Sebastian, P., Gao, R., et al. (2020). Parameterizing neural power spectra into periodic and aperiodic components. *Nat. Neurosci.* 23, 1655–1665. doi: 10.1038/s41593-020-00744-x

Einevoll, G. T., Kayser, C., Logothetis, N. K., and Panzeri, S. (2013). Modelling and analysis of local field potentials for studying the function of cortical circuits. *Nat. Rev. Neurosci.* 14, 770–785. doi: 10.1038/nrn3599

Evangelisti, S., Pittau, F., Testa, C., Rizzo, G., Gramegna, L. L., Ferri, L., et al. (2019). L-dopa modulation of brain connectivity in Parkinson's disease patients: a pilot EEG-fmri study. *Front. Neurosci.* 13:611. doi: 10.3389/fnins.2019.00611

Fang, J., Chen, H., Cao, Z., Jiang, Y., Ma, L., Ma, H., et al. (2017). Impaired brain network architecture in newly diagnosed Parkinson's disease based on graph theoretical analysis. *Neurosci. Lett.* 657, 151–158. doi: 10.1016/j.neulet.2017.08.002

Freeman, W. J., and Zhai, J. (2009). Simulated power spectral density (PSD) of background electrocorticogram (ECoG). *Cogn. Neurodyn.* 3, 97–103. doi: 10.1007/s11571-008-9064-y

Gao, L. L., and Wu, T. (2016). The study of brain functional connectivity in Parkinson's disease. *Transl. Neurodegener.* 5:18. doi: 10.1186/s40035-016-0066-0

Gao, R., Peterson, E. J., and Voytek, B. (2017). Inferring synaptic excitation/inhibition balance from field potentials. *NeuroImage* 158, 70–78. doi: 10.1016/j.neuroimage.2017.06.078

George, J. S., Strunk, J., Mak-Mccully, R., Houser, M., Poizner, H., and Aron, A. R. (2013). Dopaminergic therapy in Parkinson's disease decreases cortical beta band coherence in the resting state and increases cortical beta band power during executive control. *NeuroImage Clin.* 3, 261–270. doi: 10.1016/j.nicl.2013.07.013

Gong, R., Wegscheider, M., Mühlberg, C., Gast, R., Fricke, C., Rumpf, J. J., et al. (2021). Spatiotemporal features of β-γ phase-amplitude coupling in Parkinson's disease derived from scalp EEG. *Brain* 144, 487–503. doi: 10.1093/brain/awaa400

Hanajima, R., Ugawa, Y., Terao, Y., Ogata, K., and Kanazawa, I. (1996). Ipsilateral cortico-cortical inhibition of the motor cortex in various neurological disorders. *J. Neurol. Sci.* 140, 109–116. doi: 10.1016/0022-510X(96)00100-1

Hassan, M., Chaton, L., Benquet, P., Delval, A., Leroy, C., Plomhause, L., et al. (2017). Functional connectivity disruptions correlate with cognitive phenotypes in Parkinson's disease. *NeuroImage Clin.* 14, 591–591. doi: 10.1016/j.nicl.2017.03.002

He, B. J. (2014). Scale-free brain activity: past, present, and future. *Trends Cogn. Sci.* 18, 480–487. doi: 10.1016/j.tics.2014.04.003

He, B. J., Zempel, J. M., Snyder, A. Z., and Raichle, M. E. (2010). The temporal structures and functional significance of scale-free brain activity. *Neuron* 66, 353–369. doi: 10.1016/j.neuron.2010.04.020

Heinrichs-Graham, E., Kurz, M. J., Becker, K. M., Santamaria, P. M., Gendelman, H. E., and Wilson, T. W. (2014). Hypersynchrony despite pathologically reduced beta oscillations in patients with Parkinson's disease: a pharmacomagnetoencephalography study. *J. Neurophysiol.* 112, 1739–1747. doi: 10.1152/jn.00383.2014

Herz, D. M., Eickhoff, S. B., Løkkegaard, A., and Siebner, H. R. (2014). Functional neuroimaging of motor control in parkinson's disease: a meta-analysis. *Hum. Brain Mapp.* 35, 3227–3237. doi: 10.1002/hbm.22397

Hindriks, R. (2021). Relation between the phase-lag index and lagged coherence for assessing interactions in EEG and MEG data. *Neuroimage Rep.* 1:100007. doi: 10.1016/j.ynirp.2021.100007

Hirschmann, J., Özkurt, T. E., Butz, M., Homburger, M., Elben, S., Hartmann, C. J., et al. (2011). Distinct oscillatory STN-cortical loops revealed by simultaneous MEG and local field potential recordings in patients with Parkinson's disease. *NeuroImage* 55, 1159–1168. doi: 10.1016/j.neuroimage.2010.11.063

Hirschmann, J., Özkurt, T. E., Butz, M., Homburger, M., Elben, S., Hartmann, C. J., et al. (2013). Differential modulation of STN-cortical and cortico-muscular coherence by movement and levodopa in Parkinson's disease. *NeuroImage* 68, 203–213. doi: 10.1016/j.neuroimage.2012.11.036

Hou, Y., Wei, Q., Ou, R., Yang, J., Song, W., Gong, Q., et al. (2018). Impaired topographic organization in cognitively unimpaired drug-naïve patients with rigidity-dominant Parkinson's disease. *Park. Relat. Disord.* 56, 52–57. doi: 10.1016/j.parkreldis.2018.06.021

Jackson, N., Cole, S. R., Voytek, B., and Swann, N. C. (2019). Characteristics of waveform shape in Parkinson's disease detected with scalp electroencephalography. *eNeuro* 6:ENEURO.0151-19.2019. doi: 10.1523/ENEURO.0151-19.2019

Jech, R., Mueller, K., Schroeter, M. L., and Růžička, E. (2013). Levodopa increases functional connectivity in the cerebellum and brainstem in Parkinson's disease. *Brain* 136:e234. doi: 10.1093/brain/awt015

Kaminski, M., and Blinowska, K. J. (2018). Is graph theoretical analysis a useful tool for quantification of connectivity obtained by means of EEG/MEG Techniques? *Front. Neural Circ.* 12:76. doi: 10.3389/fncir.2018.00076

Kühn, A. A., Tsui, A., Aziz, T., Ray, N., Brücke, C., Kupsch, A., et al. (2009). Pathological synchronisation in the subthalamic nucleus of patients with Parkinson's disease relates to both bradykinesia and rigidity. *Exp. Neurol.* 215, 380–387. doi: 10.1016/j.expneurol.2008.11.008

Lantz, G., Grave de Peralta, R., Spinelli, L., Seeck, M., and Michel, C. M. (2003). Epileptic source localization with high density EEG: how many electrodes are needed? *Clin. Neurophysiol.* 114, 63–69. doi: 10.1016/S1388-2457(02)00337-1

Lindén, H., Pettersen, K. H., and Einevoll, G. T. (2010). Intrinsic dendritic filtering gives low-pass power spectra of local field potentials. *J. Comput. Neurosci.* 29, 423–444. doi: 10.1007/s10827-010-0245-4

Litvak, V., Jha, A., Eusebio, A., Oostenveld, R., Foltynie, T., Limousin, P., et al. (2011). Resting oscillatory cortico-subthalamic connectivity in patients with Parkinson's disease. *Brain* 134, 359–374. doi: 10.1093/brain/awq332

Melgari, J. M., Curcio, G., Mastrolilli, F., Salomone, G., Trotta, L., Tombini, M., et al. (2014). Alpha and beta EEG power reflects L-dopa acute administration in parkinsonian patients. *Front. Aging Neurosci.* 6:302. doi: 10.3389/fnagi.2014.00302

Michely, J., Volz, L. J., Barbe, M. T., Hoffstaedter, F., Viswanathan, S., Timmermann, L., et al. (2015). Dopaminergic modulation of motor network dynamics in Parkinson's disease. *Brain* 138, 664–678. doi: 10.1093/brain/awu381

Miller, A. M., Miocinovic, S., Swann, N. C., Rajagopalan, S. S., Darevsky, D. M., Gilron, R., et al. (2019). Effect of levodopa on electroencephalographic biomarkers of the parkinsonian state. *J. Neurophysiol.* 122, 290–299. doi: 10.1152/jn.00141.2019

Milz, P., Faber, P. L., Lehmann, D., Kochi, K., and Pascual-Marqui, R. D. (2014). sLORETA intracortical lagged coherence during breath counting in meditation-naïve participants. *Front. Hum. Neurosci.* 8:303. doi: 10.3389/fnhum.2014.00303

Mitsis, G. D., Anastasiadou, M. N., Christodoulakis, M., Papathanasiou, E. S., Papacostas, S. S., and Hadjipapas, A. (2020). Functional brain networks of patients with epilepsy exhibit pronounced multiscale periodicities, which correlate with seizure onset. *Hum. Brain Mapp.* 41, 2059–2076. doi: 10.1002/hbm.24930

Molina, J. L., Voytek, B., Thomas, M. L., Joshi, Y. B., Bhakta, S. G., Talledo, J. A., et al. (2020). Memantine effects on electroencephalographic measures of putative excitatory/inhibitory balance in schizophrenia. *Biol. Psychiatry Cogn. Neurosci. Neuroimaging* 5, 562–568. doi: 10.1016/j.bpsc.2020.02.004

Müller, E. J., and Robinson, P. A. (2018). Suppression of parkinsonian beta oscillations by deep brain stimulation: determination of effective protocols. *Front. Comput. Neurosci.* 12:98. doi: 10.3389/fncom.2018.00098

Olanow, C. W., Stern, M. B., and Sethi, K. (2009). The scientific and clinical basis for the treatment of Parkinson disease. *Neurology* 72(21 SUPPL. 4), S1–S136. doi: 10.1212/WNL.0b013e3181a1d44c

Olde Dubbelink, K. T. E., Hillebrand, A., Stoffers, D., Deijen, J. B., Twisk, J. W. R., Stam, C. J., et al. (2014). Disrupted brain network topology in Parkinson's disease: a longitudinal magnetoencephalography study. *Brain* 137, 197–207. doi: 10.1093/brain/awt316

Olde Dubbelink, K. T. E., Stoffers, D., Deijen, J. B., Twisk, J. W. R., Stam, C. J., Hillebrand, A., et al. (2013). Resting-state functional connectivity as a marker of disease progression in Parkinson's disease: a longitudinal MEG study. *NeuroImage Clin.* 2, 612–619. doi: 10.1016/j.nicl.2013.04.003

Oostenveld, R., Fries, P., Maris, E., and Schoffelen, J. M. (2011). FieldTrip: open source software for advanced analysis of MEG, EEG, and invasive electrophysiological data. *Comput. Intell. Neurosci.* 2011:156869. doi: 10.1155/2011/156869

Pascual-Marqui, R. D. (2007). Instantaneous and lagged measurements of linear and nonlinear dependence between groups of multivariate time series: frequency decomposition. *arXiv* [Preprint]. arXiv:0711.1455,

Pascual-Marqui, R. D., Lehmann, D., Koukkou, M., Kochi, K., Anderer, P., Saletu, B., et al. (2011). Assessing interactions in the brain with exact low-resolution electromagnetic tomography. *Philos. Trans. R. Soc. A Math. Phys. Eng. Sci.* 369, 3768–3784. doi: 10.1098/rsta.2011.0081

Peterson, E. J., Rosen, B. Q., Campbell, A. M., Belger, A., and Voytek, B. (2017). 1/F neural noise is a better predictor of schizophrenia than neural oscillations. *bioRxiv [Preprint]* doi: 10.1101/113449

Politis, M., and Niccolini, F. (2015). Serotonin in Parkinson's disease. *Behav. Brain Res.* 277, 136–145. doi: 10.1016/j.bbr.2014.07.037

Pollok, B., Kamp, D., Butz, M., Wojtecki, L., Timmermann, L., Südmeyer, M., et al. (2013). Increased SMA-M1 coherence in Parkinson's disease – Pathophysiology or compensation? *Exp. Neurol.* 247, 178–181. doi: 10.1016/j.expneurol.2013.04.013

Ridding, M. C., Rothwell, J. C., and Inzelberg, R. (1995). Changes in excitability of motor cortical circuitry in patients with parkinson's disease. *Ann. Neurol.* 37, 181–188. doi: 10.1002/ana.410370208

Robertson, M. M., Furlong, S., Voytek, B., Donoghue, T., Boettiger, C. A., and Sheridan, M. A. (2019). EEG power spectral slope differs by ADHD status and stimulant medication exposure in early childhood. *J. Neurophysiol.* 122, 2427–2437. doi: 10.1152/jn.00388.2019

Rockhill, A. P., Jackson, N., George, J., Aron, A., Swann, N. C., et al. (2020). *UC San Diego Resting State EEG Data from Patients with Parkinson's Disease. OpenNeuro. [Dataset]*. doi: 10.18112/openneuro.ds002778.v1.0.4

Ruan, X., Li, Y., Li, E., Xie, F., Zhang, G., Luo, Z., et al. (2020). Impaired topographical organization of functional brain networks in Parkinson's disease patients with freezing of gait. *Front. Aging Neurosci.* 12:580564. doi: 10.3389/fnagi.2020.580564

Rubinov, M., and Sporns, O. (2010). Complex network measures of brain connectivity: uses and interpretations. *NeuroImage* 52, 1059–1069. doi: 10.1016/j.neuroimage.2009.10.003

Sang, L., Zhang, J., Wang, L., Zhang, J., Zhang, Y., Li, P., et al. (2015). Alteration of brain functional networks in early-stage Parkinson's disease: a resting- state fMRI study. *PLoS One* 10:e0141815. doi: 10.1371/journal.pone.0141815

Schapira, A. H. V. (2005). Present and future drug treatment for Parkinson's disease. *Journal of Neurology, Neurosurgery and Psychiatry* 76, 1472–1478. doi: 10.1136/jnnp.2004.035980

Schaworonkow, N., and Voytek, B. (2021). Longitudinal changes in aperiodic and periodic activity in electrophysiological recordings in the first seven months of life. *Dev. Cogn. Neurosci.* 47:100895. doi: 10.1016/j.dcn.2020.100895

Sharma, A., Vidaurre, D., Vesper, J., Schnitzler, A., and Florin, E. (2021). Differential dopaminergic modulation of spontaneous cortico–subthalamic activity in parkinson's disease. *eLife* 10:e66057. doi: 10.7554/eLife.66057

Shen, Y., Hu, J., Chen, Y., Liu, W., Li, Y., Yan, L., et al. (2020). Levodopa changes functional connectivity patterns in subregions of the primary motor cortex in patients With Parkinson's Disease. *Front. Neurosci.* 14:647. doi: 10.3389/fnins.2020.00647

Siegel, M., Buschman, T. J., and Miller, E. K. (2015). Cortical information flow during flexible sensorimotor decisions. *Science* 348, 1352–1355. doi: 10.1126/science.aab0551

Silberstein, P., Pogosyan, A., Kühn, A. A., Hotton, G., Tisch, S., Kupsch, A., et al. (2005). Cortico-cortical coupling in Parkinson's disease and its modulation by therapy. *Brain* 128, 1277–1291. doi: 10.1093/brain/awh480

Smith, R. J., Alipourjeddi, E., Garner, C., Maser, A. L., Shrey, D. W., and Lopour, B. A. (2021). Infant functional networks are modulated by state of consciousness and circadian rhythm. *Netw. Neurosci.* 5, 614–630. doi: 10.1162/netn_a_00194

Stam, C. J., Jones, B. F., Nolte, G., Breakspear, M., and Scheltens, P. (2007). Small-world networks and functional connectivity in Alzheimer's disease. *Cereb. Cortex* 17, 92–99. doi: 10.1093/cercor/bhj127

Stanzione, P., Marciani, M. G., Maschio, M., Bassetti, M. A., Spanedda, F., Pierantozzi, M., et al. (1996). Quantitative EEG changes in non-demented Parkinson's disease patients before and during L-dopa therapy. *Eur. J. Neurol.* 3, 354–362. doi: 10.1111/j.1468-1331.1996.tb00229.x

Steiner, H., and Kitai, S. T. (2001). Unilateral striatal dopamine depletion: time-dependent effects on cortical function and behavioural correlates. *Eur. J. Neurosci.* 14, 1390–1404. doi: 10.1046/j.0953-816X.2001.01756.x

Stoffers, D., Bosboom, J. L. W., Deijen, J. B., Wolters, E. C., Berendse, H. W., and Stam, C. J. (2007). Slowing of oscillatory brain activity is a stable characteristic of Parkinson's disease without dementia. *Brain* 130, 1847–1860. doi: 10.1093/brain/awm034

Stoffers, D., Bosboom, J. L. W., Wolters, E. C., Stam, C. J., and Berendse, H. W. (2008). Dopaminergic modulation of cortico-cortical functional connectivity in Parkinson's disease: an MEG study. *Exp. Neurol.* 213, 191–195. doi: 10.1016/j.expneurol.2008.05.021

Sun, S., Li, X., Zhu, J., Wang, Y., La, R., Zhang, X., et al. (2019). Graph theory analysis of functional connectivity in major depression disorder with high-density resting state EEG Data. *IEEE Trans. Neural Syst. Rehabil. Eng.* 27, 429–439. doi: 10.1109/TNSRE.2019.2894423

Suo, X., Lei, D., Li, N., Cheng, L., Chen, F., Wang, M., et al. (2017). Functional brain connectome and its relation to hoehn and yahr stage in Parkinson disease. *Radiology* 285, 904–913. doi: 10.1148/radiol.2017162929

Swann, N. C., De Hemptinne, C., Aron, A. R., Ostrem, J. L., Knight, R. T., and Starr, P. A. (2015). Elevated synchrony in Parkinson disease detected with electroencephalography. *Ann. Neurol.* 78, 742–750. doi: 10.1002/ana.24507

Tahmasian, M., Bettray, L. M., van Eimeren, T., Drzezga, A., Timmermann, L., Eickhoff, C. R., et al. (2015). A systematic review on the applications of resting-state fMRI in Parkinson's disease: does dopamine replacement therapy play a role? *Cortex* 73, 80–105. doi: 10.1016/j.cortex.2015.08.005

Tessitore, A., Cirillo, M., and De Micco, R. (2019). Functional connectivity signatures of Parkinson's disease. *Journal of Parkinson's Disease* 9, 637–652. doi: 10.3233/JPD-191592

Tinkhauser, G., Pogosyan, A., Tan, H., Herz, D. M., Kühn, A. A., and Brown, P. (2017). Beta burst dynamics in Parkinson's disease off and on dopaminergic medication. *Brain* 140, 2968–2981. doi: 10.1093/brain/awx252

Utianski, R. L., Caviness, J. N., van Straaten, E. C. W., Beach, T. G., Dugger, B. N., Shill, H. A., et al. (2016). Graph theory network function in parkinson's disease assessed with electroencephalography. *Clin. Neurophysiol.* 127, 2228–2236. doi: 10.1016/j.clinph.2016.02.017

van den Heuvel, M. P., de Lange, S. C., Zalesky, A., Seguin, C., Yeo, B. T. T., and Schmidt, R. (2017). Proportional thresholding in resting-state fMRI functional connectivity networks and consequences for patient-control connectome studies: issues and recommendations. *NeuroImage* 152, 437–449. doi: 10.1016/j.neuroimage.2017.02.005

van Wijk, B. C. M., Beudel, M., Jha, A., Oswal, A., Foltynie, T., Hariz, M. I., et al. (2016). Subthalamic nucleus phase-amplitude coupling correlates with motor impairment in Parkinson's disease. *Clin. Neurophysiol.* 127, 2010–2019. doi: 10.1016/j.clinph.2016.01.015

Vecchio, F., Miraglia, F., Alù, F., Cotelli, M., Pellicciari, M. C., Judica, E., et al. (2021). Human brain networks in physiological and pathological aging: reproducibility of EEG graph theoretical analysis in cortical connectivity. *Brain Connect.* 12, 41–51. doi: 10.1089/brain.2020.0824

Voytek, B., Kramer, M. A., Case, J., Lepage, K. Q., Tempesta, Z. R., Knight, R. T., et al. (2015). Age-related changes in 1/f neural electrophysiological noise. *J. Neurosci.* 35, 13257–13265. doi: 10.1523/JNEUROSCI.2332-14.2015

Watts, D., and Strogatz, S. (1998). Collective dynamics of 'small-world' networks. *Nature* 393, 440–442. doi: 10.1038/30918

Whitmer, D., de Solages, C., Hill, B., Yu, H., Henderson, J. M., and Bronte-Stewart, H. (2012). High frequency deep brain stimulation attenuates subthalamic and cortical rhythms in Parkinson's disease. *Fron. Hum. Neurosci.* 6:155. doi: 10.3389/fnhum.2012.00155

Wingeier, B., Tcheng, T., Koop, M. M., Hill, B. C., Heit, G., and Bronte-Stewart, H. M. (2006). Intra-operative STN DBS attenuates the prominent beta rhythm in the STN in Parkinson's disease. *Exp. Neurol.* 197, 244–251. doi: 10.1016/j.expneurol.2005.09.016

Zeng, K., Wang, Y., Ouyang, G., Bian, Z., Wang, L., and Li, X. (2015). Complex network analysis of resting state EEG in amnestic mild cognitive impairment patients with type 2 diabetes. *Front. Comput. Neurosci.* 9:133. doi: 10.3389/fncom.2015.00133

Zhang, J., Idaji, M. J., Villringer, A., and Nikulin, V. V. (2021). Neuronal biomarkers of Parkinson's disease are present in healthy aging. *NeuroImage* 243:118512. doi: 10.1016/j.neuroimage.2021.118512

Zhou, S., and Yu, Y. (2018). Synaptic E-I balance underlies efficient neural coding. *Front. Neurosci.* 12:46. doi: 10.3389/fnins.2018.00046

Zhou, X., Ma, N., Song, B., Wu, Z., Liu, G., Liu, L., et al. (2021). Optimal organization of functional connectivity networks for segregation and integration with large-scale critical dynamics in human brains. *Front. Comput. Neurosci.* 15:641335. doi: 10.3389/fncom.2021.641335

Conflict of Interest: The authors declare that the research was conducted in the absence of any commercial or financial relationships that could be construed as a potential conflict of interest.

Publisher's Note: All claims expressed in this article are solely those of the authors and do not necessarily represent those of their affiliated organizations, or those of the publisher, the editors and the reviewers. Any product that may be evaluated in this article, or claim that may be made by its manufacturer, is not guaranteed or endorsed by the publisher.

frontiers | Frontiers in Aging Neuroscience

TYPE Original Research
PUBLISHED 26 January 2023
DOI 10.3389/fnagi.2023.780014

OPEN ACCESS

EDITED BY
Aneta Kielar,
University of Arizona,
United States

REVIEWED BY
Jonathan Cole,
Bournemouth University,
United Kingdom
Lars Meyer,
Max Planck Society,
Germany

*CORRESPONDENCE
Susanna Lopez
✉ susanna.lopez@uniroma1.it

SPECIALTY SECTION
This article was submitted to Neurocognitive Aging and Behavior, a section of the journal Frontiers in Aging Neuroscience

RECEIVED 20 September 2021
ACCEPTED 05 January 2023
PUBLISHED 26 January 2023

CITATION
Lopez S, Del Percio C, Lizio R, Noce G, Padovani A, Nobili F, Arnaldi D, Famà F, Moretti DV, Cagnin A, Koch G, Benussi A, Onofrj M, Borroni B, Soricelli A, Ferri R, Buttinelli C, Giubilei F, Güntekin B, Yener G, Stocchi F, Vacca L, Bonanni L and Babiloni C (2023) Patients with Alzheimer's disease dementia show partially preserved parietal 'hubs' modeled from resting-state alpha electroencephalographic rhythms. *Front. Aging Neurosci.* 15:780014. doi: 10.3389/fnagi.2023.780014

Patients with Alzheimer's disease dementia show partially preserved parietal 'hubs' modeled from resting-state alpha electroencephalographic rhythms

Susanna Lopez[1]*, Claudio Del Percio[1], Roberta Lizio[1], Giuseppe Noce[2], Alessandro Padovani[3], Flavio Nobili[4,5], Dario Arnaldi[4,5], Francesco Famà[5], Davide V. Moretti[6], Annachiara Cagnin[7], Giacomo Koch[8,9], Alberto Benussi[3], Marco Onofrj[10], Barbara Borroni[3], Andrea Soricelli[2,11], Raffaele Ferri[12], Carla Buttinelli[13], Franco Giubilei[13], Bahar Güntekin[14,15], Görsev Yener[16,17], Fabrizio Stocchi[18,19], Laura Vacca[18], Laura Bonanni[20] and Claudio Babiloni[1,21]

[1]Department of Physiology and Pharmacology "Vittorio Erspamer", Sapienza University of Rome, Rome, Italy, [2]IRCCS Synlab SDN, Naples, Italy, [3]Neurology Unit, Department of Clinical and Experimental Sciences, University of Brescia, Brescia, Italy, [4]Clinica Neurologica, IRCCS Ospedale Policlinico San Martino, Genova, Italy, [5]Dipartimento di Neuroscienze, Oftalmologia, Genetica, Riabilitazione e Scienze Materno-infantili (DiNOGMI), Università di Genova, Genova, Italy, [6]Alzheimer's Disease Rehabilitation Unit, IRCCS Istituto Centro San Giovanni di Dio Fatebenefratelli, Brescia, Italy, [7]Department of Neurosciences, University of Padua, Padova, Italy, [8]Non-Invasive Brain Stimulation Unit/Department of Behavioral and Clinical Neurology, Santa Lucia Foundation IRCCS, Rome, Italy, [9]Stroke Unit, Department of Neuroscience, Tor Vergata Policlinic, Rome, Italy, [10]Department of Neuroscience Imaging and Clinical Sciences and CESI, University "G. D'Annunzio" of Chieti-Pescara, Chieti, Italy, [11]Department of Motor Sciences and Healthiness, University of Naples Parthenope, Naples, Italy, [12]Oasi Research Institute – IRCCS, Troina, Italy, [13]Department of Neuroscience, Mental Health and Sensory Organs, Sapienza University of Rome, Rome, Italy, [14]Department of Biophysics, School of Medicine, Istanbul Medipol University, Istanbul, Türkiye, [15]Research Institute for Health Sciences and Technologies (SABITA), Istanbul Medipol University, Istanbul, Türkiye, [16]Department of Neurology, Dokuz Eylül University Medical School, Izmir, Türkiye, [17]Faculty of Medicine, Izmir University of Economics, Izmir, Türkiye, [18]Institute for Research and Medical Care, IRCCS San Raffaele Roma, Rome, Italy, [19]Telematic University San Raffaele, Rome, Italy, [20]Department of Medicine and Aging Sciences, University G. D'Annunzio of Chieti-Pescara, Chieti, Italy, [21]San Raffaele of Cassino, Cassino, Italy

Introduction: Graph theory models a network by its nodes (the fundamental unit by which graphs are formed) and connections. 'Degree' hubs reflect node centrality (the connection rate), while 'connector' hubs are those linked to several clusters of nodes (mainly long-range connections).

Methods: Here, we compared hubs modeled from measures of interdependencies of between-electrode resting-state eyes-closed electroencephalography (rsEEG) rhythms in normal elderly (Nold) and Alzheimer's disease dementia (ADD) participants. At least 5min of rsEEG was recorded and analyzed. As ADD is considered a 'network disease' and is typically associated with abnormal rsEEG delta (<4Hz) and alpha rhythms (8–12Hz) over associative posterior areas, we tested the hypothesis of abnormal posterior hubs from measures of interdependencies of rsEEG rhythms from delta to gamma bands (2–40Hz) using eLORETA bivariate and multivariate-directional techniques in ADD participants versus Nold participants. Three different definitions of 'connector' hub were used.

Results: Convergent results showed that in both the Nold and ADD groups there were significant parietal 'degree' and 'connector' hubs derived from alpha rhythms. These hubs had a prominent outward 'directionality' in the two groups, but that 'directionality' was lower in ADD participants than in Nold participants.

Discussion: In conclusion, independent methodologies and hub definitions suggest that ADD patients may be characterized by low outward 'directionality' of partially preserved parietal 'degree' and 'connector' hubs derived from rsEEG alpha rhythms.

KEYWORDS

resting-state eyes closed electroencephalographic (rseeg) rhythms, alzheimer's disease with dementia (add), interdependencies of rseeg rhythms, linear lagged connectivity, graph theory, hub topology

1. Introduction

Alzheimer's disease (AD) is the most prevalent neurodegenerative disorder in the elderly and causes cognitive deficits (e.g., episodic and working memory, executive functions, visuospatial abilities, language, etc.) and disabilities in activities of daily living progressively (i.e., loss of autonomy) belonging to dementia as a clinical syndrome (Tahami Monfared et al., 2022). It is provoked by the abnormal accumulation in the brain of Ab-42 and tau proteins, so the neurobiological *in vivo* diagnosis can be made using techniques that measure that accumulation, such as analysis of cerebrospinal fluid and positron emission tomography (Jack et al., 2019).

AD is considered a pathology affecting functional brain connectivity (Teipel et al., 2016). In this area of research, previous structural and resting-state functional magnetic resonance imaging (sMRI and rs-fMRI) studies showed colocalized abnormalities in both interhemispheric and intrahemispheric cortical connectivity in ADD patients compared with healthy elderly people (Nold) with unimpaired cognition (Delbeuck et al., 2003; Busche and Konnerth, 2016; Nakamura et al., 2017). Thanks to the high spatial resolution of MRI techniques (i.e., millimeters), those abnormalities were mainly localized as follows: (1) in the posterior parietal (precuneus) and cingulate cortices of the cortical default mode network (DMN; Bokde et al., 2006; Sorg et al., 2007; Brier et al., 2012; Wang et al., 2013, 2015; Joo et al., 2016; Eyler et al., 2019; Talwar et al., 2021; Zhang et al., 2021); (2) in the occipital and inferior parietal gyrus (Wang et al., 2021); and (3) in the medial temporal lobe and other nodes of the limbic system (Talwar et al., 2021).

Another significant contribution made by the sMRI and rs-fMRI studies, together with other brain research techniques, was to unveil the abnormal topological organization underlying the above alterations in the functional brain connectivity observed in ADD patients [see reviews by Reijneveld et al. (2007), Xie and He (2012), Stam (2014)]. In this topological organization, a cortical neural network can be formally represented by a 'graph' constituted of 'nodes' interconnected by 'edges'. Notably, the topology of 'nodes' and 'graphs' globally reflects the following properties of a network: (1) near cortical nodes can be highly interconnected to each other forming 'clusters', and the nodes with more edges may have a prominent central role and underpin the **modularity** and **segregation** of the information within a network; (2) a few cortical nodes, the 'hubs', can ensure long-range interconnections between 'clusters' and may reduce the path length between far nodes and underpin the **integration** of the information within a network; (3) the 'degree centrality' or 'nodal degree' can define the importance of the hub, the 'hub centrality', in the information transmission within a brain network; (4) a hub can be classified as 'connector', connecting several different network modules, or 'provincial', mostly connecting nodes in the same network module as measured by the hub 'participation coefficient'; (5) the number of the shortest paths that pass through a cortical node defines the node importance, the 'betweenness centrality', in the information transmission within a brain network; (6) a few highly connected cortical nodes may show dense interconnections with each other and form a sort of 'rich club' structure with a particular importance in the network information processing; (7) the topological distance between nodes, i.e., the mean number of edges to connect them, the 'global efficiency', is inversely related to effective parallel information transfer and integrated processing; and (8) an optimal balance between the network modularity (segregation) and integration of the nodes defines the so-called 'small worldness' structure, which is a favorable for information processing and shows **resilience** to insults impairing cortical nodes (Bullmore and Sporns, 2009, 2012; He and Evans, 2010; van den Heuvel and Sporns, 2011; Sporns, 2013; Wang et al., 2015; Liao et al., 2017).

Previous rs-fMRI studies also showed that compared with Nold people, ADD patients were characterized by decreased network segregation, as revealed by lower clustering/modular structure of the network graphs (Supekar et al., 2008; Chen et al., 2013) and higher network integration structure, as revealed by lower characteristic path length among the cortical nodes (Sanz-Arigita et al., 2010). Furthermore, prodromal ADD patients with mild cognitive impairment (ADMCI) compared with controls showed a higher global 'clustering coefficient', while ADD patients presented a higher hub 'participation coefficient' in the inferior parietal cortex, prefrontal cortex, precuneus, and somatomotor cortex (Ng et al., 2021). By contrast, diffusion MRI showed the following opposite picture in ADD patients over Nold persons: (1) lower network segregation, as revealed by a higher 'clustering coefficient' (Yao et al., 2010; Daianu et al., 2013); (2) lower efficiency of the network structure in relation to memory and executive performances (Lo et al., 2010; Reijmer et al., 2013); and (3) lower network integration, as revealed by higher characteristic 'path length' (Lo et al., 2010; Yao et al., 2010).

It should be remarked that the rs-fMRI has a low temporal resolution of about 1 s, which is insufficient to investigate the interdependency between the emerging activity of neural brain populations at frequencies higher than 0.5 Hz. Therefore, electroencephalographic (EEG) techniques were used to explore that interdependency at a larger frequency spectrum, as they have a high temporal resolution of <1 ms, despite a moderate spatial resolution of centimeters (de Haan et al., 2012). Previous EEG studies showed abnormalities in several measures of the interrelatedness of rsEEG rhythms at electrode or source pairs. Compared with Nold persons, ADD patients presented lower 'spectral coherence' at alpha (8–12 Hz) and beta (13–20 Hz) rhythms, especially at temporo-parieto-occipital and fronto-parietooccipital electrode pairs; notably, 'spectral coherence' is the most popular linear measure of the interrelatedness of rsEEG activity (Leuchter et al., 1992; Dunkin et al., 1994; Locatelli et al., 1998;

Jelic et al., 2000; Adler et al., 2003). Similarly, ADD and ADMCI patients exhibited lower interrelatedness of temporo-parieto-occipital and/or fronto-parietooccipital rsEEG alpha rhythms, as revealed by the following procedures: the 'phase lag index', a spectral measure of the phase difference distribution asymmetry (Stam et al., 2007b; Yu et al., 2016; Peraza et al., 2018), 'synchronization likelihood', a measure sensitive to both linear and non-linear interrelatedness of rsEEG activity (Babiloni et al., 2004b, 2006b), and 'linear lagged connectivity', a measure of the interrelatedness of rsEEG activity without the zero-lag component sensitive to the head volume conduction effects (Babiloni et al., 2018, 2019).

The above rsEEG findings were confirmed and extended by measures reflecting the directionality of the interrelatedness of rsEEG activity from one electrode/source to another, such as the 'directed transfer function' derived from Granger causality and autoregressive methods (Blinowska, 2011; Blinowska et al., 2017). ADD and ADMCI patients exhibited lower interrelatedness of the temporo-parieto-occipital and/or fronto-parietooccipital rsEEG alpha rhythms, as revealed by "directed transfer function" (Dauwels et al., 2009, 2010). Furthermore, there was a reduced prominence of the interrelatedness from parietal to frontal electrodes at the alpha and beta (13–35 Hz) rhythms (Babiloni et al., 2008, 2009a,b; Blinowska et al., 2017).

Concerning the rsEEG delta (<4 Hz) and/or theta (4–7 Hz) rhythms, most of the studies showed higher measures of the interrelatedness of topographically widespread rsEEG activity, intrahemispherically and inter-hemispherically; those measures were derived from the 'spectral coherence', 'directed transfer function', and 'linear lagged connectivity' (Babiloni et al., 2008, 2009a,b, 2010, 2018, 2019; Sankari et al., 2011; Canuet et al., 2012; Yu et al., 2016; Blinowska et al., 2017), with some exceptions (Knott et al., 2000; Adler et al., 2003).

Previous rsEEG studies also revealed the abnormal network topology of the interrelatedness of rsEEG rhythms at electrode/source pairs in ADD patients. Compared with Nold people, ADD and ADMCI patients showed a more random topology of the interrelatedness of rsEEG rhythms at an electrode or source pairs, possibly due to reduced 'small worldness' properties of brain networks (Reijneveld et al., 2007; Stam et al., 2007a; de Haan et al., 2009; Frantzidis et al., 2014; Vecchio et al., 2014, 2016; Hallett et al., 2020). This general effect was reported at the delta, alpha, and beta rhythms on the whole scalp (Stam et al., 2007a; de Haan et al., 2009; Vecchio et al., 2014, 2016) and in AD-vulnerable regions, such as the frontal and parietal regions (Frantzidis et al., 2014).

Moreover, beyond the 'small worldness' property, ADD patients were characterized by abnormalities in the following graph network indexes: (1) a shift of the 'betweenness centrality' center of mass from posterior to anterior alpha rhythms in relation to disease severity, as revealed by the 'phase lag index' (Engels et al., 2015); (2) a parietal and occipital loss of the network organization from theta and alpha rhythms, as revealed by the 'phase lag index' (Yu et al., 2016); (3) hub rearrangement and functioning at different rsEEG frequency bands, as revealed by several interrelatedness measures (Stam et al., 2007a; De Haan et al., 2009; Frantzidis et al., 2014; Engels et al., 2015; Song et al., 2019; Das and Puthankattil, 2022); (4) lower 'global efficiency', increased 'local efficiency', and lower resilience of cortical networks from the rsEEG alpha and beta rhythms, as revealed by the Granger 'directed transfer function' (Afshari and Jalili, 2017); and (5) reduced graph 'local and global efficiency' values from lower inward and outward directions of the interrelatedness derived from the whole-band rsEEG activity by another Granger measure based on a conditional multivariate vector autoregression model. Notably, the maximum abnormalities of the 'hub degree' were observed at parietal electrodes (Franciotti et al., 2019), whereas no changes in the global network organization from the whole-band rsEEG activity were found by 'mutual information' measures of that interrelatedness (Franciotti et al., 2022).

Considering the above rsEEG findings, both ADD and ADMCI patients showed reduced efficient information exchange in the cortical neural networks, as revealed by their more random topology. However, no previous study in those patients focused on the integrity of the parietal hubs derived from the rsEEG alpha rhythms, although it is well known that ADD patients show the following significant abnormalities: (1) impairment in the parietal nodes of the cortical DMN (Bokde et al., 2006; Sorg et al., 2007; Brier et al., 2012; Wang et al., 2015; Joo et al., 2016; Eyler et al., 2019; Talwar et al., 2021; Zhang et al., 2021); (2) reduced interrelatedness of the parietal rsEEG alpha rhythms electrode or source pairs (Leuchter et al., 1992; Locatelli et al., 1998; Jelic et al., 2000; Babiloni et al., 2004a, 2006a, 2018, 2019; Stam et al., 2007b; Yu et al., 2016; Peraza et al., 2018); and (3) reduced power density of the occipital and parietal rsEEG alpha rhythms (reviewed by Babiloni et al., 2021).

In ADD patients, the abnormal reduction in rsEEG alpha rhythms may be related to disorders in the regulation of quiet vigilance. This functional interpretation is based on, among others, the following findings: (1) in healthy volunteers, posterior (eyes closed) rsEEG alpha rhythms were modulated in amplitude after transcranial magnetic stimulations over angular gyrus, a core region of the DMN, but not over control regions of the dorsal attention network (Capotosto et al., 2012); (2) those rsEEG alpha rhythms also reduced in amplitude 1 min before the onset of sleep stage 1 (Morikawa et al., 2002); (3) furthermore, they decreased in amplitude and theta rhythms increased in amplitude during the transition from quiet vigilance to drowsiness, behaviorally tested by both EEG spectral measures and reaction time and decision making to auditory stimuli (Jagannathan et al., 2018, 2022); and (4) moreover, a night of sleep deprivation reduced the posterior rsEEG alpha rhythms in healthy volunteers and visual attention performances (placebo condition), whereas an acute dose of an amphetamine (experimental condition) after sleep deprivation recovered both the posterior EEG alpha rhythms and those performances (Del Percio et al., 2019).

To fill the above literature gap, the present study explored the integrity of the parietal graph-based hubs derived from the rsEEG alpha rhythms in mild-to-moderate ADD patients compared with Nold people. In the present study, all methods for estimating the directional (isolated lagged effective coherence, iCoh) and non-directional (linear lagged connectivity, LLC) interrelatedness of the rsEEG activity at electrode pairs are implemented in the freeware platform called eLORETA.[1] Along the same line, the methods for computing the Graph Theory indexes are implemented in the freeware platform called GraphVar.[2] These methods were chosen to (1) use different mathematical approaches to measure that interrelatedness, (2) compare the results, (3) promote open science, and (4) allow easier cross-validation of the present results in the future. Notably, we did not want to provide a methodological standard for applying graph theory analysis. Rather, we provided a proof of concept of how the results may be affected by different thresholds and criteria.

1 https://www.uzh.ch/keyinst/loreta

2 https://www.nitrc.org/projects/graphvar

10.3389/fnagi.2023.780014

TABLE 1 Demographic, clinical, neuropsychological, and neurophysiological characteristics of the normal elderly (Nold) subject and Alzheimer's Disease with Dementia (ADD) patients enrolled in the present study.

Group	*N*	Age (± SEM)	Education (± SEM)	Gender (M/F)	MMSE (± SEM)	TF (± SEM)	IAF (± SEM)
Nold	40	73.8 (± 1.0)	9.1 (± 0.5)	20/20	28.6 (± 0.2)	5.7 (± 0.1)	9.0 (± 0.2)
ADD	37	73.7 (± 1.0)	8.7 (± 0.8)	17/20	18.7 (± 0.6)	5.3 (± 0.2)	8.6 (± 0.3)
Statistical comparisons	–	t test, n.s.	t test, n.s.	–	Mann–Whitney, $p < 0.0001$	t test, n.s.	t test, n.s.

SEM, standard error of the mean; MMS, Mini-Mental State Examination; TF, transition frequency; IAF, individual alpha frequency; n.s., not significant.

2. Materials and methods

2.1. Subjects

For the present study, we used the clinical and rsEEG data of 40 ADD patients and 40 control Nold people carefully matched for age, gender, and education and enrolled by clinical units of our Consortium (data from three ADD patients were irremediable artifacts or relevant missing data, so were not considered further). The Local institutional Ethics Committees approved the present study. All experiments were performed with the informed and overt consent of each participant or caregiver, in line with the Code of Ethics of the World Medical Association (Declaration of Helsinki) and the standards established by the local Institutional Review Board.

Table 1 summarizes the most relevant demographic (i.e., age, gender, and education) and clinical (i.e., MMSE score) features of the Nold and ADD participants. Furthermore, it shows the results of the statistical comparisons ($p < 0.05$) of age (*t*-test), gender (Fisher test), education (*t*-test), and MMSE score (Mann–Whitney *U* test) between the two groups. As expected, a statistically significant difference was found for the MMSE score ($p < 0.001$), indicating a higher score in the Nold group than the ADD group. No difference was found for the age, gender, and education between the two groups ($p > 0.05$ uncorrected).

In Table 1, the mean values of TF and IAF for the Nold and ADD groups, together with the results of the statistical comparisons between them (*t*-test), are also reported. No statistically significant differences were observed for TF and IAF values ($p > 0.05$ uncorrected).

2.2. Diagnostic criteria

In all clinical units, probable ADD was diagnosed based on the criteria of the Diagnostic and Statistical Manual of Mental Disorders, fourth edition (DSM-IV-TR; American Psychiatric Association), and the National Institute of Neurological Disorders and Stroke-Alzheimer Disease and Related Disorders (NINCDS-ADRDA) working group (McKhann et al., 1984, 2011). Diagnostic criteria refer to the time period when diagnoses were performed. All ADD individuals underwent medical, neuropsychological, neurological, psychiatric, and neuroimaging evaluations, according to standard procedures at each center and based on the expertise of each clinician. The procedures followed by all clinical units included the Instrumental Activities of Daily Living scale (IADL; Lawton and Brody, 1969), the Mini-Mental State Examination (MMSE; Folstein et al., 1975), the Clinical Dementia Rating scale (CDR; Hughes et al., 1982), the Geriatric Depression Scale (GDS; Yesavage et al., 1982), and the Hachinski Ischemic Score scale (HIS; Rosen et al., 1980).

Inclusion criteria included the clinical diagnosis of AD based on the above procedures and the determination of a worsening episodic memory in the last 6 months, thus referring to patients with typical ADD clinical presentation. According to the Alzheimer's Disease Neuroimaging Initiative (ADNI),[3] the MMSE score had to be 24 or lower. Additionally, inclusion criteria included the visual analysis of structural T1-weighted magnetic resonance images (MRIs) by local radiologists; those images had to be compatible with ADD diagnosis (Albert et al., 2011). Cognitive deficits were assessed by standard neuropsychological tests in the domains of episodic memory, language, executive function/attention, and visuoconstruction abilities (local normative reference thresholds). Only some of the patients received the CERAD-plus battery. In general, the tests assessing episodic memory included the delayed recall of Rey figures (Rey, 1959) and/or the delayed recall of a story (Spinnler and Tognoni, 1987). The tests assessing language included the 1-min verbal fluency for letters, fruits, animals, or car trades (Novelli et al., 1986), and/or the Token test (Spinnler and Tognoni, 1987). The tests assessing executive function and attention included the Trail Making Test Part A and B (Reitan, 1958). Finally, the tests assessing visuoconstruction abilities included the copy of Rey figures (Rey, 1959). This inhomogeneity derived from the retrospective nature of the study, with data collected during a clinical routine at each center.

Exclusion criteria included major neuropsychiatric disorders and other types or causes of dementia, such as frontotemporal dementia (Rascovsky et al., 2011), vascular dementia diagnosed based on the National Institute of Neurological Disorders and Stroke and Association Internationale pour la Recherché et l'Enseignement en Neurosciences (NINDS-AIREN) working group (Gorelick et al., 2011), Parkinson disease (Gelb et al., 1999), dementia with Lewy Bodies (McKeith et al., 2005), metabolic syndrome, nutritional deficits, tumors, epilepsy, etc. Exclusion criteria also included visual analysis of structural T2-weighted MRIs by local radiologists to exclude major cerebrovascular lesions, as well as the chronic use of psychoactive drugs except for acetylcholinesterase inhibitors (all patients chronically took them) and/or NMDA receptor antagonists.

The Nold participants received a cognitive, physical, and neurological examination to exclude the presence of cognitive deficits and psychiatric disorders. According to ADNI, the MMSE score had to be 27 or higher. Additionally, all Nold participants had a GDS score lower than the threshold of 5 (no depression) or were verified as not having depression after an interview with a physician or clinical psychologist. Those affected by chronic systemic illnesses (e.g., diabetes mellitus) were excluded, as well as participants receiving chronic psychoactive drugs. Assessed Nold people were also excluded if they had, currently or historically, neurological or psychiatric diseases and drug or alcohol abuse issues.

3 http://adni.loni.usc.edu

In ADD and Nold participants, pharmacological administration (when planned) of routine drugs was postponed until after the rsEEG recordings and performed in hospital settings in the morning. Although this procedure did not guarantee a full washout of the drugs, it synchronized the timing of drug administration. Longer periods of suspension would not have been valid for obvious ethical reasons.

2.3. Resting state eyes-closed electroencephalographic recordings

In all clinical units, the Nold and ADD participants were kindly asked to stay relaxed with their eyes closed during the experiments. They were also kindly asked not to move or talk and keep their mind wandering without focused mentalization. During the experimental recordings, the researchers controlled for the subject's behavioral condition and ongoing rsEEG traces (specifically the amplitude of alpha waves on posterior regions and the onset of slow-wave activity in frontal regions), helping the participants to keep an adequate level of vigilance (i.e., avoiding drowsiness and sleep onset). These alarms were annotated in the protocol for the preliminary rsEEG data analysis phase. The above instructions and procedures were similar in all clinical units even if the respective protocols were not identical.

At least 5 min of electrophysiological data were recorded by professional digital EEG systems authorized for clinical applications (i.e., EB-Neuro Be-light, Micromed, Brain Product, etc.). For this purpose, 19 exploring scalp electrodes were placed according to the 10–20 montage system (i.e., Fp1, Fp2, F7, F3, Fz, F4, F8, T7, C3, Cz, C4, T8, P7, P3, Pz, P4, P8, O1, and O2; Figure 1).

The ground electrodes were placed in the posterior midline, while the reference electrodes were located in different positions across participating clinical units (i.e., linked earlobes, mastoids, vertex, etc.), in line with local standard protocols and clinical trials. During the rsEEG recordings, scalp electrode impedances were kept below 5 KOhm. The rsEEG recordings were performed using 128 Hz or a higher sampling rate (i.e., 128–1,024 Hz) with an adequate antialiasing band pass between 0.01 Hz and 60–100 Hz.

In addition to the rsEEG recording, bipolar vertical and horizontal electrooculographic (EOG) signals and one-channel electrocardiographic (ECG) signals were also acquired using the same sampling frequency adopted for recording the rsEEG data (128–1,024 Hz). Consequently, rsEEG, EOG, and ECG signals had the same sampling rate, so EOG and ECG signals could be used for artifact detection and their off-line correction when adequate.

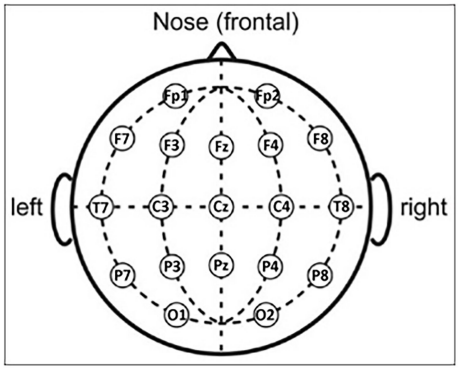

FIGURE 1
Scalp electrode positioning of the 19 electrodes according to the international standard 10–20.

As mentioned above, some rsEEG datasets were recorded using a relatively low sampling frequency of 128 Hz (i.e., 6 out of 40 rsEEG datasets collected for the Nold group and 4 out of 37 rsEEG datasets collected for the ADD group). It should be remarked that such a sampling frequency is suboptimal for an ideal reconstruction of rsEEG signal beyond 40 Hz without aliasing. Ideally, a factor of 3–4 between the low-band pass limit and the rsEEG sampling frequency should be set.

2.4. Preliminary rsEEG data analysis

Data analysis was centrally performed by the group located at the Department of Physiology and Pharmacology 'Erspamer' of Sapienza University of Rome, Italy. In the preliminary analysis, the rsEEG data were split into 2-s epochs and analyzed off-line. This segmentation allowed the use of standard toolboxes for the spectral analysis of rsEEG activity, such as fast Fourier transform (FFT) implemented in the official eLORETA platform. This analysis assumes the stationarity of rsEEG activity. Furthermore, it allowed for the minimization of the rejection of rsEEG data for artifactual activity. The use of those procedures allowed a better understanding of the present results in light of previous reference evidence of the PDWAVES Consortium (Babiloni et al., 2015, 2016; Lizio et al., 2016; more information can be found at www.pdwaves.eu), but it implied the focus on the linear components of rsEEG signals.

Two independent researchers (GN and RL) performed a visual analysis of EOG and rsEEG data blind to the clinical diagnosis associated with the electrophysiological datasets. They rejected those with artifacts due to instruments, electronic noise, head–neck movements, and face muscle tension. They also rejected rsEEG epochs with amplitude values exceeding 100 μV. Particular attention was given to the contamination of saccades and blinking on electrophysiological data recorded by frontal (i.e., F7, F3, Fz, F4, and F8) and frontopolar (Fp1 and Fp2) electrodes. This specific exam was based on the comparison of EOG and rsEEG traces. The rsEEG epochs with artifacts marked as eye movements and blinking were provided as inputs to a software toolbox based on an autoregressive model for their possible correction (MATLAB 6.5, MathWorks Inc.). Technical details and performances of this procedure have been reported elsewhere (Moretti et al., 2003) and validated in several previous studies by the present research group (Babiloni et al., 2004a, 2006a, 2008). Of note, the outcome of this procedure was visually revised by the two researchers (G. N. and R. L.). All Nold and ADD datasets showed less than 25% of artifact-free rsEEG epochs, without significant differences between the Nold and ADD groups (t-test, $p > 0.05$, two tails). More specifically, the total number of artifact-free epochs was as follows: 135 ± 11 (SE) epochs for the Nold group and 115 ± 8 (SE) epochs for the ADD group, with a total duration spanning between 3.5 and 4.5 min, respectively.

To harmonize rsEEG data recorded using different reference electrodes and sampling frequency rates, artifact-free rsEEG epochs were off-line frequency-band passed at 0.1–45 Hz and downsampled, when appropriate, to make the sampling rate of all artifact-free rsEEG datasets in the Nold and ADD participants equal to 128 Hz. For the sake of harmonization of all datasets, the recorded rsEEG data were re-referenced to the common average reference.

2.5. The spectral analysis of rsEEG epochs

A standard digital FFT-based analysis (Welch technique, Hanning windowing function, no phase shift) computed the power density of scalp rsEEG rhythms (0.5 Hz of frequency resolution). As mentioned above, only rsEEG epochs free from artifacts were used.

The EEG frequency bands of interest were individually identified based on the following frequency landmarks: the transition frequency (TF) and the individual alpha frequency (IAF) peak (Klimesch, 1999). In the EEG power density spectrum, the TF marks the transition frequency between the theta and alpha bands, defined as the minimum of the rsEEG power density between 3 and 8 Hz (between the delta and the alpha power peak). The IAF is defined as the maximum power density peak between 6 and 14 Hz. These frequency landmarks were previously well described by Dr. Wolfgang Klimesch (Klimesch, 1996, 1999; Klimesch et al., 1998). Specifically, the TF and IAF were measured on averaged rsEEG power density spectra at parietal and occipital electrodes.

The TF and IAF were computed for each subject involved in the study. Based on the TF and IAF, we estimated the individual delta, theta, and alpha bands as follows: delta from TF −4 Hz to TF −2 Hz, theta from TF −2 Hz to TF, low-frequency alpha (alpha 1 and alpha 2) from TF to IAF, and high-frequency alpha (or alpha 3) from IAF to IAF + 2 Hz. Specifically, the individual alpha 1 and alpha 2 bands were computed as follows: alpha 1 from TF to the frequency midpoint of the TF-IAF range and alpha 2 from that midpoint to IAF.

The other bands were defined based on the standard fixed frequency ranges used in the reference study series (reviewed by Babiloni et al., 2021): beta 1 from 14 to 20 Hz, beta 2 from 20 to 30 Hz, and gamma from 30 to 40 Hz. See Supplementary Figure 1 in the Supplementary materials for the graphical representation of the above-mentioned frequency bands.

Of note, important aspects of the procedure were as follows:

(1) The alpha band was divided into sub-bands because, in the rsEEG data, dominant low-frequency alpha rhythms (alpha 1 and alpha 2) may denote the synchronization of diffuse neural networks regulating the fluctuation of the subject's global awake and conscious states, while high-frequency alpha rhythms (alpha 3) may denote the synchronization of more selective neural networks specialized in the processing of modal specific or semantic information (Pfurtscheller and Klimesch, 1992; Klimesch, 1999). When the subject is engaged in sensorimotor or cognitive tasks, alpha and low-frequency beta (beta 1) rhythms do reduce in power (i.e., desynchronization or blocking) and are replaced by fast EEG oscillations at high-frequency beta (beta 2) and gamma rhythms (Pfurtscheller and Klimesch, 1992).
(2) We considered individual delta, theta, and alpha frequency bands because a clinical group may be characterized by a mean slowing in the peak frequency of the alpha power density without any substantial change in the magnitude of the power density. In that specific case, the use of fixed frequency bands would result in a statistical effect erroneously showing alpha power density values lower in the clinical group than in the control group. In some specific cases, the groups of AD patients and control participants may not show statistically significant differences in the mean values of TF and IAF. Nevertheless, we used those values as a research model to allow the identification of delta, theta, low-frequency alpha bands, and high-frequency alpha bands on an individual basis to ensure the spectral measures were accurate within those bands, in line with our reference rsEEG studies performed in patients with AD and related neurodegenerative disorders (Babiloni et al., 2017, 2018, 2019, 2020).
(3) Fixed frequency ranges were used for the beta and gamma bands because the individual beta and gamma frequency peaks were only evident in a few subjects (<10%).
(4) We selected the beginning of the beta frequency range at 14 Hz to avoid overlapping between individual alpha and fixed beta frequency ranges (i.e., the individual alpha frequency band ranged from TF to 14 Hz with an IAF of 12 Hz).

During rsEEG recording, very careful attention was paid to the amplitude of alpha rhythms on posterior regions and the abnormal slow wave on frontal regions. Overall, specific spectral features should be respected, namely:

(1) The physiological decrease of the EEG power density after the IAFp as a function of the increase of the frequencies in the range of 1–40 Hz (related to residual muscular activity);
(2) The absence of an offset of power density across all frequencies at some scalp electrodes (especially visible as big differences in gamma rsEEG power density among the ROI);
(3) The absence of several peaks of high-power density in the range of 1–40 Hz; and.
(4) Visible IAFp in the range between 6 Hz and 14 Hz, especially on posterior regions.

We carefully checked the presence of IAFp in the present cohort of AD patients, as in a mild-to-moderate dementia stage, AD neuropathology should not impair the neurophysiological synchronizing mechanism inducing a total disruption of IAFp. If an IAFp was not clearly present, we attributed the cause to substantial artifacts rather than AD neuropathology.

2.6. Estimation of linear lagged connectivity (LLC) and isolated lagged effective coherence (iCoh)

As mentioned above, LLC and iCoh are two complementary and mathematically independent approaches available at the freeware platform called LORETA (see technical details at https://www.uzh.ch/keyinst/loreta; Pascual-Marqui, 2007) for measuring the interrelatedness of rsEEG activity at electrode (source) pairs. Comparing the results with two techniques probed the intrinsic variability of this kind of readout and allowed us to select and discuss the one that was most consistent.

LLC belongs to the popular bivariate techniques that compute the non-directional interrelatedness of rsEEG activity at electrode pairs (e.g., spectral coherence, phase lag index, synchronization likelihood, etc.) without considering the interrelatedness of rsEEG activity across the other electrode (source) pairs. It has the conceptual advantage of not considering the interrelatedness of the rsEEG activity at the zero-lag phase, which may be affected by the instantaneous spread of the electric field to the well-known head volume conduction effects (Pascual-Marqui et al., 2011).

By contrast, iCoh belongs to a group of techniques based on an autoregressive model that computes the directional interrelatedness of rsEEG activity at electrode pairs (e.g., spectral coherence, phase lag index, synchronization likelihood, etc.), removing the linear component of the interrelatedness of rsEEG activity across the other electrode

(source) pairs. It has the conceptual advantage of being multivariate (as opposed to bivariate) and exploring the directionality of that interrelatedness (Pascual-Marqui et al., 2014).

Using the iCoh procedure, we obtained not only a 'directional' measure of the interdependencies of rsEEG rhythms at electrode pairs but also a 'non-directional' measure. The directional measure was computed as the absolute difference of the iCoh values between the two 'directions', while the 'non-directional' measure was obtained by the mean of the two 'directional' values. The latter measure allowed cross-validation of ('non-directional') LLC measures.

For each participant, LLC, mean iCoh between the two 'directions', and the absolute difference of the iCoh values for the two 'directions' were calculated at each frequency bin between 0.5 and 45 Hz (matrix of 19 rows × 19 columns). LLC and iCoh values within the frequency bands individually identified based on the TF and IAF landmarks were averaged to obtain delta, theta, alpha 1, alpha 2, and alpha 3 bands. LLC and iCoh values for beta 1, beta 2, and gamma LLC were based on fixed frequency bands, as mentioned above.

To reduce statistical comparisons, we averaged the LLC or iCoh values calculated between scalp electrode pairs for regions of Interests (ROI). Specifically, we considered frontal, central, parietal, temporal, and occipital ROI. For each frequency band, LLC or iCoh values for interhemispheric comparisons were calculated as follows: (1) frontal ROI, mean values of Fp1-Fp2, F3-F4, and F7-F8 electrodes; (2) central ROI, the values of C3-C4 electrodes; (3) parietal ROI, the values of P3-P4 electrodes; (4) temporal ROI, mean values of T7-T8 and P7-P8 electrodes; and (5) occipital ROI, the values of O1-O2 electrodes.

Similarly, for each frequency band, LLC or iCoh values for intrahemispheric comparisons were calculated as follows: (1) left frontal ROI, mean values of electrode pairs between Fp1, F3, and F7 electrodes and all the left hemispheric electrodes; (2) right frontal ROI, mean values of electrode pairs between Fp2, F4, and F8 electrodes and all the right hemispheric electrodes; (3) left central ROI, mean values of electrode pairs of the left hemi-scalp involving the C3 electrode and all the left hemispheric electrodes; (4) right central ROI, mean values of electrode pairs of the right hemi-scalp involving the C4 electrode and all the right hemispheric electrodes; (5) left parietal ROI, mean values of electrode pairs of the left hemi-scalp involving the P3 electrode and all the left hemispheric electrodes; (6) right parietal ROI, mean values of electrode pairs of the right hemi-scalp involving the P4 electrode and all the right hemispheric electrodes; (7) left temporal ROI, mean values of electrode pairs of the left hemi-scalp involving the T7 and P7 electrodes and all the left hemispheric electrodes; (8) right temporal ROI, mean values of electrode pairs of the right hemi-scalp involving the T6 and P8 electrodes and all the right hemispheric electrodes; (9) left occipital ROI, mean values of electrode pairs of the left hemi-scalp involving the O1 electrode and all the left hemispheric electrodes; and (10) right parietal ROI, mean values of electrode pairs of the right hemi-scalp involving the O2 electrode and all the right hemispheric electrodes.

2.7. Graph theory analysis of LLC and iCoh values

For each participant, the LLC, mean iCoh, and absolute difference of iCoh values at the frequency bands showing statistically significant differences between the ADD and Nold groups were used as input for the graph theory analysis. This analysis was performed using the GraphVar 2.0 software platform (Waller et al., 2018).

For this purpose, matrices of LLC, mean iCoh, and absolute difference of iCoh values were converted into binary matrices having '0' or '1' in the cells. LLC or iCoh values associated with '1' were considered as 'significant' and considered for the computation of the graph indexes of interest in the Nold and ADD groups. Notably, we converted the LLC and iCoh matrices into binary ('1' and '0') graphs to (1) mitigate the inclusion of 'spurious' interdependencies of rsEEG rhythms at electrode pairs and (2) compare graphs with the same number of those interdependencies for the Nold and ADD groups.

For the identification of the 'significant' values of LLC or iCoh ('1' in the binary matrices), two ***arbitrary percentage thresholds*** were used, namely 10% (0.1) and 20% (0.2). For each frequency band and group of participants (Nold and ADD), the threshold at 10% did set to '1' the 10% of the highest values of LLC (iCoh), considering all electrode pairs, and '0' for the remaining ones. This procedure was repeated for LLC, mean iCoh, and the absolute difference of iCoh values. Specifically, 10% of the highest values of LLC corresponded to 17 electrode pairs. The same number of electrode pairs was true for ('non-directional') mean iCoh and the absolute difference of the two 'directional' iCoh values.

Following the same procedure, the threshold at 20% did set to '1' the 20% of the highest values of LLC (iCoh), considering all electrode pairs, and '0' for the remaining ones. Specifically, 20% of the highest values of ('non-directional') LLC corresponded to 34 electrode pairs. Again, this procedure was repeated for LLC, mean iCoh, and the absolute difference of iCoh values.As another step of the graph theory analysis, we ***arbitrarily*** used the ***nodal degree*** (ND), ***participation coefficient*** (PC), and local ***clustering coefficient*** (CC) graph indexes to scalp electrodes as ***degree*** hubs and then differentiate them into ***provincial*** and ***connector*** hubs.

For this purpose, ND was defined as the number of links (i.e., 'significant' interdependencies of rsEEG rhythms at electrode pairs represented as '1' in the previously mentioned binary matrices) characterizing a given node (electrode). Among nodes with a high number of links (high-degree nodes = ***degree hubs***), PC denoted the discriminant feature of their connection profile. In general, ***provincial*** hubs primarily link other nodes located within a single network region. By contrast, connector hubs predominantly link nodes located in several network regions (Sporns et al., 2007; Power et al., 2013). Here, this classification as provincial hub vs. connector hub was further confirmed by the CC index, which is a measure of the tendency of network nodes to form local clusters. High CC values mainly characterize provincial hubs rather than connector hubs.

In the present experimental context, we operationally defined ***degree*** hubs and then differentiated them into ***provincial*** and ***connector*** hubs using the following three approaches:

(1) Hubs were defined according to ND and classified into connector and provincial hubs according to the PC and CC calculated at 0.1 and 0.2 graph thresholds, in line with the Franciotti and Bonanni approach.
(2) Hubs were defined according to ND and classified into connector and provincial hubs according to the PC and betweenness centrality (BC) calculated at 0.1 and 0.2 graph thresholds, in line with the approach described by Cole et al. (2015).
(3) Hubs were defined according to the within-module degree z-score and classified into connector and provincial hubs according to the PC calculated at 0.1 and 0.2 graph thresholds, in line with the approach described by Power et al. (2013).

Furthermore, we used the four following alternative criteria for testing the consistency of the results (they were applied for each frequency band and each group of participants):

(1) According to the first criterion, ***degree hubs*** were defined as nodes (electrodes) with ND (number of links) higher than ***one standard deviation*** (SD) from the group mean of significant node links (i.e., '1' in the previously mentioned binary matrices) within the network (electrode montage). ***Provincial hubs*** were then defined as degree hubs with an ND and a CC higher than one SD and PC lower than one SD from the group mean of significant node links within the network. ***Connector hubs*** were defined as degree hubs (electrodes) with an ND and a PC higher than one SD from the network mean and a CC lower than one SD from the group mean of significant node links within the network.

(2) According to the second criterion, ***degree hubs*** were defined as nodes with an ND higher than the ***80th percentile*** from the group mean of significant node links within the network. ***Provincial hubs*** were then defined as degree hubs with an ND and a CC higher than the ***80th percentile*** and a PC lower than the ***20th percentile*** from the group mean of significant node links within the network. ***Connector hubs*** were defined as degree hubs with an ND and a PC higher than the ***80th percentile*** from the network mean and a CC lower than the ***20th percentile*** from the group mean of significant node links within the network.

(3) According to the third criterion, ***degree hubs*** were defined as nodes with an ND higher than the ***70th percentile*** from the group mean of significant node links within the network. ***Provincial hubs*** were then defined as degree hubs with an ND and a CC higher than the ***70th percentile*** and a PC lower than the ***30th percentile*** from the group mean of significant node links within the network. ***Connector hubs*** were defined as degree hubs with an ND and a PC higher than the ***70th percentile*** from the network mean and a CC lower than the ***30th percentile*** from the group mean of significant node links within the network.

(4) According to the fourth criterion, ***degree hubs*** were defined as nodes with an ND higher than ***one standard error of the mean*** (SEM) from the group mean of significant node links within the network. ***Provincial hubs*** were then defined as degree hubs with an ND and a CC higher than one SEM and a PC lower than one SEM from the group mean of significant node links within the network. ***Connector hubs*** were defined as degree hubs with an ND and a PC higher than one SEM from the network mean and a CC lower than one SEM from the group mean of significant node links within the network.

All results obtained with the above criteria are reported in detail in the tables featured in the Supplementary materials (see Results). Of note, the selection of the criteria was performed to provide an index of the result variability using different mathematical threshold definitions.

2.8. Directionality of degree hubs by iCoh values

To evaluate the directionality of the interdependencies of rsEEG rhythms between degree hubs (electrodes), 'directional' iCoh values for pairs of those hubs were calculated at each frequency bin between 0.5 and 45 Hz and for each participant of the ADD and Nold groups. Then, these iCoh values were averaged according to individual frequency bands from delta to alpha 3. To limit the statistical comparisons, the subsequent analysis was focused on individual delta, alpha 2, and alpha 3 bands, which are typically abnormal in rsEEG rhythms recorded in ADD patients (Babiloni et al., 2021). For each frequency band and group of participants, the global output (outward) value of a given degree hub was obtained averaging all output iCoh values from it to the other degree hubs. The global input (inward) value of that degree hub was obtained averaging all input iCoh values to it coming from the other degree hubs.

2.9. Statistical analysis

To evaluate the study hypotheses, the following statistical sessions were performed by the commercial tool STATISTICA 10 (StatSoft Inc.).[4] As analysis of variance (ANOVA) implies that dependent variables have Gaussian distributions, we tested this feature with the LLC and iCoh values using a Kolmogorov–Smirnov test (null hypothesis of non-Gaussian distributions tested at $p > 0.05$). Both the LLC and iCoh values showed non-Gaussian distributions, so we Log10 transformed them and retested Gaussian status. Such a transformation is a popular method for transforming a skewed data distribution with all positive values, such as LLC and iCoh values, to Gaussian distributions, as required when using ANOVA. Indeed, the outcome of the procedure did approximate the distributions of LLC and iCoh values to Gaussian distributions ($p > 0.05$), allowing the use of the ANOVA model.

For the session using ANOVAs, Mauchly's test evaluated the sphericity assumption, and degrees of freedom were corrected using the Greenhouse–Geisser procedure when appropriate ($p < 0.05$). the Duncan test was used for *post-hoc* comparisons ($p < 0.05$, corrected for multiple comparisons).

The results of the following ANOVAs were controlled by the iterative (leave-one-out) Grubbs' test detecting for the presence of one or more outliers in the distribution of the LLC and iCoh values showing the significant effects in relation to the study hypotheses. The null hypothesis of the non-outlier status was tested at the arbitrary threshold of $p > 0.001$ to remove only values with the highest probability of being outliers.

In the first statistical session, we evaluated whether the LLC, mean iCoh, and absolute difference of iCoh interhemispheric values may differ between the ADD and Nold groups at parietal delta and alpha rhythms. To this aim, we developed three ANOVA designs with the Log10-transformed LLC, mean iCoh, and absolute difference of iCoh values as dependent variables, respectively. The factors were group (Nold, ADD; independent variable), ROI (frontal, central, parietal, temporal, and occipital), and band (delta, theta, alpha 1, alpha 2, alpha 3, beta 1, beta 2, and gamma). The confirmation of the hypothesis would require (1) a statistically significant ANOVA interaction, including the factors group, ROI, and band ($p < 0.05$), and (2) a *post-hoc* Duncan test indicating statistically significant ($p < 0.05$) differences in the LLC values at parietal delta and alpha rhythms between the Nold and ADD groups (i.e., Nold ≠ ADD, $p < 0.05$).

In the second session, we evaluated whether the LLC, mean iCoh, and absolute difference of iCoh intrahemispheric values may differ between the ADD and Nold groups at delta and alpha rhythms within

4 www.statsoft.com

the two hemispheres. To this aim, we developed three ANOVA designs with the Log10-transformed LLC, mean iCoh, and absolute difference of iCoh values as dependent variables, respectively. The factors were group (Nold, ADD; independent variable), hemisphere (left, right), ROI (frontal, central, parietal, temporal, and occipital), and band (delta, theta, alpha 1, alpha 2, alpha 3, beta 1, beta 2, and gamma). The confirmation of the hypothesis would require (1) a statistically significant ANOVA interaction, including the factors group, ROI, and band ($p < 0.05$), and (2) a *post-hoc* Duncan test indicating statistically significant ($p < 0.05$) differences in the LLC values at parietal delta and alpha rhythms between the Nold and ADD groups (i.e., Nold ≠ ADD, $p < 0.05$).

In the third session, we evaluated whether the global output and input iCoh values of parietal degree hubs (identified by the previous graph theory analysis) may differ between the ADD and Nold groups at delta and alpha rhythms. We also evaluated whether, within each group, a difference between global output and input iCoh values for degree hubs could be observed. To these aims, for each frequency band, we developed an ANOVA design with the Log10-transformed global iCoh values as a dependent variable and the group (Nold, ADD; independent variable), hub (all degree hubs), and direction (output, input) as factors. The confirmation of the hypothesis would require (1) a statistically significant ANOVA interaction, including the factors group, hub, and direction ($p < 0.05$), (2) a *post-hoc* Duncan test indicating statistically significant ($p < 0.05$) between-group differences in the parietal iCoh values at delta and alpha rhythms between the Nold and ADD groups (i.e., Nold ≠ ADD, $p < 0.05$), and (3) a *post-hoc* Duncan test indicating statistically significant ($p < 0.05$) within-group differences between the global output and input iCoh values (i.e., output ≠ input, $p < 0.05$).

3. Results

3.1. Demographic, clinical, neuropsychological, and rsEEG features in the Nold and Add groups

Table 1 summarizes the most relevant demographic (i.e., age, gender, and education) and clinical (i.e., MMSE score) features of the groups of Nold ($N = 40$) and ADD (N = 37) participants. Furthermore, it reports results of the statistical comparison ($p < 0.05$) of age (*t*-test), gender (Fisher test), education (*t*-test), and MMSE score (Mann–Whitney *U* test) between the two groups. As expected, a statistically significant difference was found for the MMSE score ($p < 0.001$), indicating a higher score in the Nold group than in the ADD group. No difference was found for age, gender, and education between the two groups ($p > 0.05$ uncorrected).

In Table 1, the mean values of TF and IAF for the Nold and ADD groups, together with the results of the statistical comparisons between them (*t*-test), are also reported. No statistically significant differences were observed for TF and IAF values ($p > 0.05$ uncorrected).

3.2. Interdependencies of rsEEG rhythms at parietal electrode pairs as revealed by LLC and iCoh values

Results showed a statistically significant ANOVA interaction ($F[28, 2,100] = 2.25$, $p < 0.05$) in ***interhemispheric LLC*** values among the factors group (Nold and ADD; independent variable), ROI (frontal, central, parietal, temporal, and occipital), and band (delta, theta, alpha 1, alpha 2, alpha 3, beta 1, beta 2, and gamma; Supplementary Figure 2). Compared with the ***Nold group***, the ***ADD group*** was mainly characterized by (1) lower alpha 2 and alpha 3 LLC values at parietal and temporal ROI and (2) higher delta LLC values at frontal, parietal, and occipital ROI ($p < 0.05$). No significant ANOVA effect was observed in the ***interhemispheric iCoh*** values ($p > 0.05$; see Supplementary Figures 3, 4).

Additionally, a statistically significant ANOVA interaction ($F[28, 2,100] = 3.32$, $p < 0.05$) in ***intrahemispheric (non-directional) LLC*** values among the factors group, ROI, and band (Supplementary Figure 5) was observed. Compared with the ***Nold group***, the ***ADD group*** was mainly characterized by (1) lower LLC alpha 2 and alpha 3 values at the central, parietal, and occipital ROI and (2) higher LLC delta values at frontal, parietal, and occipital ROI ($p < 0.05$).

Another statistically significant ANOVA interaction ($F[28, 2,100] = 1.91$, $p < 0.05$) was found in ***intrahemispheric (non-directional) mean iCoh*** values among the factors group, hemisphere, ROI, and band (Supplementary Figure 6). No significant *post-hoc* effect was observed in the planned tests ($p > 0.05$). There was just a trend for lower left-parietal ***iCoh*** alpha 2 and alpha 3 values in the ADD group compared with the Nold group.

Finally, a statistically significant ANOVA interaction ($F[28, 2,100] = 2.13$, $p < 0.05$) was found in the ***intrahemispheric (directional) absolute difference of iCoh values*** among the factors group, hemisphere, ROI, and band (Supplementary Figure 7). Again, no significant *post-hoc* effect was observed in the planned tests ($p > 0.05$) but there was a trend showing lower left-parietal ***iCoh*** values in the ADD group compared with the Nold group.

Table 2 reports all the results from the planned *post-hoc* tests ($p < 0.05$) for the above significant ANOVA effects. Notably, the above findings based on LLC and iCoh values were not due to outliers, as shown by Grubbs' test with an arbitrary threshold of $p > 0.001$ (see Supplementary Figures 8, 9, respectively).

Globally, the above LLC and iCoh findings showed that ***interdependencies of rsEEG alpha 2 and alpha 3 rhythms at parietal electrode pairs were lower in the ADD group than in the Nold group***. By contrast, results on interdependencies of rsEEG delta rhythms at scalp electrode pairs were inconsistent considering LLC and iCoh measures, so we did not use those measures for the graph hub analysis.

3.3. Parietal graph degree hubs from LLC and iCoh values at alpha rhythms

In the Supplementary material Tables 2–7 report detailed results about the graph degree hubs derived from LLC and iCoh alpha 2 and alpha 3 values computed in the Nold and ADD groups. As explained in the Materials and Methods section, those degree hubs were defined by the ND graph index using four different quantitative thresholds of qualification (i.e., mean + 1 SD, 80th percentile, 70th percentile, mean + 1 SEM).

Figure 2 illustrates those graph degree hubs computed from LLC and iCoh alpha 2 and alpha 3 values in the Nold and ADD groups. For sake of concision, the 0.1 and 0.2 thresholds are displayed in the same figure.

Although there was a certain spread of degree hubs over the scalp at alpha 2 and alpha 3 bands, LLC and iCoh measures showed converging evidence of parietal degree hubs at these bands in both the Nold and ADD groups. Even using the most conservative

TABLE 2 *Post-hoc p*-values (Duncan test) relative to the ANOVA interaction effects on the global output and input isolated lagged effective coherence (iCoh) in the alpha 2 and alpha 3 bands.

Global alpha2 iCoh		Global alpha3 iCoh	
Statistical comparison	*p*-value	Statistical comparison	*p*-value
Nold > ADD	*Output P3:* 0.026011 *Output Pz:* 0.038590	*Nold > ADD*	*Output Pz:* 0.021034
Input > Output (Nold)	*Fp2:* 0.044984 *F3:* 0.024305 *F4:* 0.026964 *F7:* 0.038887	*Input > Output (Nold)*	*Fp2:* 0.034870 *F3:* 0.026717 *F4:* 0.027734 *F7:* 0.026067
Input > Output (ADD)	*Pz:* 0.013233		
Output > Input (Nold)	*P3:* 0.000002 *P4:* 0.000002	*Output > Input (Nold)*	*P3:* 0.000002 *P4:* 0.000003 Pz: 0.027605
Output > Input (ADD)	*P3:* 0.014394 *P4:* 0.000001	*Output > Input (ADD)*	*P3:* 0.007453 *P4:* 0.000005

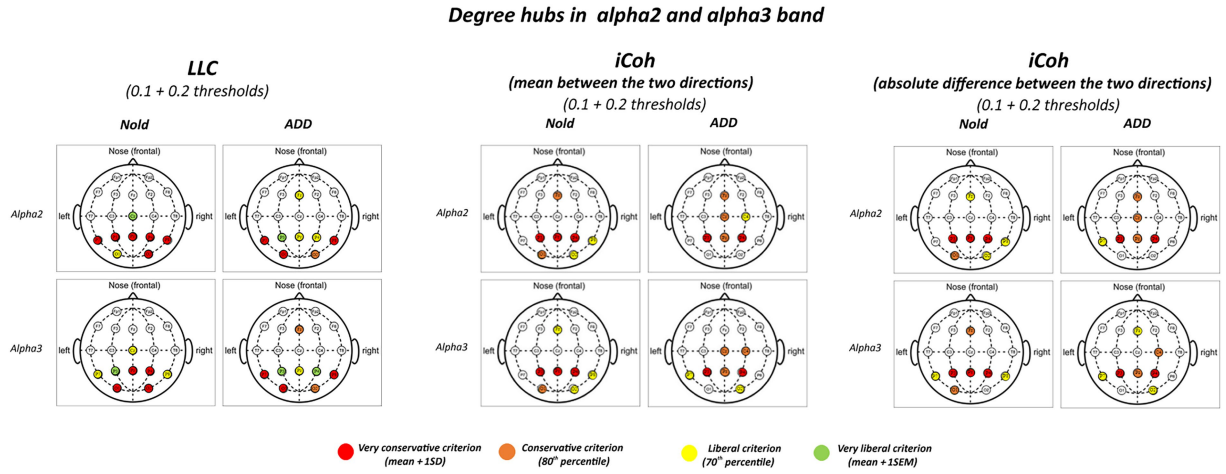

FIGURE 2
Degree hubs for the alpha 2 and alpha 3 linear lagged connectivity (LLC, left column), mean (middle column), and absolute difference isolated lagged effective coherence (iCoh, right column) values in the Nold and ADD groups defined according to nodal degree (ND) calculated at 0.1 and 0.2 graph thresholds. Colors correspond to the different criteria adopted (mean and SD, 80th percentile, 70th percentile, mean and SEM).

criterion for the degree hub qualification (i.e., mean + 1 SD), consistent degree hubs from alpha 2 and alpha 3 rhythms were observed at parietal electrodes (i.e., P3, Pz, and P4). Notably, the iCoh values showed ***no substantial between-group differences in the topology of the parietal degree hubs at the alpha 2 and alpha 3 bands***.

3.4. Parietal graph connector hubs from LLC and iCoh values at alpha 2 and alpha 3 bands

In the Supplementary material Tables 8–13 report detailed results about the graph connector and provincial hubs derived from LLC and iCoh alpha 2 and alpha 3 values computed in the Nold and ADD groups. Notably, the results showed no substantial graph provincial hub in the two groups.

Figures 3, 4 illustrate the localization of the graph connector hubs at the alpha 2 and alpha 3 bands in the Nold and ADD groups. For sake of concision, such a localization was computed considering the 0.1 and 0.2 thresholds together. There was a certain spread of connector hubs over the scalp at those bands. However, LLC and iCoh measures showed convergent evidence of parietal connector hubs at alpha 2 and alpha 3 bands in both the Nold and ADD groups. Even using the most conservative criterion for the connector hub qualification (i.e., mean + 1 SD), consistent connector hubs for alpha 2 and alpha 3 bands were observed at parietal electrodes (i.e., P3, Pz, and P4). Notably, the iCoh values showed ***no substantial between-group differences in the topology of the parietal connector hubs at the alpha 2 and alpha 3 bands***.

3.5. Directionality of hubs from LLC and iCoh values at alpha 2 and alpha 3 bands

Figures 5, 6 plot the global output (outward) and input (inward) iCoh alpha 2 and alpha 3 values at all electrodes denoted as a degree or

10.3389/fnagi.2023.780014

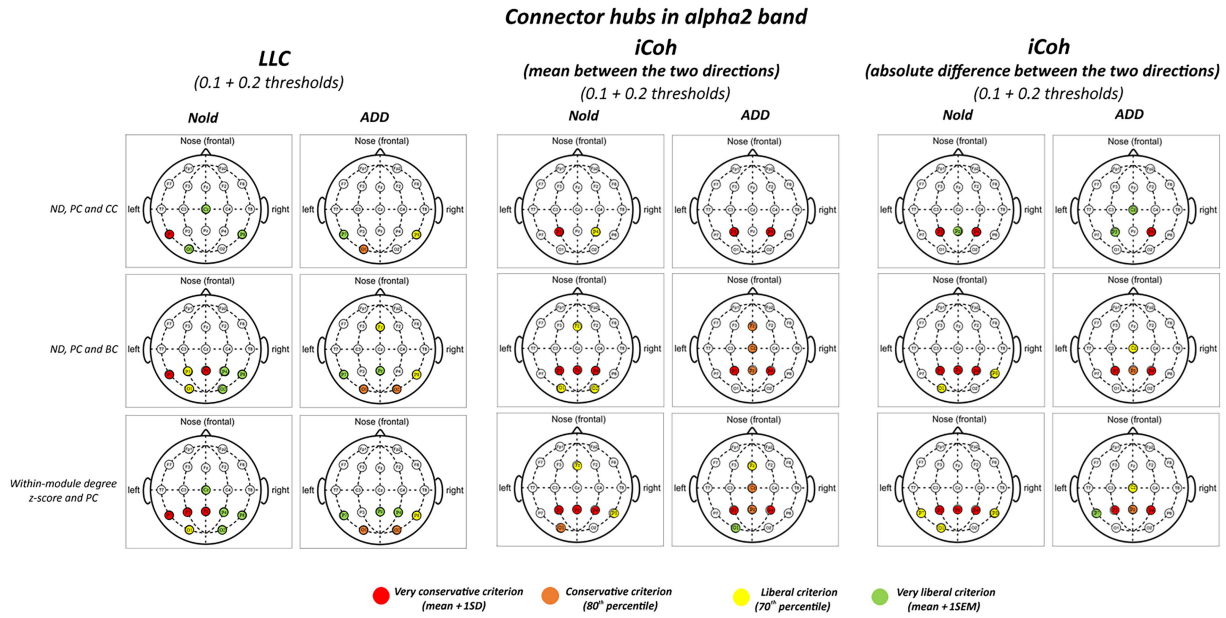

FIGURE 3
Connector and provincial hubs for the alpha 2 linear lagged connectivity (LLC, left column), mean (middle column), and absolute difference isolated lagged effective coherence (iCoh, right column) values in the Nold and ADD groups defined according to the three approaches used in the present study. Upper row: hubs were defined according to nodal degree (ND) and classified into connector and provincial hubs according to the participation coefficient (PC) and clustering coefficient (CC) calculated at 0.1 and 0.2 graph thresholds, in line with the approach described by Franciotti and Bonanni. Middle row: hubs were defined according to nodal degree (ND) and classified into connector and provincial hubs according to the participation coefficient (PC) and betweenness centrality (BC) calculated at 0.1 and 0.2 graph thresholds, in line with the approach described by Cole et al. (2015). Lower row: hubs were defined according to the within-module degree z-score and classified into connector and provincial hubs according to the participation coefficient (PC) calculated at 0.1 and 0.2 graph thresholds, in line with the approach described by Power et al. (2013). Colors correspond to the different criteria adopted (mean and SD, 80th/20th percentile, 70th/30th percentile, mean and SEM).

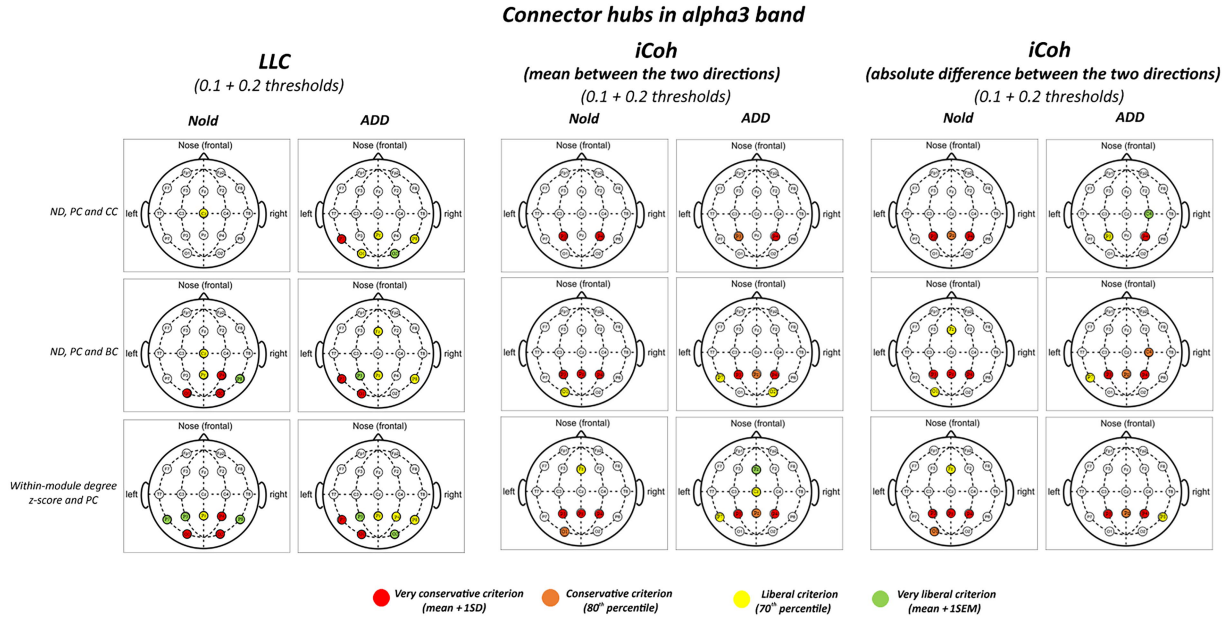

FIGURE 4
Connector and provincial hubs for the alpha 3 linear lagged connectivity (LLC, left column), mean (middle column), and absolute difference isolated lagged effective coherence (iCoh, right column) values in the Nold and ADD groups defined according to the three approaches used in the present study. Upper row: hubs were defined according to nodal degree (ND) and classified into connector and provincial hubs according to the participation coefficient (PC) and clustering coefficient (CC) calculated at 0.1 and 0.2 graph thresholds, in line with the approach described by Franciotti and Bonanni. Middle row: hubs were defined according to nodal degree (ND) and classified in connector and provincial hubs according to the participation coefficient (PC) and betweenness centrality (BC) calculated at 0.1 and 0.2 graph thresholds, in line the approach described by Cole et al. (2015). Lower row: hubs were defined according to the within-module degree z-score and classified into connector and provincial hubs according to the participation coefficient (PC) calculated at 0.1 and 0.2 graph thresholds, in line with the approach described by Power et al. (2013). Colors correspond to the different criteria adopted (mean and SD, 80th/20th percentile, 70th/30th percentile, mean and SEM).

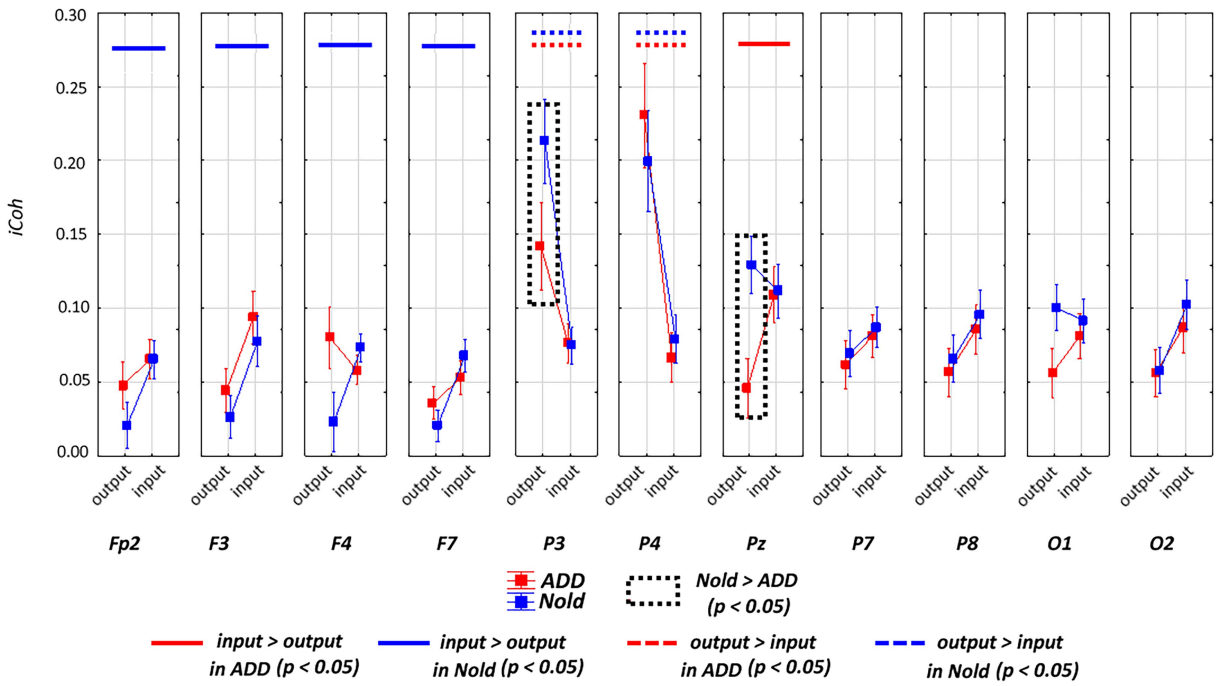

FIGURE 5
Global isolated lagged effective coherence (iCoh) values (mean across subjects ± SEM) in the alpha 2 frequency band within electrodes classified as substantial degree or connector hubs relative to a statistically significant ANOVA interaction (F [10, 750]=2.42, p<0.05) among the group (Nold and ADD), hubs (Fp2, F3, F4, F7, P3, P4, Pz, P7, P8, O1, and O2), and direction (output and input) factors. No statistically significant outliers were found according to Grubbs' test (p<0.0001).

a connector hub in the above analysis. Results showed a statistically significant ANOVA interaction of the iCoh alpha 2 values among group (Nold and ADD; independent variable), hub (electrodes with hub features), and direction (output and input) factors (F[10, 750] = 2.42, $p < 0.05$). Compared with the Nold group, the ADD group showed lower output global iCoh alpha 2 values at parietal electrodes (i.e., P3 and Pz; $p < 0.05$).

A statistically significant ANOVA interaction of the iCoh alpha 3 values was also observed among group, hub, and direction (F[10, 750] = 2.48, $p < 0.05$). Compared with the Nold group, the ADD group showed lower output global iCoh alpha 3 values at one parietal electrode (i.e., Pz; $p < 0.05$).

Additionally, a statistically significant ANOVA interaction of the iCoh alpha 3 values was observed among group, hub, and direction ($F = 2.48$, $p < 0.05$). Compared with the Nold group, the ADD group showed lower output global iCoh alpha 3 values at one parietal electrode (i.e., Pz; $p < 0.05$).

Supplementary material Table 1 reports the results of the Duncan planned *post-hoc* ($p < 0.05$) test relative to the ANOVA interaction effects. Of note, the above results were not caused by outliers, as shown by Grubbs' test with an arbitrary threshold of $p > 0.001$ (see Supplementary Figure 10).

Overall, the above iCoh results showed ***no substantial between-group differences in the topology of the iCoh alpha 2 and alpha 3 values, with those values being maximized at parietal electrodes. However, the output iCoh alpha 2 and alpha 3 values at parietal electrodes were lower in the ADD group than in the Nold group***.

3.6. Control analysis on parietal connector hubs identified at alpha 2 and alpha 3 bands by other graph theory measures

To control for the robustness of the present results about the parietal connector hubs computed at the alpha 2 and alpha 3 bands, we used the following additional graph measures and definitions of those hubs (GraphVar 2.0 platform). According to Cole et al. (2015), a connector hub can be associated with high values of ND, PC, and Betweenness Centrality (BC). Notably, BC of a node is defined as the number of shortest graph paths that goes through that node (Rubinov and Sporns, 2010). According to Power et al. (2013), a connector hub can be associated with high values of the within-module degree z-score and PC.

Figures 3, 4 illustrate the results of this control analysis. There was again a certain spread of connector hubs over the scalp at alpha 2 and alpha 3 bands. However, convergent results showed ***significant connector hubs located at the parietal electrodes (i.e., P3, Pz, and P4) in both the Nold and ADD groups***. Supplementary material Tables 14–25 report detailed results of this control analysis.

3.7. Control analysis of the influence of normalized rsEEG spectral power density on iCoh values

To evaluate the influence of potential intergroup differences in the rsEEG spectral power density on iCoh (and LLC as the second

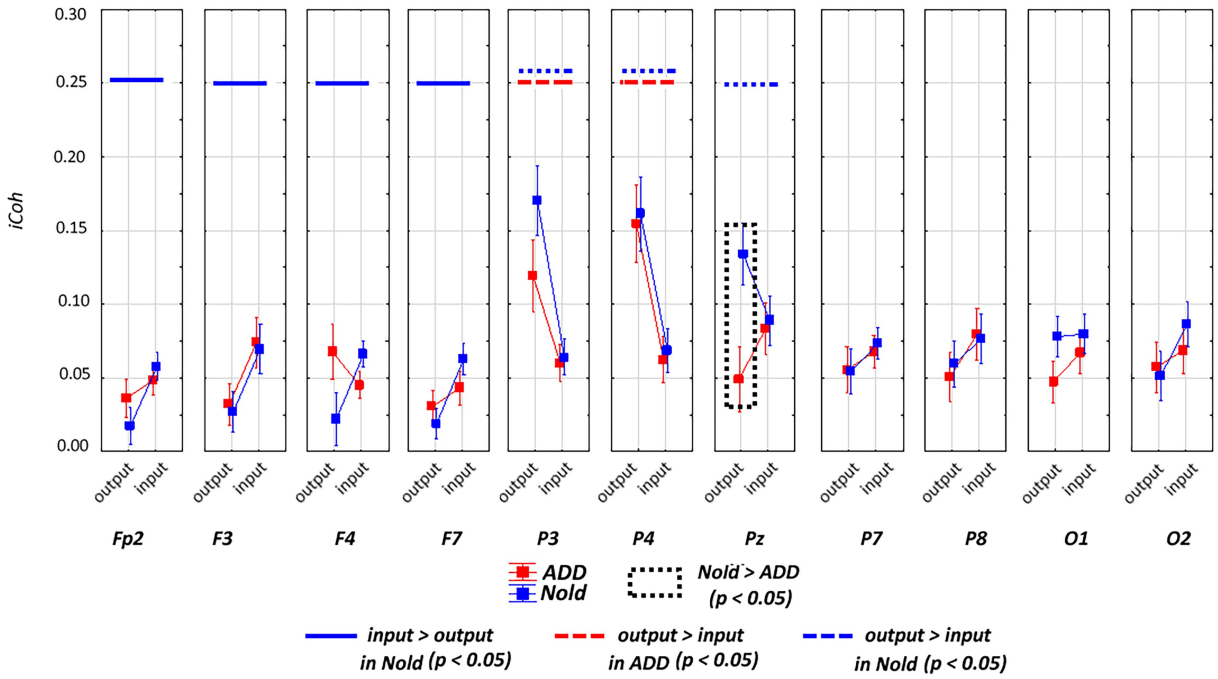

FIGURE 6
Global isolated lagged effective coherence (iCoh) values (mean across subjects ± SEM) in the alpha 3 frequency band within electrodes classified as substantial degree or connector hubs relative to a statistically significant ANOVA interaction (F [10, 750]=2.48, p<0.05) among the group (Nold and ADD), hubs (Fp2, F3, F4, F7, P3, P4, Pz, P7, P8, O1, and O2), and direction (output and input) factors. No statistically significant outliers were found according to Grubbs' test (p<0.0001).

interdependency measure) values, we included a control analysis for the comparison of the rsEEG power spectra for each frequency band of interest between the Nold and ADD groups. To this aim, we used the normalized rsEEG spectral power density calculated at each individual frequency band of interest (from delta to gamma) as the dependent variable in an ANOVA design, with group (Nold and ADD; independent variable), ROI (frontal, central, parietal, temporal, and occipital), and band (delta, theta, alpha 1, alpha 2, alpha 3, beta 1, beta 2, and gamma) as factors. The ROI were defined as those used for the interhemispheric iCoh analysis. We used the Log10-transformed rsEEG spectral power density values to meet the requirement of Gaussian distribution of the dependent ANOVA variable.

Results are illustrated in Supplementary Figure 11. Compared with the Nold group, the ADD group was characterized by (1) lower widespread alpha 2 and alpha 3 spectral power density values, especially at parietal and occipital ROI, and (2) higher widespread delta spectral power density values ($p < 0.05$).

Owing to the above-mentioned intergroup differences, we repeated the main statistical analyses by introducing the global alpha 2 or the alpha 3 regional normalized spectral power density as a covariate. Global values were calculated by averaging the regional values (as intergroup differences in the alpha 2 and alpha 3 bands were widespread). Results confirmed the previous main findings except for the intrahemispheric (non-directional) LLC values (no statistically significant interaction among the factors group, ROI, and band with global alpha 2 or alpha 3 spectral power densities as covariates; $p > 0.05$). In detail, the following results were obtained:

- intrahemispheric (non-directional) mean iCoh—covariate, global alpha 2 spectral power density: a statistically significant ANOVA interaction (F[28, 2072] = 3.55, $p < 0.05$) among the factors group, hemisphere, ROI, and band. Again, no significant *post-hoc* effect was observed in the planned tests ($p > 0.05$).
- intrahemispheric (non-directional) mean iCoh—covariate, global alpha 3 spectral power density: a statistically significant ANOVA interaction (F[28, 2072] = 3.02, $p < 0.05$) among the factors group, hemisphere, ROI, and band. Again, no significant *post-hoc* effect was observed in the planned tests ($p > 0.05$).
- intrahemispheric (non-directional) absolute difference iCoh—covariate, global alpha 2 spectral power density: a statistically significant ANOVA interaction (F[28, 2072] = 2.81, $p < 0.05$) among the factors group, hemisphere, ROI, and band. Again, no significant *post-hoc* effect was observed in the planned tests ($p > 0.05$).
- intrahemispheric (non-directional) absolute difference iCoh—covariate, global alpha 3 spectral power density: a statistically significant ANOVA interaction (F[28, 2072] = 2.02, $p < 0.05$) among the factors group, hemisphere, ROI, and band. Again, no significant *post-hoc* effect was observed in the planned tests ($p > 0.05$).
- interhemispheric LLC—covariate, global alpha 2 spectral power density: a statistically significant ANOVA interaction (F[28, 2072] = 2.22, $p < 0.05$) among the factors group, ROI, and band. A planned Duncan *post-hoc* test showed that, compared with the Nold group, the ADD group was mainly characterized by (1) lower LLC alpha 2 and alpha 3 values at the parietal and temporal ROI and (2) higher LLC delta values at frontal, parietal, and occipital ROI ($p < 0.05$).

- interhemispheric LLC—covariate, global alpha 3 spectral power density: a statistically significant ANOVA interaction ($F[28, 2072] = 2.19$, $p < 0.05$) among the factors group, ROI, and band. A planned Duncan *post-hoc* test showed that, compared with the Nold group, the ADD group was mainly characterized by (1) lower LLC alpha 2 and alpha 3 values at the parietal and temporal ROI and (2) higher LLC delta values at frontal, parietal, and occipital ROI ($p < 0.05$).

With regard to the directionality of hubs from iCoh values at alpha 2 and alpha 3 bands, we used the global alpha 2 and alpha 3 spectral power densities, respectively, as covariates in the main statistical analysis. Results with the global alpha 2 spectral power density as covariate confirmed a statistically significant ANOVA interaction of the iCoh alpha 2 values among group (Nold and ADD; independent variable), hub (electrodes with hub features), and direction (output and input) factors ($F[10, 70] = 1.97$, $p < 0.05$). Compared with the Nold group, the ADD group showed lower output global iCoh alpha 2 values at parietal electrodes (i.e., P3 and Pz; $p < 0.05$). No statistically significant ANOVA interaction ($p > 0.05$) was observed, including with global alpha 3 spectral power density as a covariate.

4. Discussion

4.1. Converging evidence of LLC and iCoh measures about the interdependencies of rsEEG rhythms at electrode pairs

In the present study, both bivariate LLC and multivariate iCoh measures showed that, compared with the Nold participants, the ADD patients were characterized by lower interdependencies of rsEEG ***alpha*** rhythms, especially at ***parietal*** electrode pairs. This effect was more spatially sharp with multivariate iCoh measures than with bivariate LLC measures. These results confirm the spatial variability of the effects derived from different techniques estimating interdependencies of rsEEG rhythms at electrode pairs and emphasize the importance of using more than one technique, including at least one multivariate approach (Blinowska, 2011; Blinowska et al., 2017).

The current results are globally in line with the bulk of previous rsEEG studies showing that ADD patients exhibit lower interrelatedness of rsEEG rhythms at alpha and higher frequencies at posterior electrode pairs (Leuchter et al., 1992, 1994; Besthorn et al., 1994; Dunkin et al., 1994; Sloan et al., 1994; Stam et al., 1995, 1996, 2003, 2009; Jelic et al., 1998, 2000; Locatelli et al., 1998; Anghinah et al., 2000; Knott et al., 2000; Adler et al., 2003; Babiloni et al., 2004a, 2006a, 2018; Pogarell et al., 2005; de Haan et al., 2009; Fonseca et al., 2011, 2013).

Additionally, the current results showed certain effects of ADD on the interdependencies of rsEEG ***delta*** rhythms at electrode pairs, but only when the ***bivariate*** LLC technique was used. Compared with the Nold group, the ADD group exhibited higher LLC values at frontal, parietal, and occipital delta rhythms. These effects were globally in agreement with previous rsEEG evidence obtained using bivariate techniques (e.g., FFT-based spectral coherence or LLC) to investigate the effects of ADD on the interdependencies of rsEEG rhythms (Locatelli et al., 1998; Babiloni et al., 2010, 2018; Hsiao et al., 2013, 2014). Given the lack of effects of ADD on interdependencies of rsEEG delta rhythms derived from multivariate iCoh measures, we did not estimate hubs at delta rhythms. Notably, the results at delta rhythms indicated that the present iCoh measures were not redundant compared with those of spectral power density, which showed greater widespread rsEEG delta power in the ADD group than the Nold group.

4.2. Converging evidence of LLC and iCoh measures about graph hubs at parietal electrodes and alpha rhythms

The present alpha LLC and iCoh measures showed converging evidence of prominent ***degree and connector hubs*** at ***parietal*** electrode pairs (i.e., P3, Pz, and P4). Furthermore, both groups were characterized by a ***prominent*** alpha iCoh ***outward direction*** (output or outflow) from parietal electrodes to other electrodes exhibiting degree hub properties. This effect was lower in the ADD group than in the Nold group and was consistent with the three definitions of connector hubs (Rubinov and Sporns, 2010; Power et al., 2013; Cole et al., 2015).

Taken together, it can be speculated that the present alpha LLC-iCoh and graph results may reflect abnormalities in parietal networks underpinning the regulation of quiet vigilance in ADD patients but with a global preservation of the parietal hub function, as revealed by the present analysis of the rsEEG alpha rhythms.

In line with this speculation, previous studies investigating directional interdependencies of rsEEG rhythms in cognitively unimpaired adults showed prominent outflow measures at alpha (and beta) rhythms from parietal electrodes, based on the computation of multivariate directed transfer function (Kuś et al., 2004; Blinowska and Kaminski, 2013). These measures were reduced in relation to a decrease in vigilance and an increase in errors during a continuous cognitive task in those adults (Liu et al., 2010). When applied to AD patients, directed transfer function measures at rsEEG alpha (and beta) rhythms exhibited lower outflow from parietal to frontal electrodes in ADD and ADMCI patients than in Nold participants (Babiloni et al., 2008, 2009a,b; Blinowska et al., 2017). These effects might be partially caused by abnormal ascending inputs coming from the thalamic and cholinergic basal forebrain regions (Hughes and Crunelli, 2005; Babiloni et al., 2006a, 2009a,b, 2020a, 2021; Wan et al., 2019).

4.3. What might graph hubs from rsEEG alpha rhythms tell us about add patients?

At this early stage of the research, we can only speculate about the neurophysiological significance of the present results. As novel and original neurophysiological findings, the present study showed evidence of prominent parietal hubs from interdependencies of the rsEEG alpha rhythms but with reduced outward iCoh measures in AD patients with mild-to-moderate dementia (mean MMSE score of approximately 19/30). An exciting hypothesis for future longitudinal studies is that the AD progression to severe dementia might be associated with (1) outward alpha iCoh measures that are even more reduced from parietal electrodes, (2) loss of degree and connector hubs from the present LLC and iCoh measures, and (3) increased disorders in the regulation and maintenance of quiet vigilance during the daytime, with frequent episodes of drowsiness, misperceptions, and light sleep. If confirmed, the present rsEEG evidence of partially preserved parietal hubs in mild-to-moderate ADD patients would reflect a sort of resilience or initial vulnerability of the brain networks underpinning quiet vigilance.

In line with this speculation, previous rsEEG evidence showed several signs of topographically widespread impairment of brain

networks in ADD patients, as revealed by graph theory indexes. Multivariate directional techniques based on a Granger causality matrix from rsEEG alpha and beta rhythms unveiled that ADD patients were globally characterized by lower global efficiency, increased local efficiency, and lower resilience of cortical networks (Afshari and Jalili, 2017). Furthermore, these patients were characterized by lower inward and outward directions of interdependencies of the whole-band rsEEG activity recorded from posterior electrodes, with maximum abnormalities of degree hubs at parietal electrodes (Franciotti et al., 2019), but not replicated with a bivariate mutual information technique (Franciotti et al., 2022).

In the ***resting state*** condition, prominent outward directionality of the present hubs at parietal electrodes and alpha rhythms might reflect the synchronization and interdependence of neural activity into posterior thalamocortical and corticothalamic loops, which might maintain cortical arousal underpinning vigilance against sleep intrusion (Hughes and Crunelli, 2005; Lörincz et al., 2008, 2009; Crunelli et al., 2015). Indeed, the greater the posterior rsEEG alpha rhythms, the greater the ***cortical inhibition*** in quiet vigilance, the lower the attention to external stimuli (Pfurtscheller and Klimesch, 1992; Boksem et al., 2005; Babiloni et al., 2020b). Those thalamic and cortical reciprocal interactions might influence several cortical areas, including the nodes of the '***default mode network***' (Raichle et al., 2001; Buckner et al., 2008). Overall, such traveling alpha rhythms may flow from higher-to lower-order areas in the visual and somatosensory cortices (Halgren et al., 2019). The effect may be to facilitate the scanning of internal and external environments (Liu et al., 2010; Al-Shargie et al., 2019), extract relevant features on demand (Ermentrout and Kleinfeld, 2001), and support communications within nodes of brain networks in relation to vigilance (Han et al., 2008; Crunelli et al., 2018).

4.4. Methodological limitations of the present study

This study was not performed within a unique multicentric clinical trial, so the present recording units did not follow the identical clinical, neuropsychological, and neuroimaging procedures during the enrollment of Nold and ADD participants. This makes the present study exploratory in nature.

Standard biomarkers of AD neuropathology (e.g., cerebrospinal diagnostic measures of Ab42/phospho tau or amyloid positron emission tomography) were not systematically measured in the present Nold and ADD participants, so only the strongest and most robust results could emerge at the group level. This limitation may explain some significant variability of graph indexes at rsEEG delta rhythms.

We used a low number of scalp electrodes to record rsEEG activity (i.e., 19 electrodes placed according to 10–20 system), two standard bivariate (LLC) and multivariate (iCoh) techniques estimating the interrelatedness of the rsEEG activity at electrode pairs, and well-known graph indexes in line with the general methodology of several previous successful studies; those studies investigated the graph-based rsEEG topology in ADD patients based on 'synchronization likelihood', 'phase lag index', 'synchronization likelihood', 'generalized composite multiscale entropy vector', and 'mutual information' techniques applied to rsEEG data recorded from ≤19 scalp electrodes (Stam et al., 2007a; De Haan et al., 2009; Engels et al., 2015; Yu et al., 2016; Song et al., 2019; Das and Puthankattil, 2022; Franciotti et al., 2022).

This intrinsic low resolution of the present rsEEG approach was partially considered by averaging the LLC and iCoh measures in large scalp ROI. Furthermore, head volume conduction effects may inflate LLC and iCoh measures. Indeed, electric fields can instantaneously spread from a brain source to several scalp electrodes, thus generating spurious (fake) interdependencies of rsEEG rhythms at electrode pairs. These effects of head volume conduction are partially mitigated by the fact that LLC and iCoh measures are insensitive to zero-lag interdependencies of rsEEG rhythms. However, the present application of those techniques at scalp electrodes ignores observational equations modeling confounding effects of head volume conduction and position/orientation of cortical sources of scalp EEG activity (Babiloni et al., 2020). Therefore, confounding non-zero-lag head volume conduction effects and false 'interrelatedness' cannot be excluded in the interpretation of the present results. In this framework, it should be remarked that bivariate techniques (including LLC) may be more prone to those confounds than multivariate techniques (including iCoh), as the latter typically remove common correlations of the rsEEG activity among the electrode pairs (Blinowska and Kaminski, 2013; Babiloni et al., 2020b).

The intrinsic methodological limits of all bivariate and multivariate techniques (including LLC and iCoh) were recently discussed by an Expert Panel of the International Federation of Clinical Neurophysiology (IFCN; Babiloni et al., 2020b). The Expert Panel agreed that all bivariate (e.g., LLC, synchronization likelihood, phase lag index, etc.) and multivariate (e.g., iCoh, directed transfer function, etc.) techniques estimating the interrelatedness of the rsEEG activity at scalp electrode pairs may be subject to unmodeled effects of (1) brain neural populations 'invisible' to EEG recordings and (2) head volume conduction. Furthermore, the Expert Panel shared the following recommendations to fruitfully tackle (Babiloni et al., 2020b): (1) the use of the locution '*measures of the interrelatedness of rsEEG activity at scalp electrodes*' rather than locutions such as "*measures of cortical functional connectivity from rsEEG activity*" to emphasize that the head volume conduction effects cannot be entirely taken into account when those techniques are applied at scalp electrode pairs; (2) the development of exploratory rsEEG studies carried out by investigators belonging to independent research institutions, to ensure a significant intersubjectivity in the interpretation of the results; (3) the use of at least two independent techniques for estimating the interrelatedness of the rsEEG activity at scalp electrodes, to compare the results and represent their intrinsic variability dependent on the methodology used; and (4) the exploitation of open science to cross-validate the research results using, when possible, freeware techniques validated by independent research groups. We grounded the present study design on these recommendations.

Keeping in mind the previously mentioned low spatial resolution and head volume conduction effects, we included a relatively low number of network nodes (corresponding to the standard 10–20 electrode montage) in the graph analysis. This low-resolution EEG method could not allow the disentanglement of the contribution of the nodes of the default mode network or associate parietal cortex. Therefore, future studies may improve the methodological approach with the following solutions: (1) large samples of the enrolled ADD, ADMCI, and Nold participants and a longitudinal design to enhance the statistical power of the study and test the impact of disease severity and progression on the topology of the interrelatedness of rsEEG activity; (2) harmonized protocols in the multicentric studies; (3) >48 scalp electrodes for the rsEEG recordings; (4) mathematical source and head volume conduction models for an rsEEG source estimation probing the activity of more

cortical nodes, including those located in the default mode and other relevant cortical networks; (5) a multimodal approach, including the rs-fMRI recordings, to correlate the AD-related abnormal topology of the cortical functional connectivity, as revealed by rs-fMRI and rsEEG data; and (6) a more systematic variation of statistical thresholds to qualify the significant associations between sensors and the criteria used to define and describe the present hubs with those thresholds.

5. Conclusion

In the present exploratory study, we compared hubs modeled from measures of interdependencies of between-electrode rsEEG alpha rhythms in Nold and mild-to-moderate ADD participants. We tested the hypothesis of abnormal posterior hubs from those measures in ADD versus Nold participants. To report robust results, we measured interdependencies of rsEEG rhythms using both bivariate LLC and multivariate (directional) iCoh measures. Furthermore, we used three different definitions of 'connector' hub.

Convergent results of LLC and iCoh measures showed that in both Nold and ADD groups there were significant 'degree' and 'connector' hubs at ***parietal*** electrodes derived from rsEEG ***alpha rhythms***. Furthermore, these hubs showed a prominent outward directionality in both groups of participants. As a main difference between the two groups, the outward 'directionality' of the hubs at parietal electrodes was lower in the ADD group than in the Nold group.

Future longitudinal high-resolution rsEEG studies in ADD patients will have to test hypotheses about the resilience or vulnerability of those parietal hubs derived from rsEEG alpha rhythms and their relationships with the neuropathological burden, derangement in the DMN, and the neurophysiological regulation and maintenance of quiet vigilance during daytime.

Data availability statement

The datasets presented in this article are not readily available because they may be made available by CB through a formal data sharing agreement and approval from the requesting researcher's local ethics committee. The presentation of a formal collaboration project outline is also suggested. Requests to access the datasets should be directed to SL, susanna.lopez@uniroma1.it.

Ethics statement

The studies involving human participants were reviewed and approved by Sapienza University of Rome. The patients/participants provided their written informed consent to participate in this study.

Author contributions

CBa and SL: conceptualization, methodology, formal analysis, investigation, data curation, validation, project administration, writing—original draft, supervision, writing—review and editing. CP, GN, and RL: formal analysis, software, writing—review and editing. AP, FN, DA, FF, DM, AC, GK, AB, MO, BB, AS, RF, CBu, FG, BG, GY, FS, LV, and LB: methodology, project administration, writing—review and editing. All authors contributed to the article and approved the submitted version.

Funding

In this study, the electroencephalographic data analysis was partially supported by the funds of "Ricerca Corrente 2021–2022" attributed by the Ministry of Health, Italy to the IRCCS Synlab SDN of Naples, IRCCS OASI Maria SS of Troina, IRCCS San Giovanni di Dio "Fatebenefratelli" of Brescia, and IRCCS San Raffaele Rome.

Acknowledgments

The research activities were partly developed in the framework of the 'PDWAVES' Consortium (https://www.pdwaves.eu/) founded by CB (Sapienza University of Rome, Italy) and Peter Fuhr (University of Basel, Basel, Switzerland).

Conflict of interest

The authors declare that the research was conducted in the absence of any commercial or financial relationships that could be construed as a potential conflict of interest.

Publisher's note

Supplementary material

The Supplementary material for this article can be found online at: https://www.frontiersin.org/articles/10.3389/fnagi.2023.780014/full#supplementary-material

References

Adler, G., Brassen, S., and Jajcevic, A. (2003). EEG coherence in Alzheimer's dementia. *J. Neural Transm.* 110, 1051–1058. doi: 10.1007/s00702-003-0024-8

Afshari, S., and Jalili, M. (2017). Directed functional networks in Alzheimer's disease: disruption of global and local connectivity measures. *IEEE J. Biomed. Health Inform.* 21, 949–955. doi: 10.1109/JBHI.2016.2578954

Albert, M. S., DeKosky, S. T., Dickson, D., Dubois, B., Feldman, H. H., Fox, N. C., et al. (2011). The diagnosis of mild cognitive impairment due to Alzheimer's disease: recommendations from the National Institute on Aging-Alzheimer's Association workgroups on diagnostic guidelines for Alzheimer's disease. *Alzheimers Dement.* 7, 270–279. doi: 10.1016/j.jalz.2011.03.008

Al-Shargie, F., Tariq, U., Hassanin, O., Mir, H., Babiloni, F., and Al-Nashash, H. (2019). Brain connectivity analysis under semantic vigilance and enhanced mental states. *Brain Sci.* 9:363. doi: 10.3390/brainsci9120363

Anghinah, R., Kanda, P. A., Jorge, M. S., Lima, E. E., Pascuzzi, L., and Melo, A. C. (2000). Alpha band coherence analysis of EEG in healthy adult's and Alzheimer's type dementia patients. *Arq. Neuropsiquiatr.* 58, 272–275. doi: 10.1590/S0004-282X2000000200011

Babiloni, C., Arakaki, X., Azami, H., Bennys, K., Blinowska, K., Bonanni, L., et al. (2021). Measures of resting state EEG rhythms for clinical trials in Alzheimer's disease: recommendations of an expert panel. *Alzheimers Dement.* 17, 1528–1553. doi: 10.1002/alz.12311

Babiloni, C., Barry, R. J., Başar, E., Blinowska, K. J., Cichocki, A., Drinkenburg, W. H. I. M., et al. (2020b). International Federation of Clinical Neurophysiology (IFCN) – EEG research workgroup: recommendations on frequency and topographic analysis of resting state EEG rhythms. Part 1: applications in clinical research studies. *Clin. Neurophysiol.* 131, 285–307. doi: 10.1016/j.clinph.2019.06.234

Babiloni, C., Blinowska, K., Bonanni, L., Cichocki, A., De Haan, W., Del Percio, C., et al. (2020a). What electrophysiology tells us about Alzheimer's disease: a window into the synchronization and connectivity of brain neurons. *Neurobiol. Aging* 85, 58–73.

Babiloni, C., Cassetta, E., Dal Forno, G., Del Percio, C., Ferreri, F., Ferri, R., et al. (2006a). Donepezil effects on sources of cortical rhythms in mild Alzheimer's disease: responders vs. non-responders. *Neuroimage* 31, 1650–1665. doi: 10.1016/j.neuroimage.2006.02.015

Babiloni, C., Del Percio, C., Boccardi, M., Lizio, R., Lopez, S., Carducci, F., et al. (2015). Occipital sources of resting-state alpha rhythms are related to local gray matter density in subjects with amnesic mild cognitive impairment and Alzheimer's disease. *Neurobiol. Aging* 36, 556–570. doi: 10.1016/j.neurobiolaging.2014.09.011

Babiloni, C., Del Percio, C., Lizio, R., Noce, G., Cordone, S., Lopez, S., et al. (2017). Abnormalities of cortical neural synchronization mechanisms in patients with dementia due to Alzheimer's and Lewy body diseases: an EEG study. *Neurobiol. Aging* 55, 143–158. doi: 10.1016/j.neurobiolaging.2017.03.030

Babiloni, C., Del Percio, C., Lizio, R., Noce, G., Lopez, S., Soricelli, A., et al. (2018). Abnormalities of resting-state functional cortical connectivity in patients with dementia due to Alzheimer's and Lewy body diseases: an EEG study. *Neurobiol. Aging* 65, 18–40.

Babiloni, C., Del Percio, C., Pascarelli, M. T., Lizio, R., Noce, G., Lopez, S., et al. (2019). Abnormalities of functional cortical source connectivity of resting-state electroencephalographic alpha rhythms are similar in patients with mild cognitive impairment due to Alzheimer's and Lewy body diseases. *Neurobiol. Aging.* 77, 112–127. doi: 10.1016/j.neurobiolaging.2019.01.013

Babiloni, C., Ferri, R., Binetti, G., Vecchio, F., Frisoni, G. B., Lanuzza, B., et al. (2009a). Directionality of EEG synchronization in Alzheimer's disease subjects. *Neurobiol. Aging* 30, 93–102.

Babiloni, C., Ferri, R., Moretti, D. V., Strambi, A., Binetti, G., Dal Forno, G., et al. (2004b). Abnormal fronto-parietal coupling of brain rhythms in mild Alzheimer's disease: a multicentric EEG study. *Eur J Neurosci.* 19, 2583–2590. doi: 10.1111/j.0953-816X.2004.03333.x

Babiloni, C., Ferri, R., Noce, G., Lizio, R., Lopez, S., Soricelli, A., et al. (2020). Resting-state electroencephalographic delta rhythms may reflect global cortical arousal in healthy old seniors and patients with Alzheimer's disease dementia. *Int. J. Psychophysiol.* 158, 259–270. doi: 10.1016/j.ijpsycho.2020.08.012

Babiloni, C., Frisoni, G. B., Pievani, M., Vecchio, F., Infarinato, F., Geroldi, C., et al. (2008). White matter vascular lesions are related to parietal-to-frontal coupling of EEG rhythms in mild cognitive impairment. *Hum. Brain Mapp.* 29, 1355–1367. doi: 10.1002/hbm.20467

Babiloni, C., Frisoni, G. B., Vecchio, F., Pievani, M., Geroldi, C., De Carli, C., et al. (2010). Global functional coupling of resting EEG rhythms is related to white-matter lesions along the cholinergic tracts in subjects with amnesic mild cognitive impairment. *J. Alzheimers Dis.* 19, 859–871.

Babiloni, C., Lizio, R., Marzano, N., Capotosto, P., Soricelli, A., Triggiani, A. I., et al. (2016). Brain neural synchronization and functional coupling in Alzheimer's disease as revealed by resting state EEG rhythms. *Int. J. Psychophysiol.* 103, 88–102. doi: 10.1016/j.ijpsycho.2015.02.008

Babiloni, C., Miniussi, C., Moretti, D. V., Vecchio, F., Salinari, S., Frisoni, G., et al. (2004a). Cortical networks generating movement-related EEG rhythms in Alzheimer's disease: an EEG coherence study. *Behav. Neurosci.* 118, 698–706. doi: 10.1037/0735-7044.118.4.698

Babiloni, C., Pievani, M., Vecchio, F., Geroldi, C., Eusebi, F., Fracassi, C., et al. (2009b). White-matter lesions along the cholinergic tracts are related to cortical sources of EEG rhythms in amnesic mild cognitive impairment. *Hum. Brain Mapp.* 30, 1431–1443. doi: 10.1016/j.neurobiolaging.2007.05.007

Babiloni, C., Vecchio, F., Bultrini, A., Luca Romani, G., and Rossini, P. M. (2006b). Pre- and poststimulus alpha rhythms are related to conscious visual perception: a high-resolution EEG study. *Cereb. Cortex* 16, 1690–1700. doi: 10.1093/cercor/bhj104

Besthorn, C., Förstl, H., Geiger-Kabisch, C., Sattel, H., Gasser, T., and Schreiter-Gasser, U. (1994). EEG coherence in Alzheimer disease. *Electroencephalogr. Clin. Neurophysiol.* 90, 242–245. doi: 10.1016/0013-4694(94)90095-7

Blinowska, K. J. (2011). Review of the methods of determination of directed connectivity from multichannel data. *Med. Biol. Engin. Comput.* 49, 521–529. doi: 10.1007/s11517-011-0739-x

Blinowska, K. J., and Kaminski, M. (2013). Functional brain networks: random, "small world" or deterministic? *PLoS One.* 8:e78763. doi: 10.1371/journal.pone.0078763

Blinowska, K. J., Rakowski, F., Kaminski, M., De Vico, F. F., Del Percio, C., Lizio, R., et al. (2017). Functional and effective brain connectivity for discrimination between Alzheimer's patients and healthy individuals: a study on resting state EEG rhythms. *Clin. Neurophysiol.* 128, 667–680. doi: 10.1016/j.clinph.2016.10.002

Bokde, A. L., Lopez-Bayo, P., Meindl, T., Pechler, S., Born, C., Faltraco, F., et al. (2006). Functional connectivity of the fusiform gyrus during a face-matching task in subjects with mild cognitive impairment. *Brain* 129, 1113–1124. doi: 10.1093/brain/awl051

Boksem, M. A., Meijman, T. F., and Lorist, M. M. (2005). Effects of mental fatigue on attention: an ERP study. *Brain Res. Cogn. Brain Res.* 25, 107–116. doi: 10.1016/j.cogbrainres.2005.04.011

Brier, M. R., Thomas, J. B., Snyder, A. Z., Benzinger, T. L., Zhang, D., Raichle, M. E., et al. (2012). Loss of intranetwork and internetwork resting state functional connections with Alzheimer's disease progression. *J Neurosci.* 32, 8890–8899. doi: 10.1523/JNEUROSCI.5698-11.2012

Buckner, R. L., Andrews-Hanna, J. R., and Schacter, D. L. (2008). The brain's default network: anatomy, function, and relevance to disease. *Ann. N. Y. Acad. Sci.* 1124, 1–38. doi: 10.1196/annals.1440.011

Bullmore, E., and Sporns, O. (2009). Complex brain networks: graph theoretical analysis of structural and functional systems Nat. *Rev. Neurosci.* 10, 186–198. doi: 10.1038/nrn2575

Bullmore, E., and Sporns, O. (2012). The economy of brain network organization. *Nat. Rev. Neurosci.* 13, 336–349. doi: 10.1038/nrn3214

Busche, M. A., and Konnerth, A. (2016). Impairments of neural circuit function in Alzheimer's disease. *Philos. Trans. R. Soc. Lond. Ser. B Biol. Sci.* 371:20150429. doi: 10.1098/rstb.2015.0429

Canuet, L., Tellado, I., Couceiro, V., Fraile, C., Fernandez-Novoa, L., Ishii, R., et al. (2012). Resting-state network disruption and APOE genotype in Alzheimer's disease: a lagged functional connectivity study. *PLoS One* 7:e46289. doi: 10.1371/journal.pone.0046289

Capotosto, P., Babiloni, C., Romani, G. L., and Corbetta, M. (2012). Differential contribution of right and left parietal cortex to the control of spatial attention: a simultaneous EEG-rTMS study. *Cereb. Cortex* 22, 446–454. doi: 10.1093/cercor/bhr127

Chen, G., Zhang, H. Y., Xie, C., Chen, G., Zhang, Z. J., Teng, G. J., et al. (2013). Modular reorganization of brain resting state networks and its independent validation in Alzheimer's disease patients. *Front. Hum. Neurosci.* 7:456. doi: 10.3389/fnhum.2013.00456

Cole, M. W., Ito, T., and Braver, T. S. (2015). Lateral prefrontal cortex contributes to fluid intelligence through multinetwork connectivity. *Brain Connect.* 5, 497–504. doi: 10.1089/brain.2015.0357

Crunelli, V., David, F., Lőrincz, M. L., and Hughes, S. W. (2015). The thalamocortical network as a single slow wave-generating unit. *Curr. Opin. Neurobiol.* 31, 72–80. doi: 10.1016/j.conb.2014.09.001

Crunelli, V., Lőrincz, M. L., Connelly, W. M., David, F., Hughes, S. W., Lambert, R. C., et al. (2018). Dual function of thalamic low-vigilance state oscillations: rhythm-regulation and plasticity. *Nat Rev Neurosci.* 19, 107–118. doi: 10.1038/nrn.2017.151

Daianu, M., Jahanshad, N., Nir, T. M., Toga, A., Jack, C. R., Weiner, M. W., et al. (2013). Breakdown of brain connectivity between normal aging and Alzheimer's disease: a structural k-core network analysis. *Brain Connect.* 3, 407–422. doi: 10.1089/brain.2012.0137

Das, S., and Puthankattil, S. D. (2022). Functional connectivity and complexity in the phenomenological model of mild cognitive-impaired Alzheimer's disease. *Front. Comput. Neurosci.* 6:877912. doi: 10.3389/fncom.2022.877912

Dauwels, J., Vialatte, F., Latchoumane, C., Jeong, J., and Cichocki, A. (2009). EEG synchrony analysis for early diagnosis of Alzheimer's disease: a study with several synchrony measures and EEG data sets. *Ann. Int. Conf. IEEE Eng. Med. Biol. Soc.*, 2224–2227. doi: 10.1109/IEMBS.2009.5334862

Dauwels, J., Vialatte, F., Musha, T., and Cichocki, A. (2010). A comparative study of synchrony measures for the early diagnosis of Alzheimer's disease based on EEG. *NeuroImage* 49, 668–693. doi: 10.1016/j.neuroimage.2009.06.056

de Haan, W., Mott, K., van Straaten, E. C., Scheltens, P., and Stam, C. J. (2012). Activity dependent degeneration explains hub vulnerability in Alzheimer's disease. *PLoS Comput Biol.* 8:e1002582. doi: 10.1371/journal.pcbi.1002582

de Haan, W., Pijnenburg, Y. A., Strijers, R. L., van der Made, Y., van der Flier, W. M., Scheltens, P., et al. (2009). Functional neural network analysis in frontotemporal dementia and Alzheimer's disease using EEG and graph theory. *BMC Neurosci.* 10:101. doi: 10.1186/1471-2202-10-101

Del Percio, C., Derambure, P., Noce, G., Lizio, R., Bartrés-Faz, D., Blin, O., et al. (2019). Sleep deprivation and Modafinil affect cortical sources of resting state electroencephalographic rhythms in healthy young adults. *Clin. Neurophysiol.* 130, 1488–1498. doi: 10.1016/j.clinph.2019.06.007

Delbeuck, X., Van der Linden, M., and Collette, F. (2003). Alzheimer's disease as a disconnection syndrome? *Neuropsychol. Rev.* 13, 79–92. doi: 10.1023/a:1023832305702

Dunkin, J. J., Leuchter, A. F., Newton, T. F., and Cook, I. A. (1994). Reduced EEG coherence in dementia: state or trait marker? *Biol. Psychiatry* 35, 870–879.

Engels, M. M., Stam, C. J., van der Flier, W. M., Scheltens, P., de Waal, H., and van Straaten, E. C. (2015). Declining functional connectivity and changing hub locations in Alzheimer's disease: an EEG study. *BMC Neurol.* 15:145. doi: 10.1186/s12883-015-0400-7

Ermentrout, G. B., and Kleinfeld, D. (2001). Traveling electrical waves in cortex: insights from phase dynamics and speculation on a computational role. *Neuron.* 29, 33–44. doi: 10.1016/s0896-6273(01)00178-7

Eyler, L. T., Elman, J. A., Hatton, S. N., Gough, S., Mischel, A. K., Hagler, D. J., et al. (2019). Resting state abnormalities of the default mode network in mild cognitive impairment: a systematic review and meta-analysis. *J Alzheimers Dis.* 70, 107–120. doi: 10.3233/JAD-180847

Folstein, M. F., Folstein, S. E., and McHugh, P. R. (1975). 'Mini mental state': a practical method for grading the cognitive state of patients for clinician. *J. Psychiatr. Res.* 12, 189–198.

Fonseca, L. C., Tedrus, G. M., Carvas, P. N., and Machado, E. C. (2013). Comparison of quantitative EEG between patients with Alzheimer's disease and those with Parkinson's disease dementia. *Clin. Neurophysiol.* 124, 1970–1974. doi: 10.1016/j.clinph.2013.05.001

Fonseca, L. C., Tedrus, G. M., Fondello, M. A., Reis, I. N., and Fontoura, D. S. (2011). EEG theta and alpha reactivity on opening the eyes in the diagnosis of Alzheimer's disease. *Clin. EEG Neurosci.* 42, 185–189. doi: 10.1177/155005941104200308

Franciotti, R., Falasca, N. W., Arnaldi, D., Famà, F., Babiloni, C., Onofrj, M., et al. (2019). Cortical network topology in prodromal and mild dementia due to Alzheimer's disease: graph theory applied to resting state EEG. *Brain Topogr.* 32, 127–141. doi: 10.1007/s10548-018-0674-3

Franciotti, R., Moretti, D. V., Benussi, A., Ferri, L., Russo, M., Carrarini, C., et al. (2022). Cortical network modularity changes along the course of frontotemporal and Alzheimer's dementing diseases. *Neurobiol. Aging* 110, 37–46. doi: 10.1016/j.neurobiolaging.2021.10.016

Frantzidis, C. A., Vivas, A. B., Tsolaki, A., Klados, M. A., Tsolaki, M., and Bamidis, P. D. (2014). Functional disorganization of small-world brain networks in mild Alzheimer's disease and amnestic mild cognitive impairment: an EEG study using relative wavelet entropy (RWE). *Front. Aging Neurosci.* 6:224. doi: 10.3389/fnagi.2014.00224

Gelb, D. J., Oliver, E., and Gilman, S. (1999). Diagnostic criteria for Parkinson disease. *Arch Neurol.* 56, 33–39. doi: 10.1001/archneur.56.1.33

Gorelick, P. B., Scuteri, A., Black, S. E., Decarli, C., Greenberg, S. M., Iadecola, C., et al. (2011). American Heart Association stroke council, council on epidemiology and prevention, council on cardiovascular nursing, council on cardiovascular radiology and intervention, and council on cardiovascular surgery and anesthesia. Vascular contributions to cognitive impairment and dementia: a statement for healthcare professionals from the american heart association/american stroke association. *Stroke* 42, 2672–2713. doi: 10.1161/STR.0b013e3182299496

Halgren, M., Ulbert, I., Bastuji, H., Fabó, D., Erőss, L., Rey, M., et al. (2019). The generation and propagation of the human alpha rhythm. *Proc Natl Acad Sci U S A.* 116, 23772–23782. doi: 10.1073/pnas.1913092116

Hallett, M., de Haan, W., Deco, G., Dengler, R., Di Iorio, R., Gallea, C., et al. (2020). Human brain connectivity: clinical applications for clinical neurophysiology. *Clin. Neurophysiol.* 131, 1621–1651. doi: 10.1016/j.clinph.2020.03.031

Han, S., Fan, Y., and Mao, L. (2008). Gender difference in empathy for pain: an electrophysiological investigation. *Brain Res.* 1196, 85–93. doi: 10.1016/j.brainres.2007.12.062

He, Y., and Evans, A. (2010). Graph theoretical modeling of brain connectivity. *Curr. Opin. Neurol.* 23, 341–350. doi: 10.1097/WCO.0b013e32833aa567

Hsiao, F. J., Chen, W. T., Wang, Y. J., Yan, S. H., and Lin, Y. Y. (2014). Altered source-based EEG coherence of resting-state sensorimotor network in early-stage Alzheimer's disease compared to mild cognitive impairment. *Neurosci. Lett.* 558, 47–52. doi: 10.1016/j.neulet.2013.10.056

Hsiao, F. J., Wang, Y. J., Yan, S. H., Chen, W. T., and Lin, Y. Y. (2013). Altered oscillation and synchronization of default-mode network activity in mild Alzheimer's disease compared to mild cognitive impairment: an electrophysiological study. *PLoS One* 8:e68792. doi: 10.1371/journal.pone.0068792

Hughes, C. P., Berg, L., Danziger, W. L., Coben, L. A., and Martin, R. L. (1982). A new clinical scale for the staging of dementia. *Br. J. Psychiatry* 140, 566–572. doi: 10.1192/bjp.140.6.566

Hughes, S. W., and Crunelli, V. (2005). Thalamic mechanisms of EEG alpha rhythms and their pathological implications. *Neuroscientist* 11, 357–372. doi: 10.1177/1073858405277450

Jack, C. R. Jr., Therneau, T. M., Weigand, S. D., Wiste, H. J., Knopman, D. S., Vemuri, P., et al. (2019). Prevalence of Biologically vs Clinically Defined Alzheimer Spectrum Entities Using the National Institute on Aging-Alzheimer's Association Research Framework. *JAMA Neurol.* 76, 1174–1183. doi: 10.1001/jamaneurol.2019.1971

Jagannathan, S. R., Bareham, C. A., and Bekinschtein, T. A. (2022). Decreasing alertness modulates perceptual decision-making. *J. Neurosci.* 42, 454–473.

Jagannathan, S. R., Ezquerro-Nassar, A., Jachs, B., Pustovaya, O. V., Bareham, C. A., and Bekinschtein, T. A. (2018). Tracking wakefulness as it fades: micro-measures of alertness. *NeuroImage* 1, 138–151. doi: 10.1016/j.neuroimage.2018.04.046

Jelic, V., Dierks, T., Amberla, K., Almkvist, O., Winblad, B., and Nordberg, A. (1998). Longitudinal changes in quantitative EEG during long-term tacrine treatment of patients with Alzheimer's disease. *Neurosci. Lett.* 254, 85–88. doi: 10.1016/S0304-3940(98)00669-7

Jelic, V., Johansson, S. E., Almkvist, O., Shigeta, M., Julin, P., Nordberg, A., et al. (2000). Quantitative electroencephalography in mild cognitive impairment: longitudinal changes and possible prediction of Alzheimer's disease. *Neurobiol. Aging* 21, 533–540. doi: 10.1016/s0197-4580(00)00153-6

Joo, S. H., Lee, C. U., and Lim, H. K. (2016). Apathy and intrinsic functional connectivity networks in amnestic mild cognitive impairment. *Neuropsychiatr Dis Treat.* 13, 61–67. doi: 10.2147/NDT.S123338

Klimesch, W. (1996). Memory processes, brain oscillations and EEG synchronization. *Int. J. Psychophysiol.* 24, 61–100.

Klimesch, W. (1999). EEG alpha and theta oscillations reflect cognitive and memory performance: a review and analysis. *Brain Res. Rev.* 29, 1169–1195.

Klimesch, W., Russegger, H., Doppelmayr, M., and Pachinger, T. (1998). A method for the calculation of induced band power: implications for the significance of brain oscillations. *Electroencephalogr. Clin. Neurophysiol.* 108, 123–130. doi: 10.1016/s0168-5597(97)00078-6

Knott, V., Engeland, C., Mohr, E., Mahoney, C., and Ilivitsky, V. (2000). Acute nicotine administration in Alzheimer's disease: an exploratory EEG study. *Neuropsychobiology* 41, 210–220. doi: 10.1159/000026662

Kuś, R., Kamiński, M., and Blinowska, K. J. (2004). Determination of EEG activity propagation: pair-wise versus multichannel estimate. *I.E.E.E. Trans. Biomed. Eng.* 51, 1501–1510. doi: 10.1109/TBME.2004.827929

Lawton, M. P., and Brody, E. M. (1969). Assessment of older people: self-maintaining and instrumental activities of daily living. *Gerontologist* 9, 179–186.

Leuchter, A. F., Dunkin, J. J., Lufkin, R. B., Anzai, Y., Cook, I. A., and Newton, T. F. (1994). Effect of white matter disease on functional connections in the aging brain. *J. Neurol. Neurosurg. Psychiatry* 57, 1347–1354. doi: 10.1136/jnnp.57.11.1347

Leuchter, A. F., Newton, T. F., Cook, I. A., Walter, D. O., Rosenberg-Thompson, S., and Lachenbruch, P. A. (1992). Changes in brain functional connectivity in alzheimer-type and multi-infarct dementia. Brain: a. *J. Neurol.* 115, 1543–1561.

Liao, X., Vasilakos, A. V., and He, Y. (2017). Small-world human brain networks: perspectives and challenges. *Neurosci. Biobehav. Rev.* 77, 286–300. doi: 10.1016/j.neubiorev.2017.03.018

Liu, J. P., Zhang, C., and Zheng, C. X. (2010). Estimation of the cortical functional connectivity by directed transfer function during mental fatigue. *Appl. Ergon.* 42, 114–121. doi: 10.1016/j.apergo.2010.05.008

Lizio, R., Del Percio, C., Marzano, N., Soricelli, A., Yener, G. G., Başar, E., et al. (2016). Neurophysiological assessment of Alzheimer's disease individuals by a single electroencephalographic marker. *J. Alzheimers Dis.* 49, 159–177. doi: 10.3233/JAD-143042

Lo, C. Y., Wang, P. N., Chou, K. H., Wang, J., He, Y., and Lin, C. P. (2010). Diffusion tensor tractography reveals abnormal topological organization in structural cortical networks in Alzheimer's disease. *J. Neurosci.* 30, 16876–16885. doi: 10.1523/JNEUROSCI.4136-10.2010

Locatelli, T., Cursi, M., Liberati, D., Franceschi, M., and Comi, G. (1998). EEG coherence in Alzheimer's disease. *Electroencephalogr. Clin. Neurophysiol.* 106, 229–237. doi: 10.1016/S0013-4694(97)00129-6

Lörincz, M. L., Crunelli, V., and Hughes, S. W. (2008). Cellular dynamics of cholinergically induced alpha (8-13 Hz) rhythms in sensory thalamic nuclei in vitro. *J. Neurosci.* 28, 660–671. doi: 10.1523/JNEUROSCI.4468-07.2008

Lörincz, M. L., Kékesi, K. A., Juhász, G., Crunelli, V., and Hughes, S. W. (2009). Temporal framing of thalamic relay-mode firing by phasic inhibition during the alpha rhythm. *Neuron* 63, 683–696. doi: 10.1016/j.neuron.2009.08.012

McKeith, I. G., Dickson, D. W., Lowe, J., Emre, M., O'Brien, J. T., Feldman, H., et al. (2005). Diagnosis and management of dementia with Lewy bodies: third report of the DLB consortium. *Neurology* 65, 1863–1872. doi: 10.1212/01.wnl.0000187889.17253.b1

McKhann, G., Drachman, D., Folstein, M., Katzman, R., Price, D., and Stadlan, E. M. (1984). Clinical diagnosis of Alzheimer's disease: report of the NINCDS-ADRDA work group under the auspices of Department of Health and Human Services Task Force on Alzheimer's disease. *Neurology* 34, 939–944.

McKhann, G. M., Knopman, D. S., Chertkow, H., Hyman, B. T., Jack, C. R. Jr., Kawas, C. H., et al. (2011). The diagnosis of dementia due to Alzheimer's disease: recommendations from the National Institute on Aging-Alzheimer's Association workgroups on diagnostic guidelines for Alzheimer's disease. *Alzheimers Dement.* 7, 263–269. doi: 10.1016/j.jalz.2011.03.005

Moretti, D. V., Babiloni, F., Carducci, F., Cincotti, F., Remondini, E., Rossini, P. M., et al. (2003). Computerized processing of EEG–EOG–EMG artifacts for multicentric studies in EEG oscillations and event-related potentials. *Int. J. Pshycophysiol.* 47, 199–216. doi: 10.1016/s0167-8760(02)00153-8

Morikawa, T., Hayashi, M., and Hori, T. (2002). Spatiotemporal variations of alpha and sigma band EEG in the waking-sleeping transition period. *Percept. Mot. Skills* 95, 131–154. doi: 10.2466/pms.2002.95.1.131

Nakamura, T., Goverdovsky, V., Morrell, M. J., and Mandic, D. P. (2017). Automatic sleep monitoring using ear-EEG. IEEE J Transl Eng. *Health Med.* 5:2800108. doi: 10.1109/JTEHM.2017.2702558

Ng, A. S. L., Wang, J., Ng, K. K., Chong, J. S. X., Qian, X., Lim, J. K. W., et al. (2021). Distinct network topology in Alzheimer's disease and behavioral variant frontotemporal dementia. *Alzheimers Res Ther.* 13:13. doi: 10.1186/s13195-020-00752-w

Novelli, G., Papagno, C., Capitani, E., Laiacona, M., Vallar, G., and Cappa, S. F. (1986). Tre test clinici di ricerca e produzione lessicale. Taratura su sogetti normali. *Arch. Psicol. Neurol. Psichiatr.* 47, 477–506.

Pascual-Marqui, R. D. (2007). Discrete, 3D distributed, linear imaging methods of electric neuronal activity. Part 1: exact, zero error localization. *Math. Phys.*, 1–16.

Pascual-Marqui, R. D., Biscay, R. J., Bosch-Bayard, J., Lehmann, D., Kochi, K., Kinoshita, T., et al. (2014). Assessing direct paths of intracortical causal information flow of oscillatory activity with the isolated effective coherence (iCoh). *Front. Hum. Neurosci.* 8:448. doi: 10.3389/fnhum.2014.00448

Pascual-Marqui, R. D., Lehmann, D., Koukkou, M., Kochi, K., Anderer, P., Saletu, B., et al. (2011). Assessing interactions in the brain with exact low-resolution electromagnetic tomography. *Philos Trans A Math Phys Eng Sci.* 369, 3768–3784. doi: 10.1098/rsta.2011.0081

Peraza, L. R., Cromarty, R., Kobeleva, X., Firbank, M. J., Killen, A., Graziadio, S., et al. (2018). Electroencephalographic derived network differences in Lewy body dementia compared to Alzheimer's disease patients. *Sci. Rep.* 8:4637. doi: 10.1038/s41598-018-22984-5

Pfurtscheller, G., and Klimesch, W. (1992). Functional topography during a visuoverbal judgment task studied with event-related desynchronization mapping. *J Clin Neurophysiol.* 9, 120–131. doi: 10.1097/00004691-199201000-00013

Pogarell, O., Teipel, S. J., Juckel, G., Gootjes, L., Möller, T., Bürger, K., et al. (2005). EEG coherence reflects regional corpus callosum area in Alzheimer's disease. *J. Neurol. Neurosurg. Psychiatry* 76, 109–111. doi: 10.1136/jnnp.2004.036566

Power, J. D., Schlaggar, B. L., Lessov-Schlaggar, C. N., and Petersen, S. E. (2013). Evidence for hubs in human functional brain networks. *Neuron* 79, 798–813. doi: 10.1016/j.neuron.2013.07.035

Raichle, M. E., MacLeod, A. M., Snyder, A. Z., Powers, W. J., Gusnard, D. A., and Shulman, G. L. (2001). A default mode of brain function. *Proc. Natl. Acad. Sci. U. S. A.* 98, 676–682. doi: 10.1073/pnas.98.2.676

Rascovsky, K., Hodges, J. R., Knopman, D., Mendez, M. F., Kramer, J. H., Neuhaus, J., et al. (2011). Miller BL. Sensitivity of revised diagnostic criteria for the behavioural variant of frontotemporal dementia. *Brain* 134, 2456–2477. doi: 10.1093/brain/awr179

Reijmer, Y. D., Leemans, A., Caeyenberghs, K., Heringa, S. M., Koek, H. L., Biessels, G. J., et al. (2013). Disruption of cerebral networks and cognitive impairment in Alzheimer disease. *Neurology.* 80, 1370–1377. doi: 10.1212/WNL.0b013e31828c2ee5

Reijneveld, J. C., Ponten, S. C., Berendse, H. W., and Stam, C. J. (2007). The application of graph theoretical analysis to complex networks in the brain. *Clin. Neurophysiol.* 118, 2317–2331. doi: 10.1016/j.clinph.2007.08.010

Reitan, R. M. (1958). Validity of the trail making test as an indicator of organic brain damage. *Percept. Mot. Skills* 8, 271–276. doi: 10.2466/PMS.8.7.271-276

Rey, A. (1959). *Reattivo della figura complessa*. Manuale del Centre de Psychologie Appliquee, Parigi.

Rosen, W. G., Terry, R. D., Fuld, P. A., Katzman, R., and Peck, A. (1980). Pathological verification of ischemic score in differentiation of dementias. *Ann. Neurol.* 7, 486–488. doi: 10.1002/ana.410070516

Rubinov, M., and Sporns, O. (2010). Complex network measures of brain connectivity: uses and interpretations. *NeuroImage* 52, 1059–1069. doi: 10.1016/j.neuroimage.2009.10.003

Sankari, Z., Adeli, H., and Adeli, A. (2011). Intrahemispheric, interhemispheric, and distal EEG coherence in Alzheimer's disease. *Clin. Neurophysiol.* 122, 897–906. doi: 10.1016/j.clinph.2010.09.008

Sanz-Arigita, E. J., Schoonheim, M. M., Damoiseaux, J. S., Rombouts, S. A., Maris, E., Barkhof, F., et al. (2010). Loss of 'small-world' networks in Alzheimer's disease: graph analysis of FMRI resting-state functional connectivity. *PLoS One* 5:e13788. doi: 10.1371/journal.pone.0013788

Sloan, E. P., Fenton, G. W., Kennedy, N. S., and MacLennan, J. M. (1994). Neurophysiology and SPECT cerebral blood flow patterns in dementia. *Electroencephalogr. Clin. Neurophysiol.* 91, 163–170. doi: 10.1016/0013-4694(94)90066-3

Song, Z., Deng, B., Wang, J., and Wang, R. (2019). Biomarkers for Alzheimer's disease defined by a novel brain functional network measure. *I.E.E.E. Trans. Biomed. Eng.* 66, 41–49. doi: 10.1109/TBME.2018.2834546

Sorg, C., Riedl, V., Mühlau, M., Calhoun, V. D., Eichele, T., Läer, L., et al. (2007). Selective changes of resting-state networks in individuals at risk for Alzheimer's disease. *Proc. Natl. Acad. Sci. U. S. A.* 104, 18760–18765. doi: 10.1073/pnas.0708803104

Spinnler, H., and Tognoni, G. (1987). Standardizzazione e taratura italiana di test neuropsicologici. *Ital. J. Neurol. Sci.* 8, 1–120.

Sporns, O. (2013). Structure and function of complex brain networks. *Dialogues Clin Neurosci.* 15, 247–262. doi: 10.31887/DCNS.2013.15.3/osporns

Sporns, O., Honey, C. J., and Kötter, R. (2007). Identification and classification of hubs in brain networks. *PLoS One* 2:e1049. doi: 10.1371/journal.pone.0001049

Stam, C. J. (2014). Modern network science of neurological disorders. *Nat. Rev. Neurosci.* 15, 683–695. doi: 10.1038/nrn3801

Stam, C. J., de Haan, W., Daffertshofer, A., Jones, B. F., Manshanden, I., Cappellen Van Wlsum, A. M., et al. (2009). Graph theoretical analysis of magnetoencephalographic functional connectivity in Alzheimer's disease. *Brain* 132, 213–224. doi: 10.1093/brain/awn262

Stam, C., Jelles, B., Achtereekte, H., Rombouts, S., Slaets, J., and Keunen, R. (1995). Investigation of EEG non-linearity in dementia and Parkinson's disease. *Electroencephalogr. Clin. Neurophysiol.* 95, 309–317. doi: 10.1016/0013-4694(95)00147-Q

Stam, C. J., Jelles, B., Achtereekte, H. A., van Birgelen, J. H., and Slaets, J. P. (1996). Diagnostic usefulness of linear and nonlinear quantitative EEG analysis in Alzheimer's disease. *Clin. Electroencephalogr.* 27, 69–77. doi: 10.1177/155005949602700205

Stam, C. J., Jones, B. F., Nolte, G., Breakspear, M., and Scheltens, P. (2007a). Small-world networks and functional connectivity in Alzheimer's disease. *Cereb. Cortex* 17, 92–99. doi: 10.1093/cercor/bhj127

Stam, C. J., Nolte, G., and Daffertshofer, A. (2007b). Phase lag index: assessment of functional connectivity from multi-channel EEG and MEG with diminished bias from common sources. *Hum. Brain Mapp.* 28, 1178–1193. doi: 10.1002/hbm.20346

Stam, C. J., van der Made, Y., Pijnenburg, Y. A., and Scheltens, P. (2003). EEG synchronization in mild cognitive impairment and Alzheimer's disease. *Acta Neurol. Scand.* 108, 90–96. doi: 10.1034/j.1600-0404.2003.02067.x

Supekar, K., Menon, V., Rubin, D., Musen, M., and Greicius, M. D. (2008). Network analysis of intrinsic functional brain connectivity in Alzheimer's disease. *PLoS Comput. Biol.* 4:e1000100. doi: 10.1371/journal.pcbi.1000100

Tahami Monfared, A. A., Byrnes, M. J., White, L. A., and Zhang, Q. (2022). We Alzheimer's disease: epidemiology and clinical progression. *Neurol. Ther.* 11, 553–569. doi: 10.1007/s40120-022-00338-8

Talwar, P., Kushwaha, S., Chaturvedi, M., and Mahajan, V. (2021). Systematic review of different neuroimaging correlates in mild cognitive impairment and Alzheimer's Disease. *Clin Neuroradiol.* 31, 953–967. doi: 10.1007/s00062-021-01057-7

Teipel, S., Grothe, M. J., Zhou, J., Sepulcre, J., Dyrba, M., Sorg, C., et al. (2016). Measuring cortical connectivity in Alzheimer's disease as a brain neural network pathology: toward clinical applications. *J. Int. Neuropsychol. Soc.* 22, 138–163. doi: 10.1017/S1355617715000995

van den Heuvel, M. P., and Sporns, O. (2011). Rich-club organization of the human connectome. *J Neurosci.* 31, 15775–15786. doi: 10.1523/JNEUROSCI.3539-11.2011

Vecchio, F., Miraglia, F., Bramanti, P., and Rossini, P. M. (2014). Human brain networks in physiological aging: a graph theoretical analysis of cortical connectivity from EEG data. *J. Alzheimers Dis.* 41, 1239–1249. doi: 10.3233/JAD-140090

Vecchio, F., Miraglia, F., Quaranta, D., Granata, G., Romanello, R., Marra, C., et al. (2016). Cortical connectivity and memory performance in cognitive decline: a study via graph theory from EEG data. *Neuroscience* 316, 143–150. doi: 10.1016/j.neuroscience.2015.12.036

Waller, L., Brovkin, A., Dorfschmidt, L., Bzdok, D., Walter, H., and Kruschwitz, J. D. (2018). GraphVar 2.0: a user-friendly toolbox for machine learning on functional connectivity measures. *J. Neurosci. Methods* 308, 21–33. doi: 10.1016/j.jneumeth.2018.07.001

Wan, L., Huang, H., Schwab, N., Tanner, J., Rajan, A., Lam, N. B., et al. (2019). From eyes-closed to eyes-open: Role of cholinergic projections in EC-to-EO alpha reactivity revealed by combining EEG and MRI. *Hum Brain Mapp.* 40, 566–577. doi: 10.1002/hbm.24395

Wang, Y., Lou, F., Li, Y., Liu, F., Wang, Y., Cai, L., et al. (2021). Clinical, neuropsychological, and neuroimaging characteristics of amyloid- positive vs. amyloid-negative patients with clinically diagnosed alzheimer's disease and amnestic mild cognitive impairment. *Curr Alzheimer Res.* 18, 523–532. doi: 10.2174/1567205018666211001113349

Wang, P., Zhou, B., Yao, H., Zhan, Y., Zhang, Z., Cui, Y., et al. (2015). Aberrant intra- and inter-network connectivity architectures in Alzheimer's disease and mild cognitive impairment. *Sci Rep.* 5:14824. doi: 10.1038/srep14824

Wang, J., Zuo, X., Dai, Z., Xia, M., Zhao, Z., Zhao, X., et al. (2013). Disrupted functional brain connectome in individuals at risk for Alzheimer's disease. *Biol. Psychiatry* 73, 472–481. doi: 10.1016/j.biopsych.2012.03.026

Xie, T., and He, Y. (2012). Mapping the Alzheimer's brain with connectomics. *Front. Psych.* 2:77. doi: 10.3389/fpsyt.2011.00077

Yao, Z., Zhang, Y., Lin, L., Zhou, Y., Xu, C., and Jiang, T. (2010). Alzheimer's Disease Neuroimaging Initiative. Abnormal cortical networks in mild cognitive impairment and Alzheimer's disease. *PLoS Comput Biol.* 6:e1001006. doi: 10.1371/journal.pcbi.1001006

Yesavage, J. A., Brink, T. L., Rose, T. L., Lum, O., Huang, V., Adey, M., et al. (1982). Development and validation of a geriatric depression screening scale: a preliminary report. *J. Psychiatr. Res.* 17, 37–49.

Yu, M., Gouw, A. A., Hillebrand, A., Tijms, B. M., Stam, C. J., Van Straaten, E. C., et al. (2016). Different functional connectivity and network topology in behavioral variant of frontotemporal dementia and Alzheimer's disease: an EEG study. *Neurobiol. Aging* 42, 150–162.

Zhang, L., Biessels, G. J., Hilal, S., Chong, J. S. X., Liu, S., Shim, H. Y., et al. (2021). Cerebral microinfarcts affect brain structural network topology in cognitively impaired patients. *J Cereb Blood Flow Metab.* 41, 105–115. doi: 10.1177/0271678X20902187

Frontiers in
Aging Neuroscience

Explores the mechanisms of central nervous system aging and age-related neural disease

The third most-cited journal in the field of geriatrics and gerontology, with a focus on understanding the mechanistic processes associated with central nervous system aging.

Discover the latest Research Topics

See more →

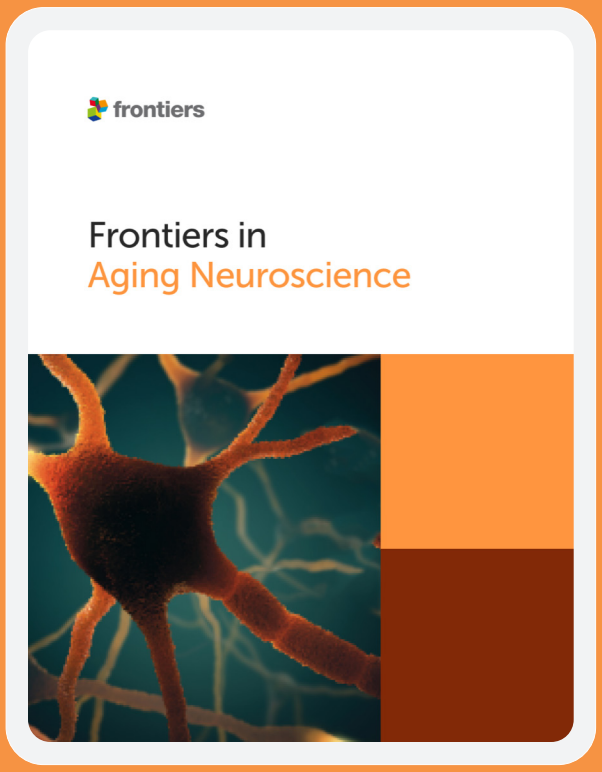

Frontiers

Avenue du Tribunal-Fédéral 34
1005 Lausanne, Switzerland
frontiersin.org

Contact us

+41 (0)21 510 17 00
frontiersin.org/about/contact